

*Assessing Axial Capacities of Auger Cast Piles from  
Measuring While Drilling*

**Final Report**

**FDOT Contract No. BDV31-977-125**

**Submitted to:**

Project Managers:

Rodrigo Herrera, P.E.

David Horhota, Ph.D., P.E.

Florida Department of Transportation

**Submitted By:**

UF Principal Investigator: Michael Rodgers, Ph.D., P.E.

UF Co-Principal Investigator: Michael McVay, Ph.D.

UF Graduate Researcher: Wyatt Kelch, E.I.

UF Graduate Researcher: Angelina Liu, E.I.

**December 1, 2021**

University of Florida

Engineering School of Sustainable Infrastructure & Environment

## **Disclaimer**

*The opinions, findings, and conclusions expressed in this publication are those of the authors and not necessarily those of the State of Florida Department of Transportation.*

## SI (Modern Metric) Conversion Factors (from FHWA) Approximate Conversions to SI Units

SYMBOL	WHEN YOU KNOW	MULTIPLY BY	TO FIND	SYMBOL
LENGTH				
in	inches	25.4	millimeters	mm
ft	feet	0.305	meters	m
yd	yards	0.914	meters	m
mi	miles	1.61	kilometers	km
SYMBOL	WHEN YOU KNOW	MULTIPLY BY	TO FIND	SYMBOL
AREA				
in <sup>2</sup>	square inches	645.2	square millimeters	mm <sup>2</sup>
ft <sup>2</sup>	square feet	0.093	square meters	m <sup>2</sup>
yd <sup>2</sup>	square yard	0.836	square meters	m <sup>2</sup>
ac	acres	0.405	hectares	ha
mi <sup>2</sup>	square miles	2.59	square kilometers	km <sup>2</sup>
SYMBOL	WHEN YOU KNOW	MULTIPLY BY	TO FIND	SYMBOL
VOLUME				
fl oz	fluid ounces	29.57	milliliters	mL
gal	gallons	3.785	liters	L
ft <sup>3</sup>	cubic feet	0.028	cubic meters	m <sup>3</sup>
yd <sup>3</sup>	cubic yards	0.765	cubic meters	m <sup>3</sup>
NOTE: volumes greater than 1000 L shall be shown in m <sup>3</sup>				
SYMBOL	WHEN YOU KNOW	MULTIPLY BY	TO FIND	SYMBOL
MASS				
oz	ounces	28.35	grams	g
lb	pounds	0.454	kilograms	kg
T	short tons (2000 lb)	0.907	megagrams (or "metric ton")	Mg (or "t")
SYMBOL	WHEN YOU KNOW	MULTIPLY BY	TO FIND	SYMBOL
TEMPERATURE (exact degrees)				
°F	Fahrenheit	5 (F-32)/9 or (F-32)/1.8	Celsius	°C
SYMBOL	WHEN YOU KNOW	MULTIPLY BY	TO FIND	SYMBOL
ILLUMINATION				
fc	foot-candles	10.76	lux	lx
fl	foot-Lamberts	3.426	candela/m <sup>2</sup>	cd/m <sup>2</sup>
SYMBOL	WHEN YOU KNOW	MULTIPLY BY	TO FIND	SYMBOL
FORCE and PRESSURE or STRESS				
lbf	pound force	4.45	newtons	N
lbf/in <sup>2</sup>	pound force per square inch	6.89	kilopascals	kPa

## Approximate Conversions to English Units

SYMBOL	WHEN YOU KNOW	MULTIPLY BY	TO FIND	SYMBOL
LENGTH				
mm	millimeters	0.039	inches	in
m	meters	3.28	feet	ft
m	meters	1.09	yards	yd
km	kilometers	0.621	miles	mi
SYMBOL	WHEN YOU KNOW	MULTIPLY BY	TO FIND	SYMBOL
AREA				
mm <sup>2</sup>	square millimeters	0.0016	square inches	in <sup>2</sup>
m <sup>2</sup>	square meters	10.764	square feet	ft <sup>2</sup>
m <sup>2</sup>	square meters	1.195	square yards	yd <sup>2</sup>
ha	hectares	2.47	acres	ac
km <sup>2</sup>	square kilometers	0.386	square miles	mi <sup>2</sup>
SYMBOL	WHEN YOU KNOW	MULTIPLY BY	TO FIND	SYMBOL
VOLUME				
mL	milliliters	0.034	fluid ounces	fl oz
L	liters	0.264	gallons	gal
m <sup>3</sup>	cubic meters	35.314	cubic feet	ft <sup>3</sup>
m <sup>3</sup>	cubic meters	1.307	cubic yards	yd <sup>3</sup>
SYMBOL	WHEN YOU KNOW	MULTIPLY BY	TO FIND	SYMBOL
MASS				
g	grams	0.035	ounces	oz
kg	kilograms	2.202	pounds	lb
Mg (or "t")	megagrams (or "metric ton")	1.103	short tons (2000 lb)	T
SYMBOL	WHEN YOU KNOW	MULTIPLY BY	TO FIND	SYMBOL
TEMPERATURE (exact degrees)				
°C	Celsius	1.8C+32	Fahrenheit	°F
SYMBOL	WHEN YOU KNOW	MULTIPLY BY	TO FIND	SYMBOL
ILLUMINATION				
lx	lux	0.0929	foot-candles	fc
cd/m <sup>2</sup>	candela/m <sup>2</sup>	0.2919	foot-Lamberts	fl
SYMBOL	WHEN YOU KNOW	MULTIPLY BY	TO FIND	SYMBOL
FORCE and PRESSURE or STRESS				
N	newtons	0.225	pound force	lbf
kPa	kilopascals	0.145	pound force per square inch	lbf/in <sup>2</sup>

## Technical Report Documentation Page

1. Report No.	2. Government Accession No.	3. Recipient's Catalog No.	
4. Title and Subtitle Assessing Axial Capacities of Auger Cast Piles from Measuring While Drilling		5. Report Date December 2021	
		6. Performing Organization University of Florida - ESSIE	
7. Author(s) Michael Rodgers, Ph.D., P.E., Michael McVay, Ph.D., Wyatt Kelch, M.E., and Angelina Liu		8. Performing Organization Report No.	
9. Performing Organization Name and Address University of Florida –Engineering School of Sustainable Infrastructure and Environment 365 Weil Hall – P.O. Box 116580 Gainesville, FL 32511-6580		10. Work Unit No. (TRAIS)	
		11. Contract or Grant No. BDV31-977-125	
12. Sponsoring Agency Name and Address Florida Department of Transportation 605 Suwannee Street, MS 30 Tallahassee, FL 32399		13. Type of Report and Period Covered Final Report 11/01/2019 – 02/28/2022	
		14. Sponsoring Agency Code	
15. Supplementary Notes			
<p>16. Abstract:</p> <p>This report focuses on the development of measuring while drilling (MWD) QA/QC procedures for South Florida auger cast-in-place (ACIP) piles, socketed into Florida limestone. The research first involved developing two MWD ACIP pile analysis spreadsheets that were used for QA/QC purposes during the installation of ACIP piles in South Florida. The first spreadsheet assessed the quality of ACIP piles using specific energy and total energy obtained from MWD. The second spreadsheet assessed the quality of ACIP piles using specific energy, unconfined compression strength, pile side shear, and pile capacity obtained from MWD. It was found that the MWD data compared well with SPT data, rock core data, and pile load test data obtained at three South Florida sites. Furthermore, modeled piles using the MWD data displayed the same behavior as the load-tested piles at the sites, which further validated the developed methods. Once the spreadsheet and methods were established, fifty production piles were analyzed to assess the QA/QC procedure developed. In addition to the development of ACIP pile MWD methods and procedures, LRFD analyses also took place that included design methods that utilized SPT data, conventional rock core data, and MWD data. It was found that the SPT methods produced the lowest resistance factor (<math>\phi</math>) values, the conventional rock core data produced the second lowest <math>\phi</math> values, MWD simulated rock coring produced the second highest <math>\phi</math> values, and MWD conducted in the footprint of the ACIP piles (QA/QC procedure) produced the highest <math>\phi</math> values. This was attributed to MWD eliminating spatial variability by monitoring the drilling process in the footprint of the piles. In conclusion, it was determined that MWD is viable to provide superior ACIP pile QA/QC.</p>			
17. Key Words ACIP piles, ACP, MWD, Florida Limestone, Rock Auger		18. Distribution Statement No restrictions.	
19. Security Classif. (of this report): Unclassified	20. Security Classif. (of this page): Unclassified	21. No. of Pages 202	22. Price

## **Acknowledgements**

The UF research team would like to thank the Florida Department of Transportation (FDOT) for supporting this research effort. A special thanks is extended to the FDOT Central Office geotechnical engineers for their continuous support, guidance, and assistance. Without their efforts, this research would not have been possible.

## Executive Summary

Measuring while drilling is an emerging application within the field of geotechnical engineering. The method involves continuously monitoring the drilling process using computerized systems with a series of sensors placed on the drill rig that measure and record individual drilling parameters. The sensors collect data for each monitored parameter continuously, in real time, without interfering with the drilling process. The continuous stream of sampled parameters produces high resolution profiles of individual and compound drilling parameters that can be used to quantify changes in subsurface conditions, assess geomechanical properties, and optimize drilling operations.

The FDOT has recently investigated using MWD for site investigation and characterization purposes (McVay and Rodgers, 2019) as well as a construction monitoring technique to provide QA/QC during drilled shaft applications (McVay and Rodgers, 2016 and 2020). In each of the prior investigations, it was found that specific energy, a compound drilling parameter obtained from MWD, was strongly correlated to the strength of Florida limestone. This provided a means to assess the strength of Florida limestone in situ during drilling, which provided a significant increase in the data obtained and provided a better understanding of the subsurface conditions at each monitored site. Similar to drilled shafts, auger cast-in-place (ACIP) piles also require QA/QC of their axial capacities during production pile installation. Because ACIP piles employ similar tooling as drilled shafts, it was believed the same MWD approach could be developed for ACIP pile axial capacity QA/QC purposes. Specifically, MWD could be used to assess specific energy on the planned instrumented load-tested piles that would allow a correlation between specific energy and ACIP side shear to be developed in layers of limestone. The established correlations could then be utilized as a new method of QA/QC for production pile capacities at each site. This research provides the basis of development for MWD conducted on ACIP piles.

To begin the research, an ACIP pile MWD analysis spreadsheet was developed that was capable of transforming time-referenced data obtained from automated monitoring equipment (AME) into depth-referenced data that was compatible with the specific energy equation. Additionally, hydraulic conversions of torque and crowd to physical measures were also undertaken to allow the use of the specific energy equation. The developed spreadsheet allowed the UF research team to assess the drilling process of South Florida ACIP piles on a 1 cm scale, providing the highest resolution MWD profiles to date. Two QA/QC methods were also developed. The first method included assessing specific energy and total energy, and the second method allowed the in situ assessment of unconfined compression strength, pile side shear, and pile capacity.

Once the spreadsheet was developed, building correlation between MWD specific energy and load-tested pile unit side shear was investigated. During the investigation, it was found that South Florida ACIP piles socketed into South Florida limestone develop curing-induced residual stresses. This required the UF research team to reanalyze the load tests in larger layers using stabilized strain gauge locations. Once the load tests were reanalyzed, a strong correlation was found between MWD specific energy and ACIP pile unit side shear. This correlation was the basis of developing the QA/QC method for South Florida ACIP piles. The correlation was also compared to SPT, rock coring, and load test data collected at three sites: I-395, Signature Bridge, and SR-836. Additionally, the MWD data collected was used to model mobilized test piles in

MultiPier. The results of the MultiPier trials indicated that the developed MWD method and correlation were highly accurate, as the modeled pile behavior was nearly identical to the pile behavior measured during the actual load tests. This further confirmed that the correlation developed was accurate. After the correlation was developed, the axial capacities of 50 production piles were assessed.

In addition to developing the ACIP pile MWD method, an assessment of LRFD resistance factor ( $\phi$ ) values was also conducted. For the LRFD assessment, the research team considered design methods that utilized SPT data, rock core data, a simulated MWD site characterization method, and MWD data obtained in the footprint of ACIP piles. The results indicated that methods that employed rock cores produced similar results to drilled shafts but higher  $\phi$  values than the original ACIP pile results presented in FDOT project BDV31-977-12 (McVay et al., 2016). Methods that employed SPT data produced the lowest  $\phi$  values as was the case in the original ACIP pile report. Conversely, the MWD methods resulted in the highest  $\phi$  values due to the excellent correlation that exists between specific energy, unconfined compression strength, side shear strength, and pile capacity.

In conclusion, it was determined that MWD is viable for ACIP pile QA/QC purposes. From this research, it was found that MWD specific energy was in agreement with the layering identified by the SPT borings, MWD agreed with the load test results, and an excellent correlation was developed between pile side shear and MWD specific energy, MWD was in agreement with the rock core strength range and layering, MWD data were able to provide accurate test pile models that showed the same behavior as the actual load tested piles, and MWD indicated the strength of rock decreased moving east-to-west which agreed with the trends of rock cores and load tests. Additionally, the drilling profiles obtained from MWD also showed the same trends as the estimated pile capacities and indicated that stronger rock takes longer to drill, which is the expected trend. From the LRFD  $\phi$  analyses, the MWD methods produced the highest LRFD  $\phi$  values, and performing MWD in the footprint of ACIP piles provided superior QA/QC as the effects of spatial variability were eliminated. All of these supporting observations indicate that the MWD correlation and procedures developed for ACIP pile capacity QA/QC are valid for the in situ assessment of rock strength and pile capacity.



## Table of Contents

Disclaimer .....	ii
SI (Modern Metric) Conversion Factors (from FHWA) Approximate Conversions to SI Units ..	iii
Approximate Conversions to English Units .....	iv
Technical Report Documentation Page .....	v
Acknowledgements.....	vi
Executive Summary .....	vii
List of Figures .....	xi
List of Tables .....	xv
1 Introduction and Background .....	1
1.1 Introduction.....	1
1.2 Background.....	1
2 MWD Data Reduction Criteria and Procedures for ACIP Pile Drill Rigs.....	3
2.1 Developing Conversion Coefficients.....	3
2.1.1 Converting Torque .....	4
2.1.2 Converting Crowd.....	5
2.2 Recommendations on Monitoring Procedures.....	6
2.3 ACIP Pile MWD Analysis Spreadsheet.....	9
2.3.1 CEI Spreadsheet.....	9
2.3.2 Enter Drill Data.....	9
2.3.3 Enter AME Pile Data .....	10
2.3.4 AME Pile Info.....	11
2.3.5 Enter AME Test Pile Data .....	12
2.3.6 AME Test Pile Info.....	13
2.3.7 Strength Analysis.....	14
2.3.8 Pile Summary Report.....	17
3 MWD Specific Energy vs. ACIP Pile Side Shear Relationships.....	19
3.1 Load Test Discrepancies .....	19
3.2 Developing Correlation.....	29
3.2.1 SR-836 Test Pile A .....	29
3.2.2 I-395 Test Pile C .....	33
3.2.3 I-395 Test Pile C Analysis .....	36
3.2.4 Signature Bridge Test Pile D .....	44
3.2.5 Developed ACIP Pile MWD Correlation for QA/QC Procedures.....	49

4	MWD Correlation Validation for ACIP Production Pile QA/QC .....	51
4.1	QA/QC Locations .....	51
4.2	Rock Core Data.....	52
4.3	Rock Core Layering.....	56
4.4	FB MultiPier Modeling.....	61
4.4.1	SR-836 Test Pile A .....	62
4.4.2	I-395 Test Pile C .....	66
4.5	Production Pile QA/QC Criteria and Reporting .....	74
4.6	Production Pile Analysis.....	75
4.7	Analyzed Production Pile Summary .....	79
5	LRFD $\phi$ Assessment of FDOT ACIP Pile Design Methods in South Florida .....	84
5.1	LRFD Methods .....	84
5.1.1	FOSM (Pre-Styler).....	84
5.1.2	FOSM (Styler) .....	85
5.1.3	Monte Carlo .....	86
5.2	SPT N Design Methods .....	86
5.2.1	SPT Design Equations .....	87
5.3	SPT LRFD $\phi$ Assessment.....	89
5.4	Core $q_u$ .....	93
5.4.1	Core $q_u$ Design Equations .....	98
5.5	Core $q_u$ LRFD $\phi$ Assessment .....	103
6	LRFD $\phi$ Assessment of MWD Specific Energy for ACIP Pile Capacity.....	108
6.1	MWD $q_u$ .....	108
6.1.1	MWD $q_u$ Design Equations .....	109
6.2	MWD $q_u$ LRFD $\phi$ Assessment.....	111
6.3	MWD $f_s$ .....	116
6.4	MWD $f_s$ LRFD $\phi$ Assessment .....	120
7	Conclusions.....	124
8	Recommendations.....	126
	References.....	128
	Appendix A – ACIP Pile QA/QC Summary Reports .....	131
	Appendix B – Sample Calculations .....	181

## List of Figures

Figure 1-1. Unit side shear – specific energy correlation for drilled shaft rock augers.....	2
Figure 2-1. Torque vs. rotational speed (T-N) chart.....	5
Figure 2-2. Proper averaging of rotational speed example.....	7
Figure 2-3. Enter Drill Rig Data tab.....	10
Figure 2-4. Enter AME Pile Data tab.....	11
Figure 2-5. AME Pile Info tab.....	12
Figure 2-6. Enter AME Test Pile Data tab.....	13
Figure 2-7. AME Test Pile Info tab.....	14
Figure 2-8. Strength Analysis tab – Specific Energy – All Data.....	15
Figure 2-9. Strength Analysis tab – Specific Energy – Above Threshold.....	16
Figure 2-10. Strength Analysis tab – MWD Auger Cast Pile QA/QC.....	17
Figure 2-11. Pile Summary Report.....	18
Figure 3-1. Load test strain gauge distribution for SR-836 Test Pile A.....	19
Figure 3-2. Load test strain gauge distribution for I-395 Test Pile B.....	20
Figure 3-3. Load test strain gauge distribution for I-395 Test Pile C.....	20
Figure 3-4. Load test strain gauge distribution for Signature Bridge Test Pile D.....	21
Figure 3-5. Load test strain gauge distribution for I-395 Test Pile E.....	21
Figure 3-6. Load test strain gauge distribution for I-395 Test Pile F.....	22
Figure 3-7. Load test strain gauge distribution for Signature Bridge Test Pile G.....	22
Figure 3-8. Load test strain gauge distribution for Signature Bridge Test Pile H.....	23
Figure 3-9. Load test strain gauge distribution for Signature Bridge Test Pile I.....	23
Figure 3-10. Load test strain gauge distribution for SR-836 Test Pile J.....	24
Figure 3-11. Load test strain gauge distribution for SR-836 Test Pile K.....	24
Figure 3-12. Continuous strain measurements during the curing of an instrumented drilled shaft (Sinnreich, 2012).....	26
Figure 3-13. Theoretical load path for SG 1 from Figure 3-12.....	27
Figure 3-14. Strain vs. load for I-395 Test Pile B.....	28
Figure 3-15. MWD specific energy and SPT profiles vs. depth.....	29
Figure 3-16. Reported load test side shear profile compared to the SPT profile.....	30
Figure 3-17. UF strain gauge load distribution for SR-836 Test Pile A.....	31
Figure 3-18. UF T-Z curves for SR-836 Test Pile A.....	31
Figure 3-19. Load test unit side shear vs. MWD specific energy for ACIP piles monitored at SR-836 compared to the previously developed drilled shaft rock auger correlation.....	32
Figure 3-20. Pile Group B and TP-B specific energy profiles.....	33
Figure 3-21. Pile Group B minimum, mean, median, and maximum specific energy, TP-B specific energy, and TP-B SPT profiles.....	34
Figure 3-22. Pile Group B combined profile compared to the TP-B MWD and SPT profiles.....	36
Figure 3-23. Group C1 (Piles 1-10) and Group C2 (Piles 11-18) specific energy profiles.....	38
Figure 3-24. Group C1 and Group C2 minimum, mean, median, and maximum specific energy profiles.....	38
Figure 3-25. SPT profiles proximal to I-395 Test Pile C.....	39
Figure 3-26. Pile Groups C1 and C2 combined profile compared to the SPT AVG profile.....	40
Figure 3-27. I-395 Test Pile C reanalyzed strain gauge load distribution.....	41
Figure 3-28. I-395 Test Pile C reanalyzed T-Z curves for the upper pile segment.....	42

Figure 3-29. I-395 Test Pile C reanalyzed T-Z curves for the lower pile segment. ....	42
Figure 3-30. Load test unit side shear vs MWD specific energy for ACIP piles monitored at SR-836 and I-395 compared to the previously developed drilled shaft rock auger correlation. ....	44
Figure 3-31. Pile Group D specific energy profiles closest to Signature Bridge TP-D. ....	45
Figure 3-32. Pile Group D minimum, mean, median, and maximum specific energy profiles. ....	45
Figure 3-33. SPT profiles close to Signature Bridge TP-7. ....	46
Figure 3-34. Pile Group D combined specific energy profile compared to the SB TP-D SPT profile. ....	48
Figure 3-35. Signature Bridge, Test Pile D reanalyzed strain gauge load distribution (upper pile segment). ....	49
Figure 3-36. Signature Bridge Test Pile D reanalyzed T-Z curves (upper pile segment). ....	49
Figure 3-37. Load test unit side shear vs. MWD specific energy for ACIP piles monitored at SR-836, I-395, and Signature Bridge compared to the drilled shaft rock auger correlation. ....	50
Figure 4-1. Map of test pile locations. ....	51
Figure 4-2. Split tension plotted as function of dry unit weight. ....	53
Figure 4-3. Unconfined compressive strength plotted as function of dry unit weight. ....	53
Figure 4-4. $q_u$ vs. $q_{st}$ relationships for MD and FLGM. ....	54
Figure 4-5. Frequency distributions for estimated $q_u$ values (MD and FLGM) compared to measured $q_u$ values. ....	55
Figure 4-6. Cumulative frequency distributions for estimated $q_u$ values (MD and FLGM) compared to measured $q_u$ values. ....	56
Figure 4-7. Depth profile of $q_u$ with the average $q_u$ for identified layering. ....	57
Figure 4-8. Depth profile of $q_u$ core samples compared to MWD specific energy at TP-B. ....	59
Figure 4-9. Depth profile of $q_u$ core samples compared to MWD specific energy at TP-C. ....	60
Figure 4-10. Depth profile of $q_u$ core samples compared to MWD specific energy at TP-D. ....	60
Figure 4-11. SR-836 Test Pile A boring. ....	62
Figure 4-12. SR-836 Test Pile A – MultiPier soil model. ....	65
Figure 4-13. Strain vs. applied load for SR-836 Test Pile A. ....	66
Figure 4-14. SR-836 Test Pile A T-Z curves with all data points plotted. ....	66
Figure 4-15. I-395 Test Pile C boring. ....	67
Figure 4-16. I-395 Test Pile C T-Z curves for the upper pile segment with Load Step 13 indicated in black and Load Step 14 indicated by dashed lines. ....	69
Figure 4-17. Synthetic limestone representing extremely weathered Florida limestone. ....	71
Figure 4-18. I-395 Test Pile C – final iteration MultiPier soil model. ....	74
Figure 4-19. ACIP pile summary report for Group B-Pile 8 QA/QC inspection using Drill Rig B. ....	76
Figure 4-20. ACIP pile summary plots for Group C1-Pile 10 QA/QC inspection using Drill Rig A. ....	78
Figure 4-21. ACIP pile summary plots for Group D-Pile 35 QA/QC inspection using Drill Rig A. ....	79
Figure 5-1. ACIP pile measured vs. predicted side shear capacity for multiple SPT design methods. ....	88
Figure 5-2. FOSM (Pre-Styler) LRFD $\phi$ vs. $\beta$ for multiple SPT design methods. ....	91
Figure 5-3. FOSM (Styler) LRFD $\phi$ vs. $\beta$ for multiple SPT design methods. ....	91
Figure 5-4. Monte Carlo LRFD $\phi$ vs. $\beta$ for multiple SPT design methods. ....	92

Figure 5-5. Rock core and MWD $q_u$ cumulative frequency distributions at I-395 and Signature Bridge.....	94
Figure 5-6. Rock core and MWD $q_u$ cumulative frequency distributions at County Road 250....	95
Figure 5-7. Rock core and MWD $q_u$ cumulative frequency distributions at Perry. ....	95
Figure 5-8. Comparison of core and MWD $q_u$ strength distributions based on elevation ranges. ....	97
Figure 5-9. Core and MWD $q_u$ distributions with an RQD adjusted core distribution for the elevation range -20' to -132.5'.....	98
Figure 5-10. Developing a new C-coefficient based on site specific load test and core data.....	101
Figure 5-11. ACIP pile measured vs. predicted side shear capacity for multiple $q_u$ design methods.....	101
Figure 5-12. FOSM (Pre-Styler) LRFD $\phi$ vs. $\beta$ for multiple $q_u$ design methods.....	105
Figure 5-13. FOSM (Styler) LRFD $\phi$ vs. $\beta$ for multiple $q_u$ design methods. ....	106
Figure 5-14. Monte Carlo LRFD $\phi$ vs. $\beta$ for multiple $q_u$ design methods. ....	106
Figure 6-1. ACIP pile measured vs. predicted side shear capacity for MWD $q_u$ design methods. ....	110
Figure 6-2. FOSM (Pre-Styler) LRFD $\phi$ vs. $\beta$ for multiple MWD $q_u$ design methods. ....	113
Figure 6-3. FOSM (Styler) LRFD $\phi$ vs. $\beta$ for multiple MWD $q_u$ design methods. ....	114
Figure 6-4. Monte Carlo LRFD $\phi$ vs. $\beta$ for multiple MWD $q_u$ design methods.....	114
Figure 6-5. Locations of all Florida MWD bored pile QA/QC investigations. ....	117
Figure 6-6. Mobilized unit side shear vs. average specific energy.....	118
Figure 6-7. ACIP pile measured vs. predicted side shear capacity for MWD $f_s$ design methods. ....	118
Figure 6-8. FOSM (Pre-Styler) LRFD $\phi$ vs. $\beta$ for MWD $f_s$ design methods. ....	122
Figure 6-9. FOSM (Styler) LRFD $\phi$ vs. $\beta$ for MWD $f_s$ design methods. ....	122
Figure 6-10. Monte Carlo LRFD $\phi$ vs. $\beta$ for MWD $f_s$ design methods.....	123
Figure A-1. ACIP pile capacity QA/QC report for Group B Pile 1.....	131
Figure A-2. ACIP pile capacity QA/QC report for Group B Pile 2.....	132
Figure A-3. ACIP pile capacity QA/QC report for Group B Pile 3.....	133
Figure A-4. ACIP pile capacity QA/QC report for Group B Pile 4.....	134
Figure A-5. ACIP pile capacity QA/QC report for Group B Pile 5.....	135
Figure A-6. ACIP pile capacity QA/QC report for Group B Pile 6.....	136
Figure A-7. ACIP pile capacity QA/QC report for Group B Pile 7.....	137
Figure A-8. ACIP pile capacity QA/QC report for Group B Pile 8.....	138
Figure A-9. ACIP pile capacity QA/QC report for Group B Pile 9.....	139
Figure A-10. ACIP pile capacity QA/QC report for Group B Pile 10.....	140
Figure A-11. ACIP pile capacity QA/QC report for Group B Pile 11.....	141
Figure A-12. ACIP pile capacity QA/QC report for Group B Pile 12.....	142
Figure A-13. ACIP pile capacity QA/QC report for Group B Pile 13.....	143
Figure A-14. ACIP pile capacity QA/QC report for Group B Pile 14.....	144
Figure A-15. ACIP pile capacity QA/QC report for Group B Pile 15.....	145
Figure A-16. ACIP pile capacity QA/QC report for Group B Pile 16.....	146
Figure A-17. ACIP pile capacity QA/QC report for Group C-1 Pile 1. ....	147
Figure A-18. ACIP pile capacity QA/QC report for Group C-1 Pile 2. ....	148
Figure A-19. ACIP pile capacity QA/QC report for Group C-1 Pile 3. ....	149
Figure A-20. ACIP pile capacity QA/QC report for Group C-1 Pile 4. ....	150
Figure A-21. ACIP pile capacity QA/QC report for Group C-1 Pile 5. ....	151

Figure A-22. ACIP pile capacity QA/QC report for Group C-1 Pile 6. ....	152
Figure A-23. ACIP pile capacity QA/QC report for Group C-1 Pile 7. ....	153
Figure A-24. ACIP pile capacity QA/QC report for Group C-1 Pile 8. ....	154
Figure A-25. ACIP pile capacity QA/QC report for Group C-1 Pile 9. ....	155
Figure A-26. ACIP pile capacity QA/QC report for Group C-1 Pile 10. ....	156
Figure A-27. ACIP pile capacity QA/QC report for Group C-2 Pile 1. ....	157
Figure A-28. ACIP pile capacity QA/QC report for Group C-2 Pile 2. ....	158
Figure A-29. ACIP pile capacity QA/QC report for Group C-2 Pile 3. ....	159
Figure A-30. ACIP pile capacity QA/QC report for Group C-2 Pile 4. ....	160
Figure A-31. ACIP pile capacity QA/QC report for Group C-2 Pile 5. ....	161
Figure A-32. ACIP pile capacity QA/QC report for Group C-2 Pile 6. ....	162
Figure A-33. ACIP pile capacity QA/QC report for Group C-2 Pile 7. ....	163
Figure A-34. ACIP pile capacity QA/QC report for Group C-2 Pile 8. ....	164
Figure A-35. ACIP pile capacity QA/QC report for Group D Pile 4. ....	165
Figure A-36. ACIP pile capacity QA/QC report for Group D Pile 5. ....	166
Figure A-37. ACIP pile capacity QA/QC report for Group D Pile 6. ....	167
Figure A-38. ACIP pile capacity QA/QC report for Group D Pile 7. ....	168
Figure A-39. ACIP pile capacity QA/QC report for Group D Pile 12. ....	169
Figure A-40. ACIP pile capacity QA/QC report for Group D Pile 13. ....	170
Figure A-41. ACIP pile capacity QA/QC report for Group D Pile 14. ....	171
Figure A-42. ACIP pile capacity QA/QC report for Group D Pile 20. ....	172
Figure A-43. ACIP pile capacity QA/QC report for Group D Pile 21. ....	173
Figure A-44. ACIP pile capacity QA/QC report for Group D Pile 28. ....	174
Figure A-45. ACIP pile capacity QA/QC report for Group D Pile 10. ....	175
Figure A-46. ACIP pile capacity QA/QC report for Group D Pile 18. ....	176
Figure A-47. ACIP pile capacity QA/QC report for Group D Pile 19. ....	177
Figure A-48. ACIP pile capacity QA/QC report for Group D Pile 26. ....	178
Figure A-49. ACIP pile capacity QA/QC report for Group D Pile 27. ....	179
Figure A-50. ACIP pile capacity QA/QC report for Group D Pile 35. ....	180
Figure B-1. Simulated torque vs. rotational speed chart.....	182

## List of Tables

Table 2-1. Drilling parameters recorded at the same depth in which specific energy is calculated after each individual drilling parameter has been averaged.....	8
Table 2-2. Drilling parameters recorded at the same depth in which specific energy is calculated for each time-referenced measurement.....	8
Table 2-3. Comparing specific energy statistics using Method 1 and Method 2 to calculate specific energy. ....	9
Table 3-1. Summary of strain vs. load for I-395 Test Pile B in descending order of maximum strain.....	28
Table 3-2. Pile Group B minimum, mean, median, and maximum specific energy, combined specific energy, TP-B specific energy, and percent error.....	35
Table 3-3. Pile Group B combined profile versus TP-B side shear.....	35
Table 3-4. Group C1 specific energy data. ....	37
Table 3-5. Group C2 specific energy data. ....	37
Table 3-6. Pile Groups C1 and C2 minimum, mean, median, and maximum specific energy and the combined specific energy tabular data.....	40
Table 3-7. Average specific energy and load test unit side shear for each I-395 Test Pile C SG zone.....	43
Table 3-8. Pile Group D specific energy data.....	47
Table 3-9. Pile Group D specific energy data continued with the combined profile.....	47
Table 3-10. Average specific energy and load test unit side shear for all monitored sites.....	50
Table 4-1. ACIP pile Miami-Dade rock core data.....	52
Table 4-2. Average split tension and unconfined compressive strength grouped by dry unit weight.....	52
Table 4-3. Summary of statistics for estimated $q_u$ values compared to measured $q_u$ values.....	55
Table 4-4. Summary of $q_u$ statistics for the Miami-Dade ACIP pile locations.....	57
Table 4-5. General strength layering at the Miami-Dade ACIP pile site.....	58
Table 4-6. $q_u$ statistics for each test pile location compared to the overall site statistics.....	61
Table 4-7. SR-836 TP-A MultiPier pile modeling input. ....	63
Table 4-8. SR-836 Test Pile 2 – MultiPier soil modeling input. ....	63
Table 4-9. I-395 Test Pile C pile modeling input. ....	68
Table 4-10. I-395 Test Pile C soil input with all layers modeled as limestone. ....	68
Table 4-11. I-395 Test Pile C soil input with layers modeled as limestone with load test T-Z curve data used in layers 4 through 7 and 13 through 16. ....	69
Table 4-12. I-395 Test Pile C soil input with layers modeled as limestone with load test T-Z curve data used in layers 4 through 8 and 13 through 17. ....	70
Table 4-13. I-395 Test Pile C soil input with layers modeled as limestone, load test T-Z curve data for layers 4 through 7 and 13 through 16, and non-cohesive IGM used in layers 8 and 17. ....	72
Table 4-14. I-395 Test Pile C soil input with layers modeled as limestone, non-cohesive IGM, and one layer modeled as sand with no shear resistance (Layer 5 – TZ Sand). ....	73
Table 4-15. Group B – Piles 1 through 10.....	80
Table 4-16. Group B – Piles 11 through 16.....	80
Table 4-17. Group C1 – Piles 1 through 10.....	80
Table 4-18. Group C2 – Piles 1 through 8.....	81
Table 4-19. Group D Piles 4, 5, 6, 7, 12, 13, 14, 20, 21, and 28. ....	81

Table 4-20. Group D Piles 10, 18, 19, 26, 27, and 35. ....	81
Table 4-21. Pile statistics for 50 ACIP production piles. ....	82
Table 4-22. Comparing pile group averages. ....	82
Table 5-1. Side shear estimates and bias per mobilized layer using SPT design methods. ....	88
Table 5-2. Bias statistics for SPT design methods. ....	89
Table 5-3. ACIP pile LRFD analysis – South Florida limestone for SPT design methods – $\beta = 2$ . .....	89
Table 5-4. ACIP pile LRFD analysis – South Florida limestone for SPT design methods – $\beta = 2.33$ . ....	89
Table 5-5. ACIP pile LRFD analysis – South Florida limestone for SPT design methods – $\beta = 2.5$ . ....	90
Table 5-6. ACIP pile LRFD analysis – South Florida limestone for SPT design methods – $\beta = 3$ . .....	90
Table 5-7. ACIP pile LRFD analysis – South Florida limestone for SPT design methods – $\beta = 3.5$ . ....	90
Table 5-8. ACIP pile LRFD analysis – South Florida limestone for SPT design methods – $\beta = 4$ . .....	90
Table 5-9. SPT design methods comparison of $\phi$ and $\phi/\lambda$ from BDV31-977-125 and BDV31-977-12. ....	93
Table 5-10. Unconfined compression strength comparison between core samples and MWD. ..	94
Table 5-11. Comparison of core and MWD $q_u$ strength statistics based on elevation ranges. ....	96
Table 5-12. Core and MWD $q_u$ statistics with RQD adjusted core statistics for El. -20' to -132.5'. .....	98
Table 5-13. Side shear estimates and bias per mobilized layer using $q_u$ design methods. ....	102
Table 5-14. Side shear estimates and bias per mobilized layer using $q_u$ design methods continued. .....	102
Table 5-15. Bias statistics for $q_u$ design methods. ....	102
Table 5-16. ACIP pile LRFD analysis – South Florida limestone for $q_u$ design methods – $\beta = 2$ . .....	103
Table 5-17. ACIP pile LRFD analysis – South Florida limestone for $q_u$ design methods – $\beta = 2.33$ . ....	103
Table 5-18. ACIP pile LRFD analysis – South Florida limestone for $q_u$ design methods – $\beta = 2.5$ . .....	104
Table 5-19. ACIP pile LRFD analysis – South Florida limestone for $q_u$ design methods – $\beta = 3$ . .....	104
Table 5-20. ACIP pile LRFD analysis – South Florida limestone for $q_u$ design methods – $\beta = 3.5$ . .....	104
Table 5-21. ACIP pile LRFD analysis – South Florida limestone for $q_u$ design methods – $\beta = 4$ . .....	105
Table 5-22. Comparison of $q_u$ design methods $\phi$ and $\phi/\lambda$ from BDV31-977-125 and BDV31-977-12. ....	107
Table 6-1. Side shear estimates and bias per mobilized layer using MWD $q_u$ design methods. ....	111
Table 6-2. Bias statistics for MWD $q_u$ design methods. ....	111
Table 6-3. ACIP pile LRFD analysis – South Florida limestone for MWD $q_u$ methods – $\beta = 2$ . .....	111



Table 6-4. ACIP pile LRFD analysis – South Florida limestone for MWD $q_u$ methods – $\beta = 2.33$ .	112
Table 6-5. ACIP pile LRFD analysis – South Florida limestone for MWD $q_u$ methods – $\beta = 2.5$ .	112
Table 6-6. ACIP pile LRFD analysis – South Florida limestone for MWD $q_u$ methods – $\beta = 3$ .	112
Table 6-7. ACIP pile LRFD analysis – South Florida limestone for MWD $q_u$ methods – $\beta = 3.5$ .	112
Table 6-8. ACIP pile LRFD analysis – South Florida limestone for MWD $q_u$ methods – $\beta = 4$ .	113
Table 6-9. Comparison of $q_u$ methods $\phi$ and $\phi/\lambda$ from BDV31-977-125 and BDV31-977-12.	116
Table 6-10. Comparing bias statistics between the MWD $q_u$ and Core $q_u$ design methods.	116
Table 6-11. Side shear estimates and bias per mobilized layer using the MWD QA/QC method.	119
Table 6-12. Bias statistics for MWD QA/QC method.	120
Table 6-13. ACIP pile LRFD analysis – South Florida limestone for MWD $f_s$ methods – $\beta = 2$ .	120
Table 6-14. ACIP pile LRFD analysis – South Florida limestone for MWD $f_s$ methods – $\beta = 2.33$ .	120
Table 6-15. ACIP pile LRFD analysis – South Florida limestone for MWD $f_s$ methods – $\beta = 2.5$ .	120
Table 6-16. ACIP pile LRFD analysis – South Florida limestone for MWD $f_s$ methods – $\beta = 3$ .	121
Table 6-17. ACIP pile LRFD analysis – South Florida limestone for MWD $f_s$ methods – $\beta = 3.5$ .	121
Table 6-18. ACIP pile LRFD analysis – South Florida limestone for MWD $f_s$ methods – $\beta = 4$ .	121
Table B-1. Simulated time-referenced data.	183
Table B-2. Converted depth-referenced data.	183
Table B-3. Simulated data used as an example to calculate the segment adjusted specific energy.	185

# 1 Introduction and Background

## 1.1 Introduction

The FDOT has developed and applied measuring while drilling (MWD) for drilled shafts to assess the axial shaft capacity of production shafts for QA/QC purposes. MWD has been applied for drilled shafts at Little River Bridge in Quincy, Overland Bridge in Jacksonville, Kanapaha in Gainesville, Selmon Expressway in Tampa, and the CR-250 Suwanee River Bridge in Dowling Park. The process involves monitoring the torque, crowd, penetration rate, and rotational speed of the drill bit in real time to obtain high resolution profiles of specific energy (measurements provided per 1” of penetration) which is then correlated to measured shaft side shear from static load tests. The developed specific energy-side shear correlation can subsequently be used for quality assurance during the installation of production shafts to ensure each shaft meets or exceeds the engineering design. Generally, the side shear versus MWD specific energy correlation must be established or verified on a site by site basis due to differences in equipment (e.g., drilling tools: rock auger, drilling bucket, etc.), the type of rock being drilled (e.g., calcite, dolomite), or other conditions (e.g., interlaced layering, drill rig type, etc.).

## 1.2 Background

Recently, the FDOT has allowed the use of auger cast-in-place (ACIP) piles for bridge piers at the I-395, Signature Bridge, and SR-836 sites in Miami. Similar to drilled shafts, ACIP piles require QA/QC of their axial capacities during production pile installation. Because ACIP piles employ an auger bit to remove soil and limestone, which creates a cylindrical excavation similar to drilled shaft tooling, it was believed the same MWD technology could be used for ACIP pile axial capacity QA/QC purposes. Specifically, MWD should be used to assess specific energy on the planned instrumented load-tested piles at each site. This would allow correlation between specific energy and ACIP side shear to be developed in layers of limestone, similar to correlations established for drilled shaft installations that use rock augers, as depicted in Figure 1-1. The established correlations could then be utilized as a new method of QA/QC for production pile capacities at each site. Alternatively, specific energy alone may be used to compare the total energy recorded at each pile (test and production) location for comparative QA/QC purposes, providing two methods of MWD QA/QC for South Florida ACIP piles.

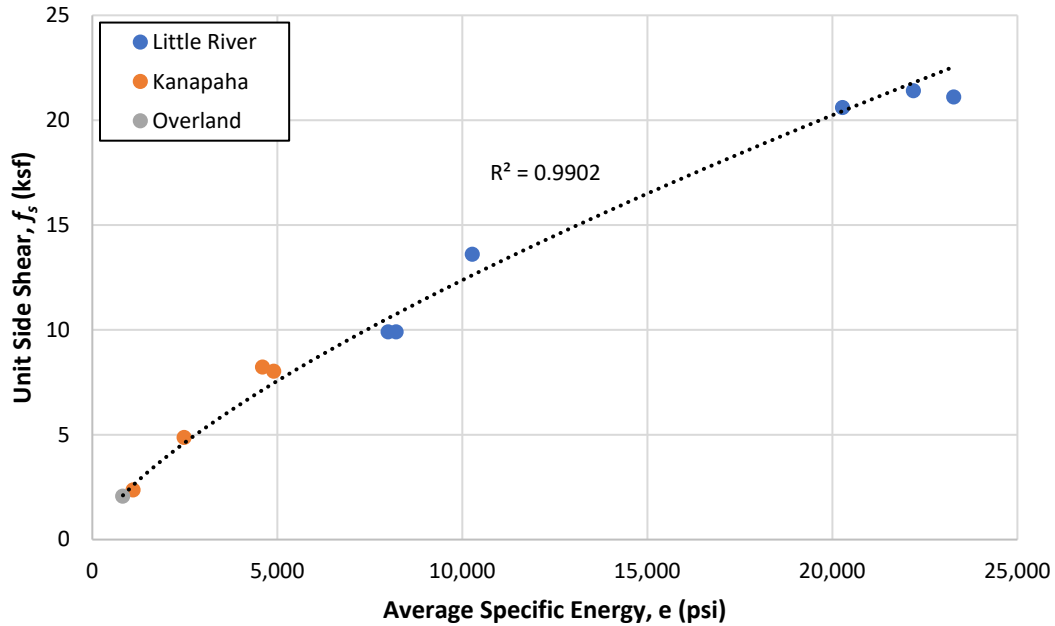


Figure 1-1. Unit side shear – specific energy correlation for drilled shaft rock augers.

Additionally, since 11 load tests were performed on the aforementioned sites, along with Standard Penetration Testing (SPT) and rock coring with laboratory strength testing, LRFD  $\phi$  assessment of different design methods should be revisited for South Florida due to the limited data available in FDOT’s prior ACIP pile project (BDV31-977-12; McVay et al., 2012). Finally, with the ACIP pile side shear versus MWD specific energy correlation established, a LRFD  $\phi$  assessment may be undertaken for the new QA/QC approach as well. The latter is important if MWD axial capacity QA/QC is used on future South Florida ACIP pile projects.

The objectives of this project were (1) use ISO-specified MWD procedures (monitoring torque, crowd, penetration rate, and rotational speed on a 1” scale or less) during Auger Cast Pile installations for load tested piles to establish a side shear versus MWD specific energy correlation on a number of sites; (2) validate the MWD correlations and developed QA/QC procedures on production piles at each of the sites; (3) use data obtained from pile load tests, recovered field cores/laboratory strength testing, and SPT testing to reassess LRFD  $\phi$  factors for Auger Cast Piles in south Florida; and (4) use the MWD pile side shear versus specific energy correlations from load tests to establish LRFD  $\phi$  factors for future south Florida axial pile capacity QA/QC.

## 2 MWD Data Reduction Criteria and Procedures for ACIP Pile Drill Rigs

The assessment of specific energy from MWD ACIP piles had never been undertaken prior to the current research effort. Like drilled shaft rigs, a method to assess specific energy on the ACIP pile drill rigs needed to be established. Drilling parameters torque, crowd, rotational speed, and penetration rate were required to be continuously monitored and recorded in real time throughout pile installations; and measurements of torque and crowd needed to be transformed from hydraulic pressures to physical measures for compatibility with the specific energy equation. This required rig-specific conversion coefficients to be developed for each drill rig used to properly make the transformations. In addition to the development of rig-specific conversion coefficients, the monitoring systems onboard the ACIP pile drill rigs provided time-referenced data which needed to be transformed into depth-referenced data for compatibility with the specific energy equation. Consequently, new raw data processing criteria and procedures were also developed to produce a workable spreadsheet in which specific energy may be assessed in a depth-referenced format. This chapter covers the development of the rig-specific conversion coefficients and the development of a workable spreadsheet to properly analyze specific energy using the recorded MWD data.

### 2.1 Developing Conversion Coefficients

There were two drill rigs used at the I-395, SR-836, and Signature Bridge sites to complete the ACIP pile installations. In order to protect the drilling contractor and the proprietary nature of the drill rigs used, generic drill rig names were designated for each drill rig. The more powerful custom drill rig will be referred to as “Drill Rig A”, and the smaller standard drill rig will be referred to as “Drill Rig B”. Both drill rigs were hydraulically driven, and therefore coefficients to convert the hydraulic pressures to physical measures for torque and crowd had to be developed for each rig. The following drill rig specifications were provided by the drilling contractor that allowed conversion coefficients to be developed for both torque and crowd for each drill rig (Note: the actual specifications are not provided to protect the proprietary nature of the contractor’s drill rigs):

- Maximum torque ( $T_{max}$ )
- Maximum operating pressure ( $OP_{max}$ )
- Baseline Torque Pressure ( $T_{BP}$ ) – Measured the day of drilling
- Hydraulic flow rate ( $Q_H$ )
- Maximum displacement ( $\delta_{max}$ )
- Minimum displacement ( $\delta_{min}$ )
- Number of hydraulic motors ( $X$ )
- Gearcase reduction for first gear ( $R_1$ )
- Gearcase reduction for second gear ( $R_2$ )
- Maximum crowd ( $F_{max}$ )
- Baseline Crowd Pressure ( $F_{BP}$ ) – Measured the day of drilling

Note: The maximum torque is often provided in the operator’s manual. However, the theoretical value should be verified through calculation using the drill rig specifications.

### 2.1.1 Converting Torque

From the specifications gathered, the minimum rotational speed ( $N_{min}$ ) that coincides with the maximum torque ( $T_{max}$ ) was determined for first gear:

$$N_{min} = \frac{Q}{\delta_{max} * R_1 * X} \quad (2-1)$$

The value of  $N_{min}$  indicates the maximum torque available on the drill rig can be achieved within a rotational speed range of 0 to  $N_{min}$ . This is often referred to as, “rock drilling mode”. The maximum torque is determined using Equation 2-2:

$$T_{max} = \frac{(P_{max} - T_{BP}) * Q}{2 * \pi * N_{min}} \quad (2-2)$$

At rotational speeds above  $N_{min}$ , the maximum torque available begins to decrease and can be determined by Equation 2-3:

$$T = \frac{(P - T_{BP}) * Q}{2 * \pi * N} \quad (2-3)$$

The transition from first gear to second gear can be determined by finding the maximum rotational speed that can be achieved while in first gear:

$$N_{max1} = \frac{Q}{\delta_{min} * R_1 * X} \quad (2-4)$$

This indicates that at rotational speeds above  $N_{max1}$  the drill rig has transitioned into second gear. The maximum rotational speed that can be achieved for second gear is found using Equation 2-5 with the gearcase reduction for second gear:

$$N_{max2} = \frac{Q}{\delta_{min} * R_2 * X} \quad (2-5)$$

This now provides the full range of rotational speeds that can be achieved with the drill rig. Because the hydraulic flow rate and number of motors were held constant, there was a seamless transition between gear shifts. Consequently, Equation 2-3 can be used to determine the maximum torque at any rotational speed above  $N_{min}$  and a torque versus rotational speed (T-N) chart can be developed as shown in Figure 2-1.

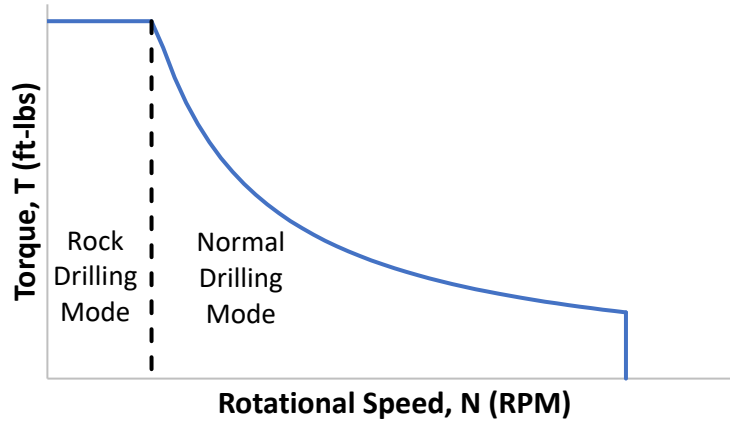


Figure 2-1. Torque vs. rotational speed (T-N) chart.

The blue line in Figure 2-1 indicates the maximum torque that can be achieved at any rotational speed for the given drill rig. Therefore, based on the rotational speed there are varying ranges of torque that can be achieved which is dependent upon the hydraulic pressure necessary (torque requirement) to keep the bit rotating at the designated rotational speed. The torque requirement is a function of the penetration rate and the strength of the rock encountered. To optimize the drilling process, the rotational speed can be adjusted to maintain an efficient penetration rate based on the material encountered and the torque requirement. For example, during rock drilling more torque is required to break apart the strong cohesive bonds of the rock and lower RPMs are ideal, whereas, drilling through soil (discontinuous mass) requires less torque, and higher RPMs are ideal to achieve higher penetration rates. These concepts also suggest that an optimum penetration rate for each rotational speed is achieved when the available torque is at a maximum. However, this approach is likely not ideal in terms rig efficiency as it could lead to quicker rig wear and downtime for repair. Therefore, a balance must be maintained between rig efficiency and drilling efficiency.

### 2.1.2 Converting Crowd

To convert crowd, a conversion coefficient ( $K_F$  - lbf/psi) must be developed. Using the specifications gathered for crowd, and the baseline hydraulic crowd pressure ( $F_{BP}$ ) solve for  $K_F$  using the identified and measured input parameters:

$$K_F = \frac{F_{max}}{P_{max} - F_{BP}} \quad (2-6)$$

The developed conversion coefficient was then used to transform the “real time” measured crowd hydraulic pressures to physical measures (lbf) as presented in Equation 2-7, where  $F_p$  is the hydraulic crowd operating pressure.

$$F \text{ (lbf)} = K_F \left( \frac{\text{lbf}}{\text{psi}} \right) \times [F_p(\text{psi}) - F_{BP}(\text{psi})] \quad (2-7)$$

Note: Hydraulic baseline pressures ( $T_{BP}$  and  $F_{BP}$ ) are typically found through visual inspection of the drill rig monitoring system after it has been warmed up. Unfortunately, researchers were not able to inspect the drill rigs used and therefore the baseline pressures were unknown. However, the baseline pressures are typically small compared to the full operating pressure range and often negligible. For example, the baseline pressure for the Bauer BG39 drill rig used at CR-250 in FDOT project BDV31-977-91 (McVay and Rodgers, 2020) accounted for 0.6% of the full range and was negligible. Therefore, assuming zero for the baseline pressure likely produced negligible error and the approach taken was considered valid. However, when possible, it is recommended to log the baseline pressures to ensure the hydraulic system is operating at an optimal level and to make any minor adjustments in the torque and crowd measurements for the most accurate in situ assessment.

After conversion of hydraulic pressure is completed for both drill rigs, measurements of torque and crowd are compatible with Teale's (1965) specific energy equation:

$$e = \frac{F}{A} + \frac{2\pi NT}{Au} \quad (2-8)$$

Where:

- $e$  = Specific Energy (psi);
- $T$  = Torque (in-lbs);
- $F$  = Crowd or downward axial force (lbf);
- $u$  = Penetration rate (in/min);
- $N$  = Rotational speed (RPMs); and
- $A$  = Cross-sectional area of the excavation ( $\text{in}^2$ ) defined by the bit diameter,  $d$  (in).

## 2.2 Recommendations on Monitoring Procedures

The monitoring system used to record the drilling data at the I-395, SR-836, and Signature Bridge sites produced time-referenced MWD data. That is, a measurement of each monitored drilling parameter was recorded for every second of drilling. The first step for proper specific energy assessment is to convert the time-referenced data to depth-referenced data. This step is required because different rates of penetration are expected due to different geomaterials being encountered throughout a pile's installation and Teale's specific energy is defined as energy per unit volume. Therefore, differences in penetration rate inherently create differences in the length of advancement achieved over the same amount of time. In order to properly average specific energy over a specified length (e.g., length of an instrumented shaft segment, i.e., volume removed) equal individual lengths of measure must be used. For example, if the rotational speed recorded for five centimeters of penetration were achieved over a 2-second interval as depicted in Figure 2-2, averaging could be completed in two ways. The first method would be to average both measurements equally:

$$N_{avg} = \frac{N_i + N_j}{n} = \frac{20 \text{ RPM} + 5 \text{ RPM}}{2} = 12.5 \text{ RPM} \quad (2-9)$$

However, the second increment ( $N = 5$  RPM) is four times the length of the first increment achieved ( $N = 20$  RPM) and a misleading higher rotational speed average would be obtained. The proper method of averaging would be to weight each measurement proportionally to the depth increment achieved (i.e., weighted averaging). To clarify, the second measurement should be weighted four times that of the first measurement as the length of the second depth increment is four times greater than that of the first depth increment. Proper averaging should be completed as follows:

$$N_{avg} = \frac{N_i + N_{j1} + N_{j2} + N_{j3} + N_{j4}}{n} = \frac{20 + 5 + 5 + 5 + 5}{5} = 8 \text{ RPM} \quad (2-10)$$

Weighted averaging produces the correct average which cannot be achieved using the time-referenced measurements alone. The time-referenced data must be broken down into depth-referenced data of equal lengths before proper averaging can take place.

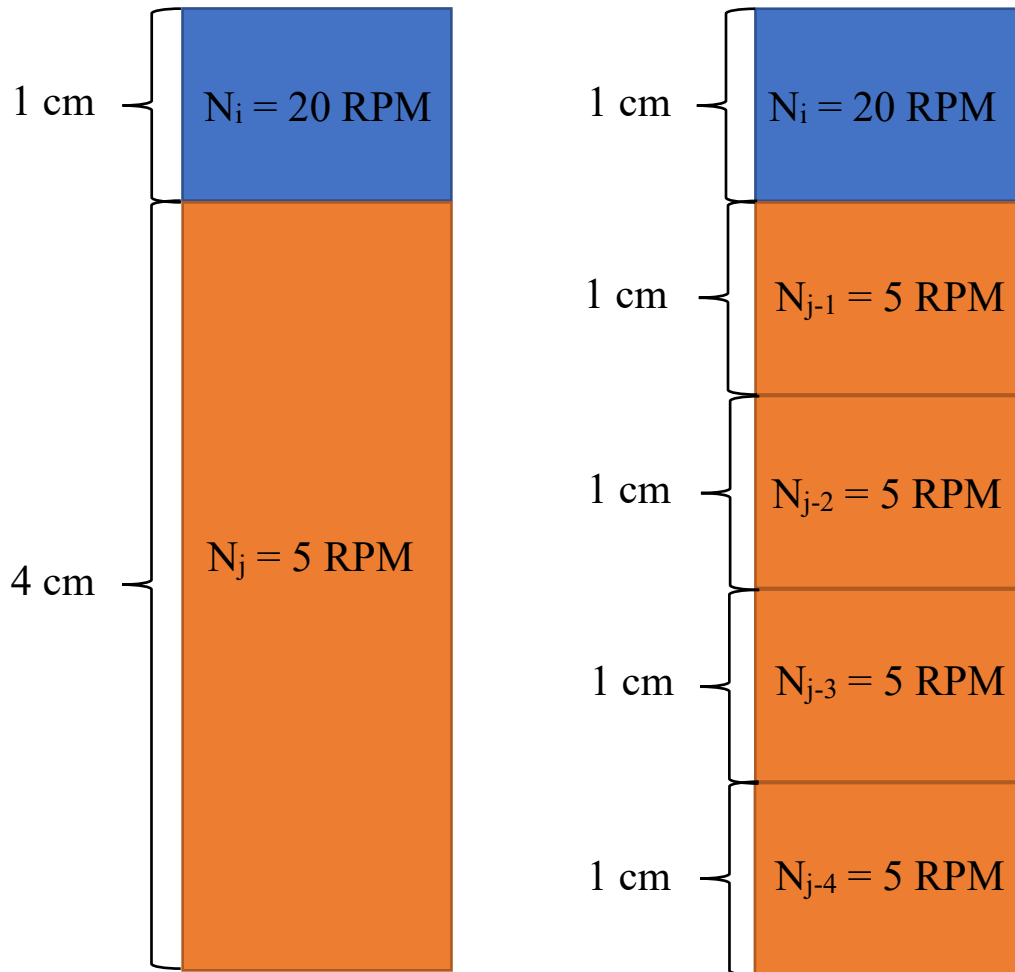


Figure 2-2. Proper averaging of rotational speed example.

When drilling into rock or harder geomaterial, the penetration rate is typically reduced and often produces several time-referenced drilling parameter data sets at the same depth increment. To properly assess specific energy for this scenario, one must average each time-referenced drilling



parameter recorded at the same depth increment individually prior to calculating the specific energy. For example, Table 2-1 shows that four time-referenced measurements for each drilling parameter were recorded at a depth of 3.48 feet. When an average is found for each individual drilling parameter and then specific energy is calculated from the parameter averages, the correct specific energy value is derived.

Table 2-1. Drilling parameters recorded at the same depth in which specific energy is calculated after each individual drilling parameter has been averaged.

Drilling Parameters Recorded at the Same Depth Increment					
Depth (ft)	N (RPM)	u (in/min)	T (in-lbs)	F (lbs)	e (psi)
3.48	39.6	31.5	435,329	30,150	
3.48	44.4	24.0	286,967	27,436	
3.48	42.0	3.9	260,778	21,151	
3.48	37.2	2.4	294,718	15,304	
Average	40.8	15.5	319,448	23,510	7,531

If specific energy is calculated for each individual time-increment (i.e., not an average calculated per unit volume of drilling) and then an average specific energy value is calculated from the four time-referenced specific energy measurements recorded at the same depth, an overestimation of specific energy would be derived (Table 2-2). This is because large fluctuations can occur for individual drilling parameters (e.g., penetration rate and torque) while the other parameters remain fairly constant. Fluctuations in drilling parameters such as penetration rate and torque can have a large effect on the calculated specific energy. Consequently, this results in a miscalculation and often times a large overestimate of specific energy and inherently rock strength.

Table 2-2. Drilling parameters recorded at the same depth in which specific energy is calculated for each time-referenced measurement.

Drilling Parameters Recorded at the Same Depth Increment					
Depth (ft)	N (RPM)	u (in/min)	T (in-lbs)	F (lbs)	e (psi)
3.48	39.6	31.5	435,329	30,150	4,908
3.48	44.4	24.0	286,967	27,436	4,755
3.48	42.0	3.9	260,778	21,151	24,759
3.48	37.2	2.4	294,718	15,304	41,277
				Average	18,925

Table 2-3 compares the two approaches of calculating specific energy for an entire pile, where Method 1 reflects the proper averaging (per unit depth or volume) found in Table 2-1 and Method 2 reflects the improper averaging (per unit time) found in Table 2-2. As indicated in Table 2-3, the average specific energy calculated for the pile using Method 2 is four times greater than the correct average calculated by Method 1. This inherently produces a large overestimate of rock strength which could lead to catastrophic failure if the true strength of the rock socket were inadequate to support the intended load. Furthermore, Method 1 produces far

more strength assessments and indicates the proper variability whereas Method 2 produces less data and indicates far more variability than is present. This would have a negative effect on the LRFD resistance assessment and lead to increased cost per shaft. Therefore, Method 1 must be used, and specific energy should only be calculated after each individual drilling parameter recorded at the same depth increment has been averaged.

Table 2-3. Comparing specific energy statistics using Method 1 and Method 2 to calculate specific energy.

Statistics	Method 1	Method 2
Mean	3,787	15,337
Median	2,316	4,158
Std. Dev	6,487	54,055
CV	1.71	3.52
Max	154,660	535,328
Min	700	1
Count	3,703	1,647

### 2.3 ACIP Pile MWD Analysis Spreadsheet

Once the rig-specific conversion coefficients, monitoring procedures, and post processing methods were established, two spreadsheets were developed to assess the axial capacity of ACIP piles using specific energy obtained from MWD. The first spreadsheet was developed for use by the construction engineering inspector (CEI) overseeing the project and the second spreadsheet was developed for research purposes. The first spreadsheet focused solely on the assessment of specific energy and the second spreadsheet was capable of assessing specific energy, unconfined compression strength ( $q_u$ ), pile side shear ( $f_s$ ), and axial pile capacity ( $P$ ). This report will focus on the procedures to use the CEI spreadsheet but will later identify the additional features that were used by the research team during the project investigation. The research-based spreadsheet is intended to illustrate the potential of MWD QA/QC procedures for future ACIP pile installations.

#### 2.3.1 CEI Spreadsheet

The CEI version of the spreadsheet is comprised of 8 tabs: Agreement, Enter Drill Rig Data, Enter AME Pile Data, AME Pile Info, Enter AME Test Pile Data, AME Test Pile Info, Strength Analysis, and Pile Summary Report. The agreement tab states that the user must be authorized by the Florida Department of Transportation (FDOT) to perform the ACIP pile analysis and states the spreadsheet is not to be modified, copied, unprotected, or distributed. Once the user agrees and checks the “I Agree” tab, the spreadsheet is unlocked and the ACIP pile MWD analysis can take place.

#### 2.3.2 Enter Drill Data

The first tab encountered is the “Enter Drill Rig Data” tab (Figure 2-3). Once the tab is accessed, the user will be able to input hydraulic drill rig specifications for both torque and crowd, for two

different drill rigs (Note: The actual drill rig specifications are not provided in Figure 2-3 to protect the proprietary nature of the contractor’s drill rigs). Once the rig specifications are input, the spreadsheet automatically updates the torque and crowd calculations based on the rig-specific specifications and a T-N chart is automatically developed for each drill rig. A “Torque Check” feature is also added to allow the user to observe how changes in hydraulic operating pressure and hydraulic baseline pressure affect the torque output at each rotational speed.

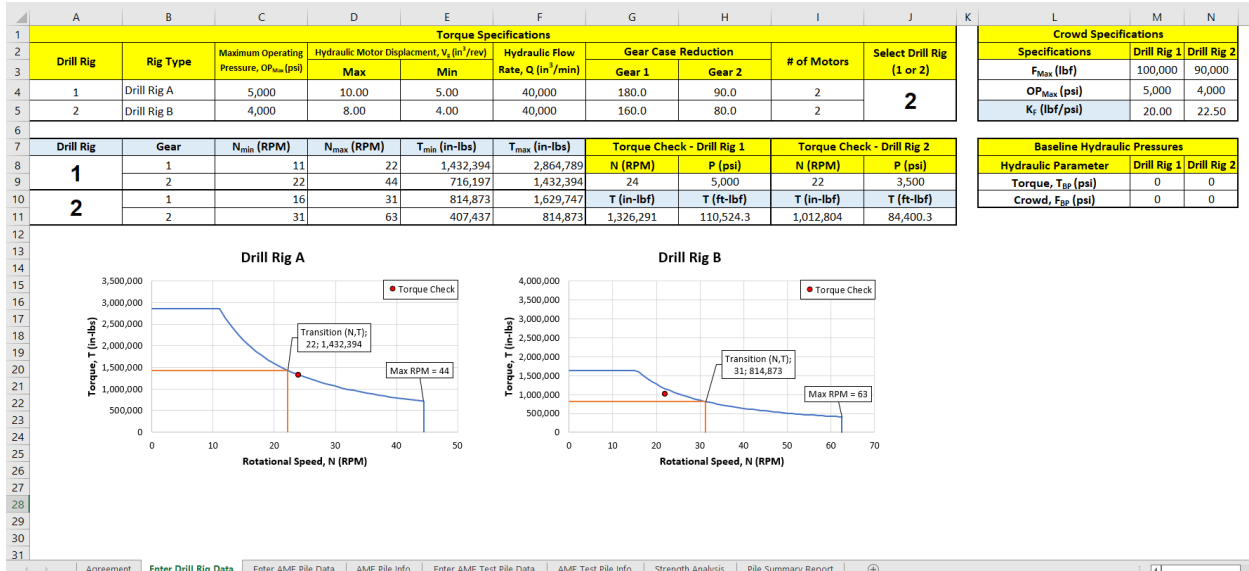


Figure 2-3. Enter Drill Rig Data tab.

### 2.3.3 Enter AME Pile Data

The next tab encountered is the “Enter AME Pile Data” tab (Figure 2-4). This tab allows the user to input AME data for up to 10 piles. The AME data must be input in the following order with the units of measured identified: time stamp (mm/dd/yyyy hh:mm:ss AM/PM), duration (min), rotational speed (RPM), penetration rate (ft/min), penetration rate (min/ft), depth (ft), torque hydraulic pressure (psi), torque (ft-lbs), crowd hydraulic pressure (psi), and crowd (lbf). Each pile input also allows the user to input the Pile ID, Top of Pile Elevation (ft), Station, and Offset. This information is automatically populated in the Strength Analysis and Pile Summary Report tabs, to be discussed later.



	A	B	C	D	E	F	G	H	I	J
			Time	Duration (min)	Depth (ft)	Penetration Rate (ft/min)	Rotational Speed (RPM)	Torque Pressure (psi)	Crowd Pressure (psi)	
1	Input		6/8/2020 7:47:33 AM	0	0	8.4645672	-19031.44	473.9832036	199.7169129	
2	Engineer		6/8/2020 7:47:34 AM	0.02	0	5.905512	-19031.33	495.0136701	202.9077423	
3	Rodgers, McVay, Kelch		6/8/2020 7:47:35 AM	0.03	0	3.5433072	-19030.87	465.8610924	201.8924784	
4	Location		6/8/2020 7:47:36 AM	0.05	0	3.1824148	-19030.93	446.4260406	196.9611966	
5	Miami, Florida		6/8/2020 7:47:37 AM	0.07	0	1.5748032	-9507.56	438.013854	201.7474407	
6	Project		6/8/2020 7:47:38 AM	0.08	0	0.0328084	17.1	460.2046221	194.7856311	
7	I-395		6/8/2020 7:47:39 AM	0.1	0.0328084	0.1968504	17.3	542.0058849	268.0296696	
8	Drill Bit Diameter (in)		6/8/2020 7:47:40 AM	0.12	0.0656168	0.7545932	17.17	515.4639858	259.9075584	
9	30.0		6/8/2020 7:47:41 AM	0.13	0.1312336	1.312336	16.98	622.211733	246.9992031	
10			6/8/2020 7:47:42 AM	0.15	0.164042	1.7716536	16.93	583.051554	157.8010176	
11	Do Not Input		6/8/2020 7:47:43 AM	0.17	0.164042	1.8700788	17.34	656.2955925	248.8846932	
12	Pile ID		6/8/2020 7:47:44 AM	0.18	0.2296588	2.1653544	18.19	709.234353	246.7091277	
13	B-16		6/8/2020 7:47:45 AM	0.2	0.2624672	2.1981628	19.28	721.9976706	239.6022804	
14	Top of Pile Elevation (ft)		6/8/2020 7:47:46 AM	0.22	0.2952756	2.1981628	20.58	769.5700362	255.4113897	
15	13.55		6/8/2020 7:47:47 AM	0.23	0.3608924	2.2637796	21.79	711.4099185	219.006927	
16	Station		6/8/2020 7:47:48 AM	0.25	0.3937008	2.7559056	22.59	703.432845	239.8923558	
17	100+00.01		6/8/2020 7:47:49 AM	0.27	0.4593176	2.8543308	22.96	710.68473	249.0297309	
18	Offset (ft)		6/8/2020 7:47:50 AM	0.28	0.482126	2.8215224	23.15	715.1808987	229.0145283	
19	10		6/8/2020 7:47:51 AM	0.3	0.5577428	2.8543308	23.23	728.9594802	262.3731993	
20	Pile Length (ft)		6/8/2020 7:47:52 AM	0.32	0.5905512	2.9199476	23.3	733.7457243	253.9610127	
21	94.09		6/8/2020 7:47:53 AM	0.33	0.656168	2.9855644	23.28	723.0129345	277.1670447	
22	Pile Length (in)		6/8/2020 7:47:54 AM	0.35	0.7217848	3.0511812	23.33	717.6465396	267.1594434	
23	1,129.13		6/8/2020 7:47:55 AM	0.37	0.7545932	3.116798	23.33	725.3335377	286.4494575	
24	Area of Excavation (ft <sup>2</sup> )		6/8/2020 7:47:56 AM	0.38	0.8530164	3.3464568	23.31	730.8449703	269.3350089	
25	4.91		6/8/2020 7:47:57 AM	0.4	0.9514436	3.8713912	23.28	773.7761295	296.0219457	
26	Area of Excavation (in <sup>2</sup> )		6/8/2020 7:47:58 AM	0.42	1.0498688	4.6259844	23.23	861.3789003	309.9455649	
27	706.86		6/8/2020 7:47:59 AM	0.43	1.2139108	5.5446196	23.14	916.3481886	282.823515	
28			6/8/2020 7:48:00 AM	0.45	1.3451444	6.6272968	22.94	955.798443	311.5409796	
29			6/8/2020 7:48:01 AM	0.47	1.5091864	7.709974	22.72	1098.660578	282.9685527	
30			6/8/2020 7:48:02 AM	0.48	1.6732284	8.4645672	22.5	1172.339729	275.7166677	
31			6/8/2020 7:48:03 AM	0.5	1.804462	8.9566932	22.29	1299.972905	268.319745	
32			6/8/2020 7:48:04 AM	0.52	1.968504	9.186352	22.16	1181.76718	279.0525348	
33			6/8/2020 7:48:05 AM	0.53	2.0997376	9.2191604	22.24	1224.118188	261.3579354	
34			6/8/2020 7:48:06 AM	0.55	2.2637796	8.9895016	22.22	1283.728683	261.5029731	
35			6/8/2020 7:48:07 AM	0.57	2.3622048	8.5958008	22.42	1145.507755	258.8922945	
36			6/8/2020 7:48:08 AM	0.58	2.3950132	7.6443572	22.58	922.7298474	207.8390241	
37			6/8/2020 7:48:09 AM	0.6	2.4278216	5.9383204	22.62	719.9671428	206.0985717	
38			6/8/2020 7:48:10 AM	0.62	2.4278216	4.1994752	22.83	667.17342	205.3733832	
39			6/8/2020 7:48:11 AM	0.63	2.4278216	2.4934384	23.22	632.364372	203.7779685	
40			6/8/2020 7:48:12 AM	0.65	2.4278216	1.0170604	23.3	610.3186416	206.6787225	
41			6/8/2020 7:48:13 AM	0.67	2.4278216	0.1312336	23.5	620.4712806	214.0756452	
42			6/8/2020 7:48:14 AM	0.68	2.4278216	0.0328084	23.76	698.5015632	369.5560596	
43			6/8/2020 7:48:15 AM	0.7	2.4934384	0.7217848	23.63	720.6923313	229.159566	
44			6/8/2020 7:48:16 AM	0.72	2.5590552	1.5419948	23.42	806.6844235	224.6633973	
45			6/8/2020 7:48:17 AM	0.73	2.624672	2.2309712	23.33	747.3792681	233.3656593	
46			6/8/2020 7:48:18 AM	0.75	2.6902888	2.9855644	23.23	820.3332312	288.0448722	
47										

Figure 2-5. AME Pile Info tab.

### 2.3.5 Enter AME Test Pile Data

The next tab encountered is the “Enter AME Test Pile Data” tab (Figure 2-6). Similar to the Enter AME Pile Data tab, the user inputs the AME data collected in the footprint of the test pile used for reference at the production pile location. This data is later used to compare the specific energy and total energy recorded at the production pile location and the referenced test pile location for QA/QC. The AME data must be input in the following order with the units of measured identified: time stamp (mm/dd/yyyy hh:mm:ss AM/PM), duration (min), rotational speed (RPM), penetration rate (ft/min), penetration rate (min/ft), depth (ft), torque hydraulic pressure (psi), torque (ft-lbs), crowd hydraulic pressure (psi), and crowd (lbf). The tab also allows the user to input the Pile ID, Top of Pile Elevation (ft), Station, and Offset for the test pile. This information is automatically populated in the Strength Analysis and Pile Summary Report tabs, to be discussed later.

	A	B	C	D	E	F	G	H	I	J	K	L	M	N	O	P	Q
1	Enter Test Pile	Time	Duration	Gear Box I	Penetrati	Penetrati	Depth (ft)	Gear Box I	Torque (f	Crowd Pre	Thrust (lbs)						
2	Pile ID	5/4/2020	0	-293.35	-36.9423	3.048	0	454.5482	0	208.5642	3233.58						
3	Test Pile B	5/4/2020	0.02	-293.26	-36.9751	3.048	0	477.4641	0	201.1673	3118.898						
4	Top of Shaft Elevation (ft)	5/4/2020	0.03	14.75	0	3.048	0	587.9828	0	351.5714	5450.763						
5	13.50	5/4/2020	0.05	16.29	0.295276	3.386667	0.032808	551.8684	0	275.8617	4276.96						
6	Station	5/4/2020	0.07	16.21	0.787402	1.27	0.065617	606.8377	0	252.9457	3921.671						
7	100+00.01	5/4/2020	0.08	16.16	1.181102	0.846667	0.098425	603.3568	0	239.8924	3719.291						
8	Offset (ft)	5/4/2020	0.1	16.16	1.574803	0.635	0.131234	665.1429	0	251.9305	3905.93						
9	10.0	5/4/2020	0.12	16.29	2.034121	0.491613	0.19685	614.5247	0	246.9992	3829.476						
10	Pile ID (B#-P#-S#)	5/4/2020	0.13	16.43	2.132546	0.468923	0.229659	641.7918	0	243.0832	3768.762						
11	B = Bridge	5/4/2020	0.15	16.5	2.001312	0.499672	0.229659	623.372	0	248.5946	3854.211						
12	P = Pier	5/4/2020	0.17	16.62	1.935696	0.51661	0.262467	643.5323	0	252.0755	3908.179						
13	S = Shaft/Pile	5/4/2020	0.18	16.78	1.935696	0.51661	0.295276	618.0056	0	246.9992	3829.476						
14		5/4/2020	0.2	16.91	1.902887	0.525517	0.328084	663.9826	0	245.6939	3809.238						
15		5/4/2020	0.22	16.98	1.870079	0.534737	0.360892	661.807	0	247.7244	3840.719						
16		5/4/2020	0.23	17.28	1.968504	0.508	0.393701	634.2499	0	250.9152	3890.19						
17		5/4/2020	0.25	17.46	2.034121	0.491613	0.459318	681.5322	0	242.6481	3762.016						
18		5/4/2020	0.27	17.47	2.034121	0.491613	0.492126	709.2344	0	255.9915	3968.893						
19		5/4/2020	0.28	17.41	2.034121	0.491613	0.524934	669.349	0	268.3197	4160.029						
20		5/4/2020	0.3	17.62	2.132546	0.468923	0.557743	682.2573	0	254.5412	3946.406						
21		5/4/2020	0.32	17.57	2.165354	0.461818	0.590551	717.2114	0	250.9152	3890.19						
22		5/4/2020	0.33	17.54	2.165354	0.461818	0.62336	695.1657	0	253.816	3935.163						
23		5/4/2020	0.35	17.62	2.198163	0.454925	0.656168	643.8224	0	263.5335	4085.823						
24		5/4/2020	0.37	17.79	2.26378	0.441739	0.688976	722.8679	0	250.9152	3890.19						
25		5/4/2020	0.38	17.6	2.26378	0.441739	0.754593	716.1962	0	258.0221	4000.374						
26		5/4/2020	0.4	17.44	2.230971	0.448235	0.787402	685.5932	0	252.9457	3921.671						
27		5/4/2020	0.42	17.49	2.26378	0.441739	0.82021	663.5475	0	270.4953	4193.759						
28		5/4/2020	0.43	17.49	2.296588	0.435429	0.853018	688.0588	0	252.0755	3908.179						
29		5/4/2020	0.45	17.46	2.296588	0.435429	0.885827	691.9749	0	258.6022	4009.369						
30		5/4/2020	0.47	17.58	2.296588	0.435429	0.918635	667.4635	0	269.48	4178.019						
31		5/4/2020	0.48	17.65	2.362205	0.423333	0.984252	715.1809	0	250.7702	3887.941						
32		5/4/2020	0.5	17.62	2.427822	0.411892	1.01706	713.0053	0	259.6175	4025.109						
33		5/4/2020	0.52	17.62	2.427822	0.411892	1.049869	696.326	0	251.0603	3892.438						
34		5/4/2020	0.53	17.66	2.46063	0.4064	1.115486	698.7916	0	253.816	3935.163						
35		5/4/2020	0.55	17.66	2.559055	0.390769	1.148294	712.4252	0	254.2511	3941.909						
36		5/4/2020	0.57	17.81	2.559055	0.390769	1.181102	703.1428	0	257.877	3998.125						
37		5/4/2020	0.58	17.82	2.526247	0.395844	1.213911	693.7153	0	252.2206	3910.428						
38		5/4/2020	0.6	17.84	2.559055	0.390769	1.279528	710.1046	0	263.8236	4090.321						

Figure 2-6. Enter AME Test Pile Data tab.

### 2.3.6 AME Test Pile Info

The next tab encountered is the “AME Test Pile Info” tab (Figure 2-7). Similar to the AME Pile Info tab, the data input in the Enter AME Test Pile Data tab is automatically populated and organized based on FDOT specifications for geotechnical MWD applications. This allows the user to more easily review the drilling parameters required to assess specific energy and to track drill rig activity. This format also allows depth-referenced data to be input directly into the spreadsheet if the monitoring system automatically produces depth-referenced data. In addition to the Engineer, Location, Project, and Drill Bit Diameter inputs, this tab also allows the user to specify which drill rig was used during the test pile installation, asks if the user wants to compare the load test data to the production pile data, and asks what percentage of the Test Pile total energy ( $E_T$ ) is required for QA/QC comparisons. If the “Compare Load Test?” box is left unchecked, the spreadsheet will not populate the Test Pile data in the Strength Analysis and Pile Summary Report tabs. If the box is checked, The Test Pile information is automatically populated in the Strength Analysis and Pile Summary Report tabs.

Note: The percentage of  $E_T$  provided in Figure 2-7 is used for demonstration purposes and is not a recommendation. The actual percentage used during ACIP production pile QA/QC will be determined by FDOT officials overseeing the project.

	A	B	C	D	E	F	G	H	I	J	K
			Time	Duration (min)	Depth (ft)	Penetration Rate (ft/min)	Rotational Speed (RPM)	Torque Pressure (psi)	Crowd Pressure (psi)		
2	Input		5/4/2020 7:12:43 AM	0	0	-36.9422584	-293.35	454.5481518	208.5642126		
3	Engineer		5/4/2020 7:12:44 AM	0.02	0	-36.9750668	-293.26	477.4641084	201.1672899		
4	Rodgers, McVay, Kelch		5/4/2020 7:12:45 AM	0.03	0	0	14.75	587.9828358	351.5713848		
5	Location		5/4/2020 7:12:46 AM	0.05	0.0328084	0.2952756	16.29	551.8684485	275.8617054		
6	Miami, Florida		5/4/2020 7:12:47 AM	0.07	0.0656168	0.7874016	16.21	606.8377368	252.9457488		
7	Project		5/4/2020 7:12:48 AM	0.08	0.0984252	1.1811024	16.16	603.356832	239.8923558		
8	I-395		5/4/2020 7:12:49 AM	0.1	0.1312336	1.5748032	16.16	665.1428922	251.9304849		
9	Drill Bit Diameter (in)		5/4/2020 7:12:50 AM	0.12	0.1968504	2.0341208	16.29	614.5247349	246.9992031		
10	30.0		5/4/2020 7:12:51 AM	0.13	0.2296588	2.132546	16.43	641.7918225	243.0831852		
11	Select Drill Rig (1 or 2)		5/4/2020 7:12:52 AM	0.15	0.2296588	2.0013124	16.5	623.3720346	248.5946178		
12	2		5/4/2020 7:12:53 AM	0.17	0.2624672	1.9356956	16.62	643.5322749	252.0755226		
13	Compare Load Test?		5/4/2020 7:12:54 AM	0.18	0.2952756	1.9356956	16.78	618.0056397	246.9992031		
14	<input checked="" type="checkbox"/> YES		5/4/2020 7:12:55 AM	0.2	0.328084	1.9028872	16.91	663.9825906	245.6938638		
15	Percentage of E <sub>r</sub> (kip-ft)		5/4/2020 7:12:56 AM	0.22	0.3608924	1.8700788	16.98	661.8070251	247.7243916		
16	90%		5/4/2020 7:12:57 AM	0.23	0.3937008	1.968504	17.28	634.2498621	250.915221		
17			5/4/2020 7:12:58 AM	0.25	0.4593176	2.0341208	17.46	681.5321523	242.6480721		
18	Do Not Input		5/4/2020 7:12:59 AM	0.27	0.492126	2.0341208	17.47	709.234353	255.9915405		
19	Pile ID		5/4/2020 7:13:00 AM	0.28	0.5249344	2.0341208	17.41	669.3489855	268.319745		
20	Test Pile B		5/4/2020 7:13:01 AM	0.3	0.5577428	2.132546	17.62	682.2573408	254.5411635		
21	Top of Pile Elevation (ft)		5/4/2020 7:13:02 AM	0.32	0.5905512	2.1653544	17.57	717.2114265	250.915221		
22	13.50		5/4/2020 7:13:03 AM	0.33	0.6233596	2.1653544	17.54	695.1656961	253.815975		
23	Station		5/4/2020 7:13:04 AM	0.35	0.656168	2.1981628	17.62	643.8223503	263.5335009		
24	100+00.01		5/4/2020 7:13:05 AM	0.37	0.6889764	2.2637796	17.79	722.8678968	250.915221		
25	Offset (ft)		5/4/2020 7:13:06 AM	0.38	0.7545932	2.2637796	17.6	716.1961626	258.0220683		
26	10		5/4/2020 7:13:07 AM	0.4	0.7874016	2.2309712	17.44	685.5932079	252.9457488		
27	Pile Length (ft)		5/4/2020 7:13:08 AM	0.42	0.82021	2.2637796	17.49	663.5474775	270.4953105		
28	107.97		5/4/2020 7:13:09 AM	0.43	0.8530184	2.296588	17.49	688.0588488	252.0755226		
29	Pile Length (in)		5/4/2020 7:13:10 AM	0.45	0.8858268	2.296588	17.46	691.9748667	258.6022191		
30	1,295.67		5/4/2020 7:13:11 AM	0.47	0.9186352	2.296588	17.58	667.4634954	269.4800466		
31	Area of Excavation (ft <sup>2</sup> )		5/4/2020 7:13:12 AM	0.48	0.984252	2.3622048	17.65	715.1808987	250.7701833		
32	4.91		5/4/2020 7:13:13 AM	0.5	1.0170604	2.4278216	17.62	713.0053332	259.617483		
33	Area of Excavation (in <sup>2</sup> )		5/4/2020 7:13:14 AM	0.52	1.0498888	2.4278216	17.62	696.3259977	251.0602587		
34	706.86		5/4/2020 7:13:15 AM	0.53	1.1154856	2.46063	17.66	698.7916386	253.815975		
35			5/4/2020 7:13:16 AM	0.55	1.148294	2.5590552	17.66	712.4251824	254.2510881		
36			5/4/2020 7:13:17 AM	0.57	1.1811024	2.5590552	17.81	703.1427696	257.8770306		
37			5/4/2020 7:13:18 AM	0.58	1.2139108	2.5262468	17.82	693.7153191	252.2205603		
38			5/4/2020 7:13:19 AM	0.6	1.2795276	2.5590552	17.84	710.1045792	263.8235763		
39			5/4/2020 7:13:20 AM	0.62	1.312336	2.5590552	17.84	745.9288911	252.8007111		
40			5/4/2020 7:13:21 AM	0.63	1.3451444	2.5262468	18.02	710.8297677	250.4801079		
41			5/4/2020 7:13:22 AM	0.65	1.4107612	2.4934384	18.32	712.4251824	266.4342549		
42			5/4/2020 7:13:23 AM	0.67	1.4435696	2.5262468	18.49	784.0738062	256.2816159		
43			5/4/2020 7:13:24 AM	0.68	1.476378	2.46063	18.69	790.455465	243.5182983		
44			5/4/2020 7:13:25 AM	0.7	1.5091864	2.3950132	18.91	736.791516	241.9228836		
45			5/4/2020 7:13:26 AM	0.72	1.5419948	2.4278216	19.15	775.2265065	250.3350702		
46			5/4/2020 7:13:27 AM	0.73	1.6076116	2.3950132	19.23	777.9822228	250.4801079		
47			5/4/2020 7:13:28 AM	0.75	1.64042	2.3622048	19.46	804.3790842	249.7549194		

Figure 2-7. AME Test Pile Info tab.

### 2.3.7 Strength Analysis

The next tab encountered is the “Strength Analysis” tab (Figures 2-8 through 2-10). When the tab is first entered, the user is presented with the specific energy data collected over the full production pile length. It is on this tab that the user will specify which pile in the Enter AME Pile Data tab to analyze. Once the pile is selected, a specific energy profile, frequency distribution, and cumulative frequency distribution are automatically generated for the entire pile length. In addition, specific energy statistics over the full pile length are generated that include the Mean, Median, Standard Deviation, Coefficient of Variation, Maximum, Minimum, and Count. The user can then input up to 30 pile segments to analyze within user-specified elevation ranges. Within each one of the elevation ranges entered, the same statistics provided for the full pile length are automatically generated for each user-specified elevation range. The user can then enter a pile segment they wish to further assess in the Pile Segment input. Once the pile segment is input, the spreadsheet will highlight the segment, elevation range, statistics, the segment in the depth profile, and populate a frequency and cumulative frequency distribution for comparison with the entire pile length.

Next, the user will specify the recorded depth increment [ $\Delta z$  Increment (cm)] at which to assess specific energy. The increment selected must be a whole number. The spreadsheet will then average specific energy over the increment selected for analysis (Note: 1 cm was used for the data analyses included in this report). The spreadsheet will also identify the ISO Class of the MWD assessment (ISO/IEC 2016). For ISO Class 1, the depth increment must be less than or

equal to 2 cm, for ISO Class 2 the depth increment must be less than or equal to 5 cm, and for ISO Class 3 the depth increment must be less than or equal to 10 cm.

Also included in the user inputs is an e Reduction input. This input reduces the specific energy per linear foot of drilling if a linear increase in the baseline specific energy is observed. In most cases, this input will only be necessary if the pile is inclined out of the intended vertical axis during drilling, which results in increased drilling resistance.

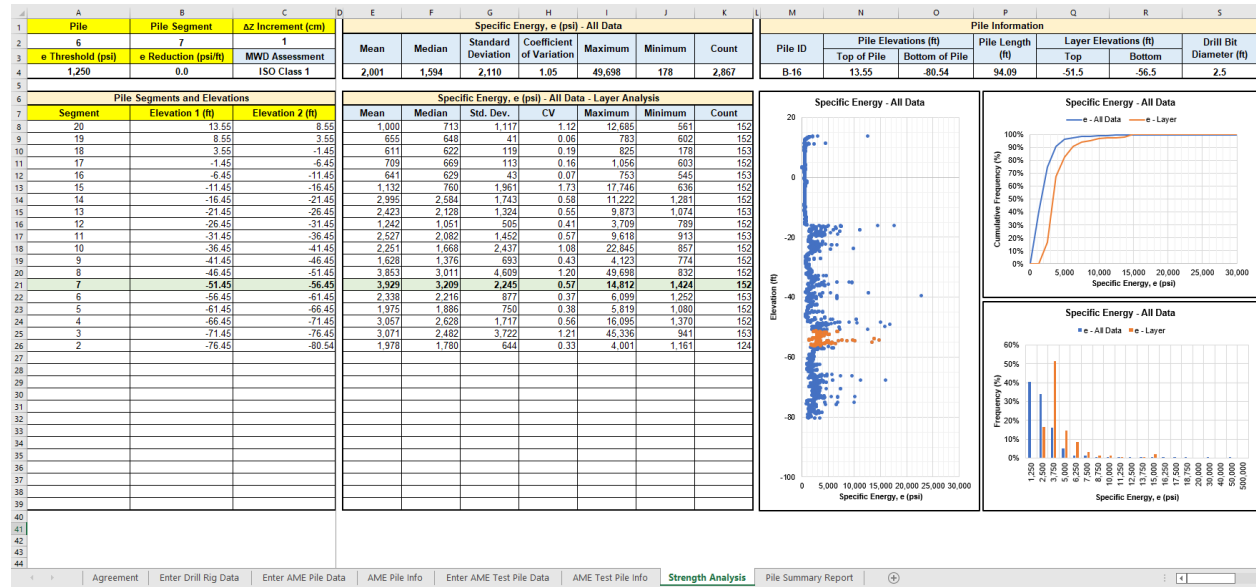


Figure 2-8. Strength Analysis tab – Specific Energy – All Data.

The final user input is the specific energy threshold (e Threshold). This input eliminates any specific energy data points that are less than the threshold specified. This is intended to remove any soil or weakly cemented sands from consideration in the rock strength and pile capacity assessment, thereby, allowing the assessment to only focus on the capacity contributions made by rock. Once the e Threshold is input, the user then scrolls the tab page to the right and is presented with the same statistical information and plots with the lower strength soil data removed from the analyses (Figure 2-9). As observed in Figure 2-9, the e Threshold removed all data from an elevation range of +8.55 ft to -11.45 ft which is observed in the tabular statistics and depth profile. The frequency distributions are also updated to only include the data above the user-specified threshold.



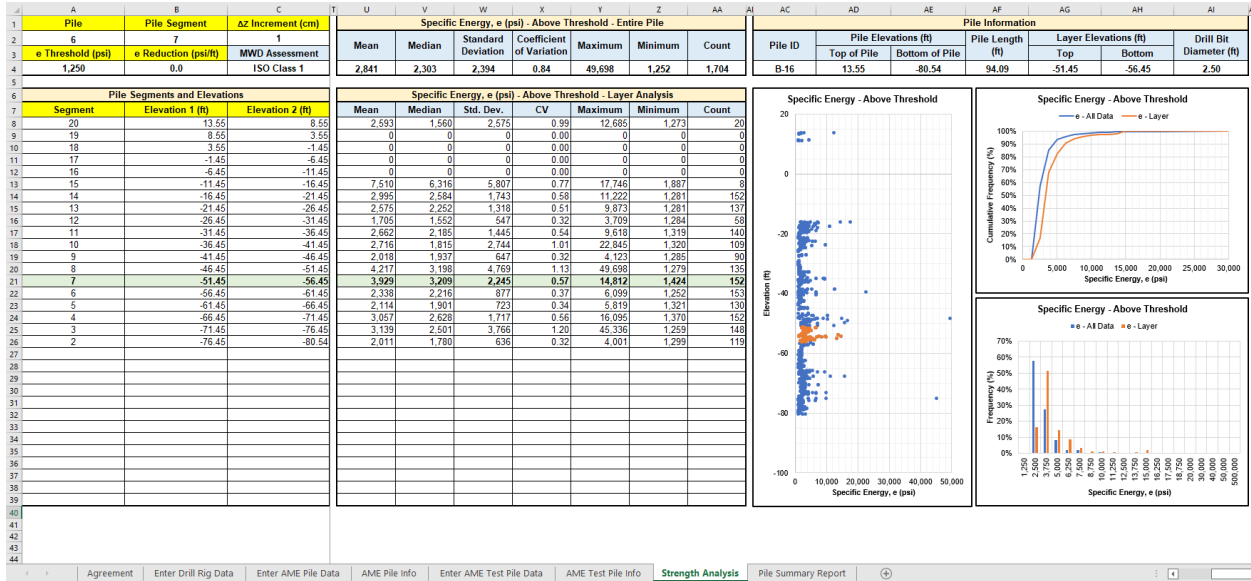


Figure 2-9. Strength Analysis tab – Specific Energy – Above Threshold.

Finally, the user scrolls the tab page further right and is presented with the QA/QC portion of the strength analysis tab (Figure 2-10). On this portion of the tab page, QA/QC statistics are provided for the production pile being analyzed and the test pile used as reference for the QA/QC procedure. For the production pile the following is provided for the full pile length: top and bottom elevations, the average specific energy above the threshold, the full pile length, the length of the rock socket above the e Threshold, the total energy above the threshold, and the average specific energy above the threshold adjusted based on the length of the rock socket per full pile length. For the production pile layer analysis, the same statistics are provided as the full pile length with the addition of the number of data points collected per layer (Count) and the average specific energy within each layer without using the e Threshold ( $e_{AVG}$ ).

Note: Total energy ( $E_T$ ) is calculated as the average specific energy recorded multiplied by the volume excavated during drilling. Because specific energy is derived in units of stress (force / area), when multiplied by the excavated volume the unit of measure is transformed into units of mechanical energy or work (force times length). Thus, a cumulative sum of the total energy required to drill a pile can be used for comparative analyses between production and/or test piles.

If a test pile is selected for comparison on the AME Test Pile Info tab, the same statistics generated for the full production pile are also generated for the test pile. For the test pile, two sets of statistics are provided. The first set of pile statistics are generated for the full test pile elevation range. The second set of statistics generated are for the test pile over the elevation range of the production pile as observed in Figure 2-10. The second set of statistics is used for direct comparison with the production pile because test piles often extend to greater depths than production piles and the lower elevation range reached at the test pile location will never be reached at the production pile location. Consequently, using the full test pile elevation range will lead to inconsistencies in the comparative strength analysis and therefore only the production pile elevations should be considered for the QA/QC procedure. In addition to the tabular statistics generated, a specific energy profile, frequency distribution, and cumulative frequency distribution are generated for comparative analyses.

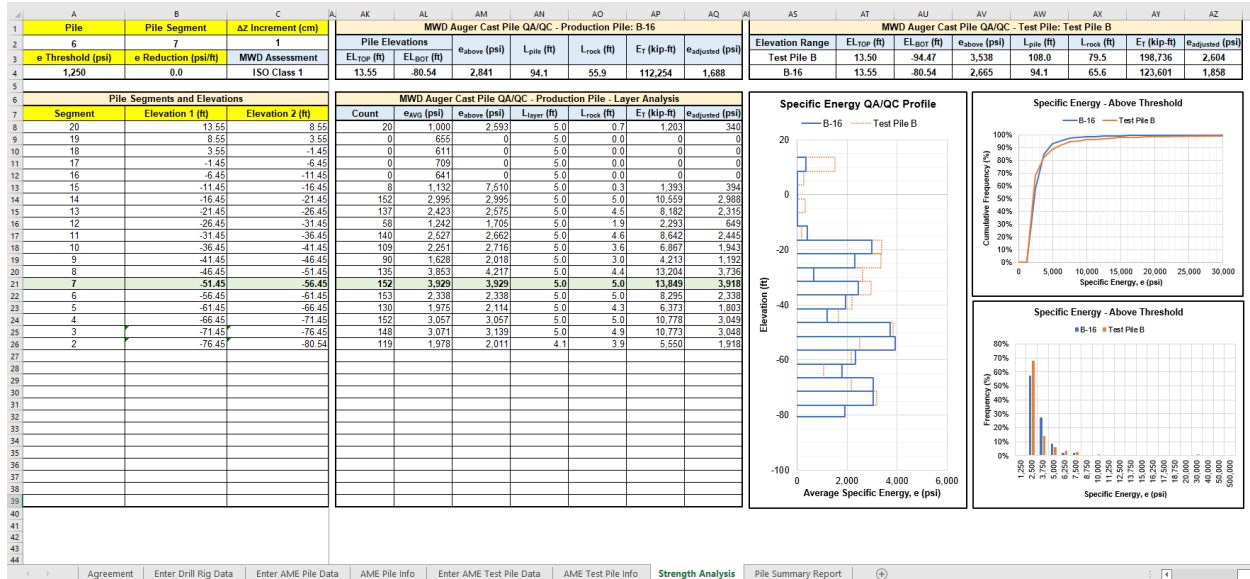


Figure 2-10. Strength Analysis tab – MWD Auger Cast Pile QA/QC.

### 2.3.8 Pile Summary Report

The final tab encountered in the spreadsheet is the “Pile Summary Report” (Figure 2-11). In the Pile Summary Report, the following tabular information is provided: project and pile information, specific energy statistics for the production pile and the test pile (if selected for comparison), a QA/QC section that includes the production pile length, the rock socket length and total energy of the production pile and test pile, a percentage of the test pile total energy required for comparison, the adjusted total energy of the test pile, and a design requirement inspection that checks to see if the production pile total energy is equal to or greater than the adjusted test pile total energy. Tabular data is also provided for the production pile installation that identifies the amount of time that was spent drilling and the amount of time that was spent on other drilling activities that include redrill, idle rotation, idle, withdrawal, and penetration without rotation. Based on the time spent drilling compared to the total time of all drilling activities, the spreadsheet will identify the drilling efficiency as a percentage of drilling time to total time.

The pile summary report also generates two plots. The first plot includes a depth profile of average specific energy above the user-defined  $e$  Threshold for the production pile and test pile, identifies the percentage of rock encountered per production pile layer based on the user-defined  $e$  Threshold and layer elevations, and plots the total energy above the threshold (cumulative mechanical energy) required to drill the pile plotted versus depth. The second plot includes a depth profile of elevation versus time and illustrates what drilling activities occurred during the drilling process, where they occurred, and what time they occurred. The second plot is intended to improve drilling efficiency in future pile installations.

The Pile summary report also allows the user to input any notes related to the drilling process. This may include problems encountered during the installation, why certain drilling activities occurred, or any relevant information that may be useful to the engineer analyzing the pile. Once

the notes are entered into the report, the user can then press print and a time-stamped PDF will be automatically generated.



### ACIP Pile - MWD Summary Report

Project	Location	Engineer	Pile ID
I-395	Miami, Florida	Rodgers, McVay, Kelch	B-16
Station	Offset (ft)	Drill Rig	Drill Bit Diameter (in)
100+00.01	10.00	Drill Rig B	30
Top of Pile Elevation (ft)	Bottom of Pile Elevation (ft)	Depth Increment Analyzed (cm)	ISO-MWD Assessment
13.55	-80.54	1	Class 1

Specific Energy, e (psi) - Summary of Statistics: B-16	
Specific Energy Threshold (psi)	1,250
Mean	2,841
Median	2,303
Standard Deviation	2,394
Coefficient of Variation (CV)	0.84
Maximum	49,698
Minimum	1,252
Number of Data Points	1,704

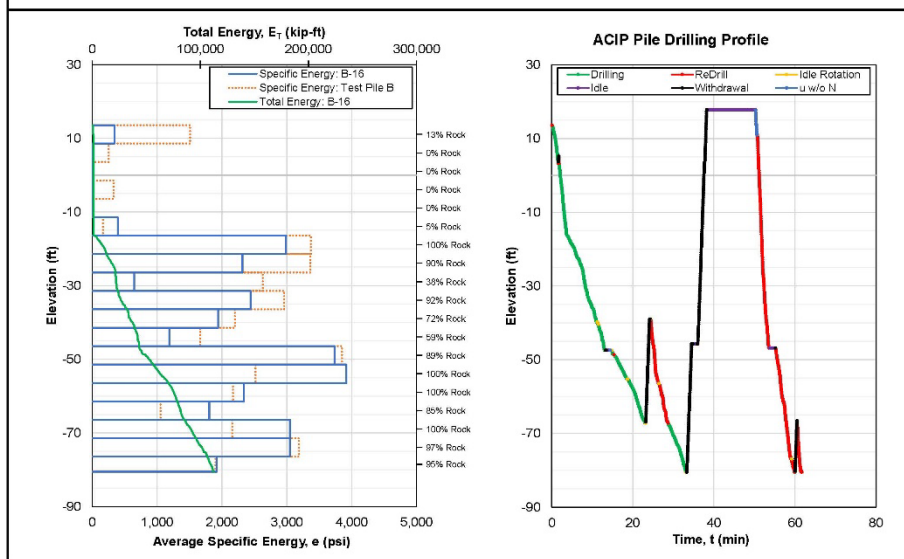
ACIP Pile QA/QC	
Pile Length (ft)	94.09
Rock Socket (ft): B-16	55.91
Total Energy (kip-ft): B-16	112,254
Rock Socket (ft): Test Pile B	65.62
Total Energy (kip-ft): Test Pile B	123,601
Total Energy Required	90% of Test Pile
Total Energy Required (kip-ft)	111,241
Design Requirement Inspection	Passed

Specific Energy, e (psi) - Summary of Statistics: Test Pile B	
Specific Energy Threshold (psi)	1,250
Mean	2,665
Median	2,073
Standard Deviation	4,539
Coefficient of Variation (CV)	1.70
Maximum	152,159
Minimum	1,252
Number of Data Points	2,000

Pile Installation Summary	
Drilling Time (min)	25.7
ReDrill Time (min)	13.4
Idle Rotation Time (min)	2.5
Idle Time (min)	14.0
Withdrawal Time (min)	5.7
Penetration w/o Rotation Time (min)	0.4
Total Time (min)	61.6
Drilling Efficiency (%)	41.6%



**Notes:**  
 Enter notes in this section.

Date of Analysis: 12/31/2021

Figure 2-11. Pile Summary Report.

### 3 MWD Specific Energy vs. ACIP Pile Side Shear Relationships

#### 3.1 Load Test Discrepancies

After thorough investigation of the load test reports, it was found that the reported side shear values, T-Z curves, and load distributions produced inconsistencies. As presented in Figures 3-1 through 3-11, in all cases, except for SR-836 Test Pile K, negative loads were generated in the strain gauge load distributions for a number of load steps, if the load test reported side shear values (given in the tables and T-Z curves) were used with the reported average pile segmental surface areas.

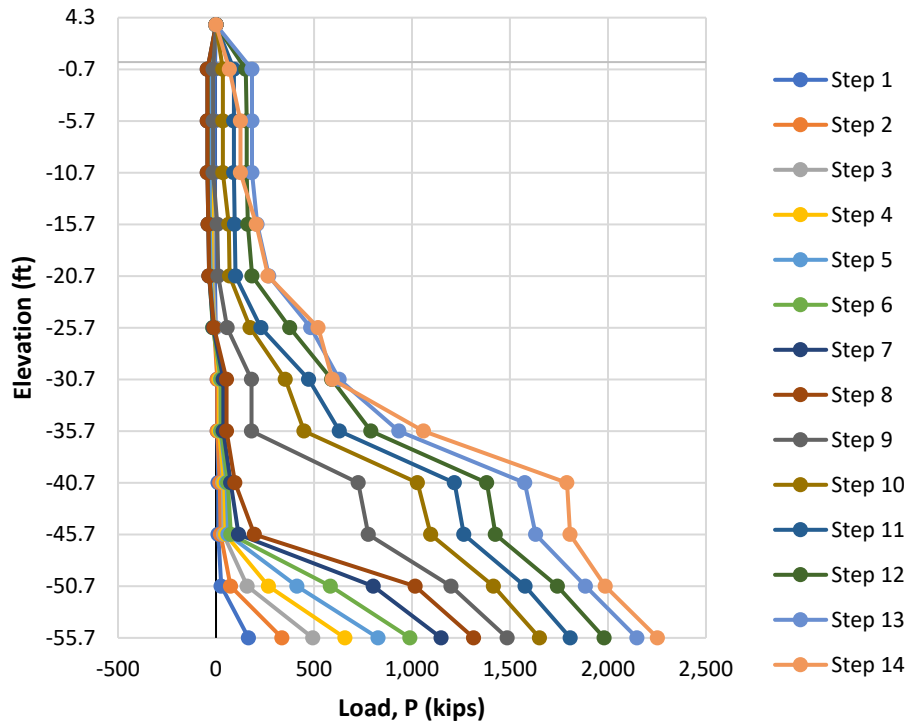


Figure 3-1. Load test strain gauge distribution for SR-836 Test Pile A.

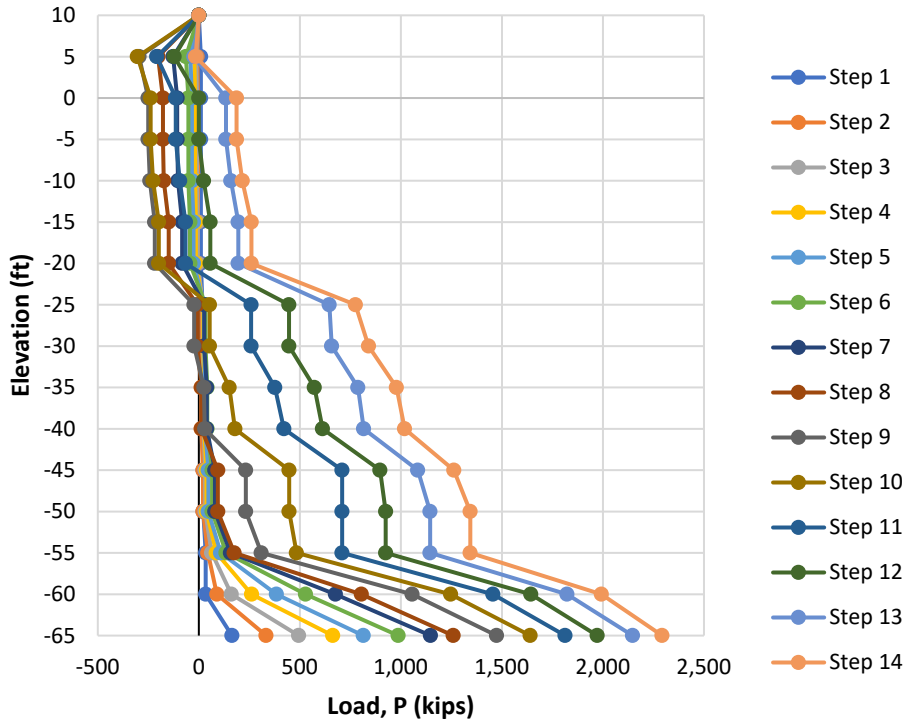


Figure 3-2. Load test strain gauge distribution for I-395 Test Pile B.

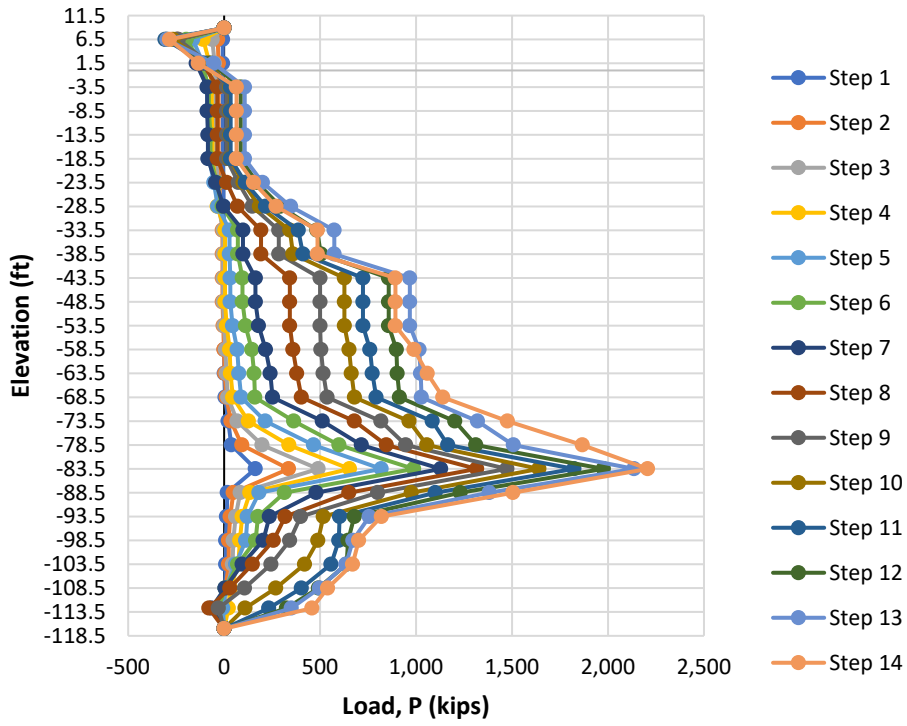


Figure 3-3. Load test strain gauge distribution for I-395 Test Pile C.

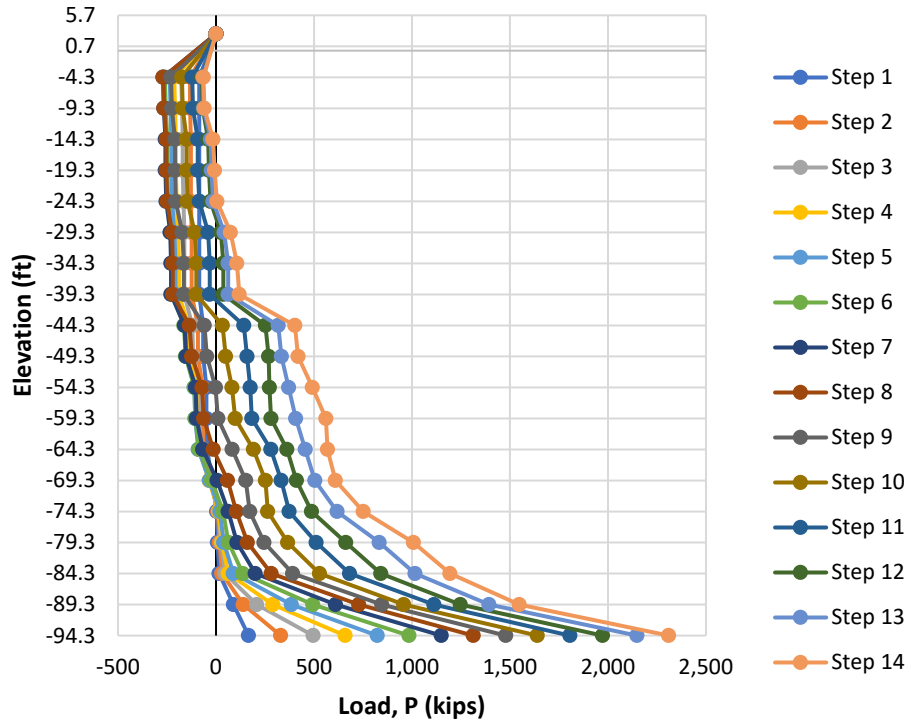


Figure 3-4. Load test strain gauge distribution for Signature Bridge Test Pile D.

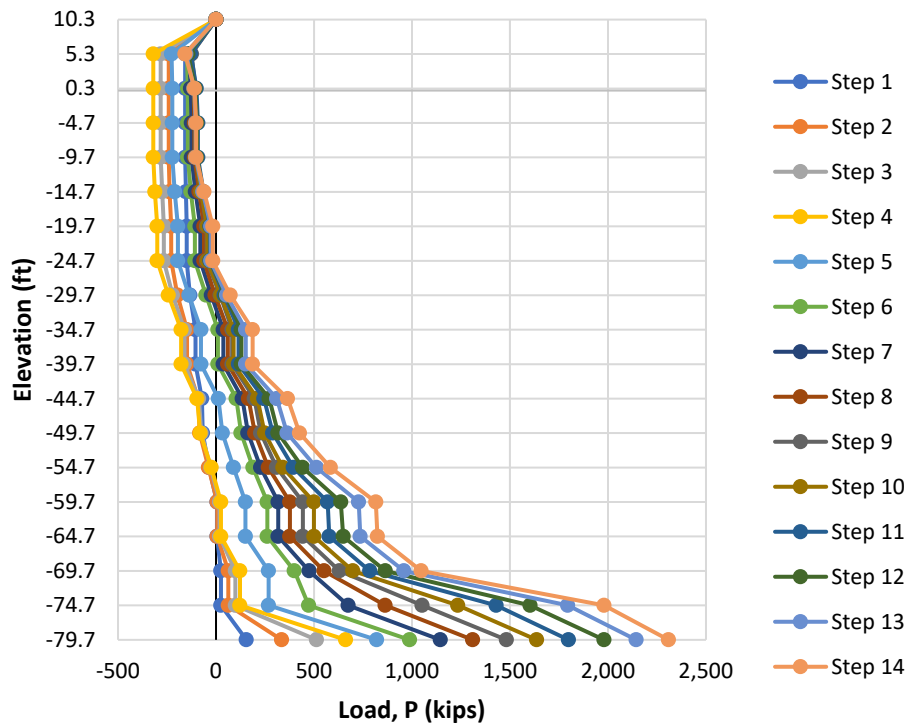


Figure 3-5. Load test strain gauge distribution for I-395 Test Pile E.

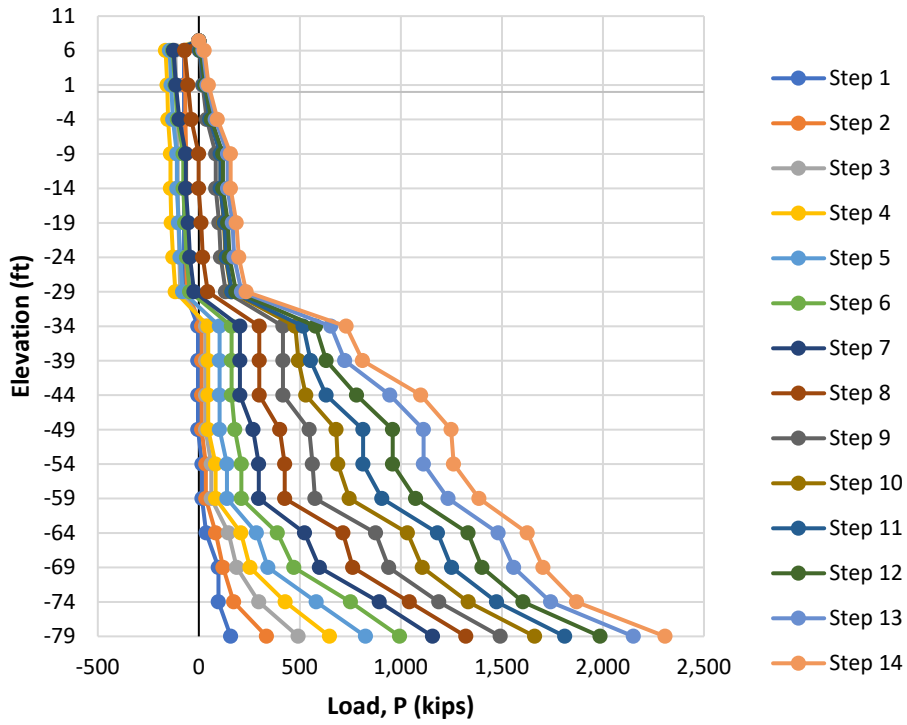


Figure 3-6. Load test strain gauge distribution for I-395 Test Pile F.

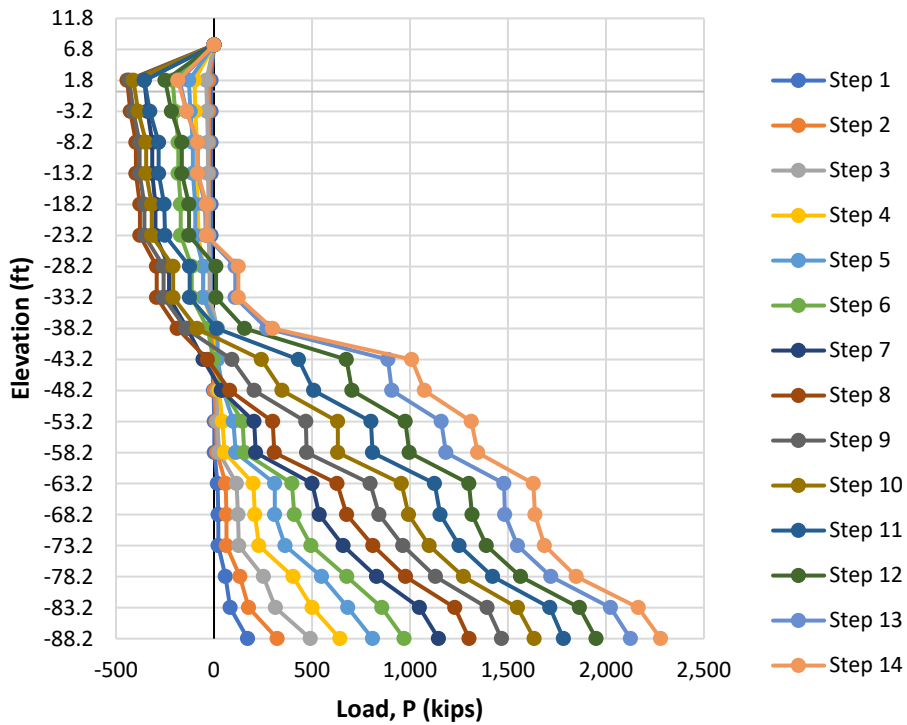


Figure 3-7. Load test strain gauge distribution for Signature Bridge Test Pile G.

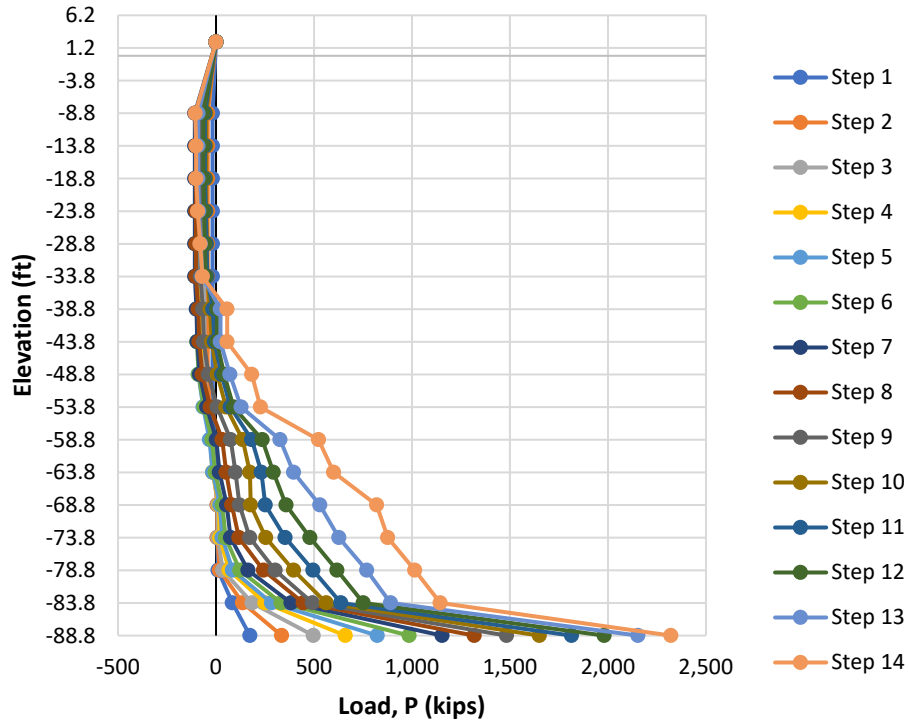


Figure 3-8. Load test strain gauge distribution for Signature Bridge Test Pile H.

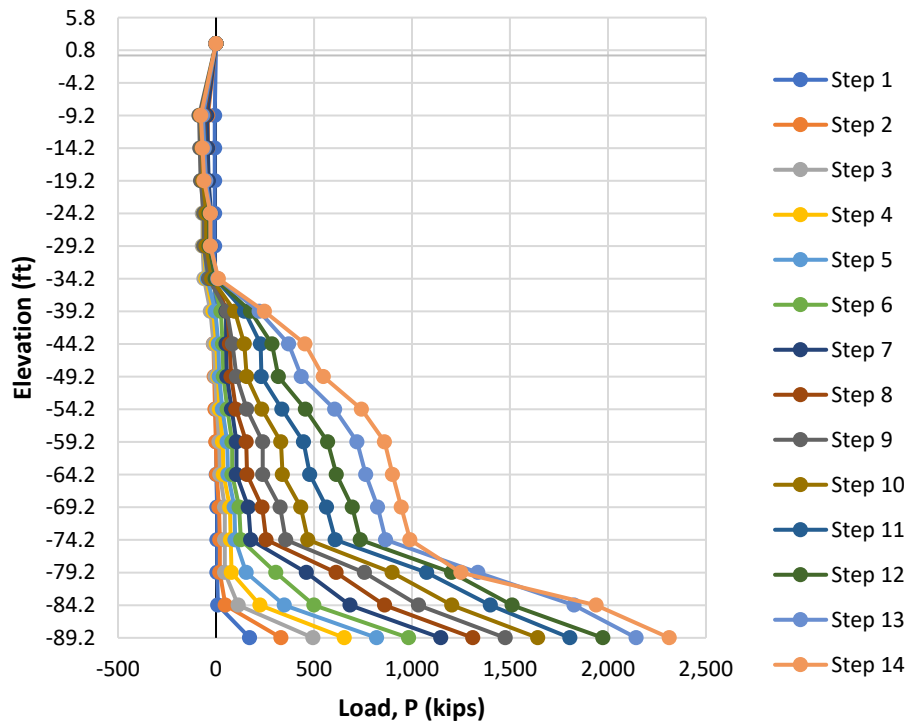


Figure 3-9. Load test strain gauge distribution for Signature Bridge Test Pile I.



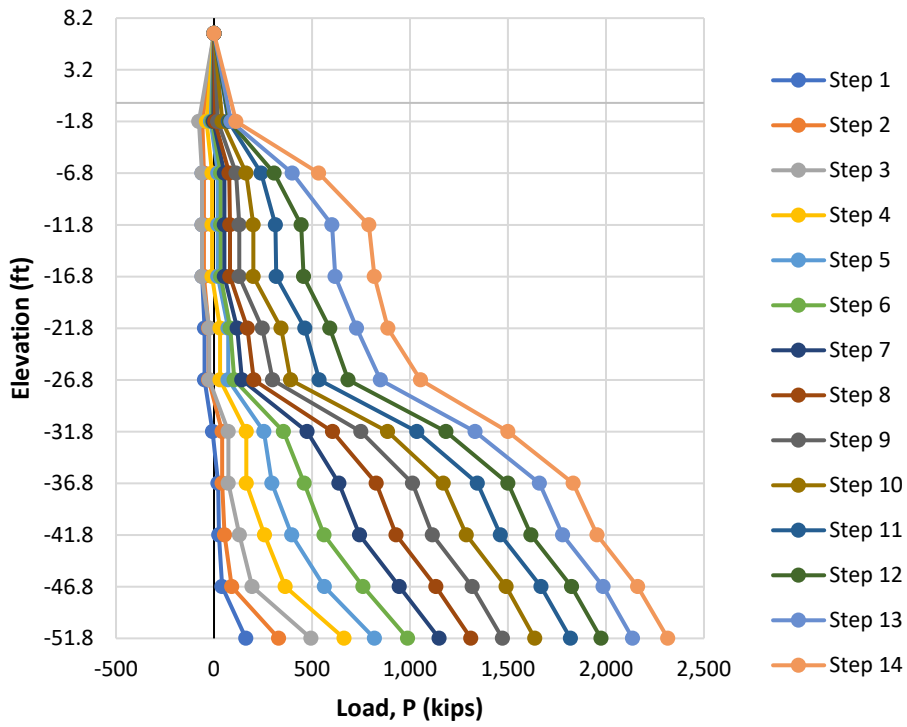


Figure 3-10. Load test strain gauge distribution for SR-836 Test Pile J.

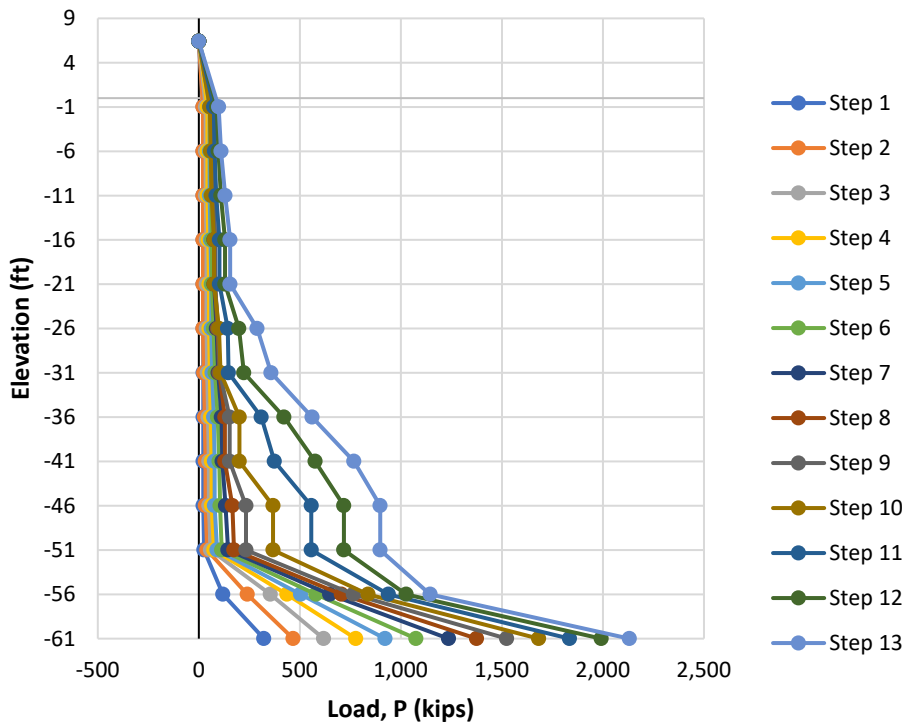


Figure 3-11. Load test strain gauge distribution for SR-836 Test Pile K.

It is possible for curing-induced residual tensile loads and stresses (negative loads and stresses) to be present in a pile; however, the negative loads must be represented in both the side shear values (T-Z curves) and the strain gauge load distribution. The fact that the side shear values reported were all positive for each load step while the strain gauge load distribution produced negative loads indicated discrepancies in the load test data reduction because there must be consistency between the reported side shear values and the strain gauge load distribution.

From each of the load test reports, the load test consultant who analyzed the data stated that high tensile curing strains (loads and stresses) were observed by comparing pre-installation strain gauge readings to those taken before active loading of the pile at the start of testing. This plus the relatively large strain increases observed during loading indicated that the piles may have experienced curing-induced residual loads, as well as tensile micro-fracturing, resulting in highly nonlinear pile rigidity. The UF researchers agreed with the load test consultant's observations. Unfortunately, strain readings were only taken while the instrumented reinforcement cage was lying on the ground and at the start of the test. Consequently, the strain influence from placing the instrumented cage in the grout-filled excavated shaft was not captured by the gauges, and thus, the true curing-induced strains and residual loads could not be accurately quantified. The load test consultant tried to account for the curing-induced residual loads in each SG level by following the method provided in Sinnreich (2012) using the pre-installation strain readings. The analysis produced positive side shear values in individual gauge levels for each load step but neglected that the cumulative load carried within all strain gauge zones must equal the applied load for each load step. Because the cumulative loads generated from adjusting the side shear values using Sinnreich (2012) began to exceed the actual load applied for each load step, negative loads were generated in the strain gauge load distribution. The method of data reduction used by the load test consultant is a viable approach to resolve curing-induced residual stresses; however, without strain measurements taken at the necessary intervals prior to load testing to quantify the true curing-induced stresses data reduction becomes challenging, and the results are questionable. UF researchers have since recommended to FDOT officials that the following procedures should be conducted to better quantify the curing-induced strains for load test data reduction:

In general, strain gauge readings should be taken immediately before (and after) every event of the piling work and not just during the actual load test. Continuous measurements would be the ideal approach. However, continuous measurements may not be feasible, currently. Therefore, readings should be conducted at the following times:

1. After installation of the gauges while the reinforcement cage is laying on the ground (to ensure all gauges are functioning).
2. Just prior to placing the instrumented cage into the ground (to validate the gauges are still working prior to cage placement).
3. **When the cage has been placed into the grouted hole and the gauges have adjusted to the ground or initial grout temperature (within 1 hour).**
4. Immediately before starting the load test.
5. After load test analysis is complete, the reported side shear in each level should be converted to load and compared to the applied load. This will ensure the measured loads within the pile do not exceed the applied load. This should be done for each load step.

6. Strain gauge data that was used to generate T-Z curves should be multiplied by segment length to obtain segment deformations that are then summed over the full pile length and compared with pile top movement, LTA movement, and tell-tale movement. The error should be within 10%.

\*Multiple readings in between Steps 3 and 4 would be ideal in an attempt to capture the thermal effects. This should be front-loaded to capture the transitional phase of the grout heating up to cooling off. In this case, readings should be taken every 12 to 24 hours over the first three days.

When curing induced tensile strains and residual loads are present within a pile and the strain gauges are simply “zeroed” prior to testing, which is common practice and was the case for all load tests included in this report, gauges within the shaft exposed to tensile stresses will exhibit higher than normal strain measurements compared to the loads applied. For example, Figure 3-12 presents continuous strain measurements recorded at each gauge level during the curing of an instrumented drilled shaft unrelated to this project.

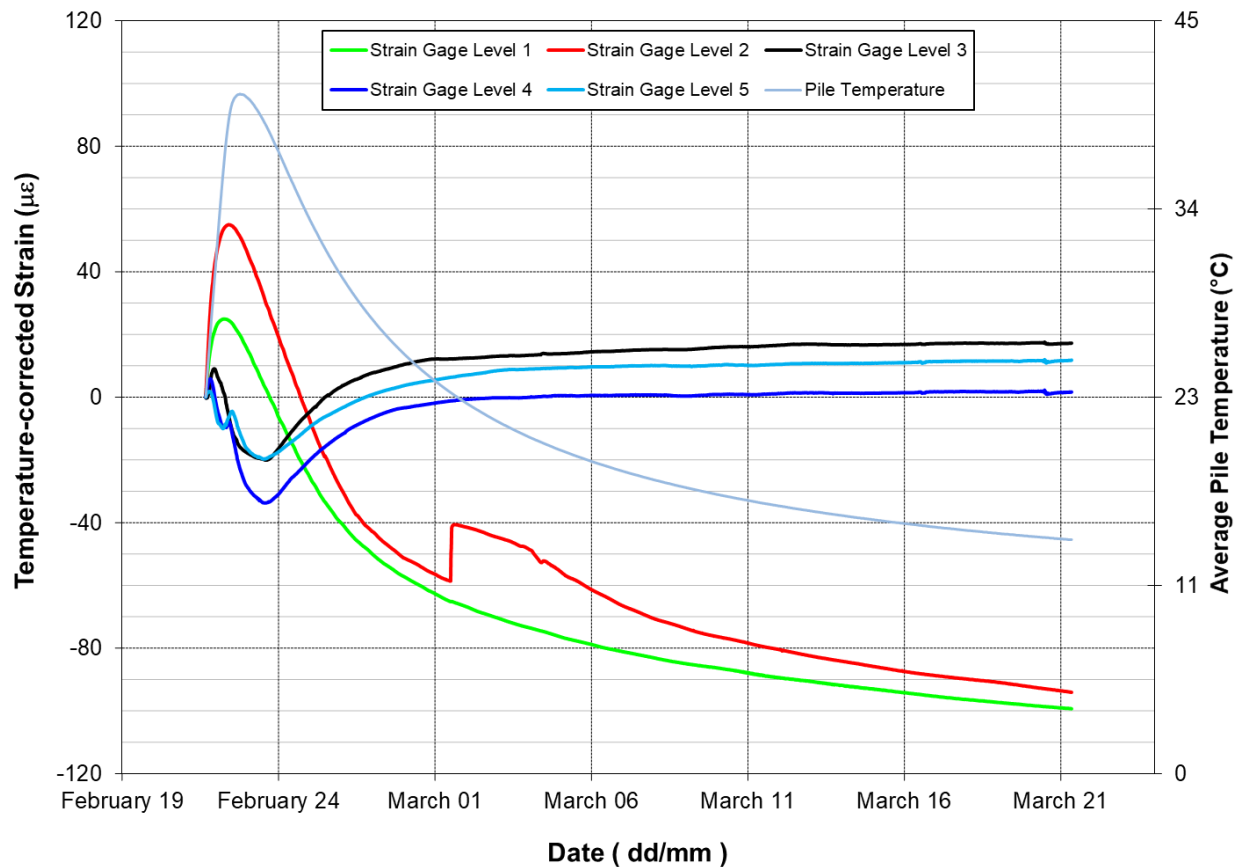


Figure 3-12. Continuous strain measurements during the curing of an instrumented drilled shaft (Sinnreich, 2012).

As observed in Figure 3-12, the curing process induced -100 µε of residual strain at Strain Gauge Level 1. Figure 3-13 presents a theoretical load path at SG Level 1 for the drilled shaft in Figure

3-12 used for demonstration where strain is plotted versus displacement. Figure 3-13 provides the load path of the shaft for compressive and tensile loading. The curing process of the drilled shaft induced  $-100 \mu\epsilon$  which indicates the shaft segment is in a state of tension prior to compressive loading (i.e., the start of a load test). Therefore, the compressive loading must first overcome the residual tensile stresses ( $-100 \mu\epsilon$ ) before being fully mobilized in compression which corresponds to  $500 \mu\epsilon$  in the theoretical load path. However, if the strain at SG Level 1 was zeroed prior to the start of the load test, as is common practice, the fully mobilized load would indicate higher shaft resistance and mobilize at  $600 \mu\epsilon$ . This is because zeroing the gauges prior to the start of a load test does not eliminate the tensile state of the pile segment, it simply neglects it which leads to inaccurate loads generated from the strain data.

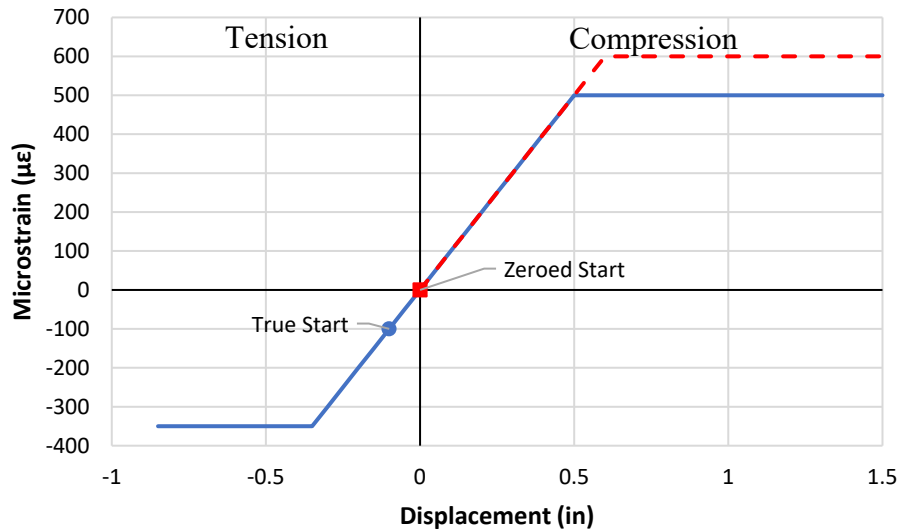


Figure 3-13. Theoretical load path for SG 1 from Figure 3-12.

This can be observed in the strain data collected during the actual load tests. Figure 3-14 presents the strain vs. load curves for Strain Gauge Levels 6 through 19 (upper portion of the pile) for I-395 Test Pile B. Observed in Figure 3-14, multiple strain gauge (SG) levels exceed the measured strains in SG levels closer to the load test assembly (LTA; i.e., load cell). This is easily observed where SG levels 7 and 9 both exceed the measured strain in SG level 6. Table 3-1 further quantifies the highly irregular strain activity by displaying the level of strain measured in each SG level in descending order of maximum strain. As observed in Table 3-1, multiple SG levels exceed the strain measured in SG levels closer to the LTA. This indicates that multiple SG levels were in a state of tension (curing induced residual load) prior to compressive loading in which the negative strain values were zeroed prior to the start of the test. When these curing induced strains and residual loads are present and not quantified by taking measurements at the necessary intervals prior to the load test, and the negative strain values are zeroed prior to compressive loading, many of the gauge readings provide false measurements that can lead to inaccurate estimates of unit side shear, T-Z curves, and loads measured within each SG zone (layering). This was the case for each of the load tests. Consequently, the SG levels that experienced curing induced tensile loads/stresses were removed from the load test reduction, and only the stable

gauge readings were used which required analyzing the load tests in larger layers in order to obtain accurate skin friction layering.

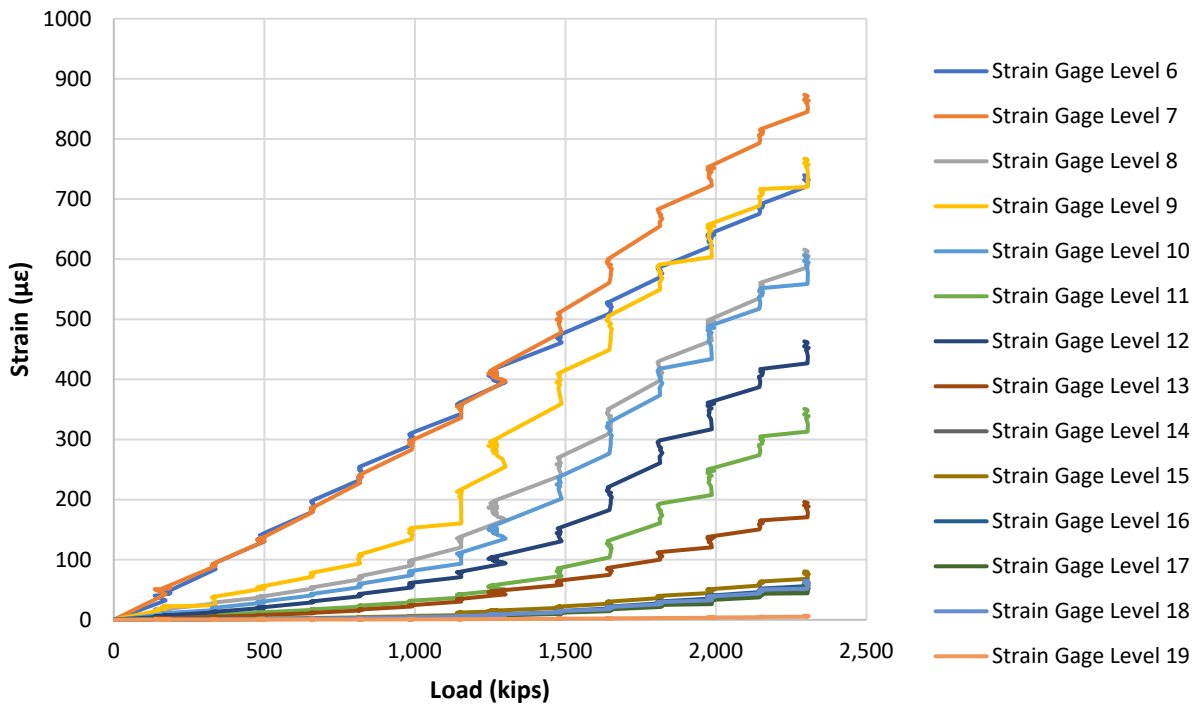


Figure 3-14. Strain vs. load for I-395 Test Pile B.

Table 3-1. Summary of strain vs. load for I-395 Test Pile B in descending order of maximum strain.

Strain Gauge Level	Maximum Strain (µε)
7	873.6
9	767.0
6	739.8
8	615.8
10	606.3
12	463.2
11	350.9
13	196.0
15	80.5
18	65.6
16	65.0
14	60.9
17	55.9
19	6.6

### 3.2 Developing Correlation

#### 3.2.1 SR-836 Test Pile A

MWD was conducted in the footprint of SR-836 Test Pile A using drill rig B in which the upper pile segment was fully mobilized and reached a final top of pile displacement of 1.87 inches with a maximum applied load of 2,253 kips. Figure 3-15 presents the MWD specific energy profile vs. depth as well as the SPT profile over the full pile length.

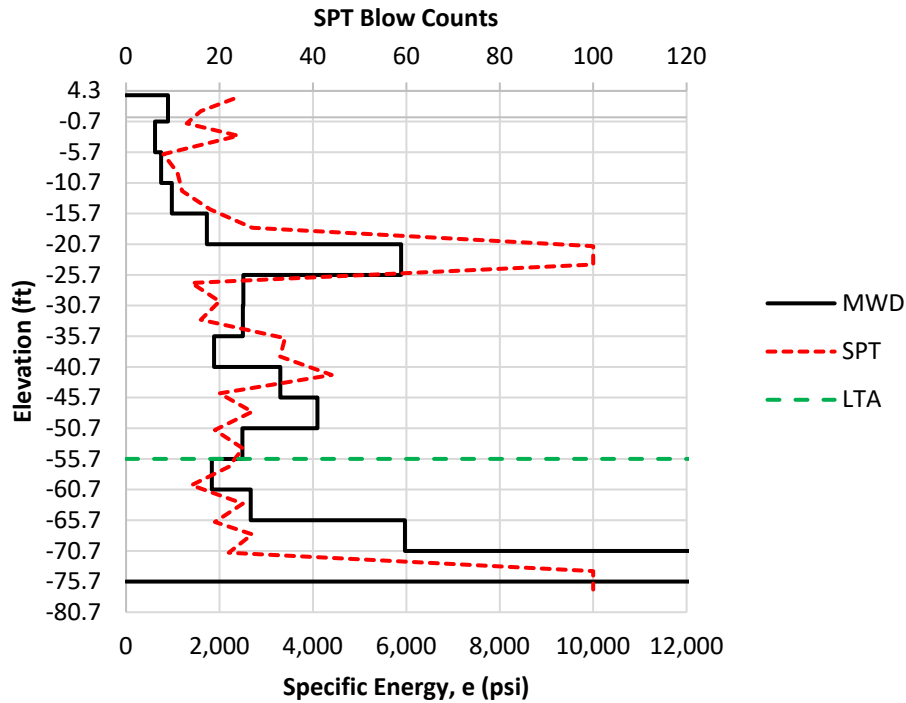


Figure 3-15. MWD specific energy and SPT profiles vs. depth.

From Figure 3-15, it is clear that the MWD and SPT profiles show similar layering throughout the full pile length. Figure 3-16 compares the unit side shear profile from the load test report to the SPT profile for the upper portion (above LTA) of the pile.

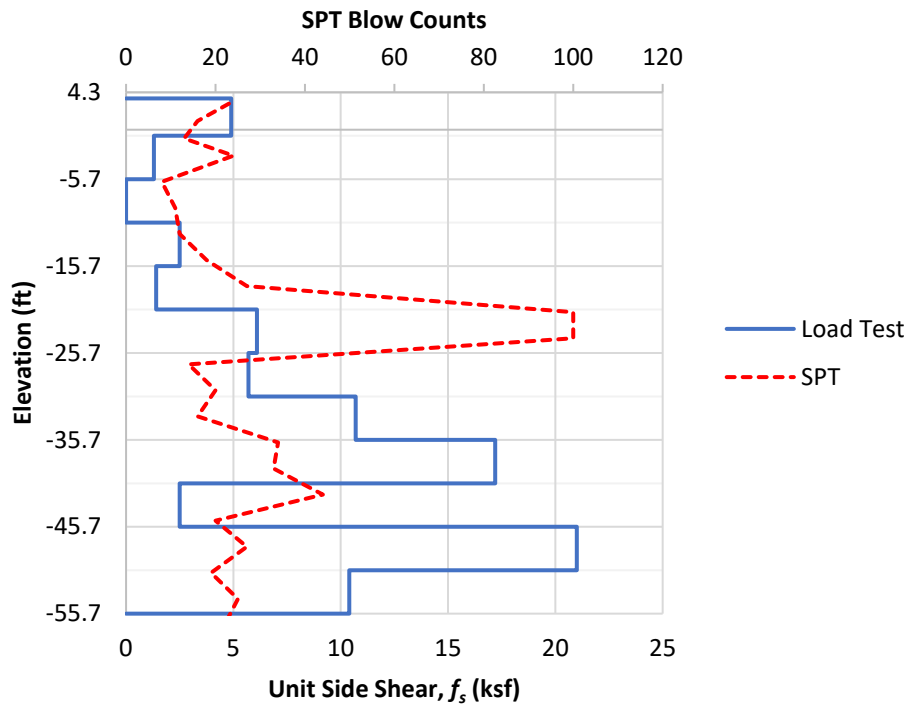


Figure 3-16. Reported load test side shear profile compared to the SPT profile.

Figure 3-16 indicates dissimilar layering between the load test (LT) side shear and the SPT profile. This further suggests the load test layer analysis was inaccurate due to the residual strain activity. Consequently, the load test was reanalyzed using larger layers in which the SG measurements used were identified as stable and a standard method of analysis was used (Note: the load test reports included an excel file with all of the raw load test data which allowed the test to be reanalyzed). Figure 3-17 presents the new strain gauge load distribution using larger layers and Figure 3-18 presents the respective T-Z curves.

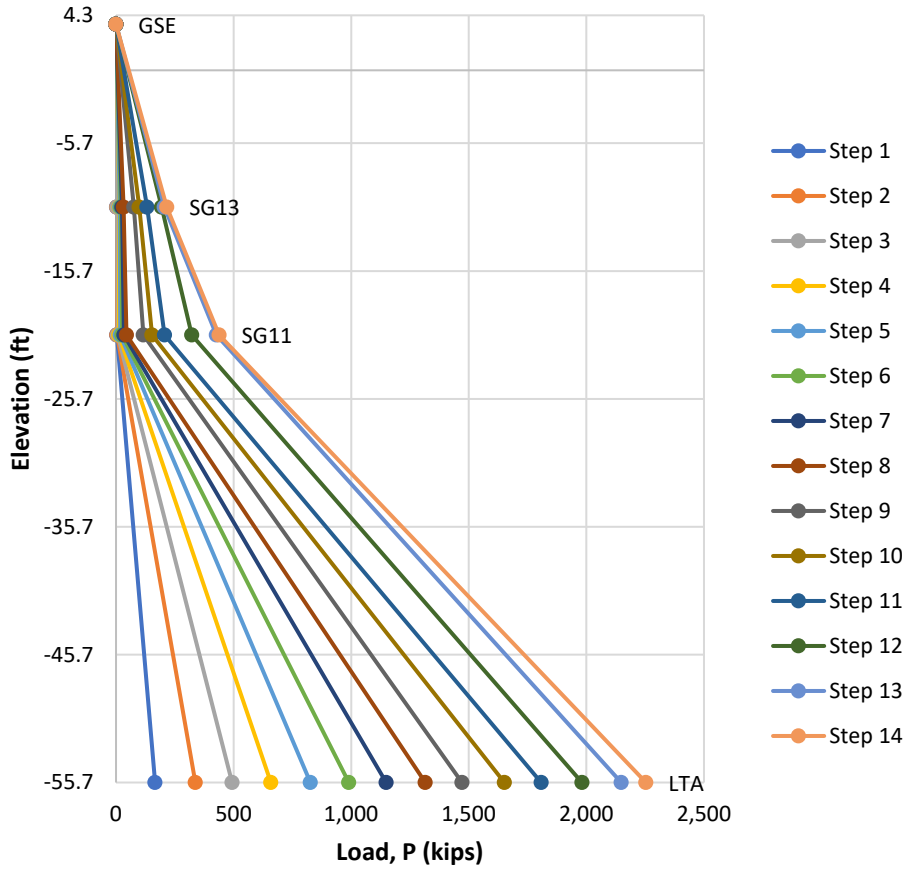


Figure 3-17. UF strain gauge load distribution for SR-836 Test Pile A.

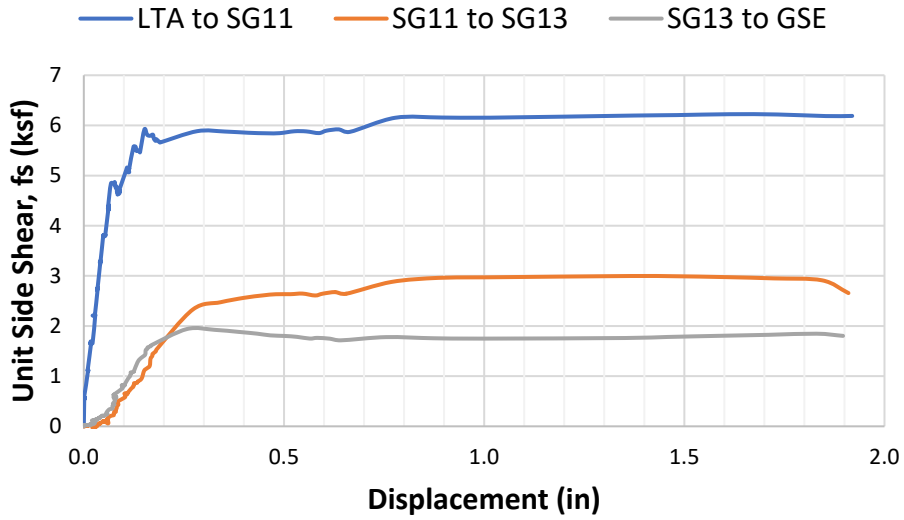


Figure 3-18. UF T-Z curves for SR-836 Test Pile A.



With the load test now reanalyzed using larger layers, correlation between MWD specific energy ( $e$ ) and load test mobilized unit side shear can be developed for the SR-836 site. For ACIP pile segments LTA to SG11, SG11 to SG13, and SG13 to ground surface elevation (GSE), the mobilized unit shear recorded over each respective segment was 5.92 ksf, 2.68 ksf, and 1.94 ksf. The unit side shear was then plotted as a function of the average specific energy recorded within each respective SG zone and compared to the previous correlation developed for drilled shaft rock augers (McVay and Rodgers, 2016 and 2020), Figure 3-19. Observed in Figure 3-19, the data points for SR-836 TP-B appear to follow the same trend as the drilled shaft rock auger correlation. Researchers projected the correlations could be similar as the rock augers used for ACIP pile excavations are fairly similar in geometry to the rock augers used for drilled shafts. However, this was simply a local correlation at the SR-836 site with only three data points spread over a small range of mobilized unit side shear. Therefore, further investigation was warranted prior to confirming ACIP pile rock augers share the same or similar correlation as drilled shaft rock augers.

Note: The regression curve and  $R^2$  value indicated in the black box of Figure 3-19 only consider the drilled shaft rock auger data points. The regression curve and  $R^2$  value indicated in the red box consider the data points from the drilled shaft and ACIP pile rock augers. The regression curves and  $R^2$  values are nearly identical for both correlations.

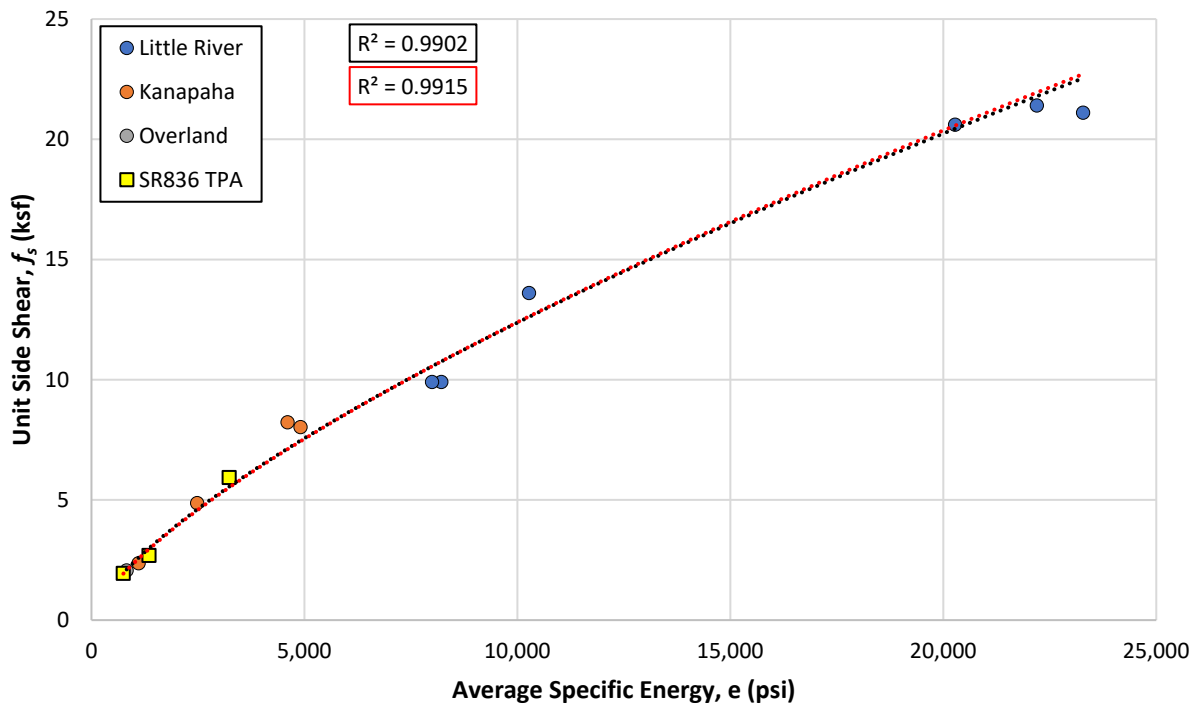


Figure 3-19. Load test unit side shear vs. MWD specific energy for ACIP piles monitored at SR-836 compared to the previously developed drilled shaft rock auger correlation.

### 3.2.2 I-395 Test Pile C

The only other test pile apart from SR-836 TP-A to achieve full mobilization was I-395 Test Pile C. During the load test of I-395 TP-C the upper pile segment was fully mobilized and reached a final top of pile displacement of 2.44 inches and the lower pile segment was fully mobilized and reached a final pile tip displacement of 2.20 inches. The maximum applied load from the LTA was 2,261 kips. Unfortunately, MWD was not conducted in the footprint of I-395 TP-C. Therefore, an alternative method of building correlation had to be developed using MWD data collected in adjacent pile groups, closest to the test pile.

#### 1.1.1.1 Developing an Alternative Method of Building Correlation

During the load test of I-395 TP-B, full mobilization was not achieved in the upper or lower segments. However, MWD was conducted in the footprint of the test pile and in an adjacent pile group in which the same drill rig (B) was used. This provided insight into the expected variability between a test pile and the closest adjacent pile group. Pile Group B comprised 16 piles and was the closest pile group to I-395 TP-B (50 ft to 80 ft in distance). Figure 3-20 indicates the variability of the pile group by plotting the depth profile of average specific energy recorded for each of the Group B piles, as well as the specific energy profile of TP-B. The layering used for averaging was based on the layering of the TP-B load test (i.e., SG zones for TP-B). Figure 3-21 provides the specific energy depth profile for the minimum, mean, median, and maximum average values recorded from Group B, the TP-B specific energy profile, and the SPT profile.

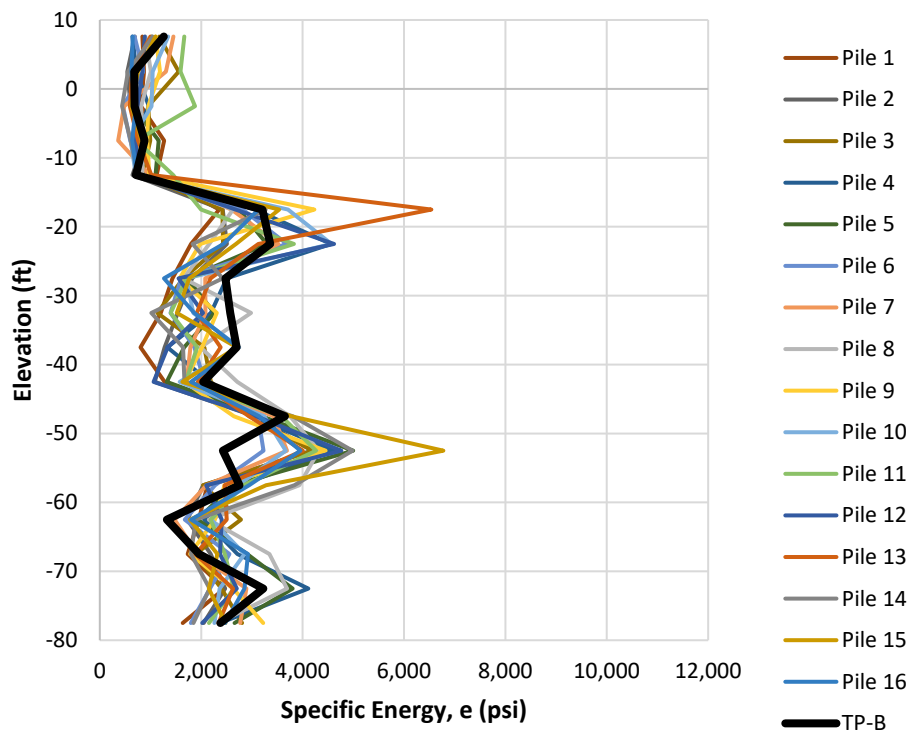


Figure 3-20. Pile Group B and TP-B specific energy profiles.

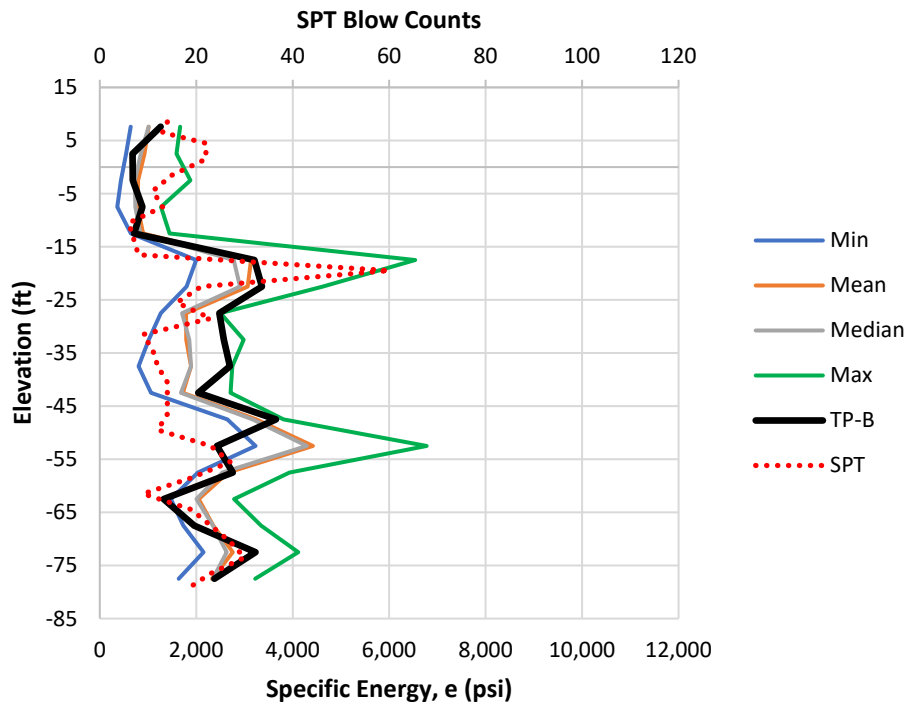


Figure 3-21. Pile Group B minimum, mean, median, and maximum specific energy, TP-B specific energy, and TP-B SPT profiles.

From Figure 3-21, it is observed that the SPT profile and specific energy profile for TP-B and Pile Group B are in general agreement and indicate similar layering. Also of interest is that the specific energy profile from TP-B generally fell within the minimum and maximum values recorded from Pile Group B but did not always follow the mean or median values. Moreover, a similar specific energy profile can be developed using the minimum, mean, median, and maximum specific energy values obtained from the Pile Group B pile segments that is nearly identical to the actual specific energy profile that was recorded in the footprint of TP-B. Table 3-2 provides the tabular data from Pile Group B which includes the minimum, mean, median, and maximum average specific energy recorded within each layer, the average specific energy recorded in each layer for TP-B, and the similar specific energy profile (Combo) that can be generated within each layer using the Pile Group B data. The percent error between the TP-B specific energy profile and the Pile Group B combined specific energy profile is 2% on average with the maximum percent error for any layer being 33%. As indicated in Figure 3-19, specific energy increases at a decreasing rate as unit side shear increases. Therefore, when specific energy is transformed into unit side shear using the rock auger equation (black box), the percent error for any layer is reduced to 22% as indicated in Table 3-3. Also from Table 3-3, in all but three layers, the percent error in side shear estimation from Pile Group B is 11% or less. Furthermore, the average error remains at 2% with a maximum error in side shear estimation from Pile Group B equal to 1 ksf, which is acceptable error.

Table 3-2. Pile Group B minimum, mean, median, and maximum specific energy, combined specific energy, TP-B specific energy, and percent error.

I-395 TPB SG Zones	SG Zone Elevations			Average Specific Energy, $e$ (psi)					Percent Error	
	$El_{top}$ (ft)	$El_{bot}$ (ft)	$El_{mid}$ (ft)	Min	Mean	Median	Max	Combo		TP-B
20	10.2	5	7.6	642	1,013	1,012	1,666	1,013	1,262	-20%
19	5	0	2.5	544	926	849	1,591	544	679	-20%
18	0	-5	-2.5	440	794	726	1,878	726	685	6%
17	-5	-10	-7.5	362	787	737	1,269	787	884	-11%
16	-10	-15	-12.5	645	895	839	1,447	645	711	-9%
15	-15	-20	-17.5	1,999	3,134	2,779	6,540	3,134	3,207	-2%
14	-20	-25	-22.5	1,799	3,066	2,907	4,620	3,066	3,362	-9%
13	-25	-30	-27.5	1,265	1,790	1,706	2,502	2,502	2,478	1%
12	-30	-35	-32.5	1,016	1,793	1,853	2,984	2,984	2,572	16%
11	-35	-40	-37.5	803	1,891	1,893	2,749	2,749	2,699	2%
10	-40	-45	-42.5	1,061	1,723	1,684	2,712	1,723	2,041	-16%
9	-45	-50	-47.5	2,645	3,246	3,169	3,808	3,808	3,652	4%
8	-50	-55	-52.5	3,229	4,419	4,292	6,777	3,229	2,429	33%
7	-55	-60	-57.5	2,036	2,660	2,542	3,935	2,660	2,756	-4%
6	-60	-65	-62.5	1,473	2,049	2,005	2,785	1,473	1,324	11%
5	-65	-70	-67.5	1,732	2,353	2,345	3,346	1,732	1,958	-12%
4	-70	-75	-72.5	2,149	2,759	2,630	4,113	2,759	3,227	-15%
3	-75	-80	-77.5	1,637	2,327	2,343	3,223	2,343	2,376	-1%
Average Error =									-2%	

Table 3-3. Pile Group B combined profile versus TP-B side shear.

I-395 TPB SG Zones	SG Zone Elevations			Unit Side Shear, $f_s$ (ksf)			Percent Error
	$El_{top}$ (ft)	$El_{bot}$ (ft)	$El_{mid}$ (ft)	TP-B	Combo	$\Delta f_s$ (ksf)	
20	10.2	5	7.6	2.85	2.43	-0.41	-14%
19	5	0	2.5	1.83	1.57	-0.27	-15%
18	0	-5	-2.5	1.85	1.92	0.08	4%
17	-5	-10	-7.5	2.21	2.04	-0.17	-8%
16	-10	-15	-12.5	1.89	1.77	-0.13	-7%
15	-15	-20	-17.5	5.52	5.43	-0.09	-2%
14	-20	-25	-22.5	5.71	5.34	-0.36	-6%
13	-25	-30	-27.5	4.60	4.63	0.03	1%
12	-30	-35	-32.5	4.72	5.24	0.52	11%
11	-35	-40	-37.5	4.88	4.95	0.06	1%
10	-40	-45	-42.5	4.00	3.55	-0.45	-11%
9	-45	-50	-47.5	6.05	6.23	0.18	3%
8	-50	-55	-52.5	4.53	5.55	1.01	22%
7	-55	-60	-57.5	4.96	4.83	-0.12	-2%
6	-60	-65	-62.5	2.94	3.18	0.23	8%
5	-65	-70	-67.5	3.89	3.56	-0.32	-8%
4	-70	-75	-72.5	5.54	4.96	-0.58	-11%
3	-75	-80	-77.5	4.46	4.42	-0.04	-1%
Average Error =							-2%

Figure 3-22 provides the specific energy profile from TP-B compared to the profile developed from Pile Group B and the SPT profile. All three profiles indicate similar layering, and the two specific energy profiles are nearly identical. Therefore, this same approach was taken for I-395

TP-C in order to develop local correlation between specific energy and unit side shear at the I-395 site.

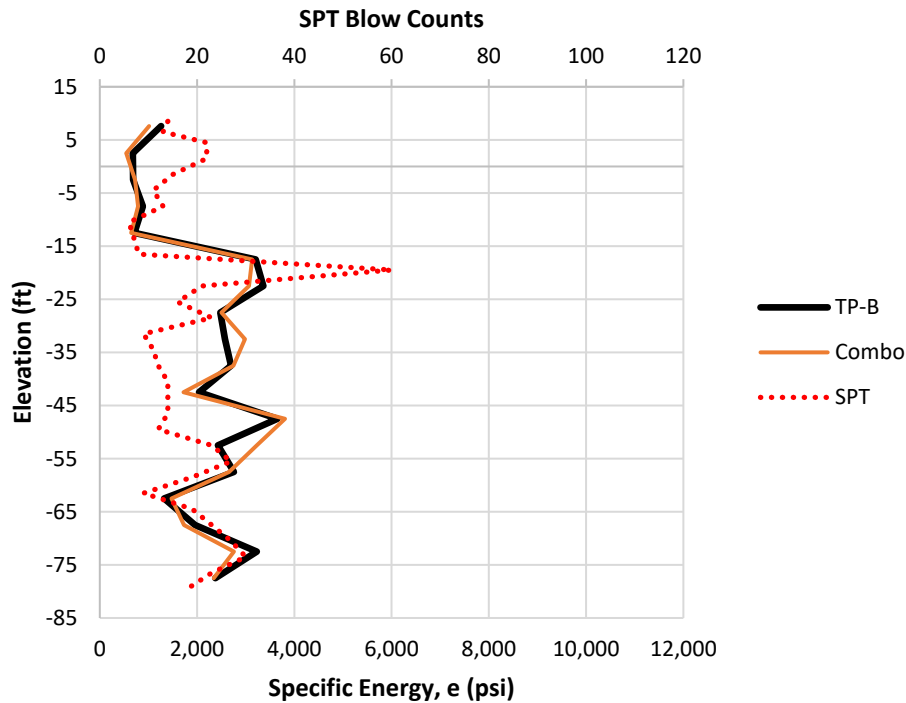


Figure 3-22. Pile Group B combined profile compared to the TP-B MWD and SPT profiles.

### 3.2.3 I-395 Test Pile C Analysis

As discussed, MWD was not completed in the footprint of I-395 Test Pile C and therefore, MWD collected in the closest adjacent pile groups (Pile Group C-1 and Pile Group C-2) were used to build correlation between MWD specific energy and load test mobilized unit side shear at the I-395 site. Table 3-4 provides the tabular results of average specific energy collected within each TP-C SG zone for all 10 piles that support Pile Group C-1. Table 3-4 provides the tabular results of average specific energy collected within each TP-C SG zone for all eight piles that support Pile Group C-2. Pile Group C-1 was located 44 ft north and 39 ft west of TP-C and Pile Group C-2 was located 54 ft south and 62 ft west of TP-C. These distances were measured to the center of each pile group with the furthest pile located 92 ft away at Pile Group C-2.

Figure 3-23 provides the specific energy depth profiles for each of the piles at Group C1 and Group C2. Figure 3-24 provides the specific energy depth profile for the minimum, mean, median, and maximum average values recorded from Group C1 and Group C2. Figures 3-23 and 3-24 show that variability exists within each pile group and between the two pile group locations. However, the figures also show that a correlated structure exists as all specific energy profiles generally show the same trends in layering as well as mean and median values with depth.

Table 3-4. Group C1 specific energy data.

I-395 TPC SG Zones	SG Zone Elevations			Group C1 - Average Specific Energy, e (psi)									
	El <sub>top</sub> (ft)	El <sub>bot</sub> (ft)	El <sub>mid</sub> (ft)	Pile 1	Pile 2	Pile 3	Pile 4	Pile 5	Pile 6	Pile 7	Pile 8	Pile 9	Pile 10
25	8.9	6.5	7.7	3,067	2,098	2,095	2,285	5,527	1,880	2,231	2,015	2,559	2,020
24	6.5	1.5	4	2,501	1,734	1,762	2,157	3,327	2,252	1,994	2,192	2,135	1,775
23	1.5	-3.5	-1	1,349	966	838	1,012	987	1,219	1,139	1,208	1,152	885
22	-3.5	-8.5	-6	577	711	627	664	830	793	1,054	677	752	496
21	-8.5	-13.5	-11	782	810	781	844	873	890	1,159	792	859	642
20	-13.5	-18.5	-16	1,050	992	960	1,097	993	1,018	1,276	949	932	846
19	-18.5	-23.5	-21	1,420	1,191	1,184	1,827	1,024	1,162	1,409	1,246	1,064	863
18	-23.5	-28.5	-26	3,473	2,714	7,368	2,490	3,547	2,016	3,071	2,526	1,662	1,337
17	-28.5	-33.5	-31	6,323	7,877	9,382	7,539	3,879	11,652	3,759	4,236	5,863	6,481
16	-33.5	-38.5	-36	3,350	3,631	5,952	5,632	3,736	4,994	4,169	4,295	8,739	7,135
15	-38.5	-43.5	-41	1,846	1,938	1,760	1,924	1,582	2,637	1,843	1,401	1,659	1,623
14	-43.5	-48.5	-46	4,424	1,416	1,013	1,608	1,240	1,682	1,538	1,019	1,332	1,295
13	-48.5	-53.5	-51	1,731	1,249	979	1,411	1,446	1,457	1,229	1,431	1,046	1,267
12	-53.5	-58.5	-56	1,562	1,538	1,732	1,431	1,356	1,333	1,527	1,350	1,111	1,163
11	-58.5	-63.5	-61	1,336	1,609	1,550	1,696	1,694	1,331	2,122	1,507	1,727	2,684
10	-63.5	-68.5	-66	1,654	2,914	1,771	1,643	1,749	1,549	1,569	1,541	2,021	2,385
9	-68.5	-73.5	-71	2,119	4,180	3,468	1,935	1,743	1,639	1,802	2,269	4,177	1,781
8	-73.5	-78.5	-76	2,503	2,204	2,836	1,608	1,519	1,312	1,643	1,259	2,187	1,578
7	-78.5	-83.5	-81	2,689	2,320	3,097	1,808	2,291	3,267	5,696	2,879	3,994	3,959
6	-83.5	-88.5	-86	8,727	2,708	3,130	5,537	5,857	5,686	3,711	6,265	4,398	6,163
5	-88.5	-93.5	-91	2,266	2,147	1,668	3,803	1,886	2,752	2,223	2,645	2,901	2,310
4	-93.5	-98.5	-96	1,890	2,310	1,858	3,143	1,424	2,410	2,245	1,942	1,946	1,955
3	-98.5	-103.5	-101	2,472	1,950	2,446	3,898	2,178	1,852	2,331	2,460	1,856	1,676
2	-103.5	-108.5	-106	6,998	5,267	6,572	14,596	4,781	4,850	5,387	4,615	7,213	3,509
1	-108.5	-112.7	-110.6	16,727	8,622	8,394	8,798	4,893	12,832	7,461	6,966	10,046	6,546

Table 3-5. Group C2 specific energy data.

I-395 TPC SG Zones	SG Zone Elevations			Group C2 - Average Specific Energy, e (psi)							
	El <sub>top</sub> (ft)	El <sub>bot</sub> (ft)	El <sub>mid</sub> (ft)	Pile 1	Pile 2	Pile 3	Pile 4	Pile 5	Pile 6	Pile 7	Pile 8
25	8.9	6.5	7.7	1,419	288	2,152	1,575	1,713	1,958	2,178	1,508
24	6.5	1.5	4	1,510	277	2,087	1,593	1,484	3,498	1,846	1,443
23	1.5	-3.5	-1	1,313	458	1,265	1,197	1,025	962	1,135	801
22	-3.5	-8.5	-6	853	737	941	694	926	704	1,071	550
21	-8.5	-13.5	-11	1,348	851	1,301	817	1,068	711	1,240	1,081
20	-13.5	-18.5	-16	871	909	1,903	897	1,157	841	1,997	1,113
19	-18.5	-23.5	-21	848	802	3,469	1,089	1,374	841	1,358	1,680
18	-23.5	-28.5	-26	4,826	2,871	6,329	2,724	2,893	1,520	2,415	3,517
17	-28.5	-33.5	-31	6,577	3,942	3,899	1,968	4,412	3,646	7,445	3,003
16	-33.5	-38.5	-36	6,226	7,428	7,492	7,752	8,794	7,158	8,104	5,657
15	-38.5	-43.5	-41	1,649	1,955	2,292	2,050	3,737	1,753	2,380	1,619
14	-43.5	-48.5	-46	1,960	1,410	1,663	1,870	1,788	1,718	2,190	1,206
13	-48.5	-53.5	-51	1,706	1,305	2,093	1,626	2,451	1,824	1,377	870
12	-53.5	-58.5	-56	1,676	1,623	2,059	2,483	1,929	1,490	1,339	1,320
11	-58.5	-63.5	-61	2,867	1,352	1,766	2,399	1,829	1,432	1,627	1,234
10	-63.5	-68.5	-66	2,072	1,343	1,627	1,470	5,685	1,262	1,717	1,428
9	-68.5	-73.5	-71	2,646	2,038	2,061	2,211	4,394	1,653	2,481	2,904
8	-73.5	-78.5	-76	1,939	1,454	1,498	1,894	2,377	1,308	1,993	1,871
7	-78.5	-83.5	-81	4,285	3,319	1,842	4,202	3,851	4,698	2,681	3,260
6	-83.5	-88.5	-86	5,660	2,760	3,859	4,335	6,394	5,157	4,289	6,167
5	-88.5	-93.5	-91	1,771	1,404	1,975	2,233	3,774	2,188	2,567	7,201
4	-93.5	-98.5	-96	1,868	1,575	2,297	1,906	4,847	1,506	2,759	4,456
3	-98.5	-103.5	-101	2,225	2,077	4,302	2,260	3,703	2,927	3,105	5,104
2	-103.5	-108.5	-106	N/A	N/A	N/A	N/A	N/A	N/A	N/A	N/A
1	-108.5	-112.7	-110.6	N/A	N/A	N/A	N/A	N/A	N/A	N/A	N/A

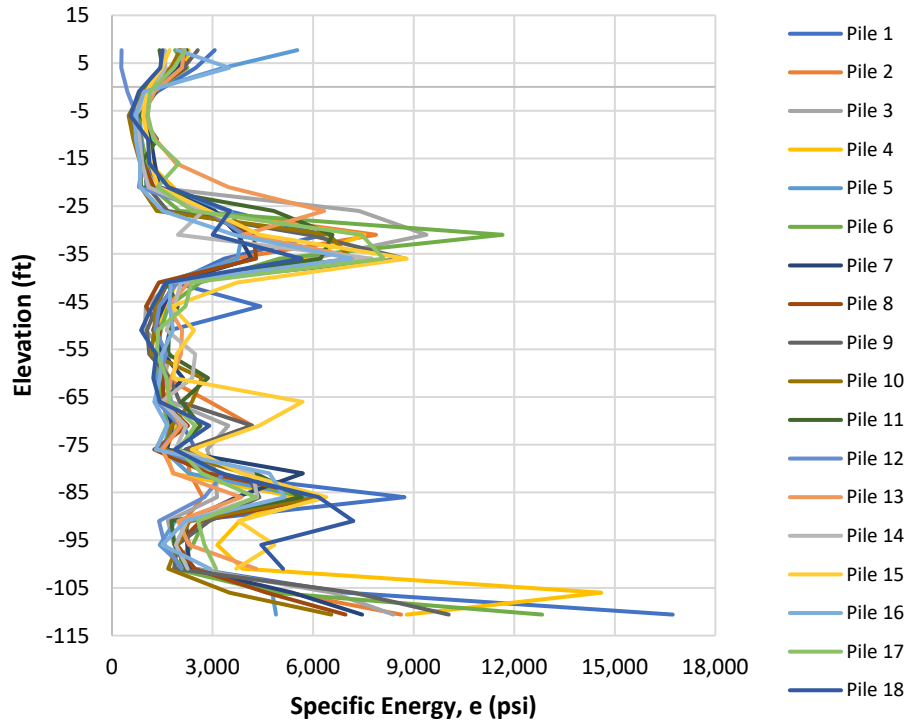


Figure 3-23. Group C1 (Piles 1-10) and Group C2 (Piles 11-18) specific energy profiles.

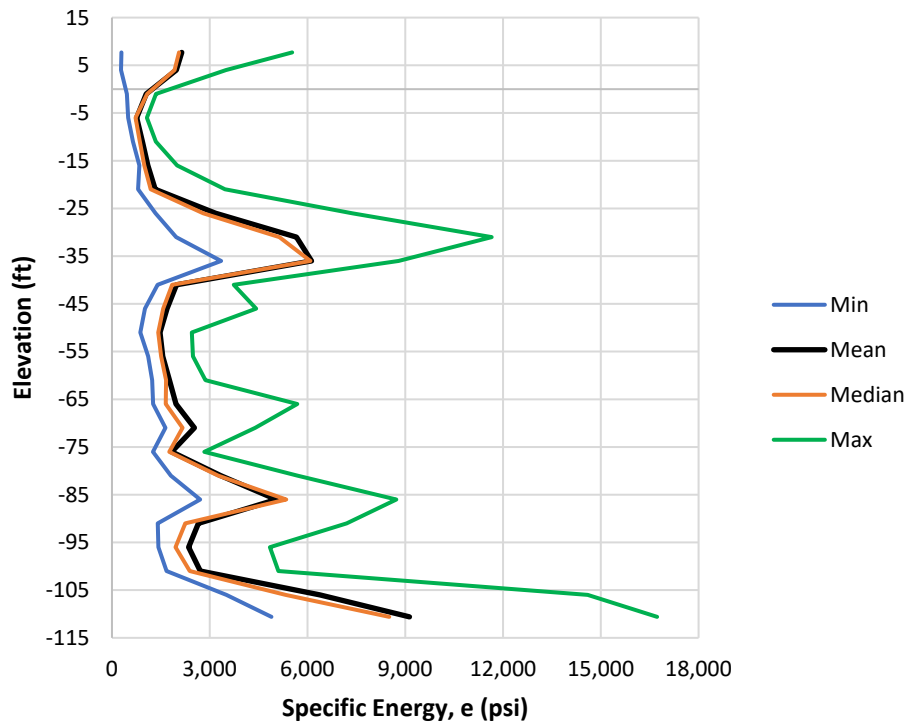


Figure 3-24. Group C1 and Group C2 minimum, mean, median, and maximum specific energy profiles.

Also available within proximity to I-395 Test Pile C were four SPT borings which included two borings located inside Group C1 (54 ft and 64 ft NW of TP1), one boring outside Group C2 (located 60 ft southwest of TP-C), and one boring at the test pile location. Figure 3-25 provides the SPT depth profiles and the average SPT value within each of the I-395 TP-C SG zones.

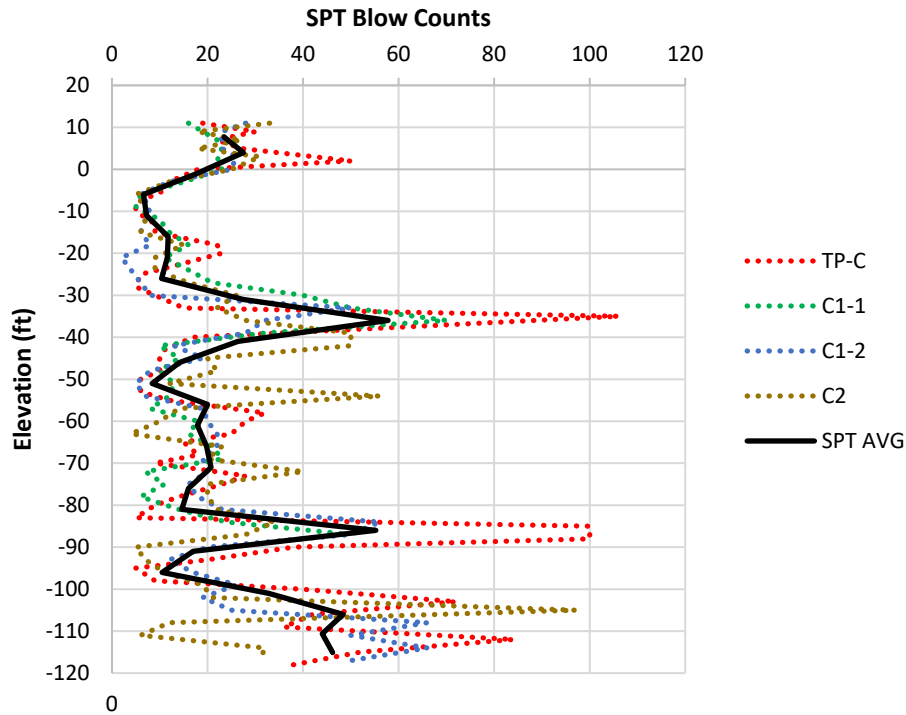


Figure 3-25. SPT profiles proximal to I-395 Test Pile C.

Similar to the specific energy profiles from the two pile groups, the SPT borings also indicate variability within Group C1 and between the two pile group locations. Furthermore, the SPT borings also indicate a correlated structure exists within proximity of TP-C with similar layering to the specific energy profiles. Consequently, the SPT borings were used to help develop a combined specific energy profile to build correlation with load test unit side shear at the I-395 site. Table 3-6 provides the minimum, mean, median and maximum average specific energy values for each SG zone at TP-C, as well as the specific energy profile developed from a combination of Group C1 and Group C2 piles (MWD). Figure 3-26 compares the specific energy depth profile developed with the average SPT profile. Observed in Figure 3-26, the MWD and SPT profiles show very similar layering.



Table 3-6. Pile Groups C1 and C2 minimum, mean, median, and maximum specific energy and the combined specific energy tabular data.

I-395 TPC SG Zones	SG Zone Elevations			Average Specific Energy, e (psi)				
	El <sub>top</sub> (ft)	El <sub>bot</sub> (ft)	El <sub>mid</sub> (ft)	Min	Mean	Median	Max	Combo
25	8.9	6.5	7.7	288	2,143	2,058	5,527	2,143
24	6.5	1.5	4.0	277	1,976	1,920	3,498	3,498
23	1.5	-3.5	-1.0	458	1,051	1,080	1,349	1,051
22	-3.5	-8.5	-6.0	496	759	724	1,071	496
21	-8.5	-13.5	-11.0	642	936	855	1,348	642
20	-13.5	-18.5	-16.0	841	1,100	992	1,997	841
19	-18.5	-23.5	-21.0	802	1,325	1,188	3,469	802
18	-23.5	-28.5	-26.0	1,337	3,183	2,798	7,368	1,337
17	-28.5	-33.5	-31.0	1,968	5,660	5,138	11,652	1,968
16	-33.5	-38.5	-36.0	3,350	6,125	6,089	8,794	8,794
15	-38.5	-43.5	-41.0	1,401	1,980	1,845	3,737	1,980
14	-43.5	-48.5	-46.0	1,013	1,687	1,573	4,424	1,013
13	-48.5	-53.5	-51.0	870	1,472	1,421	2,451	870
12	-53.5	-58.5	-56.0	1,111	1,557	1,509	2,483	1,111
11	-58.5	-63.5	-61.0	1,234	1,765	1,661	2,867	1,234
10	-63.5	-68.5	-66.0	1,262	1,967	1,649	5,685	1,262
9	-68.5	-73.5	-71.0	1,639	2,528	2,165	4,394	1,639
8	-73.5	-78.5	-76.0	1,259	1,832	1,757	2,836	2,836
7	-78.5	-83.5	-81.0	1,808	3,341	3,263	5,696	1,808
6	-83.5	-88.5	-86.0	2,708	5,045	5,347	8,727	8,727
5	-88.5	-93.5	-91.0	1,404	2,651	2,249	7,201	2,249
4	-93.5	-98.5	-96.0	1,424	2,352	1,951	4,847	1,424
3	-98.5	-103.5	-101.0	1,676	2,712	2,388	5,104	2,388
2	-103.5	-108.5	-106.0	3,509	6,379	5,327	14,596	5,327
1	-108.5	-112.7	-110.6	4,893	9,129	8,508	16,727	9,129

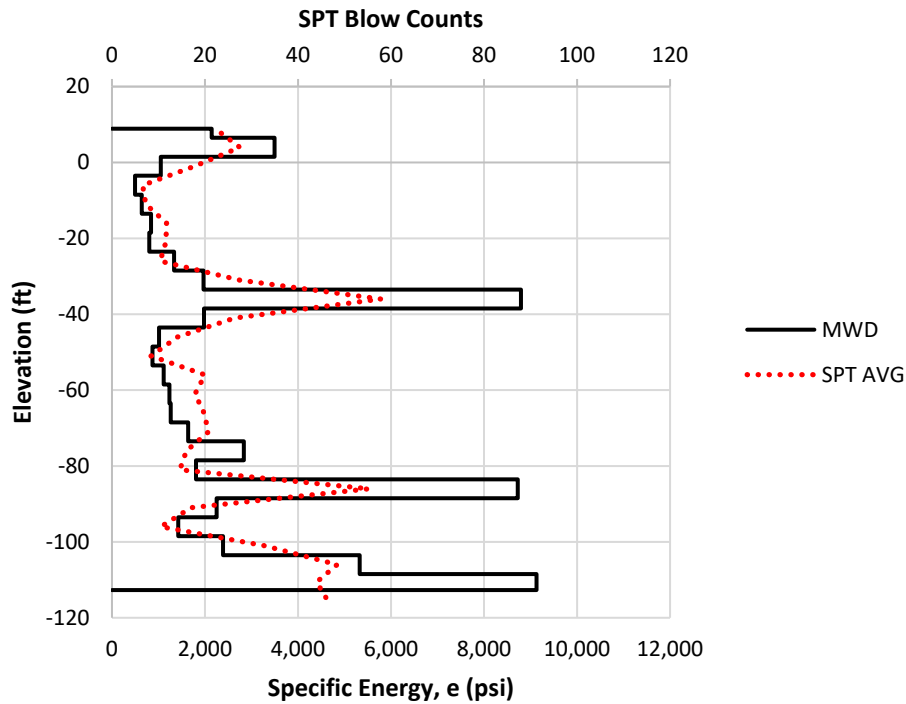


Figure 3-26. Pile Groups C1 and C2 combined profile compared to the SPT AVG profile.

Figure 3-27 presents the strain gauge load distribution after I-395 Test Pile C was reanalyzed using larger layers developed from stable strain gauge locations as previously discussed. Figures 3-28 and 3-29 provide the T-Z curves from the reanalyzed load test. Based on the strain gauge load distribution and T-Z curves, researchers estimate the pile was fully mobilized during Load Step 13.

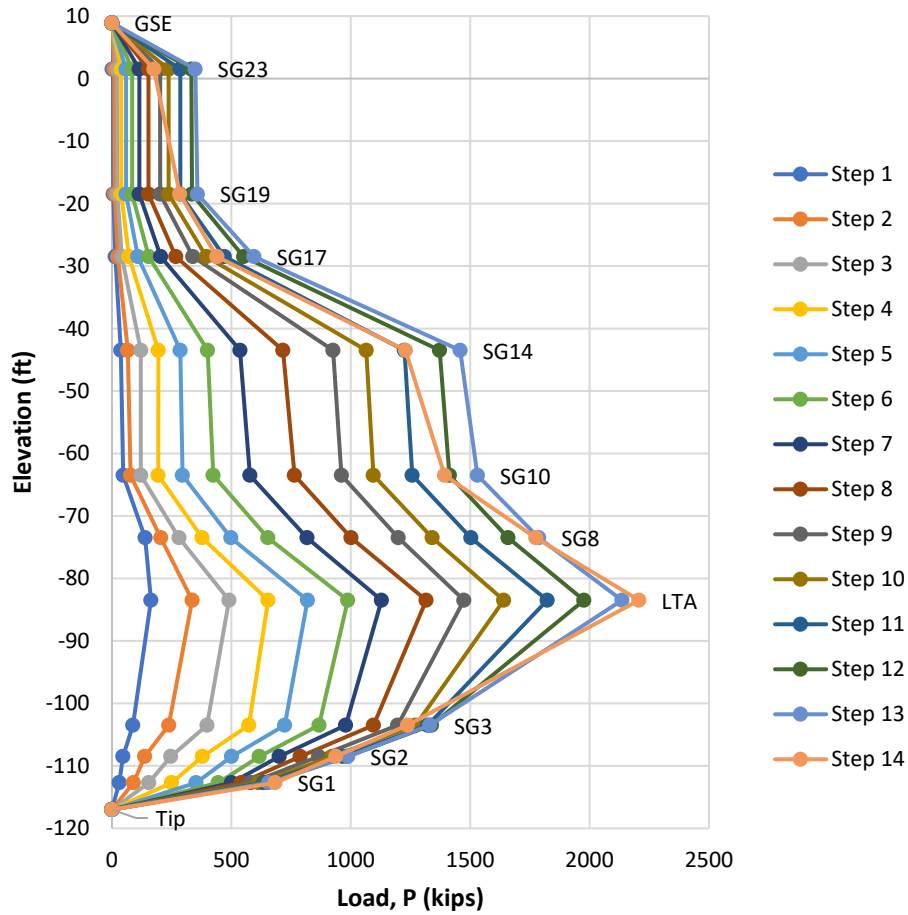


Figure 3-27. I-395 Test Pile C reanalyzed strain gauge load distribution.

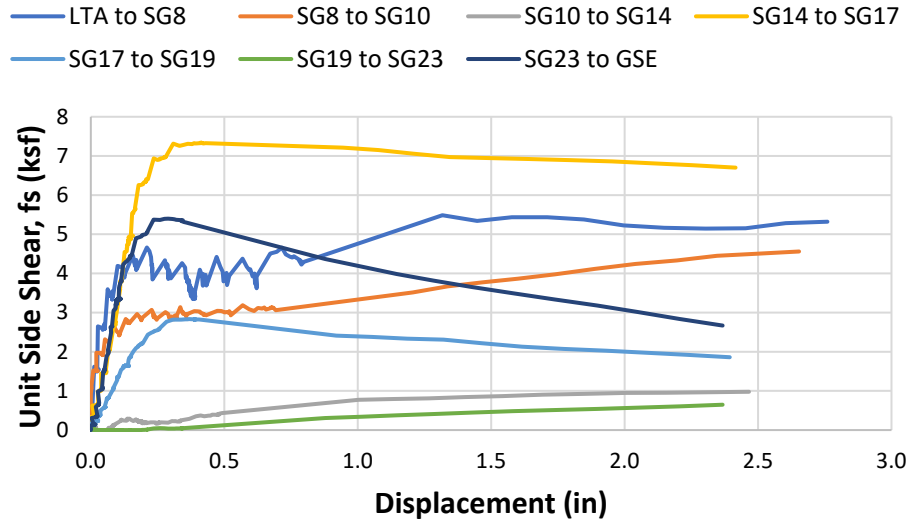


Figure 3-28. I-395 Test Pile C reanalyzed T-Z curves for the upper pile segment.

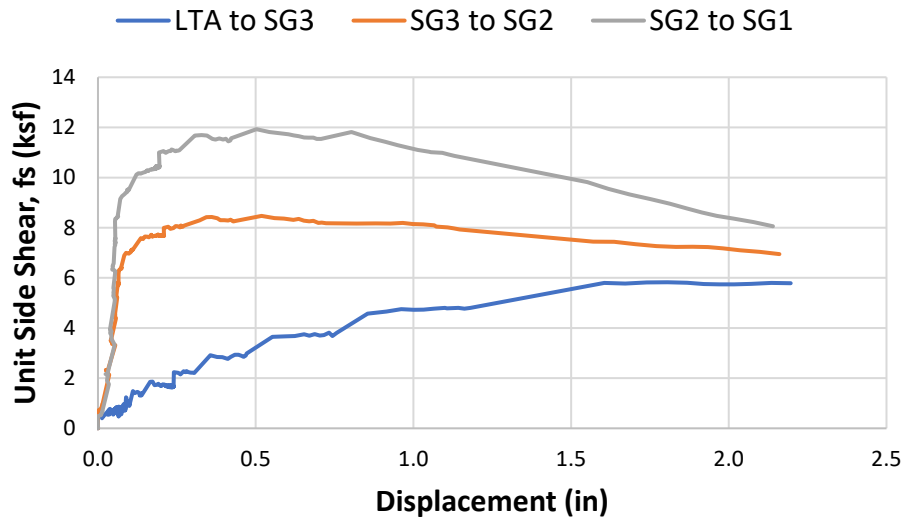


Figure 3-29. I-395 Test Pile C reanalyzed T-Z curves for the lower pile segment.

Table 3-7 includes the unit side shear in each respective SG zone from Figures 3-27 through 3-29. Table 3-7 does not include Zones SG10 to SG14 or SG19 to SG23 because these were identified as soil layers and LTA to SG3 is not included because a definitive side shear value could not be determined to compare with specific energy.

Note: For LTA to SG3, the range of average specific energy from the Group C1 and Group C2 piles matched the unit side shear range in Figure 3-29 for a displacement range of 0.5 to 1.6 inches. For example, at 1.6 inches of displacement, the specific energy profile that matches the SPT profile (Figure 3-26) produced an average specific value of  $e = 3,697$  psi over this portion of the shaft which corresponds to  $f_s = 6.1$  ksf using the drilled shaft rock auger relationship in

Figure 3-19. The mobilized unit side shear from the T-Z curves for this segment in Figure 3-29 was  $f_s = 5.8$  ksf which is in near perfect agreement with the specific energy assessment. However, this zone was not included in further development of correlation as the general trend of the T-Z curve indicates side shear mobilization occurred at much higher displacement than is typical. Although the zone was not included in correlation development, this zone may be an indicator of the pile behavior that occurs in pile segments in which large residual tensile stresses are present prior to top-down compressive loading. This indicates piles that contain segments with large residual tensile stresses may compress and displace more than typical prior to full side shear mobilization. The lower pile segment which experienced side shear resistance and end bearing compressed 0.30 inches over a shaft length of 29.2 feet whereas the upper pile segment that was loaded in isolated shear compressed 0.46 inches over a shaft length of 92.4 feet. This indicates the lower pile segment that was loaded top-down compressed twice as much per shaft length as the upper pile segment that was loaded bottom-up. If this pile behavior held true and the entire pile was loaded top-down, the total pile compression would have been 1.2 inches at full side shear mobilization.

Table 3-7. Average specific energy and load test unit side shear for each I-395 Test Pile C SG zone.

I-395 TPC SG Zone	LT Unit Side Shear $f_s$ (ksf)
SG23 to GSE	5.30
SG17 to SG19	2.83
SG14 to SG17	7.33
SG8 to SG 10	3.06
LTA to SG8	4.30
SG3 to SG2	8.28
SG2 to SG1	11.57

The average specific energy recorded within each respective SG zone of Table 3-7 is plotted with unit side shear in Figure 3-30 and compared to the previous correlation presented in Figure 3-19. Again, the ACIP pile data points follow the same trend as the drilled shaft rock auger correlation and produced a nearly identical regression curve and  $R^2$  value when combined with the drilled shaft rock auger data points. This further indicates that ACIP pile and Drilled Shaft rock augers share the same or a similar correlation between MWD specific energy and load test mobilized unit side shear.

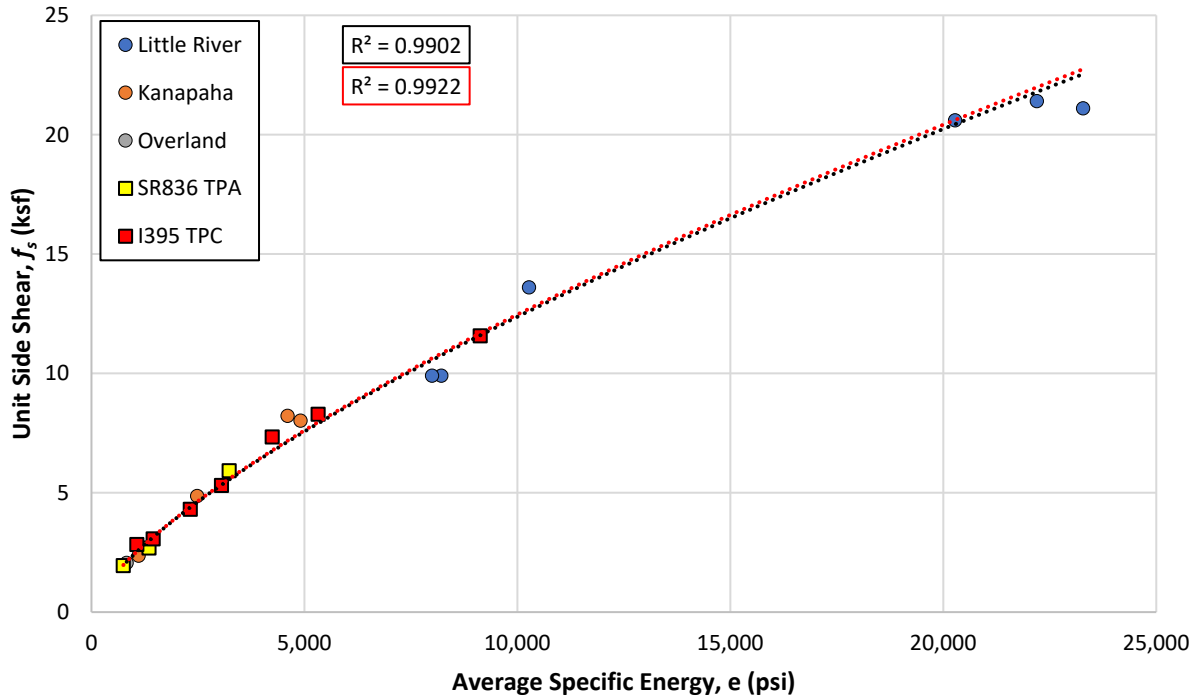


Figure 3-30. Load test unit side shear vs MWD specific energy for ACIP piles monitored at SR-836 and I-395 compared to the previously developed drilled shaft rock auger correlation.

### 3.2.4 Signature Bridge Test Pile D

The third site investigated for the development of MWD ACIP correlation was Signature Bridge. At the Signature Bridge site, Test Pile D located southwest of Group D was loaded with 2,310 kips with an LTA expansion of 0.39 inches upward and a top of pile displacement of 0.24 inches. During the test, a shaft segment 20 ft in length directly above the LTA was fully mobilized while the remainder of the pile was not. At the Signature Bridge site, MWD was not conducted in the footprint of the test pile. Therefore, the same approach taken at I-395 Test Pile C was used to develop correlation at this site.

From Group D, 16 piles located 20 ft to 57 ft northwest of TP-D were used to build correlation. Figure 3-31 provides the average specific energy profiles for the 16 closest piles to TP-D from Group D using the TP-D SG zone layering. Figure 3-32 provides the specific energy depth profile for the minimum, mean, median, and maximum average values recorded from Group D. Figures 3-31 and 3-32 show that variability exists within the pile group, with greater variability observed in the lower portion of the profiles. However, the figures also show that a correlated structure exists as all specific energy profiles generally show the same trends in layering.

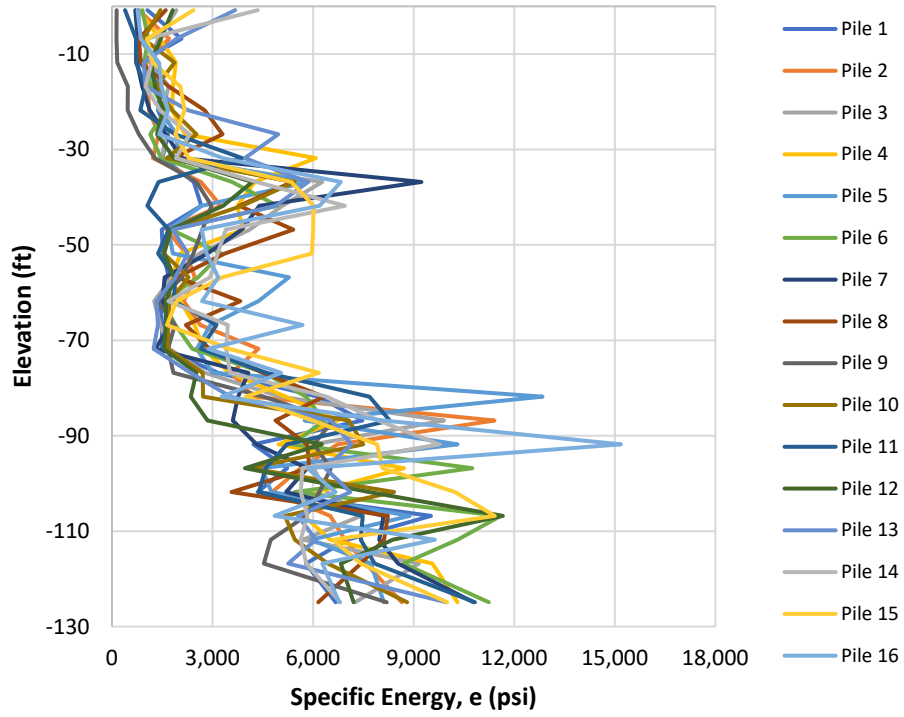


Figure 3-31. Pile Group D specific energy profiles closest to Signature Bridge TP-D.

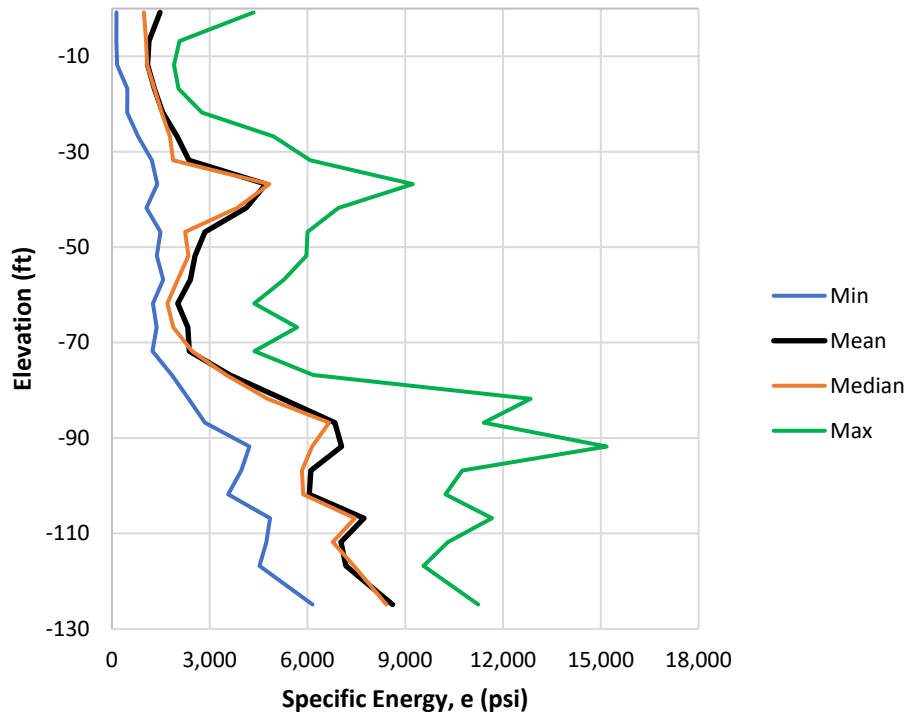


Figure 3-32. Pile Group D minimum, mean, median, and maximum specific energy profiles.

Also available within proximity to Signature Bridge Test Pile D were two SPT borings which included one boring located inside Pile Group D (SB 4-1), 55 ft northwest of TP-D, and one boring at the TP-D location. Figure 3-33 provides the SPT depth profiles and the average SPT value within each of the Signature Bridge TP-D SG zones.

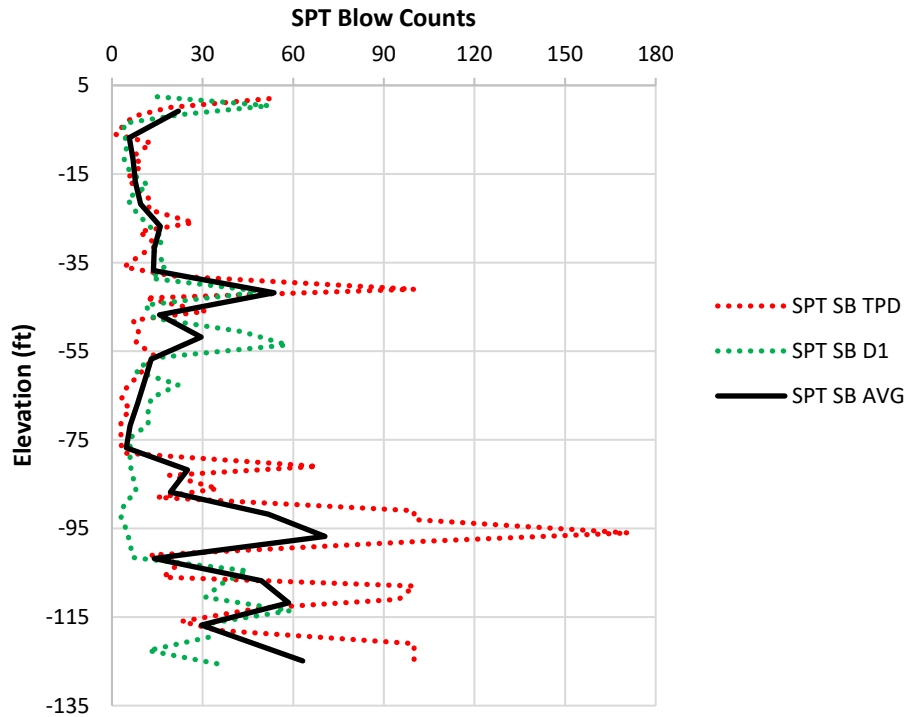


Figure 3-33. SPT profiles close to Signature Bridge TP-7.

Similar to the specific energy profiles from Group D, the SPT borings also indicate variability within the vicinity of TP-D, with more variability observed in the lower portion of the profile. Furthermore, the SPT borings also indicate a correlated structure exists within proximity of TP-D with similar layering to the specific energy profiles. Consequently, the SPT borings were used to help develop a combined specific energy profile to build correlation with load test unit side shear at the Signature Bridge site, with more emphasis placed on the TP-D SPT boring due to its close proximity to the test pile. Tables 3-8 and 3-9 provide the tabular specific energy data for each individual Group D pile considered, the minimum, mean, median and maximum average specific energy values, as well as the specific energy profile developed from a combination of Group D piles for each SG zone at TP-D (MWD). Figure 3-34 compares the specific energy depth profile developed with the TP-D SPT profile. Observed in Figure 3-34, the MWD and SPT profiles show very similar layering.

Figure 3-35 presents the strain gauge load distribution after Signature Bridge Test Pile D was reanalyzed using larger layers developed from stable strain gauge locations as previously discussed. Figure 3-36 provides the T-Z curves from the upper pile segment for the reanalyzed load test.

Table 3-8. Pile Group D specific energy data.

S.B. TPD SG Zones	SG Zone Elevations			Signature Bridge Group D - Average Specific Energy, e (psi)									
	El <sub>top</sub> (ft)	El <sub>bot</sub> (ft)	El <sub>mid</sub> (ft)	Pile 1	Pile 2	Pile 3	Pile 4	Pile 5	Pile 6	Pile 7	Pile 8	Pile 9	Pile 10
24	2.7	-4.3	-0.8	1,054	803	1,925	802	793	906	696	1,605	140	1,449
23	-4.3	-9.3	-6.8	2,072	1,703	1,375	1,427	812	1,081	772	801	134	935
22	-9.3	-14.3	-11.8	830	1,016	1,146	1,904	1,375	960	744	858	159	1,866
21	-14.3	-19.3	-16.8	1,441	1,074	1,690	1,819	1,439	1,177	905	1,694	472	1,322
20	-19.3	-24.3	-21.8	1,374	1,106	1,514	1,794	1,442	1,601	1,126	2,763	469	1,799
19	-24.3	-29.3	-26.8	1,673	1,389	1,620	2,177	1,919	1,142	1,608	3,298	801	2,522
18	-29.3	-34.3	-31.8	1,505	1,225	1,491	6,082	1,988	1,464	2,081	1,827	1,286	1,638
17	-34.3	-39.3	-36.8	2,442	2,656	6,273	4,255	5,864	3,583	9,233	5,384	2,520	5,455
16	-39.3	-44.3	-41.8	2,662	3,247	5,086	3,743	2,680	4,929	4,398	3,795	2,969	3,883
15	-44.3	-49.3	-46.8	1,487	1,626	4,112	3,905	1,683	1,755	3,874	5,407	2,697	1,769
14	-49.3	-54.3	-51.8	1,519	2,216	2,612	2,045	1,814	3,268	2,849	3,368	2,431	1,541
13	-54.3	-59.3	-56.8	1,702	2,472	1,779	1,780	5,278	2,570	1,570	1,938	2,095	2,289
12	-59.3	-64.3	-61.8	1,439	2,138	1,259	2,043	4,366	1,512	1,511	3,826	1,358	1,717
11	-64.3	-69.3	-66.8	1,499	2,635	1,439	2,464	2,934	1,891	1,728	2,208	1,876	1,679
10	-69.3	-74.3	-71.8	1,482	4,368	1,713	2,738	2,529	2,396	1,301	2,910	1,670	1,658
9	-74.3	-79.3	-76.8	3,171	3,566	2,777	3,497	3,003	4,548	4,068	4,508	1,835	2,709
8	-79.3	-84.3	-81.8	6,146	4,208	5,022	5,182	12,844	5,792	3,763	6,316	4,532	2,718
7	-84.3	-89.3	-86.8	7,470	11,410	9,907	6,729	5,747	6,324	3,605	4,878	6,599	7,071
6	-89.3	-94.3	-91.8	4,219	6,731	6,021	4,971	10,309	5,382	4,315	5,820	6,020	7,492
5	-94.3	-99.3	-96.8	5,228	5,624	6,004	8,711	4,473	10,748	5,823	5,888	6,531	4,102
4	-99.3	-104.3	-101.8	4,342	4,776	6,417	6,103	4,754	5,450	5,195	3,565	6,185	8,417
3	-104.3	-109.3	-106.8	9,515	6,510	7,430	5,727	8,881	11,598	8,107	8,231	5,789	5,162
2	-109.3	-114.3	-111.8	7,027	6,952	5,702	6,509	5,947	10,309	7,973	8,115	4,737	5,456
1	-114.3	-119.3	-116.8	5,785	7,569	9,156	9,560	7,724	8,694	8,535	7,428	4,530	6,439
0	-119.3	-130.5	-124.9	6,672	8,645	7,257	10,307	8,107	11,239	10,786	6,153	8,196	8,805

Table 3-9. Pile Group D specific energy data continued with the combined profile.

S.B. TPD SG Zones	Elevation El <sub>mid</sub> (ft)	Signature Bridge Group D - Average Specific Energy, e (psi)										
		Pile 11	Pile 12	Pile 13	Pile 14	Pile 15	Pile 16	Minimum	Mean	Median	Maximum	MWD
24	-0.8	390	1,813	3,677	4,348	2,432	764	140	1,475	980	4,348	980
23	-6.8	717	1,458	1,923	1,043	1,053	861	134	1,135	1,048	2,072	134
22	-11.8	718	1,171	947	1,184	1,216	1,405	159	1,094	1,081	1,904	159
21	-16.8	1,004	1,279	1,006	999	2,041	1,478	472	1,302	1,300	2,041	472
20	-21.8	848	1,537	2,267	1,433	2,169	1,678	469	1,557	1,525	2,763	469
19	-26.8	1,883	1,345	4,958	2,315	1,891	1,407	801	1,997	1,778	4,958	801
18	-31.8	3,888	1,847	3,962	1,910	2,293	3,302	1,225	2,362	1,878	6,082	1,878
17	-36.8	1,392	4,188	5,848	4,308	5,349	6,824	1,392	4,723	4,829	9,233	1,392
16	-41.8	1,058	3,317	4,887	6,948	6,016	6,191	1,058	4,113	3,839	6,948	6,948
15	-46.8	1,696	1,748	1,810	3,392	6,000	2,678	1,487	2,852	2,244	6,000	2,852
14	-51.8	1,376	1,558	2,265	3,152	5,966	2,823	1,376	2,550	2,348	5,966	1,376
13	-56.8	1,878	1,857	1,892	2,927	3,285	3,168	1,570	2,405	2,017	5,278	1,570
12	-61.8	1,856	1,616	1,331	1,682	1,926	2,687	1,259	2,017	1,699	4,366	1,259
11	-66.8	3,116	1,611	1,370	3,457	1,640	5,683	1,370	2,327	1,883	5,683	1,370
10	-71.8	2,649	1,546	1,244	3,407	3,498	2,870	1,244	2,374	2,462	4,368	1,244
9	-76.8	4,609	2,520	2,344	3,517	6,174	5,046	1,835	3,618	3,507	6,174	1,835
8	-81.8	7,680	2,351	3,535	6,404	3,988	3,271	2,351	5,234	4,777	12,844	4,777
7	-86.8	8,286	2,852	6,534	7,947	5,979	8,104	2,852	6,840	6,664	11,410	2,852
6	-91.8	5,219	6,262	7,147	9,760	7,908	15,179	4,219	7,047	6,141	15,179	15,179
5	-96.8	4,583	3,967	6,360	5,680	8,070	5,831	3,967	6,101	5,827	10,748	10,748
4	-101.8	4,381	7,669	7,112	5,635	10,234	6,668	3,565	6,056	5,869	10,234	3,565
3	-106.8	7,479	11,660	5,554	5,827	11,419	4,850	4,850	7,734	7,455	11,660	7,734
2	-111.8	7,424	8,376	6,080	5,626	6,599	9,632	4,737	7,029	6,775	10,309	10,309
1	-116.8	7,834	6,827	5,255	5,798	7,419	6,279	4,530	7,177	7,424	9,560	4,530
0	-124.9	10,827	7,208	9,975	6,809	10,002	6,779	6,153	8,610	8,421	11,239	11,239



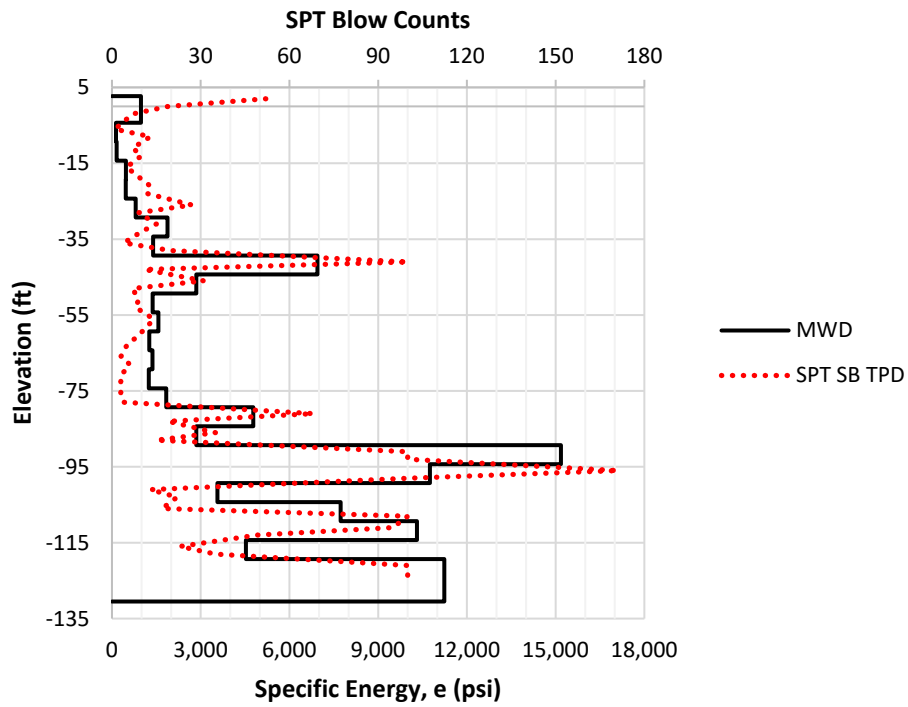


Figure 3-34. Pile Group D combined specific energy profile compared to the SB TP-D SPT profile.

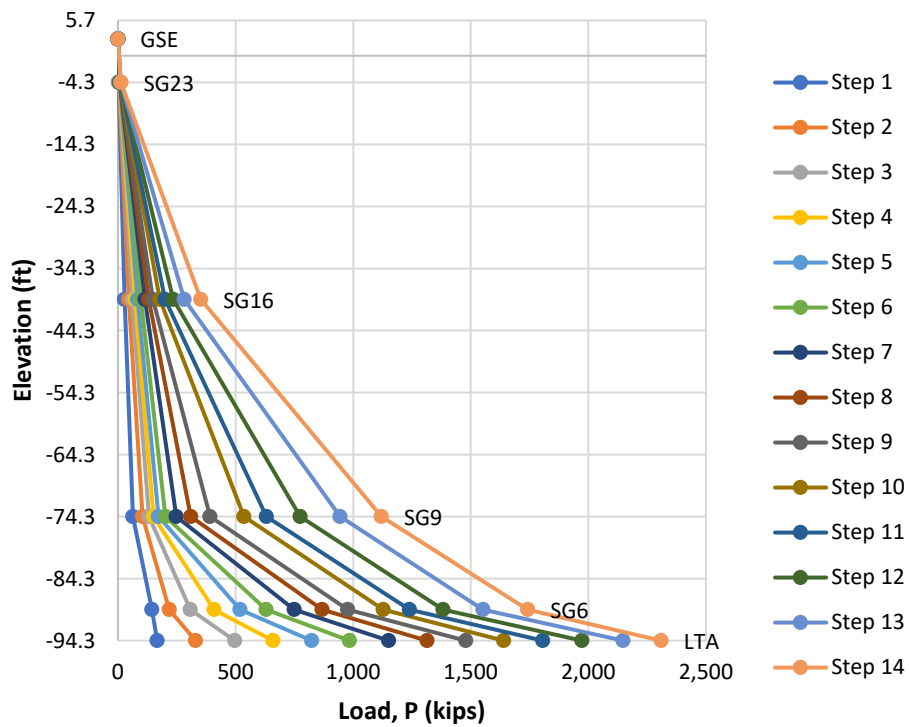


Figure 3-35. Signature Bridge, Test Pile D reanalyzed strain gauge load distribution (upper pile segment).

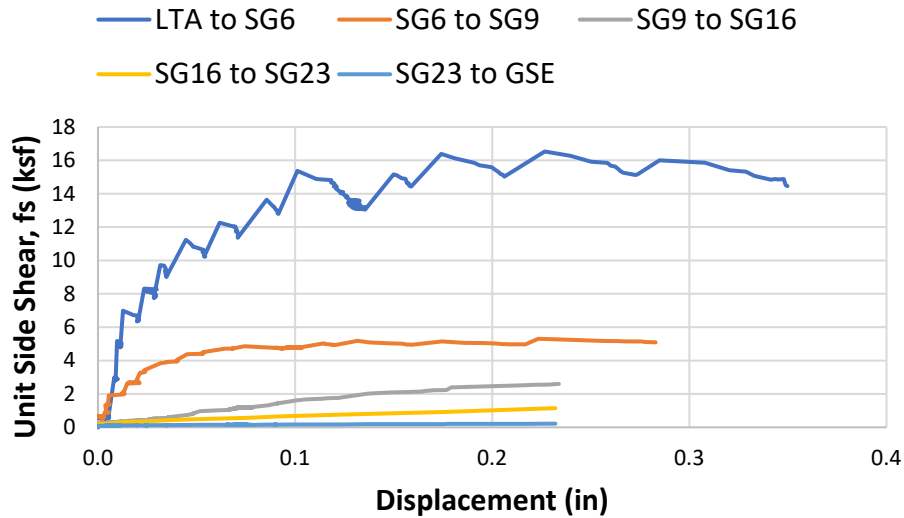


Figure 3-36. Signature Bridge Test Pile D reanalyzed T-Z curves (upper pile segment).

### 3.2.5 Developed ACIP Pile MWD Correlation for QA/QC Procedures

Table 3-10 provides the load test unit side shear for each mobilized zone in limestone for each of the investigated sites. From all three sites, 12 data points were acquired to build regional correlation for ACIP piles socketed into south Florida limestone. Figure 3-37 presents the developed correlation in red which uses a combination of 11 data points acquired from monitoring drilled shafts using rock augers and 12 data points from monitoring ACIP piles using rock augers. Observed in Figure 3-37, each local correlation investigated (I-395, SR-836, and Signature Bridge) followed the trends of the drilled shaft rock auger correlation quite well. When considering both data sets, the regression curve and  $R^2$  value are nearly identical to the original drilled shaft rock auger correlation. This is a good indicator that drilled shaft and ACIP pile rock augers share the same or a similar relationship between specific energy and load test unit side shear, which is likely due to the similar bit geometry of each bored pile drilling tool.

Table 3-10. Average specific energy and load test unit side shear for all monitored sites.

Load Test Site Location	Strain Gauge Zones	LT Unit Side Shear $f_s$ (ksf)
SR-836 Test Pile A	GSE to SG13	1.94
	SG13 to SG11	2.68
	SG11 to LTA	5.92
I-395 Test Pile C	GSE to SG23	5.30
	SG19 to SG17	2.83
	SG17 to SG14	7.33
	SG10 to SG8	3.06
	SG8 to LTA	4.30
	SG3 to SG2	8.28
	SG2 to SG1	11.57
Signature Bridge Test Pile D	SG9 to SG6	5.09
	SG6 to LTA	15.16

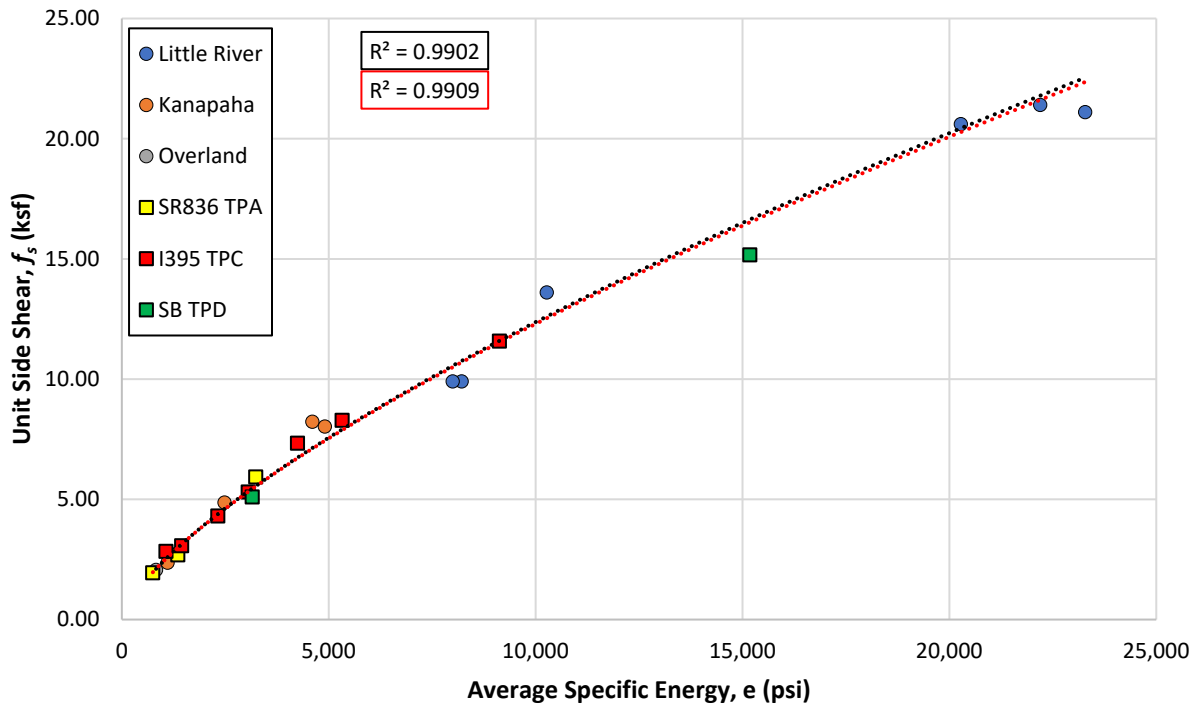


Figure 3-37. Load test unit side shear vs. MWD specific energy for ACIP piles monitored at SR-836, I-395, and Signature Bridge compared to the drilled shaft rock auger correlation.

## 4 MWD Correlation Validation for ACIP Production Pile QA/QC

### 4.1 QA/QC Locations

The production piles monitored during the project were intended to be in locations SR-836, I-395, and Signature Bridge. However, minimal core samples were collected in the SR-836 location for comparison at the time of the research investigation and the MWD data collected for the piles available in the SR-836 location do not include all of the necessary monitored drilling parameters for proper analyses. Specifically, at the SR-836 location, the rig had a malfunctioning rotational speed sensor which was observed at the end of SR-836 Test Pile A drilling and continued through the drilling of SR-836 Test Piles J & K, based on the drilling data received by the UF research team. The UF researchers notified the FDOT about the RPM sensor because it prevented QA/QC procedures from occurring for the SR-836 location. For this work, production Pile Group B was used as a replacement for the nonfunctioning pile occurrences. Pile Group B is located within close proximity to Test Pile B identified in Figure 4-1 and was discussed in Chapter 3. This location is approximately the same distance from I-395 Test Pile C as is Signature Bridge Test Pile D and it is one of the closer monitored locations to SR-836 Test Pile A with the required data currently available. Consequently, the following pile groups were used for the QA/QC procedures (Figure 4-1):

- Pile Group B – I-395 Test Pile B
- Pile Groups C1 and C2 – I-395 Test Pile C
- Pile Group D – Signature Bridge Test Pile D

Specifically, 16 production piles were used from Group B, 10 piles from Group C1, 8 piles from Group C2, and 16 piles from Group D. This provided a total of 50 production piles analyzed throughout the sites.

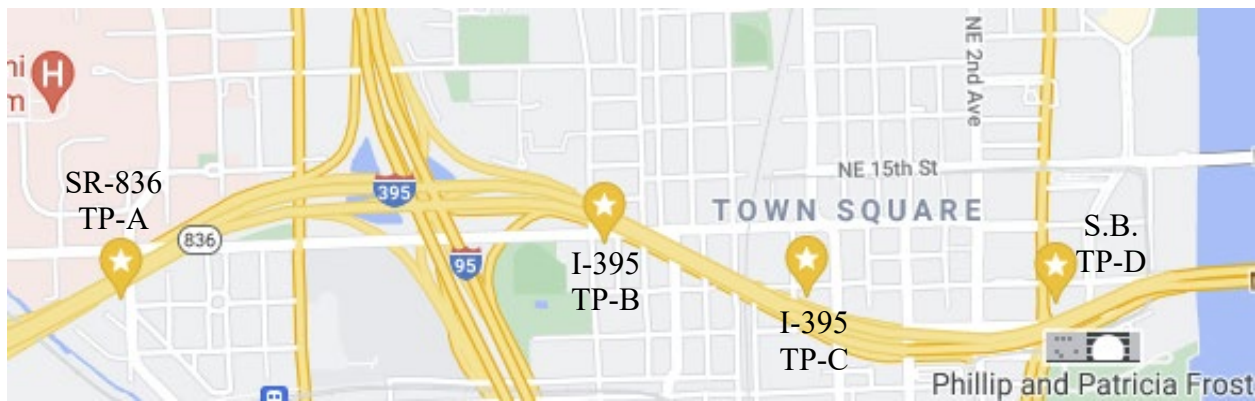


Figure 4-1. Map of test pile locations.

## 4.2 Rock Core Data

From the I-395 and Signature Bridge locations, a total of 204 unconfined compressive strength ( $q_u$ ) samples were collected and 218 split tension ( $q_{st}$ ) samples were collected, totaling 422 samples collected and tested in the laboratory with summary statistics given in Table 4-1.

Table 4-1. ACIP pile Miami-Dade rock core data.

Miami-Dade Rock Core Data		
Statistics	$q_{st}$ (psi)	$q_u$ (psi)
Mean	195	1,281
Median	153	717
Std. Dev.	150	1,354
CV	0.77	1.06
Maximum	698	5,172
Minimum	9	24
Count	218	204

It is common practice to use  $q_u$  samples in design, therefore, it is of great interest to identify if  $q_{st}$  samples can be correlated to the  $q_u$  samples and used as additional  $q_u$  estimates for design purposes. The UF researchers have developed a method based on index testing that allows the  $q_{st}$  samples to be used as  $q_u$  samples. This was covered in FDOT projects BDV31-977-20 (McVay and Rodgers, 2016) and BDV31-977-91 (McVay and Rodgers, 2020) as well as Rodgers et al. (2019). This same approach was taken during this project and the following will provide a brief description of the process.

First, the samples are grouped based on ranges of dry unit weight and the average strength value for each group is determined (Table 4-2). Typically, moisture content is also considered but that data was not available for this project.

Table 4-2. Average split tension and unconfined compressive strength grouped by dry unit weight.

$\gamma_d$ Range (pcf)	$q_{st}$ (psi)	$q_u$ (psi)
90	95	42
95	100	64
100	105	77
105	110	109
110	115	140
115	120	103
120	125	172
125	130	146
130	135	204
135	140	314
140	145	281
145	150	243
150	155	348
155	160	332

Next, the average strength values for each dry unit weight range are plotted in red as strength vs. dry unit weight (Miami-Dade Mean; MD Mean) and compared to the data collected from 23 different sites throughout the state of Florida plotted in black (Rodgers et al., 2019; FL Mean).

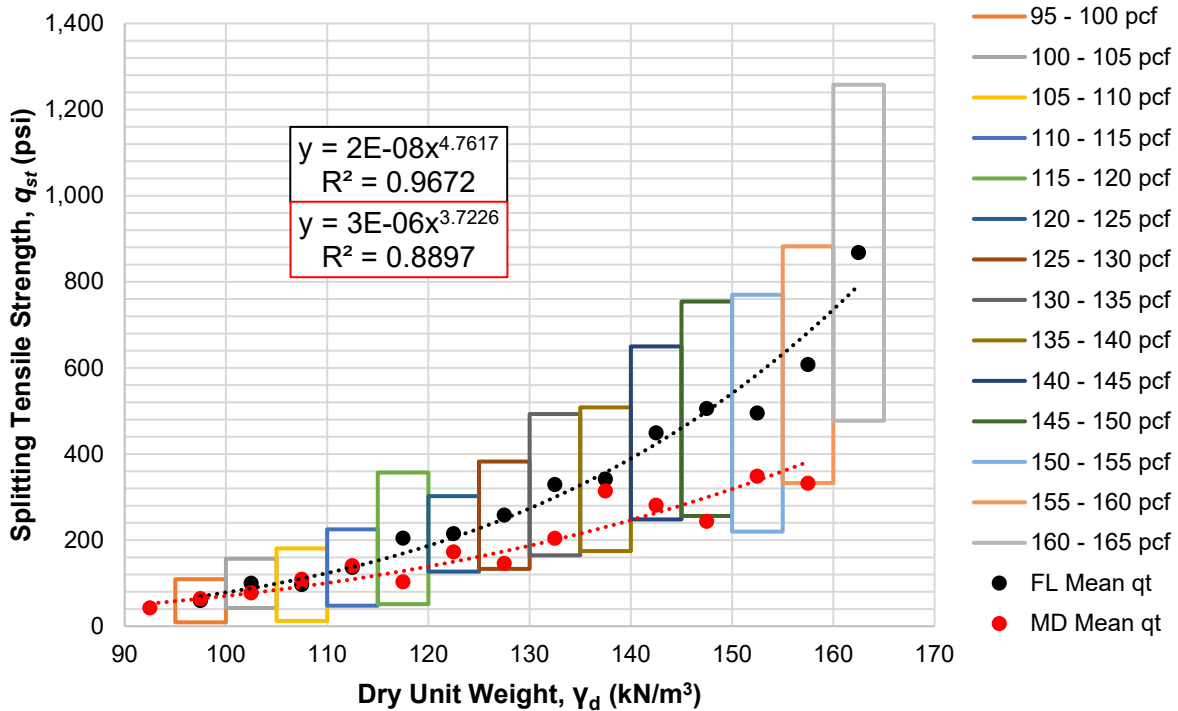


Figure 4-2. Split tension plotted as function of dry unit weight.

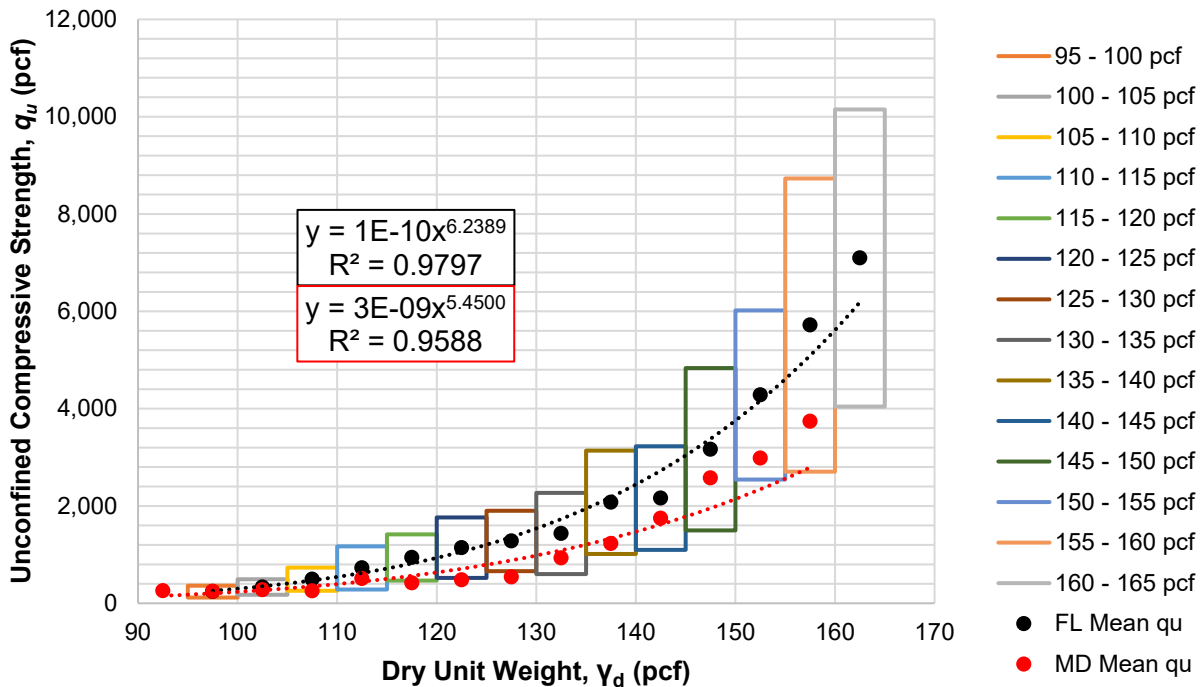


Figure 4-3. Unconfined compressive strength plotted as function of dry unit weight.

Evident from Figures 4-2 and 4-3, the MD Mean generally followed the same trends as the FL Mean as expected. However, it is noticed that the MD Mean is lower than the FL Mean in nearly all dry unit weight ranges but typically falls within one standard deviation from the FL Mean as indicated by the colored boxes for each range. The lower MD values may be due to the core samples resting in the core boxes for an extended period of time prior to laboratory testing (possible micro-cracking -drying out). Also note, it is common practice that a large majority of core samples collected are not tested for the design of ACIP piles. Fortunately, the FDOT collected the untested samples and performed the additional testing at the State Materials Office (SMO) for this research. This provided a significant increase in tested core samples for analyses and comparison with MWD results.

The next step in the  $q_u$ - $q_{st}$  correlation development was to take the regression equations from Figures 4-2 and 4-3 and plot  $q_u$  vs.  $q_{st}$  for a strength range representative of the core samples collected and compare the relationship to the relationship developed for all of Florida, the Florida Geomaterials equation (FLGM; Figure 4-4).

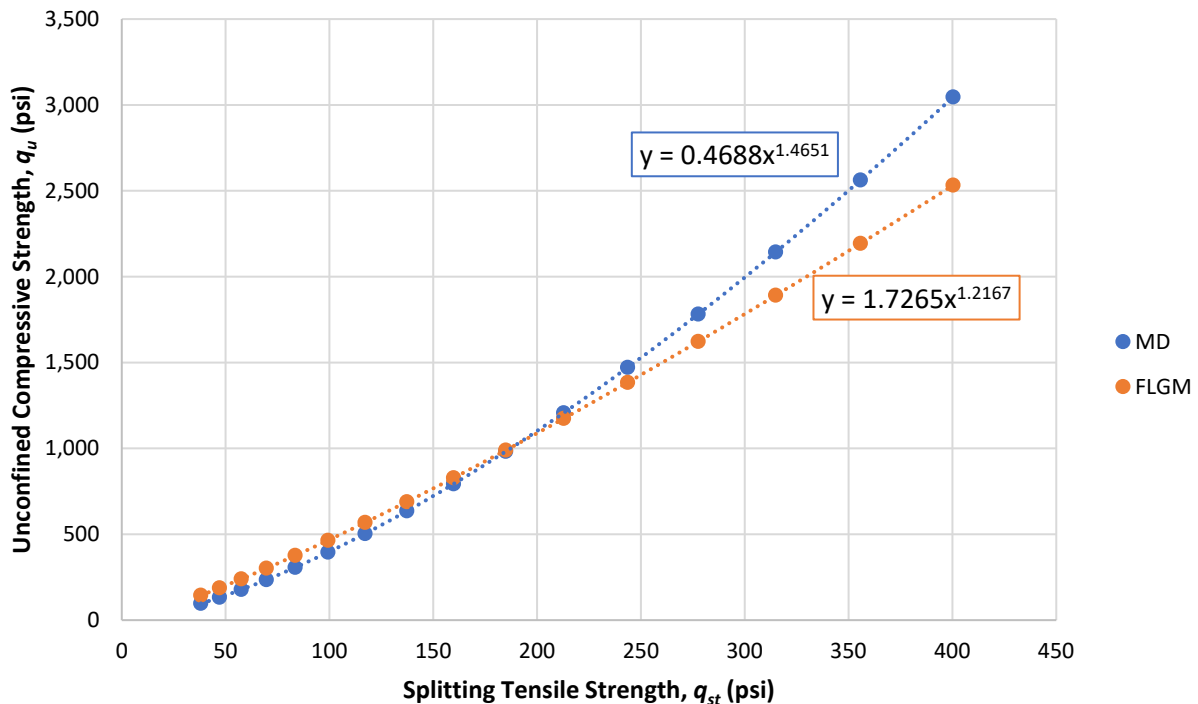


Figure 4-4.  $q_u$  vs.  $q_{st}$  relationships for MD and FLGM.

Once the new correlation was developed (Figure 4-4),  $q_u$  estimates from the MD and FLGM regression equations were compared to the measured  $q_u$  values collected at the MD site. Table 4-3 provides the tabular data, Figure 4-5 provides the frequency distributions, and Figure 4-6 provides the cumulative frequency distributions.

Table 4-3. Summary of statistics for estimated  $q_u$  values compared to measured  $q_u$  values.

Statistics	Unconfined Compressive Strength, $q_u$ (psi)		
	Measured	Estimated - FLGM	Estimated - MD
Mean	1,281	1,136	1,268
Median	717	784	743
Std. Dev.	1,354	1,032	1,351
CV	1.06	0.91	1.07
Maximum	5,172	4,984	6,885
Minimum	24	25	12
Count	204	218	218

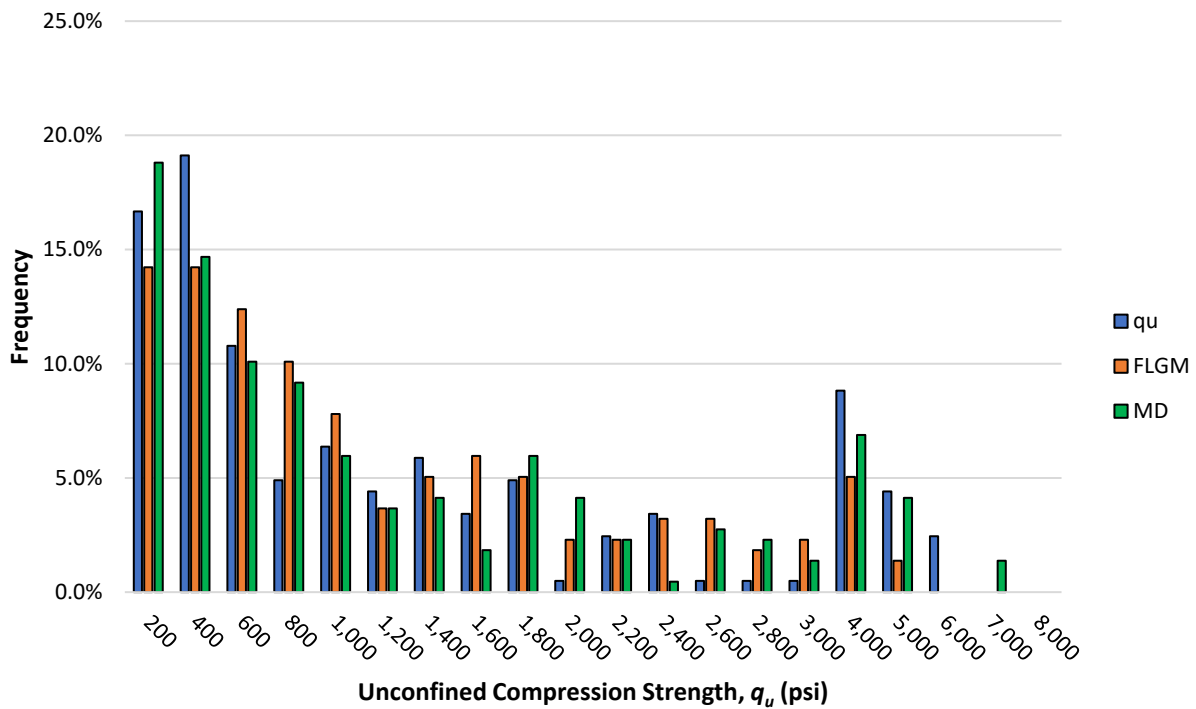


Figure 4-5. Frequency distributions for estimated  $q_u$  values (MD and FLGM) compared to measured  $q_u$  values.



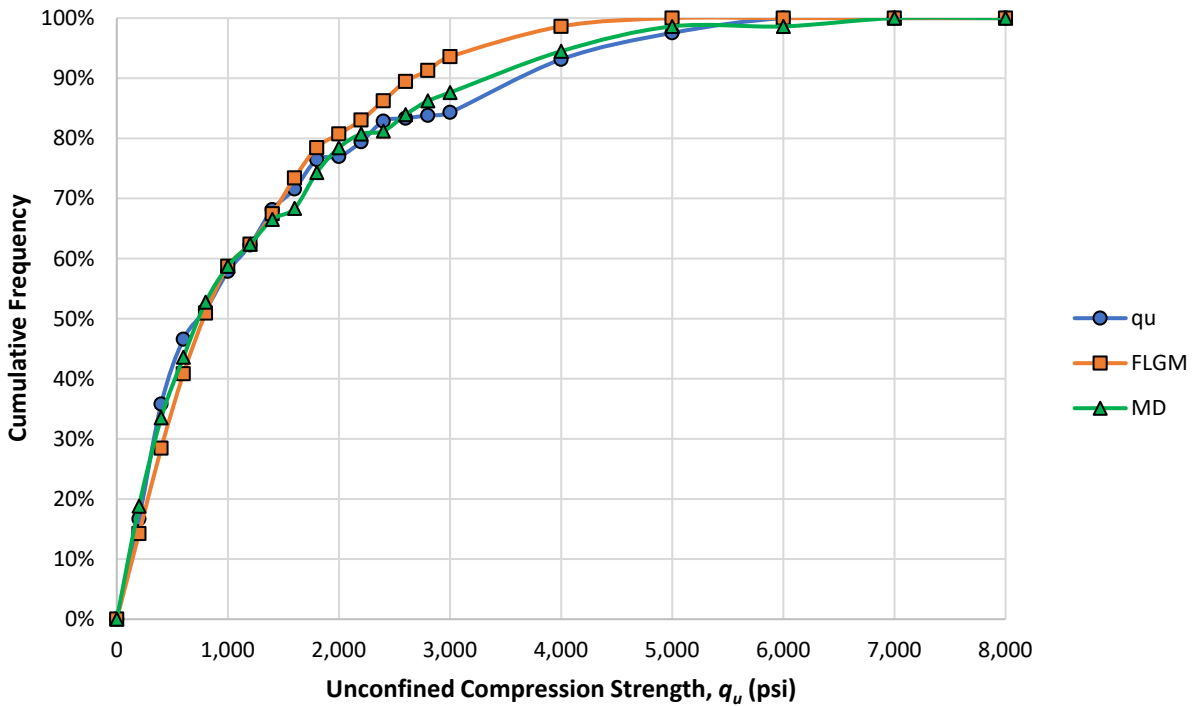


Figure 4-6. Cumulative frequency distributions for estimated  $q_u$  values (MD and FLGM) compared to measured  $q_u$  values.

From Table 4-3 along with Figures 4-5 and 4-6, it is observed that both  $q_u$  estimates from  $q_{st}$  are quite accurate. Both correlations indicated similar strength distributions as the measured  $q_u$  samples. FLGM showed a similar mean and a nearly identical strength range whereas MD showed a nearly identical mean and CV but a wider range of strengths than the measured  $q_u$  samples. The latter is likely due to the lower than typical MD split tension strengths for the higher dry unit weight ranges compared to the trends observed throughout Florida. This would cause the developed correlation to overestimate  $q_u$  as  $q_{st}$  increases which can be observed in Figure 4-4. Consequently, the FLGM correlation was chosen to estimate  $q_u$  at the Miami-Dade site to increase the number of  $q_u$  strengths available for analyses.

### 4.3 Rock Core Layering

From the  $q_u$ - $q_{st}$  correlation, 218  $q_u$  estimates were derived which provides a total of 422  $q_u$  strength assessments available for analyses. Table 4-4 summarizes the whole  $q_u$  strength assessment for the project site research project.

Table 4-4. Summary of  $q_u$  statistics for the Miami-Dade ACIP pile locations.

Statistics	$q_u$ (psi)
Mean	1,206
Median	779
Std. Dev.	1,199
CV	0.99
Maximum	5,172
Minimum	24
Count	422

Figure 4-7 provides the depth profile of the rock strength assessments ( $q_u$ ) for the project site with proposed layering, along with means, max, min and counts for each layer identified in Table 4-5.

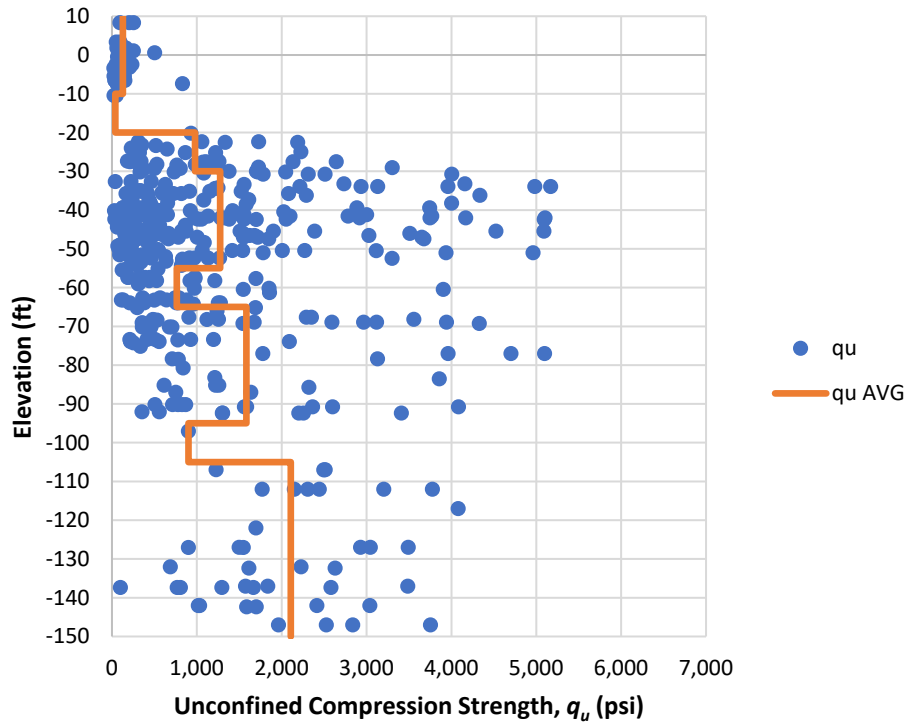


Figure 4-7. Depth profile of  $q_u$  with the average  $q_u$  for identified layering.

Table 4-5. General strength layering at the Miami-Dade ACIP pile site.

Elevations		Unconfined Compressive Strength, $q_u$ (psi)			
El <sub>top</sub> (ft)	El <sub>bot</sub> (ft)	Mean	Max	Min	Count
10	-10	128	832	24	43
-10	-20	40	53	26	2
-20	-30	979	3,304	185	35
-30	-55	1,275	5,172	32	192
-55	-65	764	3,906	112	41
-65	-95	1,583	5,099	212	68
-95	-105	902	902	902	1
-105	-150	2,107	4,081	101	40

From Figure 4-7 and Table 4-5, it is observed that variable strength with layering is present on the site. Evidently, lower strength rock was collected in the elevation range from 10 to -10 feet, which is where the tops of the piles generally were located. In the elevation range of -10 to -20 feet, only two samples were collected with strengths of 26 psi and 56 psi. This strength range is representative of the extremely weathered synthetic limestone cored in FDOT project BDV31-820-006 (McVay and Rodgers, 2019). It is also worth mentioning that these core samples were collected at an elevation of 10.5 feet, which the elevation represents the midspan of the core run (this is the case for all rock core elevations). Therefore, it is reasonable that no samples were collected in this elevation range. At elevations -20 to -30 feet, 35 samples were collected, and the strength began to significantly increase compared to the cores collected at higher elevation. At elevations -30 to -55 feet, the most core samples (192) were collected, and the strength continued to increase compared to the core samples collected in higher elevations. In the elevation range -55 to -65 feet, the strength of rock and number of samples collected per linear foot began to decrease compared to elevation range -30 to -55 feet. Between elevations -65 to -95 feet, the strength of rock began to increase, but the number of core samples collected per linear foot continued to decrease. In elevation range -95 to -105 feet, the strength of rock decreased again, and only one sample was collected. Again, it is possible that this sample could have been recovered in the elevation range above because it bordered both ranges. In the lowest elevation range, -105 to -150 feet, the average strength of rock was the highest, but the samples collected per linear foot were less than the other higher strength ranges, -30 to -55 feet and -65 to -95 feet. This may be due to fewer core borings completed within the elevation range.

At each of the test pile locations, 16 to 18 ACIP production piles close to the test pile were analyzed. Any MWD data point with a specific energy value over 1,250 psi was considered rock (the  $e$  threshold of 1,250 psi will be discussed later) and a  $q_u$  estimate was made using the rock auger equation from FDOT Project BDV31-977-20 (McVay and Rodgers, 2016) and Rodgers et al. (2017 and 2018). The rock auger equation was considered valid for  $q_u$  estimation because the ACIP pile specific energy-side shear correlation presented in Chapter 3 indicated the same relationship for ACIP pile rock augers and drilled shaft rock augers. Figures 4-8 through 4-10 present the MWD estimated  $q_u$  strengths for ACIP Test Piles I-395 TP-B, I-395 TP-C, and Signature Bridge TP-D, respectively, as well as the rock core strengths from the core specimens recovered within a radius of 500 feet from each of the test piles. Also included in the plots are percentages of MWD  $q_u$  estimates recorded within 5-foot layers starting at the tops of the piles. For example, 16 piles were analyzed close to Test Pile B with MWD measurements provided for

every 1 cm of penetration. Therefore, each 5-foot layer at the TP-B location had total of 2,438 possible  $q_u$  data points that could have been recorded from the 16 piles. Based on the strength of the material drilled, some of the data may be eliminated if the specific energy value was below 1,250 psi. The percentages in the plots represent the percentage of data points that were above the specific energy threshold within each 5-foot layer from all 16 production piles analyzed. For the TP-B location (Figure 4-8) in the top five foot layer, 20% is reported. This indicates that out of the 2,438 possible strength assessments for the layer, only 477 of the MWD specific energy strength assessments recorded were above 1,250 psi. This indicates that some rock is present within the elevation range but that core recoveries and the RQD from traditional rock coring would likely be low. It is important to note that the core samples had to be at least 4 inches in length to test in  $q_{st}$  and 8 inches in length to test in  $q_u$  based on their diameter of 4 inches. At the smallest testable sample size of 4 inches, MWD would have produced 10.2 measurements. However, the MWD measurements logged in the figures are not necessarily sequential with depth or even from the same pile location. For a single pile, a minimum of 11 MWD data points would have to be logged sequentially with depth for a  $q_{st}$  sample to be recovered and 21 sequential data points would have to be logged for a  $q_u$  sample. This equates to a maximum of only 43  $q_{st}$  samples or 22  $q_u$  samples that could have possibly been recovered from the 16 MWD sampled locations which is quite low. Observing Figures 4-8 through 4-10 within the elevation range of -10 to -20 feet where only two rock cores were collected, the MWD percentages are typically the lowest indicating agreement between the lack of core samples recovered and the MWD assessment within the elevation range.

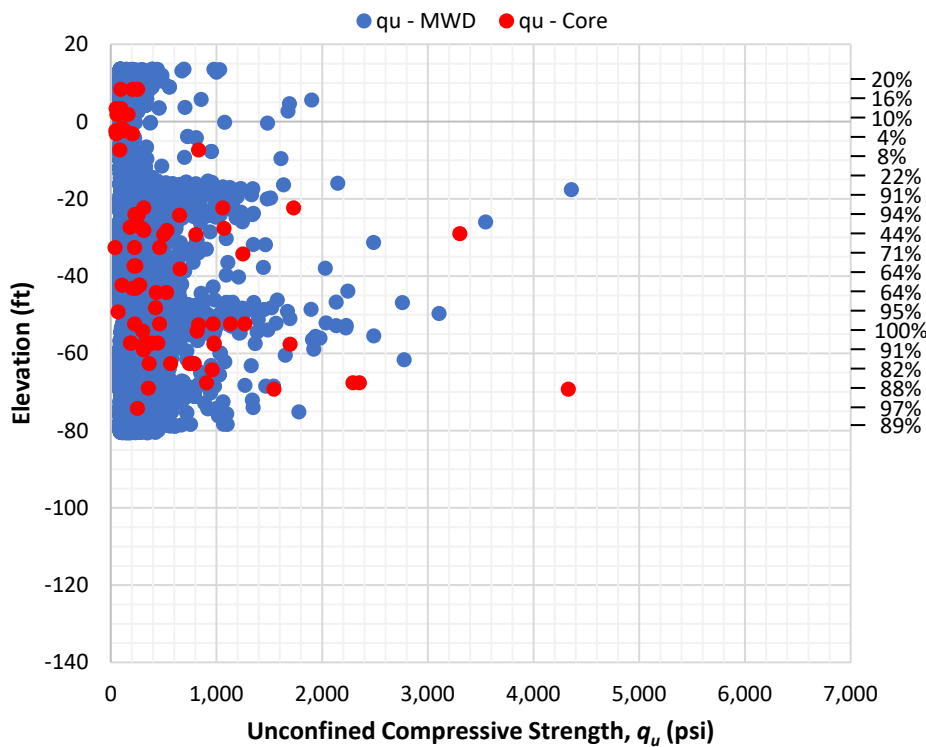


Figure 4-8. Depth profile of  $q_u$  core samples compared to MWD specific energy at TP-B.

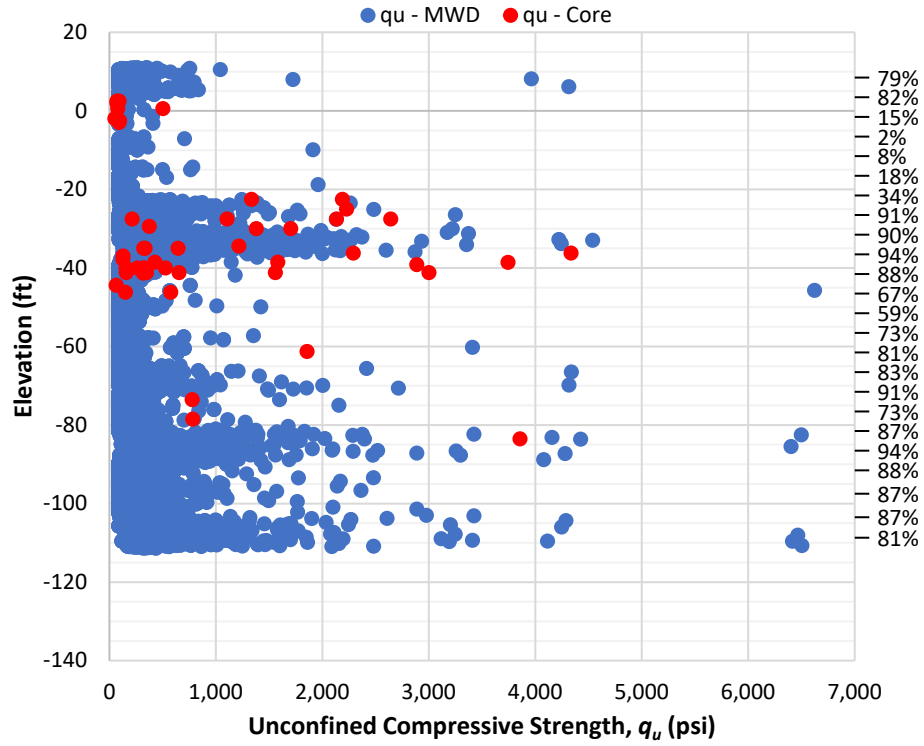


Figure 4-9. Depth profile of  $q_u$  core samples compared to MWD specific energy at TP-C.

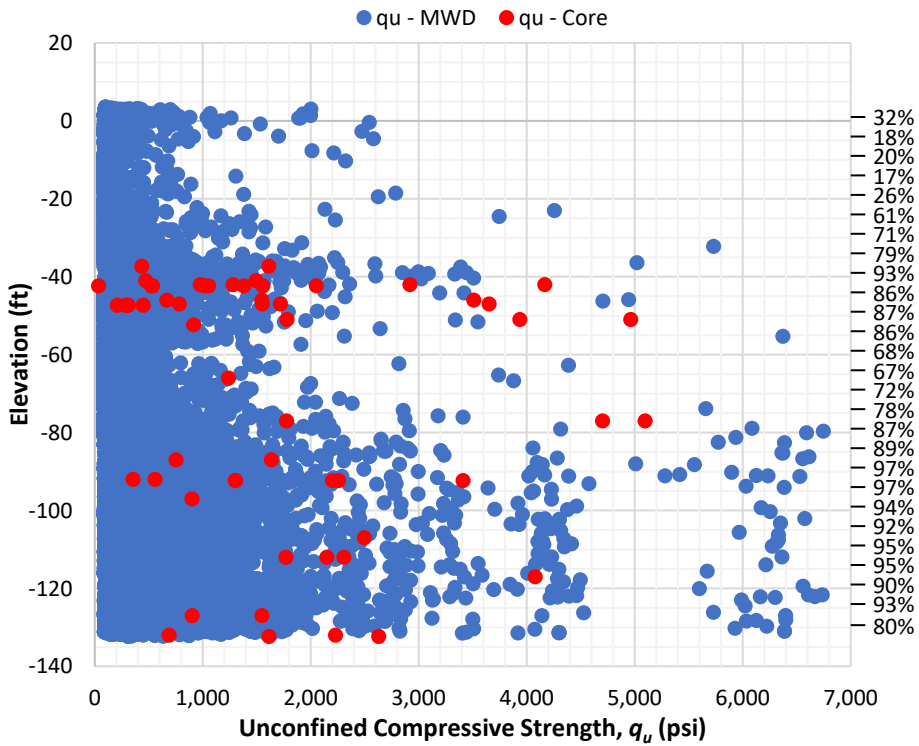


Figure 4-10. Depth profile of  $q_u$  core samples compared to MWD specific energy at TP-D.

Also observed in Figures 4-8 through 4-10 is that the MWD  $q_u$  data points generally agree with the recovered rock core strength range and layering. The rock cores were generally collected in the elevation ranges in which MWD identified that higher strength geomaterial was present and had a higher percentage of reported values. Additionally, in all cases, the general layering identified in Figure 4-7 was also observed for the test pile locations by MWD. At Test Piles B and C, the layering trends were more defined but could also be observed at the Test Pile D location. This indicated that a correlated structure likely exists throughout the site with expected variability with zones that are likely present within the investigated project location. Table 4-6 summarizes the statistics of the rock core strengths at each test pile location and compares them to the statistics for the entire site. In Table 4-6, the TP-C statistics are closer to the entire site statistics compared to the other two test pile locations. The MWD  $q_u$  profile in Figure 4-9 also more closely resembles the  $q_u$  profile from the core strengths in Figure 4-7, compared to the other test pile locations. This is likely due to Test Pile C being located in the middle of the investigated area which shares attributes of Test Pile D located east of Test Pile C and Test Pile B located west of Test Pile D, suggesting zonal changes. Table 4-6 indicates that the strength of rock is decreasing moving east-to-west which supports this observation.

Table 4-6.  $q_u$  statistics for each test pile location compared to the overall site statistics.

Statistics	Unconfined Compressive Strength, $q_u$ (psi)			
	MD	TP-B	TP-C	TP-D
Mean	1,206	573	1,059	1,708
Median	779	312	528	1,575
Std Dev	1,199	735	1,162	1,155
CV	0.99	1.28	1.10	0.68
Maximum	5,172	4,330	4,337	5,099
Minimum	24	50	53	36
Count	422	58	45	67

Based on these observations and the observations made in Chapter 3, MWD appears to be accurately identifying the strength of the geomaterial as well as the layering at the ACIP pile bridge site. Specifically, MWD showed similar strength layering compared to the SPT borings and rock core borings, and the specific energy recorded in mobilized load test layers showed excellent correlation ( $R^2 = 0.99$ ) with the measured side shear. To further investigate the accuracy of the MWD strength assessments prior to analyzing the production piles, FB MultiPier modeling was completed for Test Piles SR-836 TP-A and I-395 TP-C.

#### 4.4 *FB MultiPier Modeling*

FB MultiPier modeling was completed for SR-836 Test Pile A and I-395 Test Pile C. Both of these test piles were fully mobilized in the upper pile segment. The upper pile segments were loaded in isolated shear (i.e., no pile tip influence) which is ideal for comparison with MWD specific energy. This is because MWD specific energy is correlated to pile side shear as presented in Chapter 3. Therefore, modeling the upper pile segments using the MWD data provides a direct comparison of the MWD predicted side shear behavior versus the load test measured side shear behavior without the influence of the pile tip. Note: The specific energy threshold of 1,250 psi was not used during the MultiPier trials ( $e_{\text{threshold}} = 0$  psi).

#### 4.4.1 SR-836 Test Pile A

Modeling begins with SR-836 Test Pile A as the geomaterial present was predominantly rock, indicated by the SR-836 TP-A boring (Figure 4-11), and MWD data was available in the footprint of the test pile. Table 4-7 provides the modeling input for the pile properties in which the steel inputs are identical to the actual test pile layout included in the load test reports and the concrete compressive strength ( $f'_c$ ) and modulus ( $E_c$ ) are derived from the pile rigidity ( $AE$ ) used to analyze the load test.

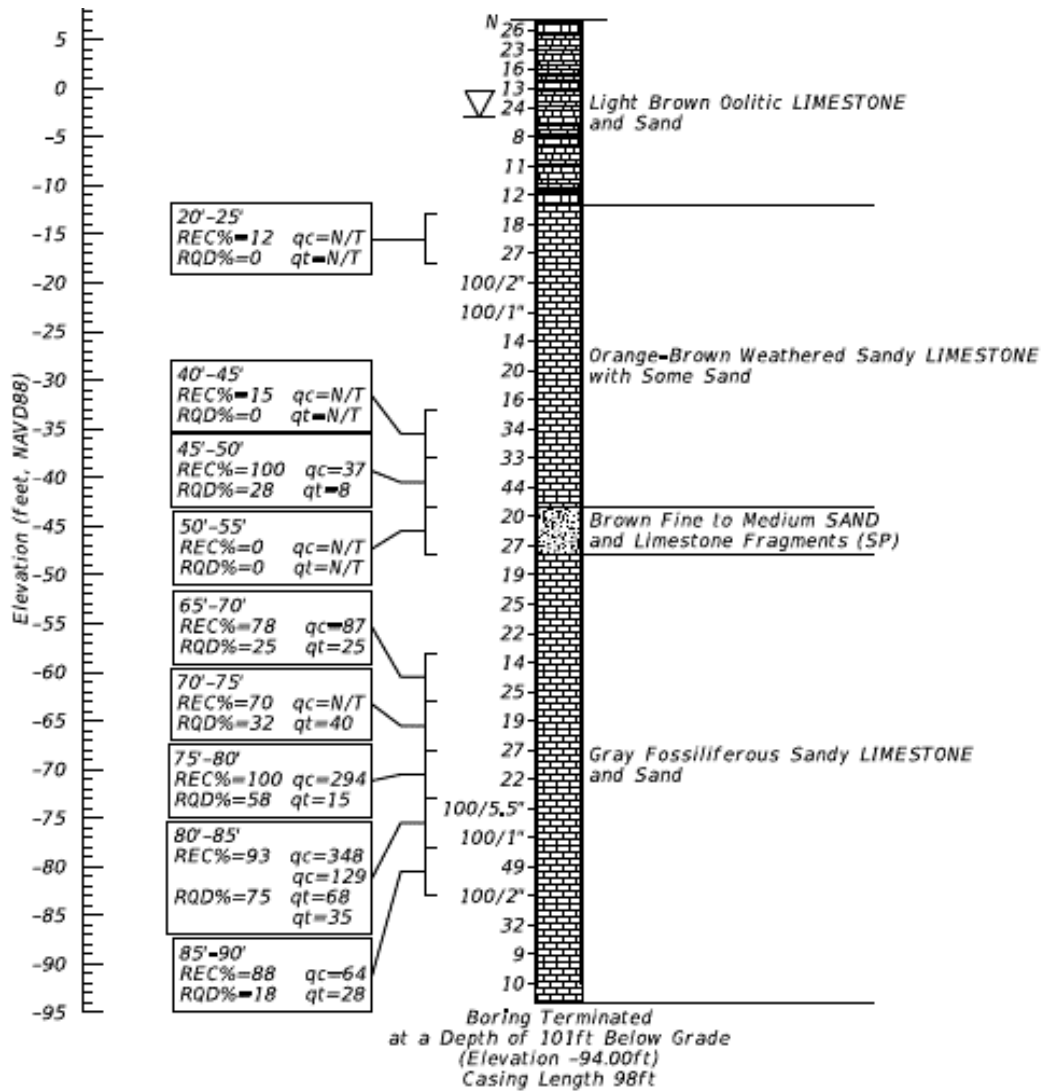


Figure 4-11. SR-836 Test Pile A boring.

Table 4-7. SR-836 TP-A MultiPier pile modeling input.

SR-836 Test Pile A MultiPier Pile Modeling Input	
Concrete, f'c (ksi)	3.5
Concrete, Ec (ksi)	3,400
Steel, fy (ksi)	60
Steel, Es (ksi)	29,000
Bar Type	11
Number of Bars	8
Bar Area (in <sup>2</sup> )	1.56
Cage Diameter (in)	21
Bar Spacing (in)	8.247

Table 4-8 provides the soil modeling inputs used for SR-836 Test Pile A. Layers 1 and 14 are modeled as sand with no shear strength as these layers are not relevant to the pile behavior. Layer 1 was used to provide 5-foot increments between pile nodes to ensure each node was located in a strain gauge location. The top node represents the top of the pile above the ground surface elevation (GSE) and the bottom node (Layer 14) represents the location of loading from the Load Test Assembly (LTA). Layers 2 through 13 were modeled based on MWD measurements ( $e$ ,  $q_u$ ,  $f_s$ , and  $\gamma_d$ ) and the pile diameters were derived from measurements provided in the load test report obtained from thermal integrity profiling (TIP). For example, in Layer 2 MWD produced an average specific energy value of  $e = 899$  psi which produces a  $q_u = 63$  psi based on the methods developed in Rodgers et al. (2017) for rock augers, a dry unit weight of 79.5 pcf based on the relationship provided in Figure 4-3, a side shear value for the layer of  $f_s = 2.24$  ksf based on the correlation developed in Chapter 3, and the pile diameter of 34.6 inches was derived from the TIP data included in the load test report. This was done for each of the layers, 2 through 13 in which the layering is identical to the original load test layers defined by each strain gauge elevation. The ground water table (GWT) elevation of -3 feet was based on the load test reported GWT.

Table 4-8. SR-836 Test Pile 2 – MultiPier soil modeling input.

SR-836 Test Pile 2 - MultiPier Soil Modeling Input											
Layer	El <sub>top</sub> (ft)	El <sub>bot</sub> (ft)	Dia. (in)	e (psi)	Model	$\gamma_d$ (pcf)	$q_u$ (psi)	$f_s$ (ksf)	SPT	$v$	
1	4.3	3.6	34.6	N/A	Sand	62.4	0	0.00	N/A	N/A	
2	3.6	-0.7	34.6	899	Limestone	79.5	63	2.24	N/A	N/A	
3	-0.7	-5.7	33.6	619	Limestone	75.3	44	1.72	N/A	N/A	
4	-5.7	-10.7	33.1	749	Limestone	77.5	53	1.97	N/A	N/A	
5	-10.7	-15.7	33.0	978	Limestone	80.6	69	2.38	N/A	N/A	
6	-15.7	-20.7	32.7	1,732	Limestone	87.3	117	3.57	N/A	N/A	
7	-20.7	-25.7	32.1	5,890	Limestone	103.3	353	8.48	N/A	N/A	
8	-25.7	-30.7	32.6	2,512	Limestone	92.3	168	4.64	N/A	N/A	
9	-30.7	-35.7	33.1	2,501	Limestone	92.1	166	4.63	N/A	N/A	
10	-35.7	-40.7	32.6	1,883	Limestone	88.6	129	3.78	N/A	N/A	
11	-40.7	-45.7	30.8	3,303	Limestone	95.6	213	5.63	N/A	N/A	
12	-45.7	-50.7	30.0	4,098	Limestone	98.4	257	6.56	N/A	N/A	
13	-50.7	-55.7	30.1	2,491	Limestone	92.2	168	4.61	N/A	N/A	
14	-55.7	-95.7	N/A	N/A	Sand	62.4	0	0.00	N/A	N/A	



Figure 4-12 provides the modeled layering as well as the bottom-up loading that was provided by the LTA. For SR-836 Test Pile A, a maximum load of 2,290 kips was provided by the LTA. This produced an LTA recorded upward expansion of 2.1 inches and a top of pile displacement of 1.87 inches during the final loading phase, Load Step 14. As the pile was unloaded, the LTA continued to expand upward and reached a maximum expansion of 2.5 inches and a top of pile displacement of 2.28 inches was measured, indicating the pile continued to creep upward after loading.

For the MultiPier simulation, a prescribed upward displacement of 2.1 inches was used at the LTA location as shown in Figure 4-12. The prescribed displacement resulted in an LTA load of 1,921 kips and a pile top displacement of 1.87 inches which is the exact displacement measured during the load test. Based on the MultiPier model, MWD indicates the pile was likely fully mobilized between Load Steps 12 and 13 which induced a load of 1,989 kips and 2,171 kips respectively during the test. Based on the observed creep at the end of the load test, it is very likely the pile was fully mobilized during Load Step 12, but as a result of the short load duration (i.e., ten minutes) the load transmission throughout the entire pile did not occur prior to the next load increment of 2,171 kips in Load Step 13. Discussed in Chapter 3, each of the test piles experienced curing induced residual stresses that could not be accurately quantified because strain readings were not taken after the instrumented cage was placed in the grout-filled shaft. These stresses are locked into the pile and must be overcome before load transmission can take place throughout the remainder of pile segments, above the residual stress concentrated locations. For SR-836 Test Pile A, the load test had to be broken up into three larger layers due to the residual stress effects. Figure 4-13 provides the strain activity vs the LTA load for TP-A. In Figure 4-13, during Load Step 9, an LTA load of 1,500 kips was sustained for one hour in which the strain continuously increased in multiple strain gauge locations. UF researchers suspect this pile behavior is the applied LTA load overcoming the residual stresses that were locked into this portion of the pile, which delayed transmission of the load up the remainder of the pile, thereby explaining the creep behavior observed at the end of the load test. To further investigate this, a prescribed displacement of 2.5 inches was induced at the LTA for the modeled pile, similar to the actual unloading LTA behavior, which resulted in the same modeled load of 1,921 kips with a top of pile displacement of 2.27 inches which is nearly identical to the 2.28 inches of top pile displacement measured during the load test. The T-Z curves in Figure 4-14 also support these observations as they indicate the pile was mobilized between Load Steps 12 and 13, indicated in the black portions of the colored T-Z curves. These observations indicate the MWD rock strength assessments are highly accurate as the MWD modeled pile behavior was nearly identical to the actual pile behavior observed during the load test.

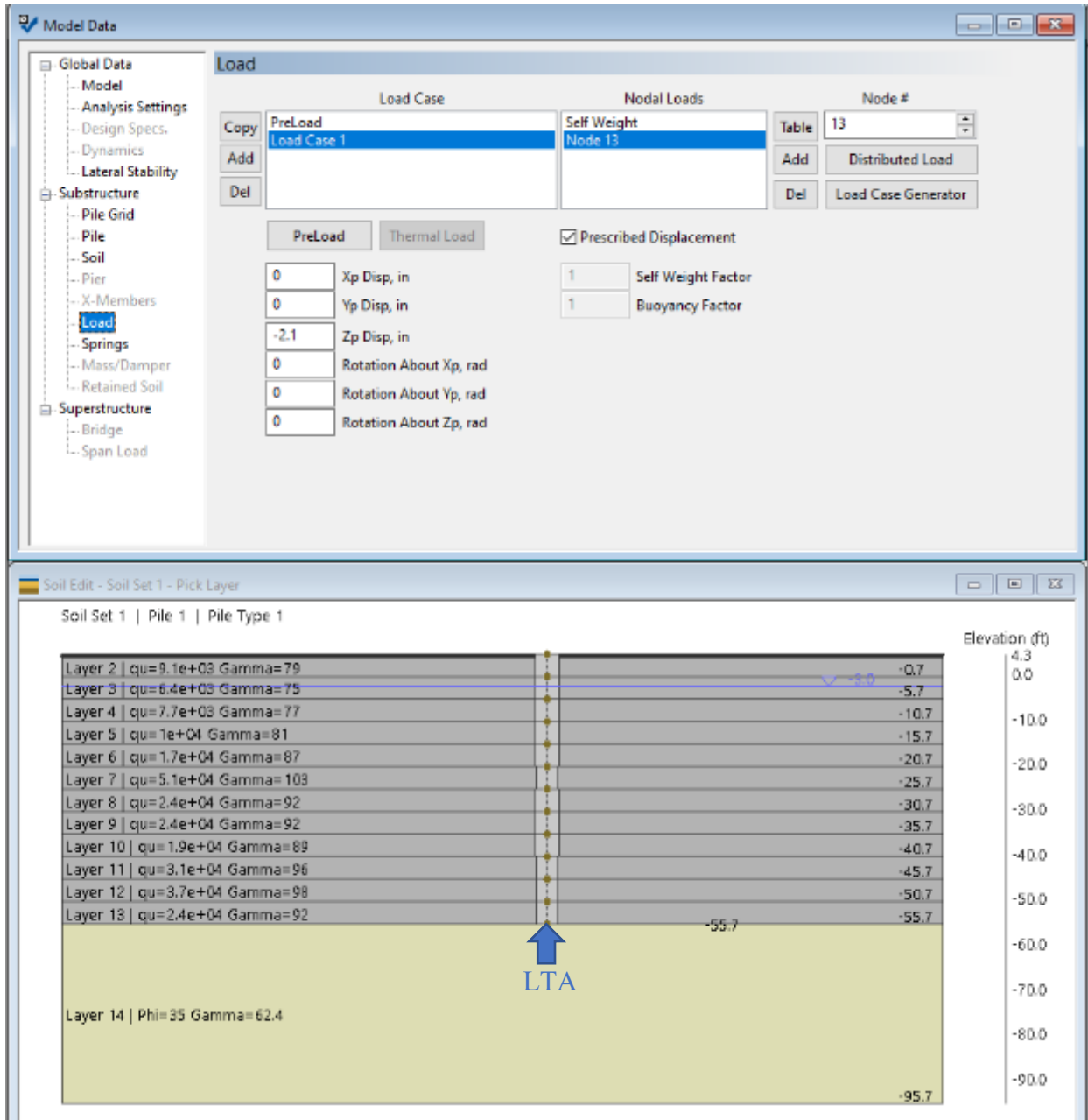


Figure 4-12. SR-836 Test Pile A – MultiPier soil model.

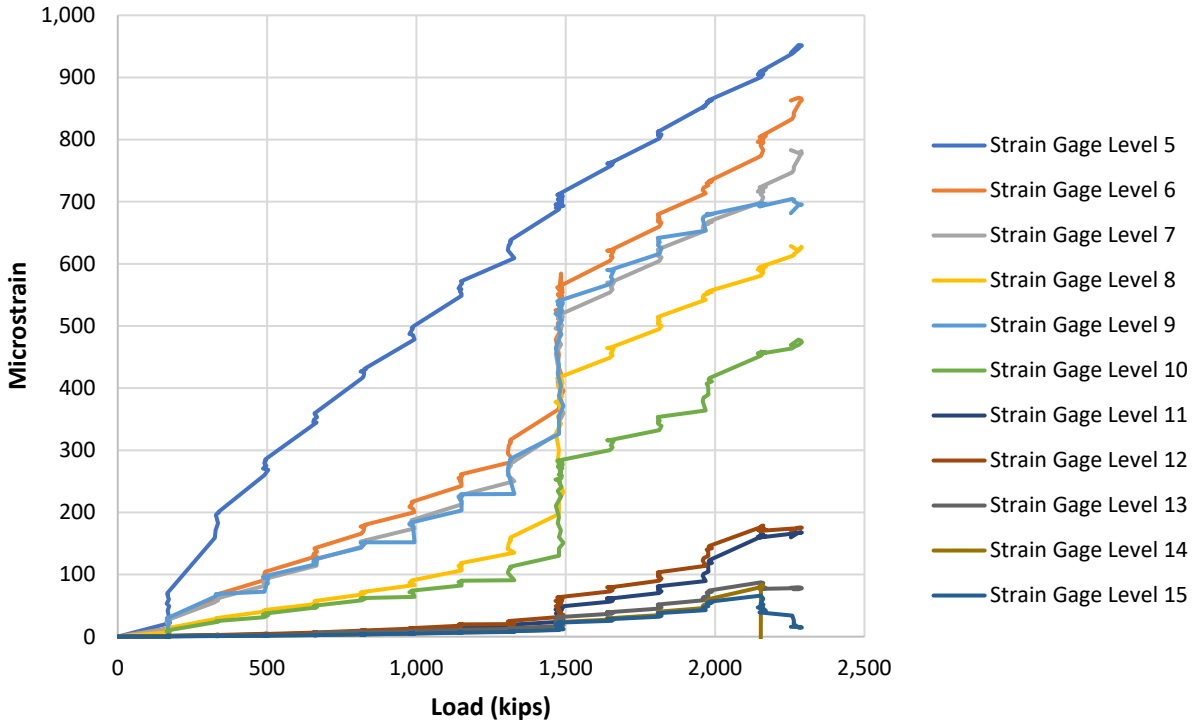


Figure 4-13. Strain vs. applied load for SR-836 Test Pile A.

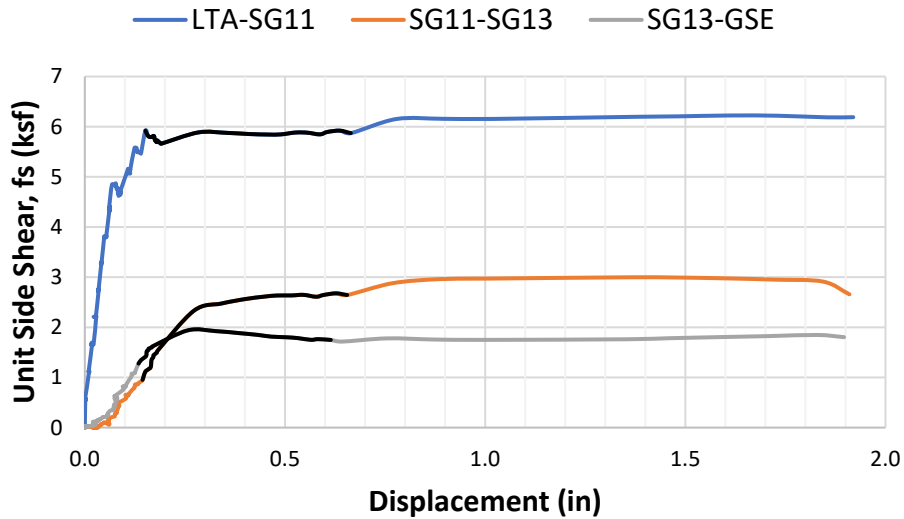


Figure 4-14. SR-836 Test Pile A T-Z curves with all data points plotted.

#### 4.4.2 I-395 Test Pile C

The second Test Pile modeled was I-395 Test Pile C. Figure 4-15 provides the TP-1 boring in which layers of sand, rock, and IGM are all present. Therefore, TP-C provided an excellent opportunity to compare MWD measurements recorded in layers of geomaterial other than rock to

begin delineating what range of specific energy should be discounted as rock during the production pile capacity QA/QC procedure.

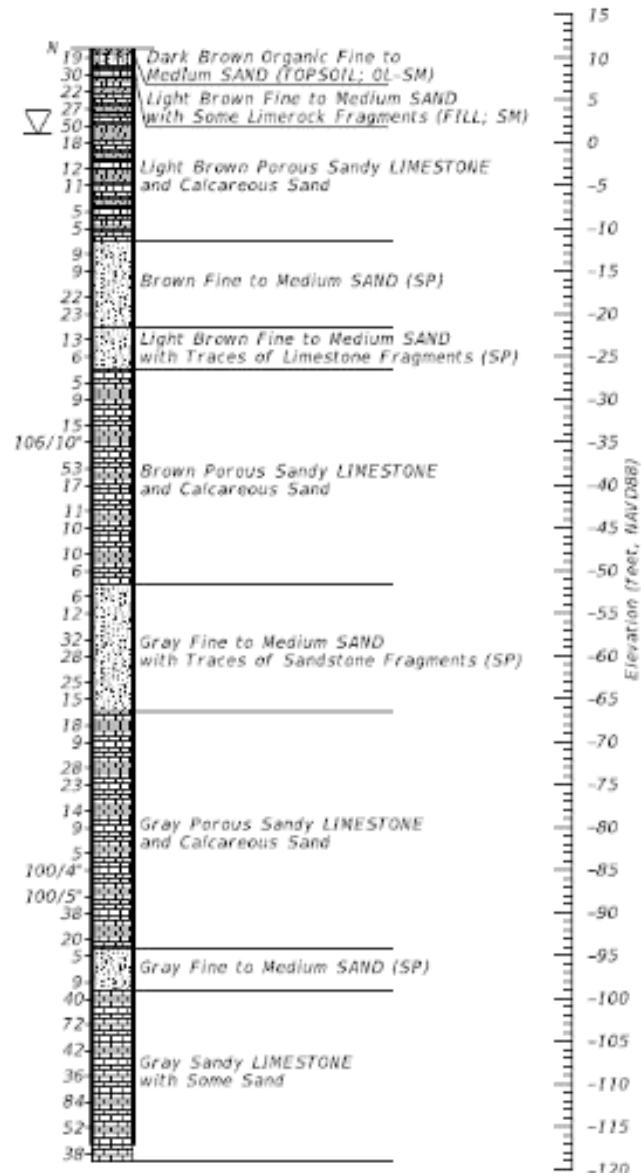


Figure 4-15. I-395 Test Pile C boring.

Table 4-9 provides the modeling input for the pile properties in which the steel inputs are identical to the actual test pile layout included in the load test report and the concrete compressive strength ( $f'_c$ ) and modulus ( $E_c$ ) are derived from the pile rigidity ( $AE$ ) used to analyze the load test.

Table 4-9. I-395 Test Pile C pile modeling input.

I-395 Test Pile C MultiPier Pile Modeling Input	
Concrete, f'c (ksi)	3.7
Concrete, Ec (ksi)	3,500
Steel, fy (ksi)	60
Steel, Es (ksi)	29,000
Bar Type	11
Number of Bars	8
Bar Area (in <sup>2</sup> )	1.56
Cage Diameter (in)	21
Bar Spacing (in)	8.247

Modeling TP-C was an iterative process which began assuming all geomaterial was limestone. Table 4-10 provides the soil model input for the first iteration. The layering is identical to the strain gauge layers from the load test and the GWT is modeled at an elevation of +1 ft based on the load test report. During the actual load test the LTA produced a maximum load of 2,261 kips with an LTA upward expansion of 2.9 inches and a top of pile displacement of 2.44 inches. From the first modeled iteration a prescribed LTA displacement of 2.9 inches was induced which resulted in a maximum LTA load of 2,653.5 kips and a top of pile displacement of 2.29 inches. This indicates the first model overestimated the capacity of the pile by assuming all geomaterial was limestone. This further suggests that the geomaterial present at TP-C was not all rock as indicated by the TP-C boring.

Table 4-10. I-395 Test Pile C soil input with all layers modeled as limestone.

I-395 Test Pile C - MultiPier Soil Modeling Input											
Layer	El <sub>top</sub> (ft)	El <sub>bot</sub> (ft)	Dia. (in)	e (psi)	Model	$\gamma_d$ (pcf)	q <sub>u</sub> (psi)	f <sub>s</sub> (ksf)	SPT	v	
1	11.5	8.9	34.0	N/A	Sand	62.4	0	0.00	N/A	N/A	
2	8.9	6.5	34.0	2,143	Limestone	90.3	146	4.15	N/A	N/A	
3	6.5	1.5	31.8	3,498	Limestone	96.8	230	5.86	N/A	N/A	
4	1.5	-3.5	31.8	1,051	Limestone	81.5	74	2.51	N/A	N/A	
5	-3.5	-8.5	31.8	496	Limestone	72.9	36	1.47	N/A	N/A	
6	-8.5	-13.5	31.8	642	Limestone	75.7	46	1.77	N/A	N/A	
7	-13.5	-18.5	31.8	841	Limestone	78.8	60	2.14	N/A	N/A	
8	-18.5	-23.5	31.8	802	Limestone	78.3	57	2.07	N/A	N/A	
9	-23.5	-28.5	31.8	1,337	Limestone	84.4	93	2.97	N/A	N/A	
10	-28.5	-33.5	30.0	1,968	Limestone	89.2	135	3.91	N/A	N/A	
11	-33.5	-38.5	30.0	8,794	Limestone	109.4	515	11.26	N/A	N/A	
12	-38.5	-43.5	30.0	1,980	Limestone	89.3	136	3.92	N/A	N/A	
13	-43.5	-48.5	31.8	1,013	Limestone	81.0	72	2.44	N/A	N/A	
14	-48.5	-53.5	31.8	870	Limestone	79.2	62	2.19	N/A	N/A	
15	-53.5	-58.5	31.8	1,111	Limestone	82.1	78	2.61	N/A	N/A	
16	-58.5	-63.5	31.8	1,234	Limestone	83.4	87	2.81	N/A	N/A	
17	-63.5	-68.5	31.8	1,262	Limestone	83.7	89	2.85	N/A	N/A	
18	-68.5	-73.5	31.8	1,639	Limestone	86.9	114	3.43	N/A	N/A	
19	-73.5	-78.5	32.5	2,836	Limestone	94.0	190	5.06	N/A	N/A	
20	-78.5	-83.5	31.0	1,808	Limestone	88.2	125	3.68	N/A	N/A	
21	-83.5	-88.5	N/A	N/A	Sand	62.4	0	0.00	N/A	N/A	

From the TP-C load test, the T-Z curves (Figure 4-16) indicated lower strength geomaterial was present in elevation ranges +1.5 to -18.5 feet (SG10 to SG14) and -43.5 to -63.5 feet (SG19 to SG23) which agrees with the layering indicated in the TP-C boring (Figure 4-15). Consequently, the second modeled iteration considered all layers as limestone except for the elevation ranges identified. For the weaker layers identified, the load test T-Z curve data was used as indicated in Table 4-11. Note: The T-Z curves in Figure 4-16 only show measurements at the end of each load step whereas the TP-C T-Z curves from Chapter 3 showed every data point recorded.

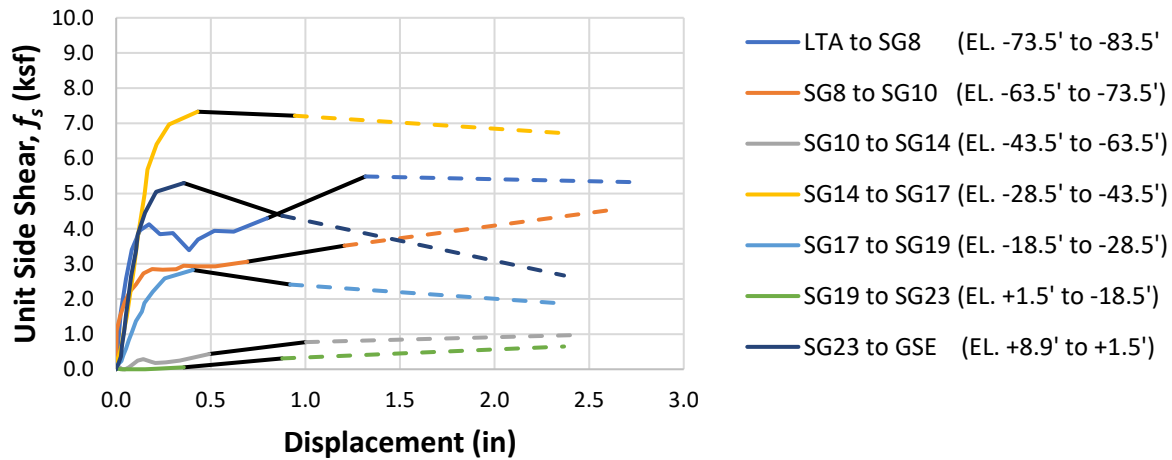


Figure 4-16. I-395 Test Pile C T-Z curves for the upper pile segment with Load Step 13 indicated in black and Load Step 14 indicated by dashed lines.

Table 4-11. I-395 Test Pile C soil input with layers modeled as limestone with load test T-Z curve data used in layers 4 through 7 and 13 through 16.

I-395 Test Pile C - MultiPier Soil Modeling Input										
Layer	El <sub>top</sub> (ft)	El <sub>bot</sub> (ft)	Dia. (in)	e (psi)	Model	$\gamma_d$ (pcf)	$q_u$ (psi)	$f_s$ (ksf)	SPT	$\nu$
1	11.5	8.9	34.0	N/A	Sand	62.4	0	0.00	N/A	N/A
2	8.9	6.5	34.0	2,143	Limestone	90.3	146	4.15	N/A	N/A
3	6.5	1.5	31.8	3,498	Limestone	96.8	230	5.86	N/A	N/A
4	1.5	-3.5	31.8	1,051	TZ Curves	81.5	74	N/A	N/A	N/A
5	-3.5	-8.5	31.8	496	TZ Curves	72.9	36	N/A	N/A	N/A
6	-8.5	-13.5	31.8	642	TZ Curves	75.7	46	N/A	N/A	N/A
7	-13.5	-18.5	31.8	841	TZ Curves	78.8	60	N/A	N/A	N/A
8	-18.5	-23.5	31.8	802	Limestone	78.3	57	2.07	N/A	N/A
9	-23.5	-28.5	31.8	1,337	Limestone	84.4	93	2.97	N/A	N/A
10	-28.5	-33.5	30.0	1,968	Limestone	89.2	135	3.91	N/A	N/A
11	-33.5	-38.5	30.0	8,794	Limestone	109.4	515	11.26	N/A	N/A
12	-38.5	-43.5	30.0	1,980	Limestone	89.3	136	3.92	N/A	N/A
13	-43.5	-48.5	31.8	1,013	TZ Curves	81.0	72	N/A	N/A	N/A
14	-48.5	-53.5	31.8	870	TZ Curves	79.2	62	N/A	N/A	N/A
15	-53.5	-58.5	31.8	1,111	TZ Curves	82.1	78	N/A	N/A	N/A
16	-58.5	-63.5	31.8	1,234	TZ Curves	83.4	87	N/A	N/A	N/A
17	-63.5	-68.5	31.8	1,262	Limestone	83.7	89	2.85	N/A	N/A
18	-68.5	-73.5	31.8	1,639	Limestone	86.9	114	3.43	N/A	N/A
19	-73.5	-78.5	32.5	2,836	Limestone	94.0	190	5.06	N/A	N/A
20	-78.5	-83.5	31.0	1,808	Limestone	88.2	125	3.68	N/A	N/A
21	-83.5	-88.5	N/A	N/A	Sand	62.4	0	0.00	N/A	N/A

The modeled pile again used a prescribed displacement of 2.9 inches at the LTA which resulted in a maximum applied load 2,179.3 kips and a top of pile displacement of 2.43 inches which is nearly identical to the 2.44 inches observed during the load test. Observing the tabular data in Table 4-11 indicates that Layer 8 was nearly identical to Layer 7 (modeled using the T-Z curves) in strength based on the specific energy (841 psi vs. 802 psi) and the average SPT blow counts (N = 12 vs. N = 12) from the four SPT borings considered for TP-C in Chapter 3. Layer 17 was also nearly identical to Layer 16 (modeled using the T-Z curves) in strength based on the specific energy (1,234 psi vs. 1,262 psi) and the average SPT blow counts (N = 20 vs. N = 18) from the four SPT borings considered for TP-C in Chapter 3. It is entirely possible these similar layers indicated by MWD and SPT behaved the same during the actual load test, however this behavior was not captured as larger load test layers had to be used for proper load test analyses due residual stresses as explained in Chapter 3. Consequently, for the third iteration Layer 8 was modeled using the T-Z curves from SG19 to SG23 and Layer 17 was modeled using the T-Z curves from SG10 to SG14 as indicated in Table 4-12.

Table 4-12. I-395 Test Pile C soil input with layers modeled as limestone with load test T-Z curve data used in layers 4 through 8 and 13 through 17.

I-395 Test Pile C - MultiPier Soil Modeling Input										
Layer	El <sub>top</sub> (ft)	El <sub>bot</sub> (ft)	Dia. (in)	e (psi)	Model	$\gamma_d$ (pcf)	q <sub>u</sub> (psi)	f <sub>s</sub> (ksf)	SPT	v
1	11.5	8.9	34.0	N/A	Sand	62.4	0	0.00	N/A	N/A
2	8.9	6.5	34.0	2,143	Limestone	90.3	146	4.15	N/A	N/A
3	6.5	1.5	31.8	3,498	Limestone	96.8	230	5.86	N/A	N/A
4	1.5	-3.5	31.8	1,051	TZ Curves	81.5	74	N/A	N/A	N/A
5	-3.5	-8.5	31.8	496	TZ Curves	72.9	36	N/A	N/A	N/A
6	-8.5	-13.5	31.8	642	TZ Curves	75.7	46	N/A	N/A	N/A
7	-13.5	-18.5	31.8	841	TZ Curves	78.8	60	N/A	N/A	N/A
8	-18.5	-23.5	31.8	802	TZ Curves	78.3	57	N/A	N/A	N/A
9	-23.5	-28.5	31.8	1,337	Limestone	84.4	93	2.97	N/A	N/A
10	-28.5	-33.5	30.0	1,968	Limestone	89.2	135	3.91	N/A	N/A
11	-33.5	-38.5	30.0	8,794	Limestone	109.4	515	11.26	N/A	N/A
12	-38.5	-43.5	30.0	1,980	Limestone	89.3	136	3.92	N/A	N/A
13	-43.5	-48.5	31.8	1,013	TZ Curves	81.0	72	N/A	N/A	N/A
14	-48.5	-53.5	31.8	870	TZ Curves	79.2	62	N/A	N/A	N/A
15	-53.5	-58.5	31.8	1,111	TZ Curves	82.1	78	N/A	N/A	N/A
16	-58.5	-63.5	31.8	1,234	TZ Curves	83.4	87	N/A	N/A	N/A
17	-63.5	-68.5	31.8	1,262	TZ Curves	83.7	89	N/A	N/A	N/A
18	-68.5	-73.5	31.8	1,639	Limestone	86.9	114	3.43	N/A	N/A
19	-73.5	-78.5	32.5	2,836	Limestone	94.0	190	5.06	N/A	N/A
20	-78.5	-83.5	31.0	1,808	Limestone	88.2	125	3.68	N/A	N/A
21	-83.5	-88.5	N/A	N/A	Sand	62.4	0	0.00	N/A	N/A

The same prescribed displacement of 2.9 inches at the LTA was used again which resulted in a maximum applied load of 2,041.9 kips with a top of pile displacement of 2.46 inches. Based on the results of the second and third modeled iterations, UF researchers suspected the mobilized load was in the range of 2,041.9 kips to 2,179.3 kips.

Because strength variability existed within each of the original T-Z curve layers (modeled iteration 2), based on MWD specific energy measurements, it is likely that the T-Z curve data

produced side shear resistance that was too low and not representative of the pile behavior for Layers 8 and 17. Consequently, for the fourth modeled iteration, T-Z curve data was only used in the same layers as iteration 2 (Table 4-11) and Layers 8 and 17 were now modeled as non-cohesive IGM (NC IGM) as indicated in Table 4-13. The SPT values were obtained from the four SPT borings within the vicinity of TP-1 as discussed in Chapter 3 with a Poisson's ratio of 0.25 used. MultiPier defines non-cohesive IGM as very dense granular material that includes residual, decomposed rock, and gravel which fits the descriptions of the materials in the TP-C SPT boring (Figure 4-15) that identified calcareous sand, fine to medium sand with limestone fragments, and fine to medium sand with sandstone fragments. Furthermore, the MWD estimated  $q_u$  strengths fall within the range of strengths measured while coring synthetic limestone representative of extremely weathered limestone (decomposed rock) in FDOT Project BDV31-820-006 (McVay and Rodgers, 2019; Rodgers et al., 2020; and Rodgers et al., 2021). On average the strength of the synthetic limestone was  $q_u = 56$  psi with core strengths ranging from 24 psi to 73 psi and MWD estimated strengths ranging from 35 psi to 95 psi on average from 12 different core runs. SPT testing was also conducted on the synthetic limestone with  $N = 24$  and  $N = 26$ . Figure 4-17 illustrates the synthetic limestone where it can be seen that the material can be broken by hand which would not be considered competent rock in a true assessment of RQD. The synthetic material when broken by hand appears to be fine to medium sand with limestone fragments which fits the TP-C boring descriptors. Therefore, it is likely that similar material should not be treated as competent limestone during the ACIP pile MWD QA/QC procedures and the use of non-cohesive IGM in the layers indicated is likely valid.



Figure 4-17. Synthetic limestone representing extremely weathered Florida limestone.



The fourth modeled iteration (Table 4-13) used a prescribed LTA displacement of 2.9” which produced a maximum LTA load of 2,078 psi with a top of pile displacement of 2.45 inches which is nearly identical to the load test displacement of 2.44 inches.

Table 4-13. I-395 Test Pile C soil input with layers modeled as limestone, load test T-Z curve data for layers 4 through 7 and 13 through 16, and non-cohesive IGM used in layers 8 and 17.

I-395 Test Pile C - MultiPier Soil Modeling Input										
Layer	El <sub>top</sub> (ft)	El <sub>bot</sub> (ft)	Dia. (in)	e (psi)	Model	$\gamma_d$ (pcf)	q <sub>u</sub> (psi)	f <sub>s</sub> (ksf)	SPT	$\nu$
1	11.5	8.9	34.0	N/A	Sand	62.4	0	0.00	N/A	N/A
2	8.9	6.5	34.0	2,143	Limestone	90.3	146	4.15	N/A	N/A
3	6.5	1.5	31.8	3,498	Limestone	96.8	230	5.86	N/A	N/A
4	1.5	-3.5	31.8	1,051	TZ Curves	81.5	74	N/A	N/A	N/A
5	-3.5	-8.5	31.8	496	TZ Curves	72.9	36	N/A	N/A	N/A
6	-8.5	-13.5	31.8	642	TZ Curves	75.7	46	N/A	N/A	N/A
7	-13.5	-18.5	31.8	841	TZ Curves	78.8	60	N/A	N/A	N/A
8	-18.5	-23.5	31.8	802	NC IGM	78.3	57	N/A	12	0.25
9	-23.5	-28.5	31.8	1,337	Limestone	84.4	93	2.97	N/A	N/A
10	-28.5	-33.5	30.0	1,968	Limestone	89.2	135	3.91	N/A	N/A
11	-33.5	-38.5	30.0	8,794	Limestone	109.4	515	11.26	N/A	N/A
12	-38.5	-43.5	30.0	1,980	Limestone	89.3	136	3.92	N/A	N/A
13	-43.5	-48.5	31.8	1,013	TZ Curves	81.0	72	N/A	N/A	N/A
14	-48.5	-53.5	31.8	870	TZ Curves	79.2	62	N/A	N/A	N/A
15	-53.5	-58.5	31.8	1,111	TZ Curves	82.1	78	N/A	N/A	N/A
16	-58.5	-63.5	31.8	1,234	TZ Curves	83.4	87	N/A	N/A	N/A
17	-63.5	-68.5	31.8	1,262	NC IGM	83.7	89	N/A	20	0.25
18	-68.5	-73.5	31.8	1,639	Limestone	86.9	114	3.43	N/A	N/A
19	-73.5	-78.5	32.5	2,836	Limestone	94.0	190	5.06	N/A	N/A
20	-78.5	-83.5	31.0	1,808	Limestone	88.2	125	3.68	N/A	N/A
21	-83.5	-88.5	N/A	N/A	Sand	62.4	0	0.00	N/A	N/A

Based on the observations from the first four iterations, the final modeled iteration did not use the T-Z curve data and instead modeled the pile using only MultiPier inputs with data gathered from MWD and the SPT borings. As indicated in Table 4-14, non-cohesive IGM was modeled in Layers 4, 6, 7, 8, 13, 14, 15, 16 and 17. Layer 5 was modeled as sand with no shear resistance, similar to Layers 1 and 21. This layer had an average specific energy of 496 psi measured from MWD, which equates to 36 psi if the geomaterial were limestone, and an average SPT blow count of N = 7 from all four borings within proximity to TP-C. Additionally, Figure 4-9 indicates only 60 of 2,743 (2%) MWD specific energy measurements from Pile Groups C1 and C2 (18 piles total) were above 1,250 psi and the TP-C boring (Figure 4-15) indicates the material in this elevation range is fine to medium sand and fine to medium sand with trace limestone. The model first used built-in MultiPier sand inputs, but this increased the capacity of the pile more so than if a non-cohesive IGM was modeled in the layer which seemed incorrect. In the MultiPier Help Manual it is stated that the measured data used for drilled shaft sand modeling exhibited considerable scatter which should be considered. Consequently, the sand layer was modeled with zero shear resistance using custom T-Z curves which is likely more accurate for a bored pile in which the layer in question is only 15 to 20 feet below the GSE and 4.5 feet below the GWT.

Table 4-14. I-395 Test Pile C soil input with layers modeled as limestone, non-cohesive IGM, and one layer modeled as sand with no shear resistance (Layer 5 – TZ Sand).

I-395 Test Pile C - MultiPier Soil Modeling Input											
Layer	El <sub>top</sub> (ft)	El <sub>bot</sub> (ft)	Dia. (in)	e (psi)	Model	$\gamma_d$ (pcf)	$q_u$ (psi)	$f_s$ (ksf)	SPT	$\nu$	
1	11.5	8.9	34.0	N/A	Sand	62.4	0	0.00	N/A	N/A	
2	8.9	6.5	34.0	2,143	Limestone	90.3	146	4.15	N/A	N/A	
3	6.5	1.5	31.8	3,498	Limestone	96.8	230	5.86	N/A	N/A	
4	1.5	-3.5	31.8	1,051	NC IGM	81.5	74	N/A	18	0.25	
5	-3.5	-8.5	31.8	496	TZ Sand	62.4	0	0.00	7	N/A	
6	-8.5	-13.5	31.8	642	NC IGM	75.7	46	N/A	7	0.25	
7	-13.5	-18.5	31.8	841	NC IGM	78.8	60	N/A	12	0.25	
8	-18.5	-23.5	31.8	802	NC IGM	78.3	57	N/A	12	0.25	
9	-23.5	-28.5	31.8	1,337	Limestone	84.4	93	2.97	N/A	N/A	
10	-28.5	-33.5	30.0	1,968	Limestone	89.2	135	3.91	N/A	N/A	
11	-33.5	-38.5	30.0	8,794	Limestone	109.4	515	11.26	N/A	N/A	
12	-38.5	-43.5	30.0	1,980	Limestone	89.3	136	3.92	N/A	N/A	
13	-43.5	-48.5	31.8	1,013	NC IGM	81.0	72	N/A	14	0.25	
14	-48.5	-53.5	31.8	870	NC IGM	79.2	62	N/A	8	0.25	
15	-53.5	-58.5	31.8	1,111	NC IGM	82.1	78	N/A	20	0.25	
16	-58.5	-63.5	31.8	1,234	NC IGM	83.4	87	N/A	18	0.25	
17	-63.5	-68.5	31.8	1,262	NC IGM	83.7	89	N/A	20	0.25	
18	-68.5	-73.5	31.8	1,639	Limestone	86.9	114	3.43	N/A	N/A	
19	-73.5	-78.5	32.5	2,836	Limestone	94.0	190	5.06	N/A	N/A	
20	-78.5	-83.5	31.0	1,808	Limestone	88.2	125	3.68	N/A	N/A	
21	-83.5	-88.5	N/A	N/A	Sand	62.4	0	0.00	N/A	N/A	

For the final modeled iteration (Table 4-14 and Figure 4-18), a prescribed LTA displacement of 2.9 inches was used which produced a maximum LTA load of 2,120.1 kips with a top of pile displacement of 2.44 inches which is in perfect agreement with the actual load test top of pile displacement. Furthermore, the maximum load indicates the upper segment of the test pile was mobilized during Load Step 13 which produced a maximum load of 2,152.8 kips. The T-Z curves in Figure 4-16 also suggest the pile was mobilized during Load Step 13, indicated by the black portions of each colored curve. At the end of the 10-minute sustained loading for Load Step 13, the top of pile was displaced 0.48 inches and at the start of Load Step 14 the top of Pile displacement was 0.99 inches, indicating the pile continuously moved upward after Load Step 13 suggesting the pile was fully mobilized at this stage of loading. Furthermore, Load Step 14 (Figure 4-16, dashed lines) which induced a maximum LTA load of 2,261 kips further displaced the entire pile 1.45 inches over the final 10-minute sustained loading which strongly supports these observations. Finally, similar to the unloading of SR-836 TP-A, I-395 TP-C continued to move upward as the LTA was unloaded. During this phase, the maximum LTA upward displacement was 3.06 inches with a top of pile displacement of 2.63 inches. The final modeled iteration then used this same prescribed LTA displacement of 3.06 inches which resulted in a maximum LTA load of 2,119.8 kips and a top of pile displacement of 2.61 inches which is in near perfect agreement with the actual load test and further supports the MultiPier model based on MWD data and SPT boring observations.

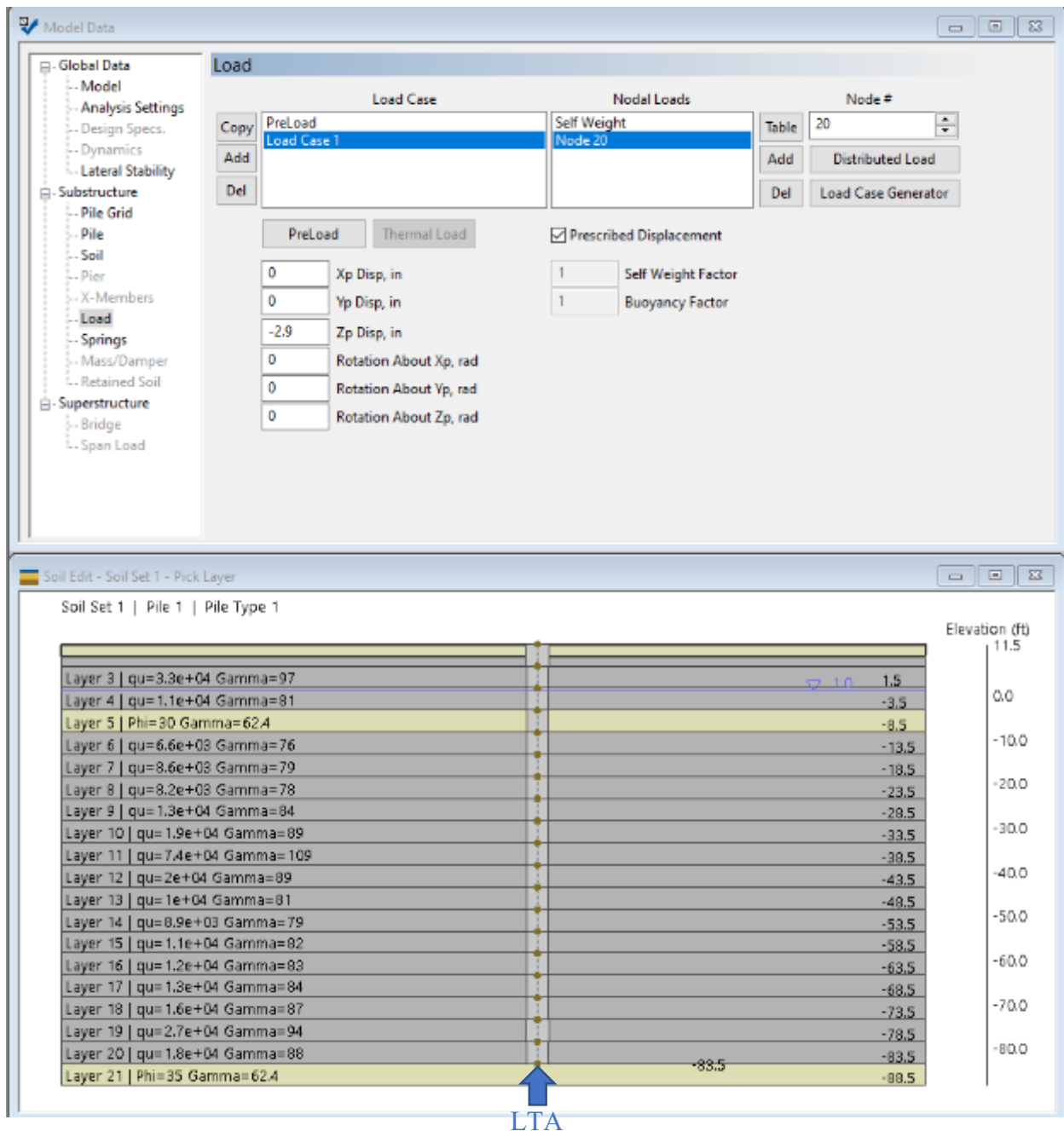


Figure 4-18. I-395 Test Pile C – final iteration MultiPier soil model.

#### 4.5 Production Pile QA/QC Criteria and Reporting

Based on the MultiPier ACIP pile modeling trials, UF researchers determined a specific energy threshold of 1,250 psi should be used to reduce the risk of sand or weakly-cemented sand layers being counted as rock. To clarify, the specific energy threshold of 1,250 psi eliminates any MWD data point with a specific energy value of 1,250 psi or less from counting towards the estimated pile capacity. This value was chosen because the MWD  $q_u$  strength range associated

with this is 88 psi or less which based on the observations discussed for Figure 4-17 includes extremely weathered limestone that can be crushed by hand that would not count as competent rock in a true RQD assessment. Additionally, the final TP-C MultiPier iteration modeled the material within this specific energy range as non-cohesive IGM and sand with no shear resistance which showed excellent agreement with the actual load test behavior. It is likely that some low strength limestone will be discounted from the pile capacity estimations as the SR-836 Test Pile A model indicated that limestone within this strength range is present at the site and can contribute to the overall pile capacity. The rock core strengths also support this as the lowest core strength was  $q_u = 24$  psi. However, any low strength limestone that is eliminated by the specific energy threshold would only contribute extra pile capacity above what is counted for the QA/QC analysis which is a conservative approach undertaken in the development of ACIP pile MWD procedures.

#### **4.6 Production Pile Analysis**

The results of the 50 production piles analyzed are provided in an excel-based summary format as illustrated in Figure 4-19. In Figure 4-19, a pile summary report is produced similar to the Pile Summary report discussed in Chapter 2. However, the spreadsheet developed for the UF research team analysis focused on specific energy, unconfined compression strength, pile side shear, and pile capacity rather than specific energy and total energy. The unconfined compression strength was estimated using the rock auger equation developed in FDOT Project BDV31-977-20 (McVay and Rodgers, 2016) and Rodgers et al. (2017) and the pile shear was estimated using the regression curve developed in Chapter 3. In the research-based Pile summary report, similar tabular data is provided for general pile information:

- Project,
- Location,
- Station and Offset,
- Top and bottom pile elevations,
- Engineer,
- Pile ID,
- Drill Rig used to excavate the pile,
- Drill bit diameter,
- Depth increment analyzed and the ISO-MWD assessment class.

In addition to the general pile information, detailed tabular data is provided for the ACIP pile QA/QC assessment which includes:

- Specific energy statistics above the specific energy threshold,
- Unconfined compressive strength statistics above the specific energy threshold,
- ACIP pile capacity QA/QC summary and,
- The pile installation summary.

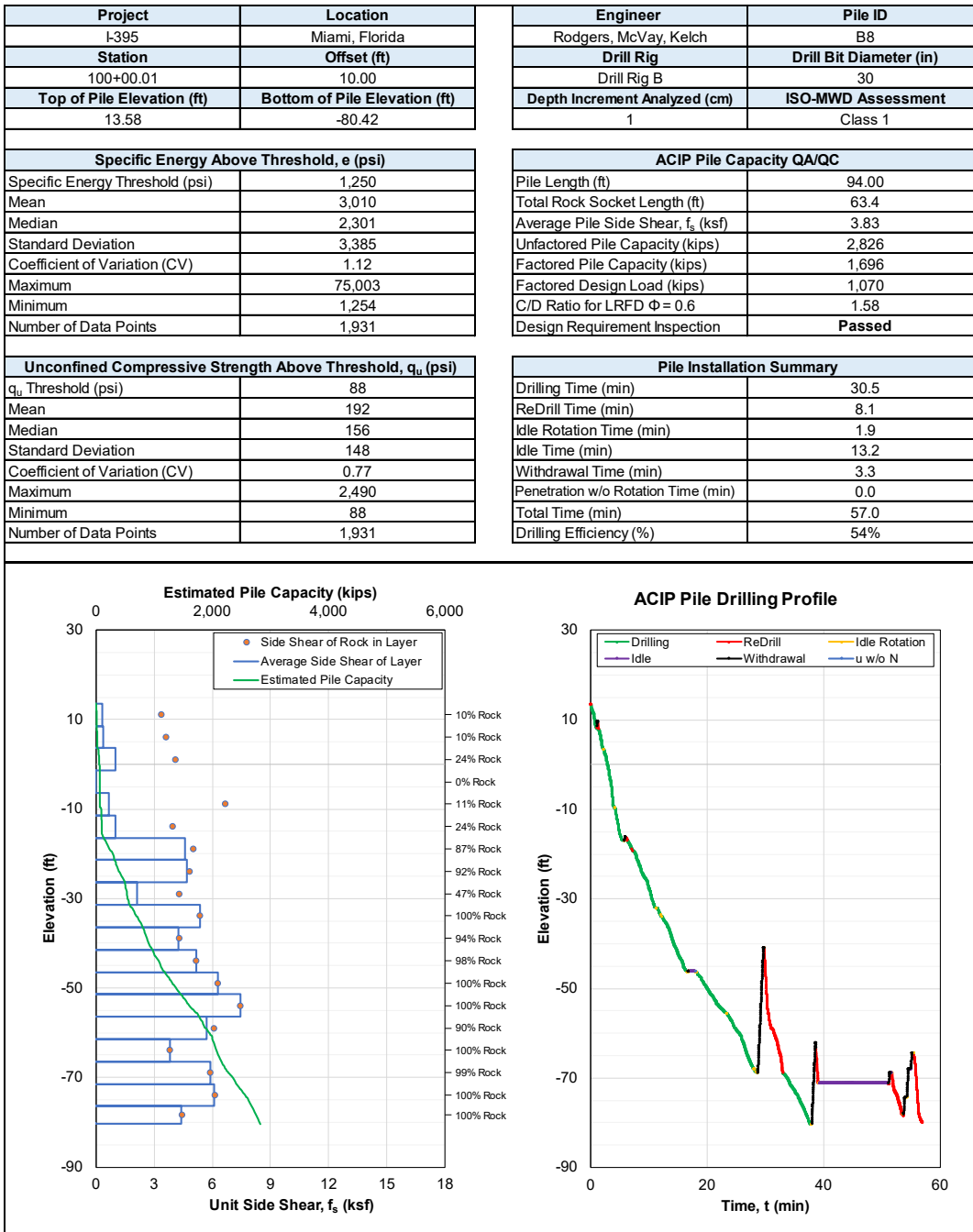


Figure 4-19. ACIP pile summary report for Group B-Pile 8 QA/QC inspection using Drill Rig B.

In the ACIP pile capacity QA/QC summary, the pile length is identified, the rock socket length based on the specific energy threshold is derived, the average pile side shear from all rock above the specific energy threshold is estimated, and then the unfactored pile capacity is calculated based on the pile length multiplied by the average side shear times pi times the drill bit diameter. Based on the LRFD-phi factor used in the actual pile design, the factored pile capacity is then calculated. The factored design load is listed, and the capacity-to-demand (C/D) ratio is then calculated. If the C/D ratio is equal to or greater than one, the design requirement inspection will

list “**Passed**” in bold. If the C/D ratio falls below one, the design requirement inspection will list “**Failed**” in bold red. The Pile installation summary details where time was spent during the pile excavation and lists the total time to drill the pile out. The pile installation summary includes drilling, redrilling, idle rotation, idle, withdrawal, and penetration without rotation. As explained in Chapter 2, only drilling time is considered for rock strength assessments and pile capacity estimations for ACIP piles.

In addition to the tabular data provided in the QA/QC summary report, two plots are also provided. The first plot (left side) indicates the shear strength of the rock present in each of the layers by an orange circle outlined in blue. If no rock is present, an orange circle will not be plotted. Also provided in the first plot is the average side shear of each layer, outlined in blue, based on the percentage of rock present which is identified on the right side of the plot in the y-axis. Therefore, the orange circle indicates the strength of the rock, and the blue bars indicate the adjusted shear strength based on the percentage of rock present which is similar to the FDOT’s method of side shear calculation where side shear is adjusted based on the average core recovery for a layer. The orange circles and blue bars correspond to the bottom x-axis. For the QA/QC procedure, five foot layer increments were used starting at the top of the pile. The bottom layer may be slightly smaller or larger than five feet depending on the pile length. The continuous green line indicates the estimated pile capacity (based on layer side shear) versus elevation. The green line corresponds to the top x-axis. The right side plot includes the drilling activities throughout the excavation process and plots them as elevation versus time. Interestingly, the drilling profile (right side) closely resembles the pile capacity profile (left side) as depicted in Figure 4-20. In Figure 4-20 it can be seen that weaker layers required less drilling time whereas the stronger layers required more drilling time which further supports the strength layering provided by MWD as it takes longer to drill through stronger geomaterial.

Note: The percentage of rock determined per layer in the Pile Summary Report is based on the specific energy threshold of  $e = 1,250$  psi. Any data point with  $e < 1,250$  psi was considered soil and removed from the rock strength analysis. The percentage of rock was then calculated as the number of data points with  $e > 1,250$  psi divided by the total number of data points possible in the layer. This is referred to as the MWD recovery ( $REC_{MWD}$ ) later in the report.

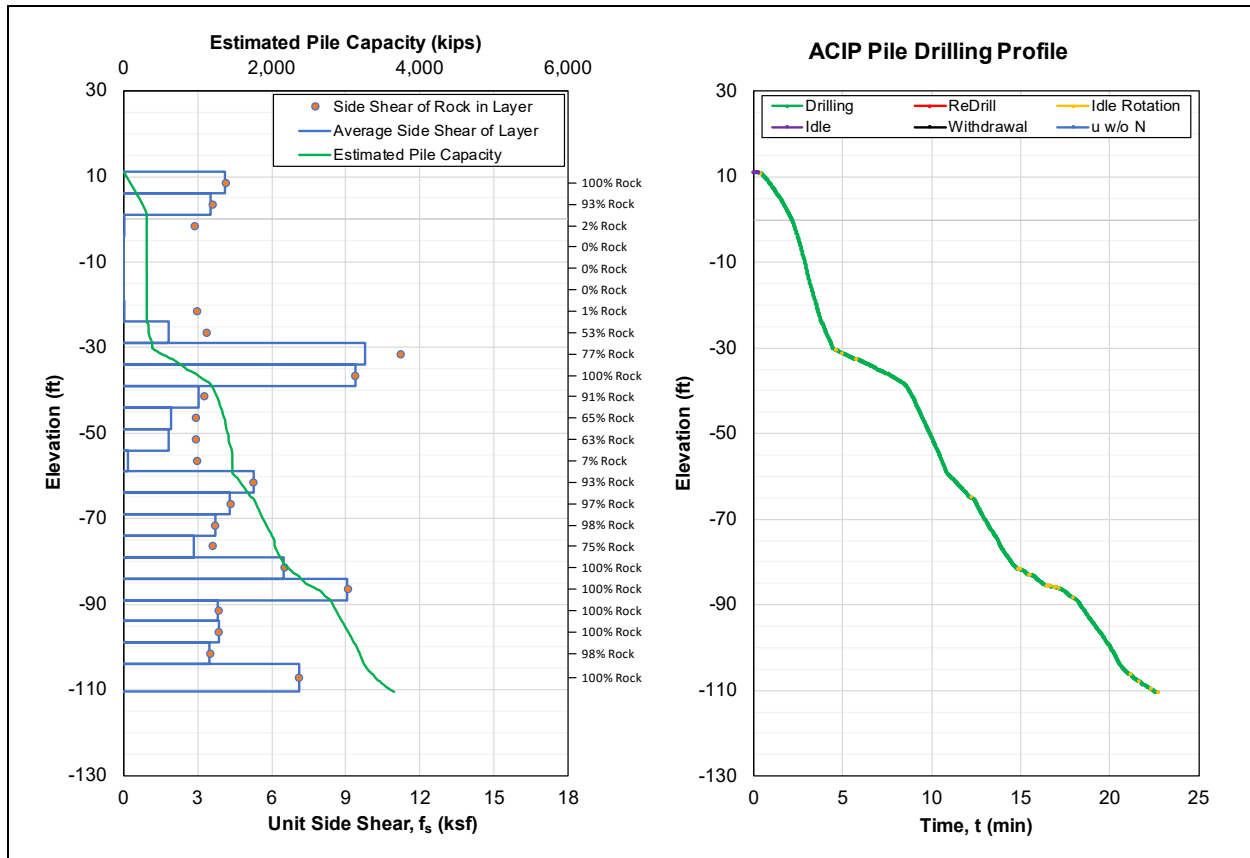


Figure 4-20. ACIP pile summary plots for Group C1-Pile 10 QA/QC inspection using Drill Rig A.

Also of interest, Figures 4-19 and 4-20 provide drilling profiles from the two different drill rigs used on the site while drilling into the same average strength of rock ( $f_s = 3.83$  ksf). Figure 4-19 presents drilling data from Drill Rig B while drilling Pile 8 from Group B and Figure 4-20 presents drilling data from the more powerful Drill Rig A while drilling Pile 10 from Group C1. It is observed that the smaller drill rig (B) required more time to drill through 63.4 feet of rock than Drill Rig A required to drill through 82.1 feet of rock of the same average strength. Additionally, Drill Rig B indicated more problems during the drilling process as more time was spent on drilling activities other than “drilling”. This indicates Drill Rig A is better suited to complete the drilling on site which is an added benefit of the QA/QC procedure as the drilling contractor could learn from these observations to better prepare for future work in the area. This also helps to ensure that the right drilling equipment is brought on site for future projects in the area to reduce the time of completion. Figure 4-21 provides drilling data from Drill Rig A while drilling Pile 35 from Group D where the side shear strength of rock is 6.2 ksf on average and nearly double the strength of the other two locations. From Figure 4-21, it can be seen that the stronger rock began to create difficulties for the more powerful drill rig as more time was spent on drilling activities other than “drilling”. Based on the observations from Figures 4-19 through 4-21, Drill Rig B would likely have struggled to complete the Group D pile that had much stronger rock present.

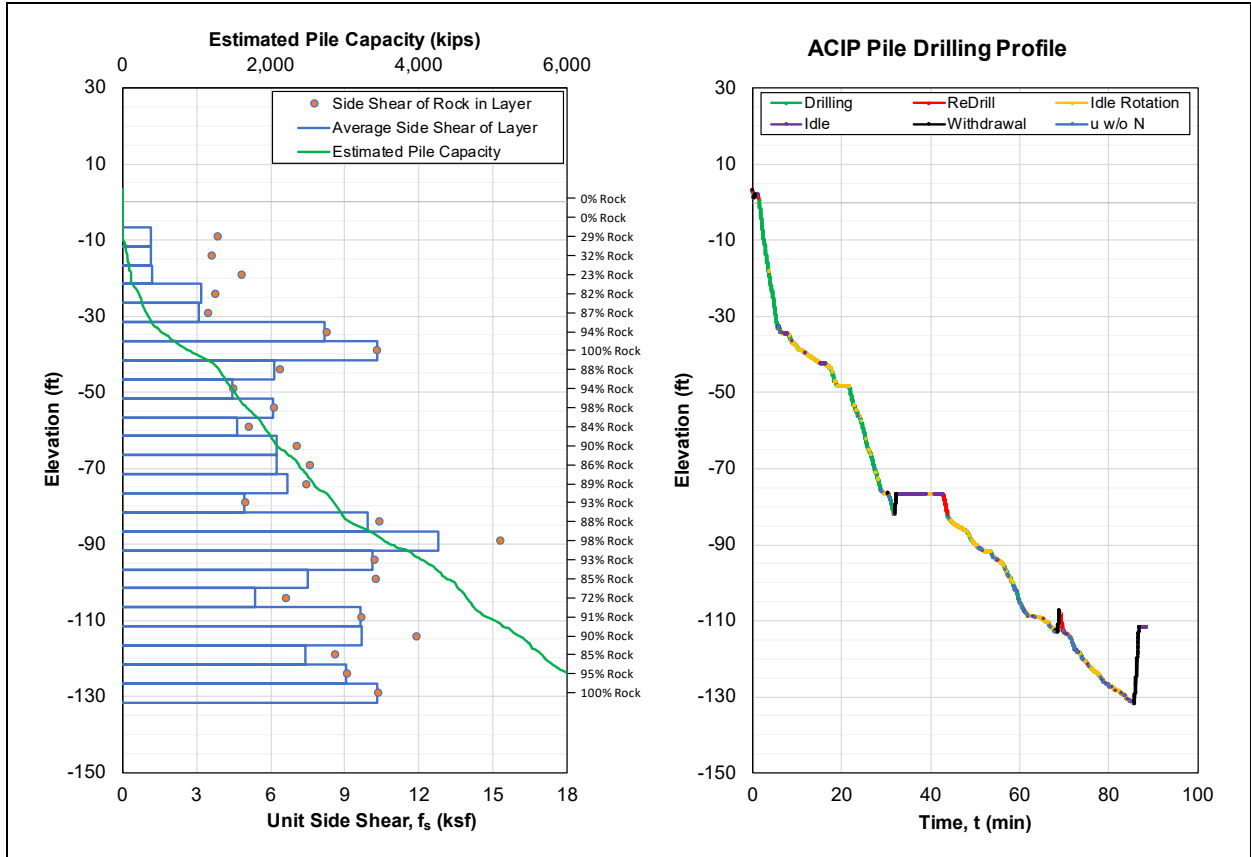


Figure 4-21. ACIP pile summary plots for Group D-Pile 35 QA/QC inspection using Drill Rig A.

#### 4.7 Analyzed Production Pile Summary

The following section includes Tables 4-15 through 4-22 that summarize the QA/QC inspections from the 50 production piles analyzed from Pile Groups B, C1, C2, and D. The data in Tables 4-15 through 4-20 includes the Pile ID, pile length, total rock socket length, average pile side shear, unfactored pile capacity, factored pile capacity, factored design load, C/D ratio with phi identified, and the design requirement inspection result. Table 4-21 provides an overall summary from all analyzed piles and Table 4-22 provides a comparative summary from the four different pile groups analyzed.



Table 4-15. Group B – Piles 1 through 10.

Group B - Piles 1 through 10										
Pile	1	2	3	4	5	6	7	8	9	10
Pile Length (ft)	94.0	94.0	94.3	94.0	94.0	94.0	94.0	94.0	94.0	94.1
Total Rock Socket Length (ft)	50.6	50.0	56.7	55.4	57.1	55.8	63.2	63.4	58.6	61.8
Average Pile Side Shear, $f_s$ (ksf)	2.6	2.7	3.1	3.6	3.5	3.0	3.5	3.8	3.3	3.7
Unfactored Pile Capacity (kips)	1,904	2,001	2,312	2,635	2,556	2,217	2,581	2,826	2,464	2,743
Factored Pile Capacity (kips)	1,142	1,201	1,387	1,581	1,534	1,330	1,549	1,696	1,478	1,646
Factored Design Load (kips)	1,070	1,070	1,070	1,070	1,070	1,070	1,070	1,070	1,070	1,070
C/D Ratio for LRFD $\Phi = 0.6$	1.07	1.12	1.30	1.48	1.43	1.24	1.45	1.58	1.38	1.54
Design Requirement Inspection	<b>Passed</b>	<b>Passed</b>	<b>Passed</b>	<b>Passed</b>	<b>Passed</b>	<b>Passed</b>	<b>Passed</b>	<b>Passed</b>	<b>Passed</b>	<b>Passed</b>

Table 4-16. Group B – Piles 11 through 16.

Group B - Piles 11 through 16						
Pile	11	12	13	14	15	16
Pile Length (ft)	94.1	94.0	94.1	94.0	94.2	94.1
Total Rock Socket Length (ft)	62.0	48.8	62.5	49.5	57.5	55.9
Average Pile Side Shear, $f_s$ (ksf)	3.6	3.0	3.6	2.9	3.5	3.3
Unfactored Pile Capacity (kips)	2,624	2,203	2,674	2,164	2,584	2,419
Factored Pile Capacity (kips)	1,574	1,322	1,604	1,299	1,551	1,451
Factored Design Load (kips)	1,070	1,070	1,070	1,070	1,070	1,070
C/D Ratio for LRFD $\Phi = 0.6$	1.47	1.24	1.50	1.21	1.45	1.36
Design Requirement Inspection	<b>Passed</b>	<b>Passed</b>	<b>Passed</b>	<b>Passed</b>	<b>Passed</b>	<b>Passed</b>

Table 4-17. Group C1 – Piles 1 through 10.

Group C1 - Piles 1 through 10										
Pile	1	2	3	4	5	6	7	8	9	10
Pile Length (ft)	121.5	121.5	121.5	121.5	121.5	121.5	121.5	121.5	121.5	121.5
Total Rock Socket Length (ft)	102.3	89.0	81.6	98.3	85.9	90.8	99.2	79.3	81.5	82.1
Average Pile Side Shear, $f_s$ (ksf)	4.8	4.1	4.4	4.9	3.7	4.3	4.2	3.6	4.2	3.8
Unfactored Pile Capacity (kips)	4,590	3,943	4,178	4,710	3,560	4,137	4,031	3,408	3,974	3,652
Factored Pile Capacity (kips)	2,754	2,366	2,507	2,826	2,136	2,482	2,419	2,045	2,384	2,191
Factored Design Load (kips)	920	920	920	920	920	920	920	920	920	920
C/D Ratio for LRFD $\Phi = 0.6$	2.99	2.57	2.72	3.07	2.32	2.70	2.63	2.22	2.59	2.38
Design Requirement Inspection	<b>Passed</b>	<b>Passed</b>	<b>Passed</b>	<b>Passed</b>	<b>Passed</b>	<b>Passed</b>	<b>Passed</b>	<b>Passed</b>	<b>Passed</b>	<b>Passed</b>

Table 4-18. Group C2 – Piles 1 through 8.

Group C2 - Piles 1 through 8								
Pile	1	2	3	4	5	6	7	8
Pile Length (ft)	111.5	111.5	111.5	111.5	111.5	111.5	111.0	111.5
Total Rock Socket Length (ft)	81.4	62.4	100.0	81.2	84.2	76.1	92.7	70.4
Average Pile Side Shear, $f_s$ (ksf)	4.1	2.8	4.7	3.7	4.9	3.5	4.5	3.8
Unfactored Pile Capacity (kips)	3,583	2,486	4,100	3,260	4,266	3,038	3,907	3,338
Factored Pile Capacity (kips)	2,150	1,491	2,460	1,956	2,559	1,823	2,344	2,003
Factored Design Load (kips)	980	980	980	980	980	980	980	980
C/D Ratio for LRFD $\Phi = 0.6$	2.19	1.52	2.51	2.00	2.61	1.86	2.39	2.04
Design Requirement Inspection	<b>Passed</b>	<b>Passed</b>	<b>Passed</b>	<b>Passed</b>	<b>Passed</b>	<b>Passed</b>	<b>Passed</b>	<b>Passed</b>

Table 4-19. Group D Piles 4, 5, 6, 7, 12, 13, 14, 20, 21, and 28.

Group D - Piles										
Pile	4	5	6	7	12	13	14	20	21	28
Pile Length (ft)	135.0	135.0	135.0	135.0	135.0	135.0	135.0	135.0	135.0	135.2
Total Rock Socket Length (ft)	106.1	89.2	110.8	93.2	107.7	98.2	95.8	104.0	90.8	98.4
Average Pile Side Shear, $f_s$ (ksf)	5.0	5.3	6.0	5.6	6.1	5.9	5.6	6.2	4.8	5.1
Unfactored Pile Capacity (kips)	5,276	5,569	6,331	5,924	6,438	6,252	5,931	6,578	5,071	5,382
Factored Pile Capacity (kips)	3,166	3,341	3,799	3,554	3,863	3,751	3,558	3,947	3,042	3,229
Factored Design Load (kips)	1,050	1,050	1,050	1,050	1,050	1,050	1,050	1,050	1,050	1,050
C/D Ratio for LRFD $\Phi = 0.6$	3.02	3.18	3.62	3.39	3.68	3.57	3.39	3.76	2.90	3.08
Design Requirement Inspection	<b>Passed</b>	<b>Passed</b>	<b>Passed</b>	<b>Passed</b>	<b>Passed</b>	<b>Passed</b>	<b>Passed</b>	<b>Passed</b>	<b>Passed</b>	<b>Passed</b>

Table 4-20. Group D Piles 10, 18, 19, 26, 27, and 35.

Group D - Piles						
Pile	10	18	19	26	27	35
Pile Length (ft)	134.9	135.5	135.0	135.0	135.0	135.0
Total Rock Socket Length (ft)	79.4	97.2	100.4	107.2	105.3	103.3
Average Pile Side Shear, $f_s$ (ksf)	5.0	5.0	5.8	6.2	6.9	6.2
Unfactored Pile Capacity (kips)	5,328	5,293	6,165	6,624	7,338	6,579
Factored Pile Capacity (kips)	3,197	3,176	3,699	3,974	4,403	3,947
Factored Design Load (kips)	1,050	1,050	1,050	1,050	1,050	1,050
C/D Ratio for LRFD $\Phi = 0.6$	3.04	3.02	3.52	3.78	4.19	3.76
Design Requirement Inspection	<b>Passed</b>	<b>Passed</b>	<b>Passed</b>	<b>Passed</b>	<b>Passed</b>	<b>Passed</b>

Table 4-21. Pile statistics for 50 ACIP production piles.

Category	Pile Statistics for 50 ACIP Production Piles						
	Mean	Median	Std Dev	CV	Max	Min	Count
Pile Length (ft)	115.4	121.5	16.9	0.15	135.5	94.0	50
Total Rock Socket Length (ft)	80.7	81.8	19.3	0.24	110.8	48.8	50
Average Pile Side Shear, $f_s$ (ksf)	4.3	4.1	1.1	0.25	6.9	2.6	50
Unfactored Pile Capacity (kips)	4,063	3,925	1,544	0.38	7,338	1,904	50
Factored Pile Capacity (kips)	2,438	2,355	926	0.38	4,403	1,142	50
Factored Design Load (kips)	1,019	1,050	58	0.06	1,070	920	50
C/D Ratio for LRFD $\Phi = 0.6$	2.4	2.5	0.9	0.37	4.2	1.1	50

Table 4-22. Comparing pile group averages.

Category	Pile Group Averages			
	Group A	Group C2	Group C1	Group D
Pile Length (ft)	94.1	111.4	121.5	135.0
Total Rock Socket Length (ft)	56.8	81.0	89.0	99.2
Rock Socket per Pile Length	0.604	0.727	0.733	0.735
Pile Side Shear, $f_s$ (ksf)	3.3	4.0	4.2	5.7
Unfactored Pile Capacity (kips)	2,432	3,497	4,018	6,005
Factored Pile Capacity (kips)	1,459	2,098	2,411	3,603
Factored Design Load (kips)	1,070	980	920	1,050
C/D Ratio for LRFD $\Phi = 0.6$	1.4	2.1	2.6	3.4

From Tables 4-15 through 4-22, the average side shear strength of rock ranged from 2.6 ksf to 6.9 ksf and the total rock socket length ranged from 48.8 feet to 110.8 feet. These ranges indicate large variability throughout the site. Fortunately, in all cases the production piles passed the design requirement inspection. In Table 4-22, the pile groups are listed moving west-to-east. Observed in Table 22, the strength of rock, total rock socket length, rock socket length per pile length, average pile side shear, unfactored capacity, factored capacity, and C/D ratio all decreased in sequential order moving east-to-west. This indicates that the pile capacities are decreasing moving in the direction of SR-836 in which MWD data was not available to analyze for this report. Therefore, it is of great importance to fix the rotational speed sensor on the drill rig completing the SR-836 piles so MWD data and subsequent analyses of soil/rock layering and pile capacities can occur. It should also be noted that the rock core strength data also support the decreasing rock strength and pile capacities as drilling moves from east-to-west (Table 4-6).

From Chapters 3 and 4, it was shown that MWD specific energy was in agreement with the layering identified by the SPT borings, MWD agreed with the load test results as an excellent correlation was developed between unit side shear and specific energy, MWD was in agreement with the rock core strength range and layering, MWD data were able to provide accurate test pile models that showed the same behavior as the actual load tested piles, and observed in the QA/QC pile summaries MWD indicated the strength of rock decreased moving east-to-west which agrees with the trends of rock cores and load tests. Furthermore, the drilling profiles also

show the same trends as the estimated pile capacities and indicated stronger rock takes longer to drill which is the expected trend. All of these supporting observations indicate the MWD correlation and procedures developed for ACIP pile capacity QA/QC are valid for the assessment of rock strength and pile capacity. The full ACIP Pile QA/QC summary report for each of the 50 production piles analyzed can be found in Appendix A.

## 5 LRFD $\phi$ Assessment of FDOT ACIP Pile Design Methods in South Florida

The focus of this chapter is further assessment of LRFD resistance factors,  $\phi$ , for Auger Cast-in-Place (ACIP) piles constructed in south Florida limestone. Prior work was completed in FDOT project BDV31-977-12 (McVay et al., 2016) in which the effort assessed LRFD resistance factors for ACIP piles in sand, clay, IGM, and limestone using SPT, CPT, and rock core data. Further assessment of ACIP piles in sand, clay, and IGM is beyond the scope of this effort and will not be reported. Also, the use of CPT data is not relevant in the assessment of rock strength and will therefore not be covered as well. Comparisons of the previously developed LRFD resistance factors in south Florida limestone will be compared to the new assessment developed in this research effort with more core data and fully mobilized pile segments within proximity to the core samples available. As discussed in Chapters 3 and 4, this included eight mobilized segments from I-395 Test Pile C and two mobilized segments from Signature Bridge Test Pile D.

In the prior report, LRFD resistance factors were assessed using a revised First Order Second Moment (FOSM) approach. This report will cover three different methods of assessment which includes the original FOSM approach (FOSM Pre-Styler) used in FDOT's Structural Design Guidelines (SDG), the revised FOSM approach (FOSM Styler) used in FDOT Report BDV31-977-12, and Monte Carlo simulations (Monte Carlo). Additionally, this report will assess each LRFD approach using six different Reliability Indices,  $\beta$ , ranging from 2 to 4. The prior report assessed one  $\beta$  equal to 2.33 which is recommended for redundant deep foundations such as ACIP piles. This report will focus on four different SPT design methods and seven different design methods using unconfined compression strength,  $q_u$ , data acquired from laboratory testing recovered rock core specimens. In total, this amounts to 198 LRFD resistance factor assessments for ACIP piles in south Florida limestone. In addition to developing resistance factors for each LRFD approach and design method, an evaluation of efficiency ( $\phi/\lambda$ ; McVay et al. 2000) will be reported that identifies how well the method performed and provides a percentage (%) of side shear available for design. Finally, LRFD  $\phi$  vs.  $\beta$  curves will be developed for each LRFD approach and design method to provide guidance in future south Florida ACIP pile designs that utilize SPT and/or  $q_u$  data.

### 5.1 LRFD Methods

#### 5.1.1 FOSM (Pre-Styler)

The first implementation of resistance factor,  $\phi$ , in AASHTO and FHWA was the first order second moment (FOSM) by Barker et al. (1991) and Withiam et al. (1997), with the assumption of a log-normal distribution function for resistance ( $R_n$ ), load ( $Q$ ), and/or bias factors ( $\lambda_R$ ,  $\lambda_{QD}$ , and  $\lambda_{QL}$ ), which resulted in resistance factor,  $\phi$  :

$$\phi = \frac{\lambda_R \left( \gamma_D \frac{Q_D}{Q_L} + \gamma_L \right) \sqrt{\frac{1 + COV_{QD}^2 + COV_{QL}^2}{1 + COV_R^2}}}{\left( \lambda_{QD} \frac{Q_D}{Q_L} + \lambda_{QL} \right) \exp \left( \beta_T \sqrt{\ln \left[ (1 + COV_R^2) (1 + COV_{QD}^2 + COV_{QL}^2) \right]} \right)} \quad (5-1)$$

where,

- $\gamma_D$  = dead load factor = 1.25
- $\gamma_L$  = live load factor = 1.75
- $Q_D/Q_L$  = dead/live load ratio = 3
- $\lambda_R$  = Resistance bias factor
- $COV_R$  = resistance coefficient of variability
- $\lambda_{QD}$  = dead load bias factor = 1.08
- $\lambda_{QL}$  = live load bias factor = 1.15
- $COV_{QD}$  = dead load coefficient of variability = 0.128
- $COV_{QL}$  = live load coefficient of variability = 0.180
- $\beta_T$  = Target reliability index = 2, 2.33, 2.5, 3, 3.5, and 4

### 5.1.2 FOSM (Styler)

Paikowsky et al. (2004) evaluated LRFD  $\phi$  for deep foundation design using both AASHTO's (Barker et al., 1991) FOSM and the more labor intensive and accurate First Order Reliability Method (FORM). They found the FORM resistance values were 10% - 15% greater than those developed using the original FOSM methods. Styler (2006) reviewed Paikowsky and Barker's work and identified that the original FOSM LRFD  $\phi$  could be improved if the full expression for COV of the load were used in the FOSM equation instead of its approximation. Specifically, Styler showed that resistance factors using FOSM with the full expression of  $COV_Q$  were within 3% of those developed using the FORM method. Consequently, the revised FOSM method will be used as replacement to the FORM method here. The revised expression for CV (FOSM Styler) is currently used in GeoStat, adopted from McVay et al. (2012), and presented in Equation 5-2:

$$\phi = \frac{\lambda_R \left( \gamma_D \cdot \frac{Q_D}{Q_L} + \gamma_L \right) \cdot \sqrt{\frac{1 + COV_Q^2}{1 + COV_R^2}}}{\left( \lambda_{QD} \cdot \frac{Q_D}{Q_L} + \lambda_{QL} \right) \cdot \exp \left( \beta \cdot \sqrt{\ln \left( (1 + COV_R^2) \cdot (1 + COV_Q^2) \right)} \right)} \quad (5-2)$$

where  $COV_Q$  is the coefficient of variation with respect to loading as stipulated by Styler (2006) which combines the live load and dead load coefficients of variation as presented in Equation 5-3. All other component terms used in calculating  $\phi$  are listed under Equation 5-1.

$$COV_Q^2 = \frac{\left( \lambda_{QD} \cdot \frac{Q_D}{Q_L} \cdot COV_{QD} \right)^2 + \left( \lambda_{QL} \cdot COV_{QL} \right)^2}{\left( \lambda_{QD} \cdot \frac{Q_D}{Q_L} \right)^2 + 2 \cdot \frac{Q_D}{Q_L} \cdot \lambda_{QD} \cdot \lambda_{QL} + \lambda_{QL}^2} \quad (5-3)$$

### 5.1.3 Monte Carlo

In addition to the FOSM (original, i.e., Pre-Styler) and FOSM (Styler; FORM alternative) methods discussed, Monte Carlo simulations were also investigated for the LRFD assessments. The method was initially outlined by Transportation Research Circular E-C079 (Allen et al. 2005) and is intended to estimate the reliability index ( $\beta$ ) using the tails of the log normal distribution from load and resistance where failure is more likely to occur. For the evaluation, strength limit state I was employed,

$$g = \phi R - \gamma_{LL} LL - \gamma_{DL} DL \quad (5-4)$$

where  $g$  is the performance limit state function,  $\gamma_{LL}$  and  $\gamma_{DL}$  are the live and dead load factors;  $R$  is the nominal resistance bias described as a random variable, and  $LL$  and  $DL$  are the live load and dead load biases which are also described as random variables. The bias is defined as measured nominal resistance divided the predicted resistance. Each of the random variables ( $R$ ,  $DL$  and  $LL$ ) were modeled with a lognormal distribution which matched the histogram and probability density function (PDF) of the data better than a normal distribution. In the case of live load and dead load, the additional component terms used in calculating  $\phi$  are listed under Equation 5-1.

The assessment of the Monte Carlo LRFD  $\phi$  for the associated target reliability index was performed as follows:

1. Select a resistance factor  $\phi$ ;
2. Independently randomly generate  $N$  (50,000) trial values of  $LL$ ,  $DL$  and  $R$  using Monte Carlo with bias summary statistics;
3. For each trial value of  $LL$ ,  $DL$  and  $R$ , the function  $g(x_i)$  (Eq. 5-4) was evaluated;
4. Based on all the trials, the number of cases in which  $g(x_i) \leq 0$  was tallied and the probability of failure was computed as,
5. 
$$P_f = \frac{\text{count}(g(x_i))}{N}$$
6. Using the inverse of the standard normal cumulative function,  $\phi$ , the reliability index,  $\beta = \phi^{-1}(P_f)$  is found;
7. If the reliability index,  $\beta$ , is less than or larger than the target values,  $\beta_T$  (e.g., 2.33, 3.0, etc.), the resistance factor  $\phi$  is adjusted upward or downward until  $|\beta - \beta_T| < \text{tolerance}$ .

## 5.2 SPT N Design Methods

The first design methods assessed were the SPT approaches that used data collected within 100 ft from the load tested ACIP piles at I-395 and Signature Bridge. Generally, this consisted of one boring either in the footprint or adjacent to a load tested pile and neighboring borings performed in the footprint of nearby pier groups. All borings considered at each location were combined to produce an average blow count value for each mobilized pile segment. Each average SPT  $N$  calculated per mobilized segment was then used with four different SPT design equations and the

predicted side shear was compared to the measured side shear acquired from the load test. The SPT design equations considered were Crapps (1986), Ramos et al. (1994), Frizzi and Meyer (2000), and BDV12 which was developed in the prior FDOT ACIP project, BDV31-977-12 (McVay et al., 2016). The measured side shear is plotted vs. predicted side shear in Figure 5-1, the tabular results are presented in Table 5-1, and the bias statistics for each method are provided in Table 5-2.

### 5.2.1 SPT Design Equations

Crapps (1986)

$$f_s(ksf) = 0.8 * N - 10.4, \text{ for } N \geq 11 \quad (5-5)$$

Ramos et al. (1994)

$$f_s(ksf) = 0.4 * N + 4, \text{ for } 60 \geq N \geq 5 \quad (5-6)$$

$$f_s(ksf) = 0.2 * N + 16, \text{ for } N > 60 \quad (5-7)$$

Frizzi & Meyer (2000)

$$f_s = (0.35 * N - 1) * 2 (ksf/tsf) \quad (5-8)$$

BDV12 (McVay et al., 2016)

$$f_s = 0.15 * N * 2 (ksf/tsf) \quad (5-9)$$



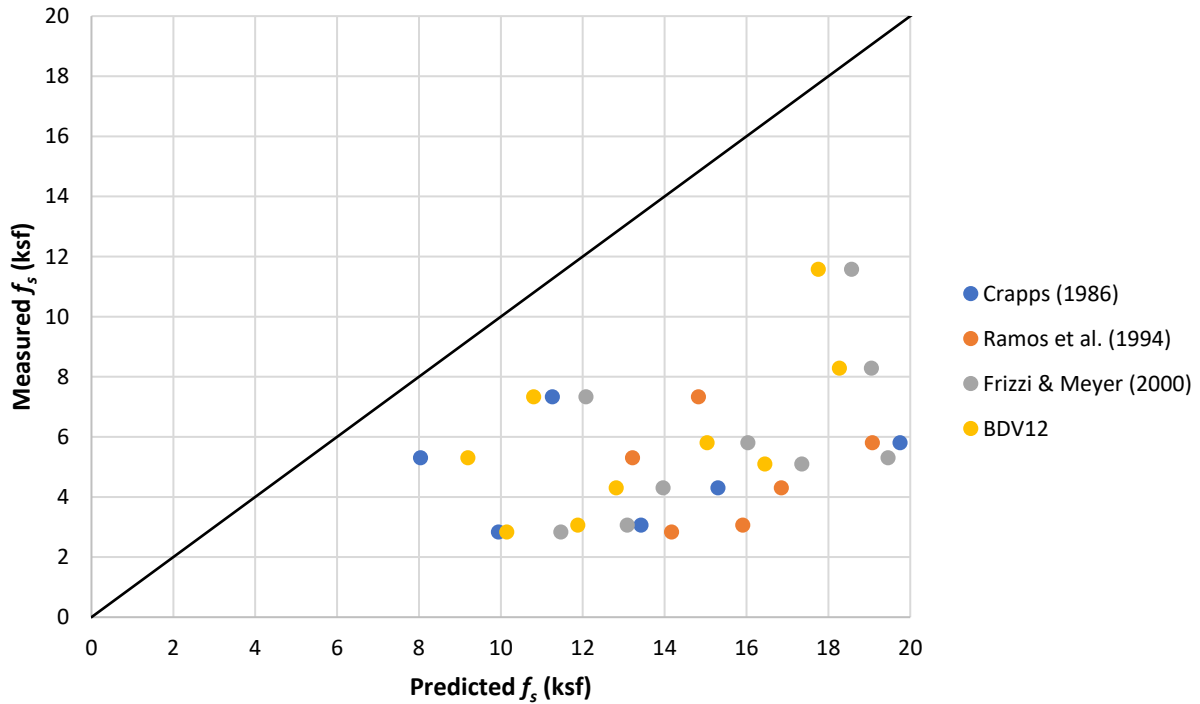


Figure 5-1. ACIP pile measured vs. predicted side shear capacity for multiple SPT design methods.

Table 5-1. Side shear estimates and bias per mobilized layer using SPT design methods.

Location	Segment	Load Test fs (ksf)	Crapps (1986)		Ramos et al. (1994)		Frizzi & Meyer (2000)		BDV12	
			fs (ksf)	Bias	fs (ksf)	Bias	fs (ksf)	Bias	fs (ksf)	Bias
I395 TP-C	GSE to SG23	5.30	8.04	0.66	13.22	0.40	19.46	0.27	9.20	0.58
	SG19 to SG17	2.83	9.94	0.28	14.17	0.20	11.47	0.25	10.15	0.28
	SG17 to SG14	7.33	11.26	0.65	14.83	0.49	12.08	0.61	10.80	0.68
	SG10 to SG8	3.06	13.43	0.23	15.91	0.19	13.09	0.23	11.88	0.26
	SG8 to LTA	4.30	15.31	0.28	16.85	0.26	13.97	0.31	12.82	0.34
	SG3 to SG2	8.28	26.24	0.32	22.32	0.37	19.06	0.43	18.27	0.45
	SG2 to SG1	11.57	25.20	0.46	21.80	0.53	18.57	0.62	17.76	0.65
	LTA to SG3	5.80	19.75	0.29	19.08	0.30	16.04	0.36	15.04	0.39
SB TP-D	SG9 to SG6	5.09	22.58	0.23	20.49	0.25	17.35	0.29	16.45	0.31
	SG6 to LTA	15.16	30.49	0.50	24.44	0.62	21.03	0.72	20.39	0.74

Table 5-2. Bias statistics for SPT design methods.

Design Method	Mean	Std Dev	CV <sub>R</sub>
Crapps (1986)	0.39	0.16	0.40
Ramos et al. (1994)	0.36	0.14	0.39
Frizzi & Meyer (2000)	0.41	0.17	0.41
BDV12	0.47	0.17	0.37

### 5.3 SPT LRFD $\phi$ Assessment

Once the bias statistics were derived, LRFD  $\phi$  assessment took place for each reliability index:  $\beta = 2, 2.33, 2.5, 3, 3.5,$  and  $4$ . The dead-to-live load ratio ( $Q_D/Q_L$ ) which is generally dependent on the bridge span length was set to three for LRFD calibration based on McVay et al. (2000) where it was found that the calibrated resistance factor ( $\phi$ ) is insensitive to a  $Q_D/Q_L$  ratio greater than three. Tables 5-3 through 5-8 provide the LRFD  $\phi$  and efficiency ( $\phi / \lambda$ ) for each  $\beta$  using the four SPT design methods and three LRFD methods. Figures 5-2 through 5-4 provide the LRFD  $\phi$  vs.  $\beta$  curves for each LRFD method, FOSM (Pre-Styler), FOSM (Styler), and Monte Carlo, respectively.

Table 5-3. ACIP pile LRFD analysis – South Florida limestone for SPT design methods –  $\beta = 2$ .

Design Method	SPT N - $\beta = 2$					
	FOSM - Pre-Styler		FOSM - Styler		Monte Carlo	
	$\phi$	$\phi / \lambda$	$\phi$	$\phi / \lambda$	$\phi$	$\phi / \lambda$
Crapps (1986)	0.19	49%	0.20	52%	0.19	50%
Ramos et al. (1994)	0.18	50%	0.20	54%	0.19	52%
Frizzi & Meyer (2000)	0.20	48%	0.21	51%	0.20	49%
BDV12	0.24	52%	0.26	56%	0.25	54%

Table 5-4. ACIP pile LRFD analysis – South Florida limestone for SPT design methods –  $\beta = 2.33$ .

Design Method	SPT N - $\beta = 2.33$					
	FOSM - Pre-Styler		FOSM - Styler		Monte Carlo	
	$\phi$	$\phi / \lambda$	$\phi$	$\phi / \lambda$	$\phi$	$\phi / \lambda$
Crapps (1986)	0.16	42%	0.18	46%	0.17	43%
Ramos et al. (1994)	0.16	44%	0.17	47%	0.16	45%
Frizzi & Meyer (2000)	0.17	41%	0.18	45%	0.18	43%
BDV12	0.21	45%	0.23	50%	0.22	47%

Table 5-5. ACIP pile LRFD analysis – South Florida limestone for SPT design methods –  $\beta = 2.5$ .

Design Method	SPT N - $\beta = 2.5$					
	FOSM - Pre-Styler		FOSM - Styler		Monte Carlo	
	$\phi$	$\phi / \lambda$	$\phi$	$\phi / \lambda$	$\phi$	$\phi / \lambda$
Crapps (1986)	0.15	39%	0.17	43%	0.16	40%
Ramos et al. (1994)	0.15	40%	0.16	44%	0.15	42%
Frizzi & Meyer (2000)	0.16	38%	0.17	42%	0.16	40%
BDV12	0.20	42%	0.22	47%	0.21	44%

Table 5-6. ACIP pile LRFD analysis – South Florida limestone for SPT design methods –  $\beta = 3$ .

Design Method	SPT N - $\beta = 3$					
	FOSM - Pre-Styler		FOSM - Styler		Monte Carlo	
	$\phi$	$\phi / \lambda$	$\phi$	$\phi / \lambda$	$\phi$	$\phi / \lambda$
Crapps (1986)	0.12	31%	0.14	35%	0.13	33%
Ramos et al. (1994)	0.12	33%	0.13	37%	0.12	35%
Frizzi & Meyer (2000)	0.13	31%	0.14	34%	0.13	32%
BDV12	0.16	34%	0.18	39%	0.17	37%

Table 5-7. ACIP pile LRFD analysis – South Florida limestone for SPT design methods –  $\beta = 3.5$ .

Design Method	SPT N - $\beta = 3.5$					
	FOSM - Pre-Styler		FOSM - Styler		Monte Carlo	
	$\phi$	$\phi / \lambda$	$\phi$	$\phi / \lambda$	$\phi$	$\phi / \lambda$
Crapps (1986)	0.10	25%	0.11	28%	0.11	27%
Ramos et al. (1994)	0.09	26%	0.11	30%	0.10	29%
Frizzi & Meyer (2000)	0.10	24%	0.11	28%	0.11	26%
BDV12	0.13	28%	0.15	32%	0.14	31%

Table 5-8. ACIP pile LRFD analysis – South Florida limestone for SPT design methods –  $\beta = 4$ .

Design Method	SPT N - $\beta = 4$					
	FOSM - Pre-Styler		FOSM - Styler		Monte Carlo	
	$\phi$	$\phi / \lambda$	$\phi$	$\phi / \lambda$	$\phi$	$\phi / \lambda$
Crapps (1986)	0.08	20%	0.09	23%	0.09	23%
Ramos et al. (1994)	0.08	21%	0.09	25%	0.09	24%
Frizzi & Meyer (2000)	0.08	19%	0.09	23%	0.09	22%
BDV12	0.11	23%	0.12	27%	0.12	26%

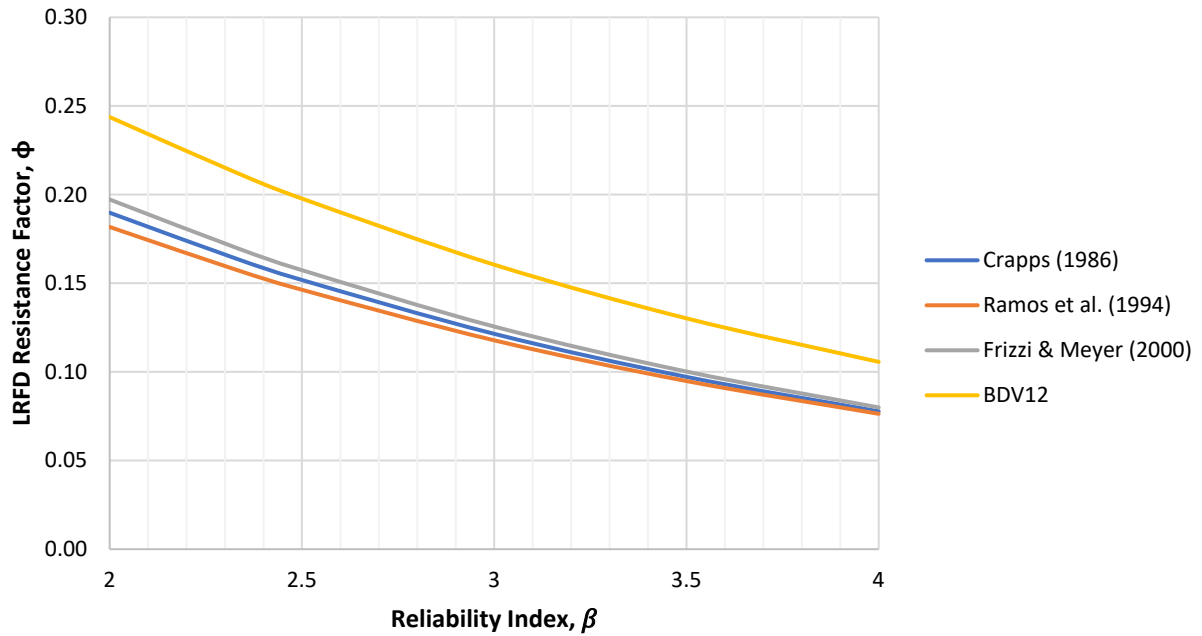


Figure 5-2. FOSM (Pre-Styler) LRFD  $\phi$  vs.  $\beta$  for multiple SPT design methods.

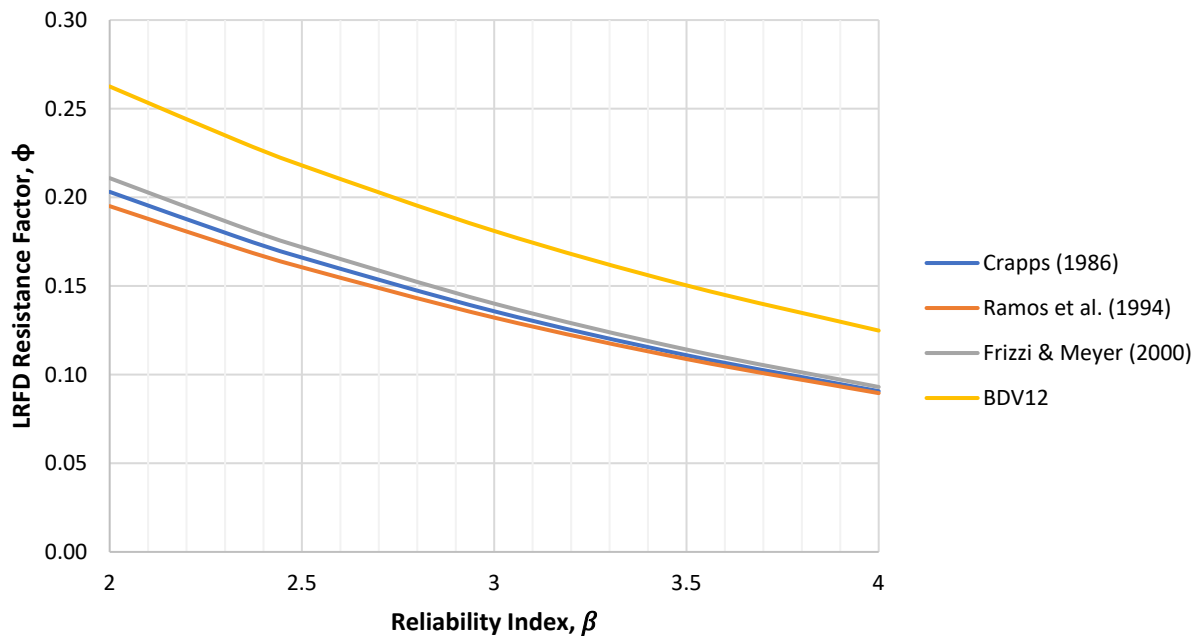


Figure 5-3. FOSM (Styler) LRFD  $\phi$  vs.  $\beta$  for multiple SPT design methods.

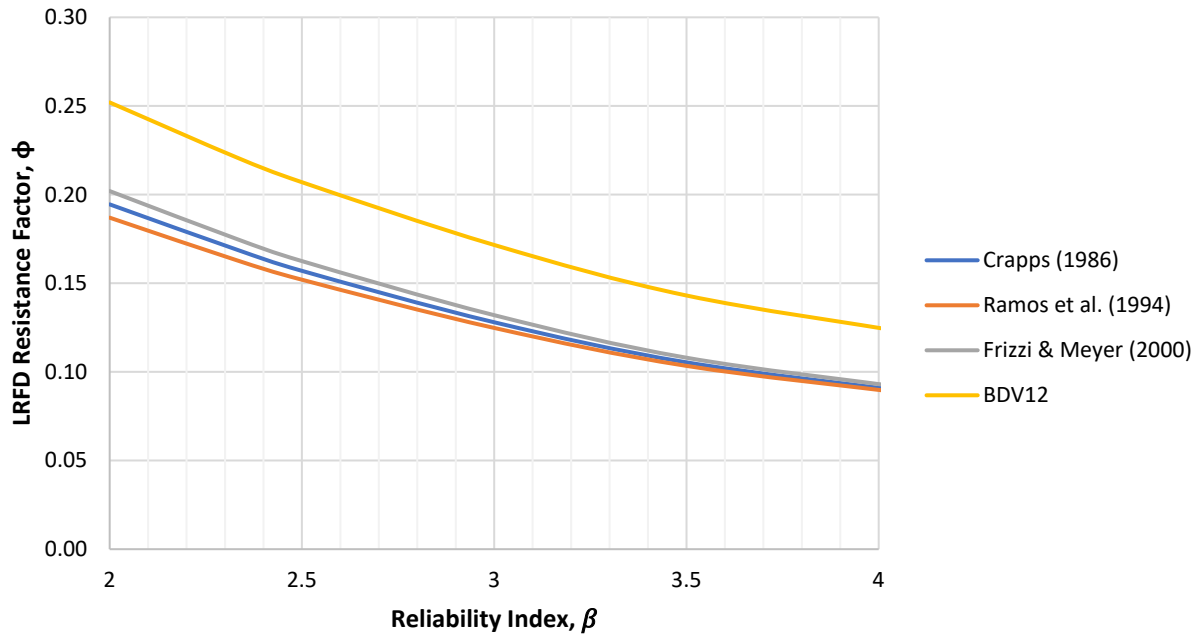


Figure 5-4. Monte Carlo LRFD  $\phi$  vs.  $\beta$  for multiple SPT design methods.

From Tables 5-3 through 5-8 and Figures 5-2 through 5-4, it is observed that the FOSM (Styler) and Monte Carlo methods produced similar results. Over the full  $\beta$  range the average percent difference between the two methods ranged from 3% to 6%. The FOSM (Pre-Styler) method was the most conservative and over the full  $\beta$  range the average percent difference compared to the FOSM (Styler) method ranged from 7% to 16%, with the percent difference increasing as  $\beta$  increased. The FOSM (Styler) method was used for comparison because this was the method used in FDOT Project BDV31-977-12 (McVay et al., 2016). Table 5-9 provides a comparison between the findings of this research effort with those included in BDV31-977-12. For the results from BDV31-977-12, two values are provided for  $\phi$  and  $(\phi / \lambda)$ . This is because in BDV31-977-12, the  $\phi$  assessments were separated by the limestone formation encountered. In Table 5-7, the Miami formation results are presented on the left side and the Fort Thompson formation results are presented on the right side. During this research effort, only one mobilized segment occurred in the Miami formation and therefore both formations were analyzed together. Also, only  $\beta = 2.33$  was analyzed in the prior research effort and therefore, this is the only comparison that can be made. From the results in Table 5-9, it can be seen that the new assessment falls within the range of the prior assessment. In both cases, the  $\phi$  values are quite low, suggesting SPT design is not an ideal approach for ACIP piles socketed into Florida limestone.

Table 5-9. SPT design methods comparison of  $\phi$  and  $\phi/\lambda$  from BDV31-977-125 and BDV31-977-12.

Design Method	SPT N - $\beta = 2.33$			
	FOSM - Styler		BDV31-977-12	
	$\phi$	$\phi / \lambda$	$\phi$	$\phi / \lambda$
Crapps (1986)	0.18	46%	N/A	N/A
Ramos et al. (1994)	0.17	47%	0.20 / 0.13	38% / 30%
Frizzi & Meyer (2000)	0.18	45%	0.14 / 0.25	19% / 37%
BDV12	0.23	50%	0.20 / 0.33	21% / 51%

**5.4 Core  $q_u$**

The next design methods evaluated employed unconfined compression strength ( $q_u$ ) data obtained from laboratory-tested cores collected throughout the site. In general, the number of core specimens recovered and tested in the lab were low considering the core data available for analysis was collected from 25 boring locations and 370 core runs. The average site recovery (REC) was 42%, and the average site rock quality designation (RQD) was 19%. As reported in Chapter 4, 218 split tension tests ( $q_{st}$ ) were completed, and 204 unconfined compression tests were completed. To increase the number of  $q_u$  assessments available for the analysis, the Florida geomaterials  $q_u$ - $q_t$  relationship (Rodgers et al. 2019) was used to estimate  $q_u$  from  $q_{st}$ , which increased the total number of  $q_u$  assessments from 204 to 422. Within the investigated elevation range (+15 to -132.5 ft), based on the deepest ACIP pile elevations, 403  $q_u$  assessments were available for analysis. Due to the poor recoveries and RQD, there was an insufficient amount of core samples collected within proximity (<100 to 500 ft) of the mobilized load-tested ACIP piles to only consider samples collected within a short distance. Consequently, samples collected throughout the site had to be used within each elevation range of the mobilized pile segments for the LRFD assessment.

When the core  $q_u$  strengths were first compared to the MWD  $q_u$  strengths, the core data indicated much higher strength rock was present at the site, and a significant difference in mean strengths was found, as indicated in Table 5-10. The cumulative frequency distributions presented in Figure 5-5 also indicated the strength distributions were dissimilar due to the core strengths showing a much larger percentage of higher strength rock present at the site. However, the large disagreement in mean strengths and the distributions were not typical, based on prior MWD investigations. Presented in Figures 5-6 and 5-7 are the cumulative frequency distributions for core strengths and MWD strengths at County Road 250 (CR-250) and at Perry. Similar to the ACIP pile site, core samples were collected throughout the site, and MWD was also performed throughout the site.

Comparison of the cumulative frequency distributions shows there is generally good agreement between the two strength assessments. The only time disagreement was typically found between MWD and core strengths was when REC and the RQD were low (e.g., Kanapaha; McVay and Rodgers, 2016). This gave indication that the core strength distribution was incomplete and underrepresented the amount of low strength limestone present at the site. The agreement between MWD side shear estimates and the measured load tested side shear presented in Chapter

4 support this notion. Furthermore, if side shear was estimated from the mean strength of the core samples (1,173 psi), using the FDOT recommended side shear equation (McVay et al., 1992), the average side shear would be 30.1 ksf. In only one mobilized segment did the measured side shear reach half this value and the average side shear from all mobilized segments used in these analyses (i.e., Table 5-1) was 6.87 ksf. The side shear estimated using the MWD mean  $q_u$  (223 psi) is 6.61 ksf which is in near perfect agreement with the load test data and further supports this hypothesis.

Table 5-10. Unconfined compression strength comparison between core samples and MWD.

Statistics	Core $q_u$	MWD $q_u$
Mean	1,173	223
Median	716	152
Std. Dev	1,200	282
CV	1.02	1.27
Max	5,172	6,749
Min	24	88
Count	403	120,458

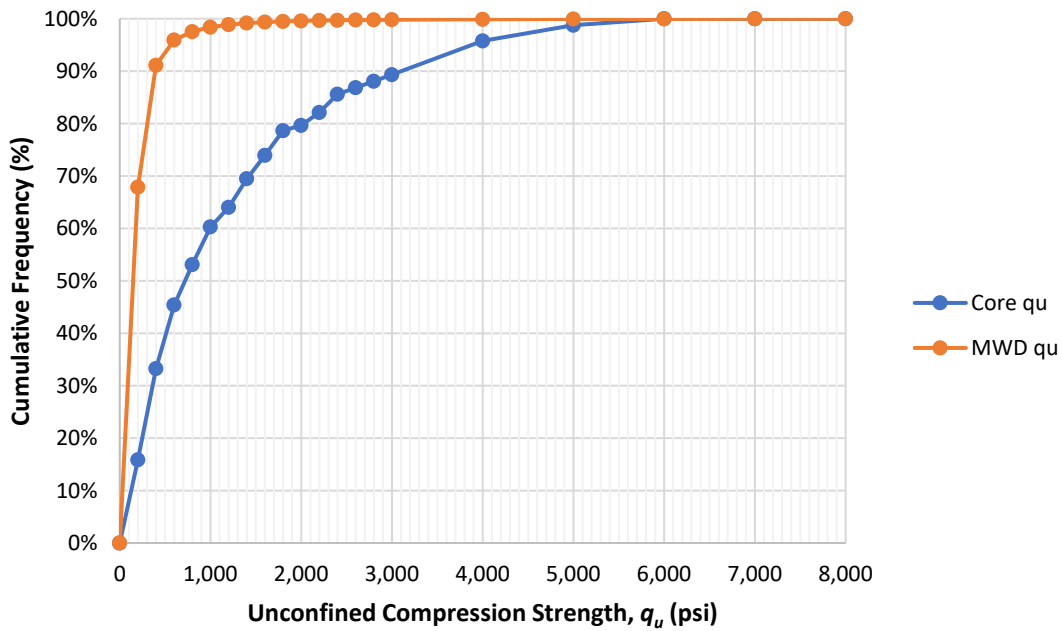


Figure 5-5. Rock core and MWD  $q_u$  cumulative frequency distributions at I-395 and Signature Bridge.

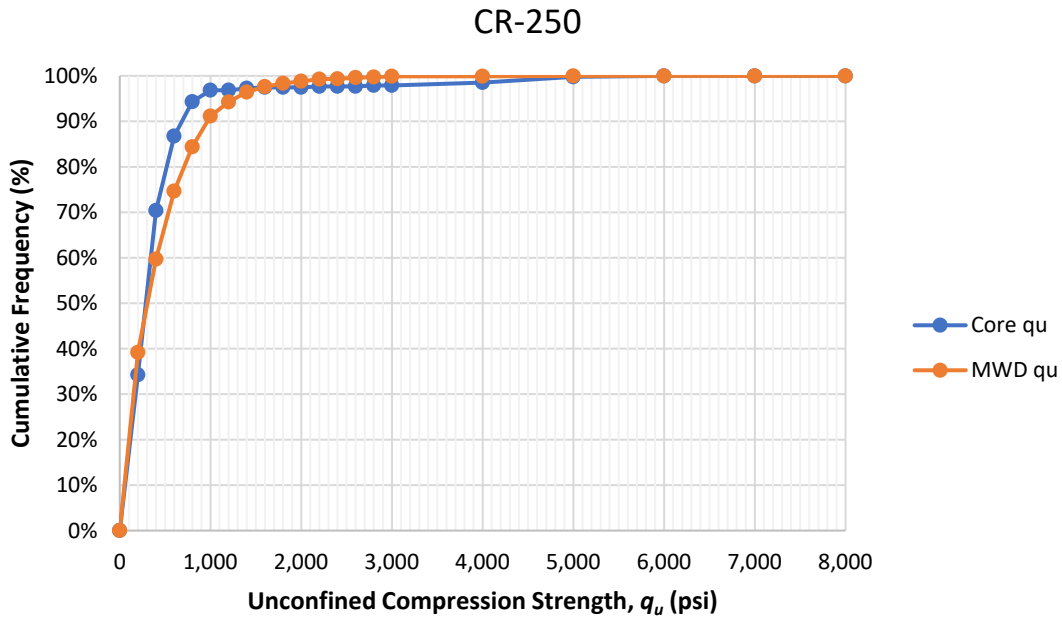


Figure 5-6. Rock core and MWD  $q_u$  cumulative frequency distributions at County Road 250.

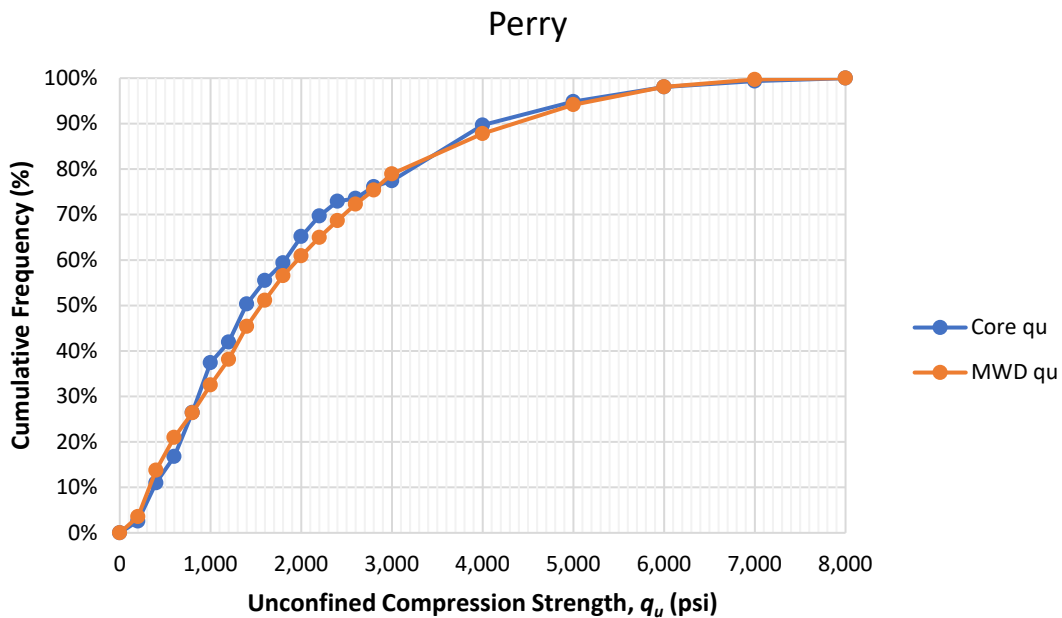


Figure 5-7. Rock core and MWD  $q_u$  cumulative frequency distributions at Perry.

UF researchers believe the poor recoveries and low RQDs were likely a result of the coring operations and the large percentage of lower strength rock present at the site. Specifically, MWD indicated that 68% of the rock had a  $q_u$  less than 200 psi, 91% of the rock had a  $q_u$  less than 400 psi, and 98.9% of the rock was less than 1,200 psi, which is the approximate mean strength indicated by the core samples. Based on the findings of Rodgers et al. (2021), when rock coring



is performed outside of the operational limits of the core bit, which occurs often in conventional coring, recoveries and the RQD are diminished, and lower strength rock less than  $q_u \leq 400$  psi is often significantly damaged and less likely to be recovered in testable lengths. Due to the four inch core diameters, the testable  $q_u$  length required was eight inches, and four-inch sample lengths were required for split tension testing which made recovering testable samples more difficult in the lower strength rock. The findings of Rodgers et al. (2021) also showed that coring outside the operational limits in rock with a  $q_u \leq 200$  psi often results in minimal REC and a RQD = 0%. Of the 370 core runs completed, 51 resulted in REC = 0% and 190 (over half the core runs) resulted in RQD = 0% which further suggests coring took place outside the operational limits and greatly reduced the amount of lower strength rock collected for testing. As coring depths become deeper, operating outside of the operational limits can become more frequent due to added vibration from overcrowding the bit and induced eccentric rotation of the long slender drill string. Consequently, UF researchers iteratively investigated different elevation ranges to determine if there was an elevation range in which MWD and the core strengths did agree. From the investigation, it was found that in the elevation range of +15 to -20 feet, the MWD and core  $q_u$  strengths were in good agreement but below this elevation range the strength statistics and cumulative frequency distributions began to deviate as indicated in Table 5-11 and Figure 5-8. The deviation was likely due to the discussed difficulties coring lower strength rock at greater depths. Therefore, the strength statistics at greater depths needed to be adjusted to account for the untested volume of rock. This was essential for the LRFD analyses as the initial resistance factors developed using the raw core data were significantly lower than the resistance factors found in McVay et al. (2016) due to the incomplete strength distribution sampled and reported.

Table 5-11. Comparison of core and MWD  $q_u$  strength statistics based on elevation ranges.

Statistics	El. +15' to -20'		El. -20' to -132.5' ft	
	Core $q_u$	MWD $q_u$	Core $q_u$	MWD $q_u$
Mean	125	159	1,305	230
Median	88	127	869	156
Std. Dev	138	150	1,210	292
CV	1.11	0.95	0.93	1.27
Max	832	4,359	5,172	6,749
Min	24	88	32	88
Count	45	11,908	358	108,550

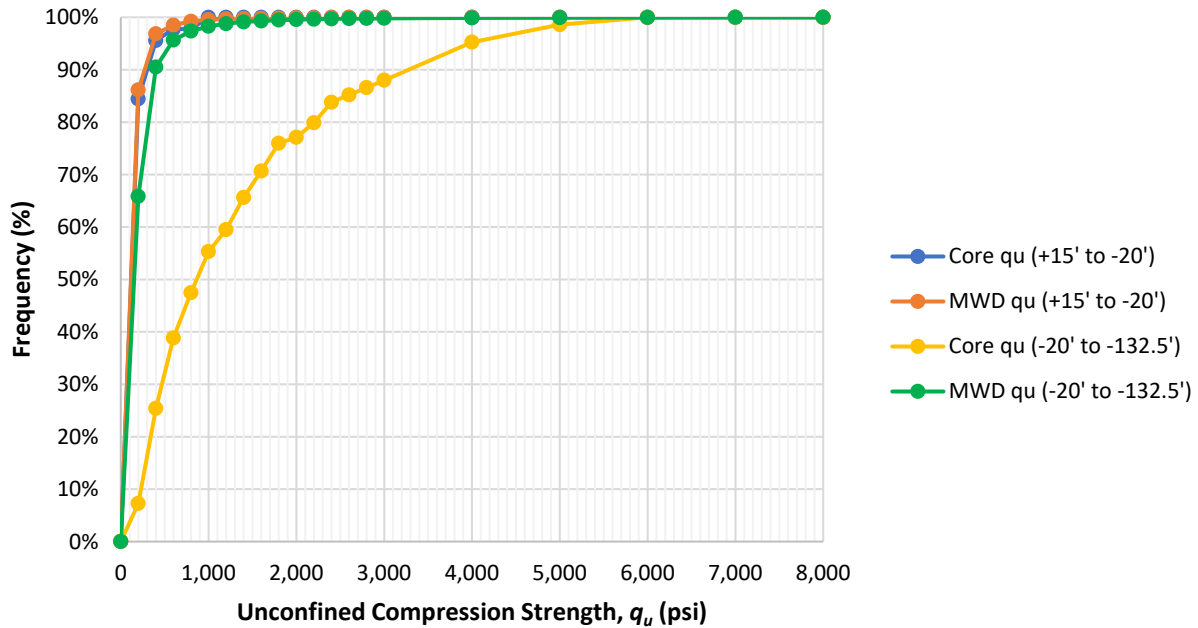


Figure 5-8. Comparison of core and MWD  $q_u$  strength distributions based on elevation ranges.

As noted, the core samples collected at the site were 4 inches in diameter, which indicates the RQD was representative of the tested volume. The very low RQD (19%) for the site indicates that only a small portion of the investigated volume was testable. Therefore, the core strengths in the lower elevation range needed to be adjusted to account for the untested volume of rock. It is common practice to use the core recovery percentage to adjust the rock strengths. However, this can lead to overestimates in the adjustment if the recovery percentage is not representative of the tested volume of rock which was the case at this site. For example, if the average REC = 42% were multiplied by the average  $q_u = 1,173$  psi, the adjusted average  $q_u$  strength for the site would be 507 psi which overestimates the average  $q_u = 223$  psi indicated by MWD. However, this assumes that the untested volume was 58% which is much lower than the true untested volume which was 81% based on the RQD = 19% and the smallest testable sample size (qst) of 4 inches. If the average RQD = 19% were multiplied by the average core  $q_u = 1,173$  psi, the adjusted average  $q_u$  strength for the site would be 223 psi which is in perfect agreement with MWD. This is because the true untested volume (81%) was accounted for by the adjustment. Table 5-12 provides the adjusted strength statistics in the lower elevation range and Figure 5-9 illustrates how accounting for the untested volume adjusts the cumulative frequency distribution. Table 5-12 and Figure 5-9, both indicate the RQD adjusted strength statistics and cumulative distribution are more representative of the MWD results which agreed with the mobilized load test data. Consequently, for the LRFD analysis, the side shear ( $f_s$ ) calculated for each mobilized pile segment located below an elevation of -20 ft was adjusted by multiplying  $f_s$  with the average RQD calculated within the same elevation range. The one mobilized segment located in the +15 to -20 ft elevation range was not adjusted because the correct strength distribution was found from the core samples collected.

Table 5-12. Core and MWD  $q_u$  statistics with RQD adjusted core statistics for El. -20' to -132.5'.

Statistics	El. +15' to -20'		El. -20' to -132.5' ft	
	Core $q_u$	MWD $q_u$	Core $q_u$	MWD $q_u$
Mean	125	159	248	230
Median	88	127	165	156
Std. Dev	138	150	229	292
CV	1.11	0.95	0.93	1.27
Max	832	4,359	981	6,749
Min	24	88	6	88
Count	45	11,908	358	108,550

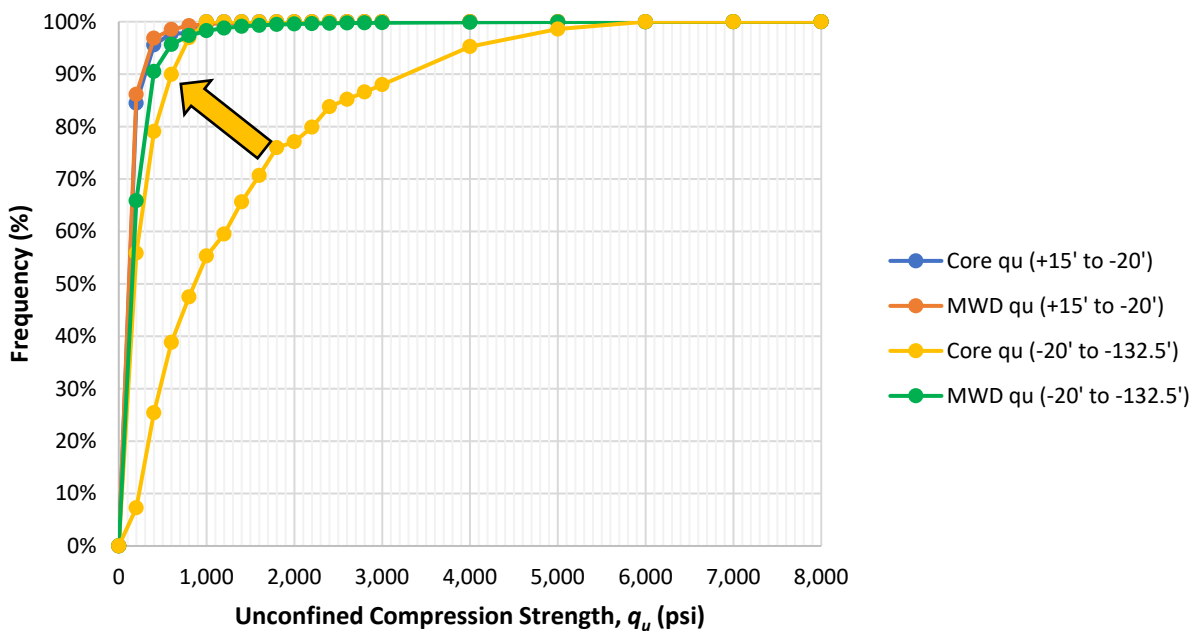


Figure 5-9. Core and MWD  $q_u$  distributions with an RQD adjusted core distribution for the elevation range -20' to -132.5'.

#### 5.4.1 Core $q_u$ Design Equations

The  $q_u$  design equations considered for the analysis included McVay et al. (1992) with the Florida Geomaterials equation used to simplify the equation as discussed in Rodgers et al. (2019), Gupton and Logan (1984), Reese and O’Neill (1987), the FDOT’s Soils and Foundation Handbook (SFH) recommended method which is McVay et al. (1992) with plus or minus one standard deviation from the mean  $q_u$  removed, and three versions of the BDV12 method developed in BDV31-977-12 (Note: the FDOT method was also simplified using the Florida Geomaterials equation). Equations 5-10 through 5-18 provide each design equation form used for the analysis.

McVay et al. (1992)

$$f_s = 1/2 * \sqrt{q_u} * \sqrt{q_t} * RQD \rightarrow (FL \text{ Geomaterials EQN used to estimate } q_t) \quad (5-10)$$

$$q_t = 0.436 \times q_u^{0.825} \rightarrow (FL \text{ Geomaterials EQN}) \quad (5-11)$$

$$f_s = 0.3302 \times q_u^{0.9125} \times 144 \frac{\text{in}^2}{\text{ft}^2} / 1,000 \frac{\text{lb}}{\text{kip}} \rightarrow (Simplified EQN) \quad (5-12)$$

Gupton and Logan (1984)

$$f_s = 0.2 * q_u * RQD * 2 (ksf/tsf) \quad (5-13)$$

Reese and O'Neill (1987)

$$f_s = 0.15 * q_u * RQD * 2 (ksf/tsf) \quad (5-14)$$

FDOT SFH Method

$$f_s = 1/2 * \sqrt{q_u} * \sqrt{q_t} * RQD \quad (5-10)$$

where,

- the FL Geomaterials equation was used to estimate  $q_t$  as shown in Eq. 5-11 and 5-12, and
- $q_u \pm 1$  standard deviation from the mean  $q_u$  was removed.

BDV12 (McVay et al., 2016)

$$f_s = 1.111 * \sqrt{q_u} * REC * 2 (ksf/tsf) \rightarrow \text{Miami Formation} \quad (5-15)$$

$$f_s = 1.643 * \sqrt{q_u} * REC * 2 (ksf/tsf) \rightarrow \text{Fort Thompson Formation} \quad (5-16)$$

BDV12 using Old C w/ RQD in Fort Thompson

$$f_s = 1.111 * \sqrt{q_u} * REC * 2 (ksf/tsf) \rightarrow \text{Miami Formation} \quad (5-15)$$

$$f_s = 1.643 * \sqrt{q_u} * RQD * 2 (ksf/tsf) \rightarrow \text{Fort Thompson Formation} \quad (5-17)$$

BDV12 using New C w/ RQD in Fort Thompson

$$f_s = 1.111 * \sqrt{q_u} * REC * 2 (ksf/tsf) \rightarrow \text{Miami Formation} \quad (5-15)$$

$$f_s = 1.500 * \sqrt{q_u} * RQD * 2 (ksf/tsf) \rightarrow \text{Fort Thompson Formation} \quad (5-18)$$

Note: McVay et al. (1992) and the FDOT's SFH method typically use REC to adjust the calculated side shear strength ( $f_s$ ). RQD was used as a replacement at the Miami-Dade site to account for the untested volume of rock. UF researchers are not recommending REC to be replaced with RQD for all cases. However, the UF researchers do recommend that any adjustment made should be representative of the untested volume of rock and account for layers used in design that are partially rock and partially soil.

As seen in Equations 5-15 through 5-18, each version of the BDV12 method used two different equations. One equation was used in the Miami formation (El. +15 to -20 feet) for every version of the method, and a different equation was used in the Fort Thompson formation (El. -20 to -132.5 feet) for each version of the method. The equation form of the BDV12 method was developed so that the C-coefficient is unique based on site specific conditions. In FDOT Project BDV31-977-12, (McVay et al., 2016),  $C = 1.111$  in the Miami formation, and  $C = 1.643$  in the Fort Thompson formation. The equation then multiplies the C-coefficient by the square root of the mean  $q_u$  and the REC to account for the volume of rock present. The original C-coefficient and REC in the Miami formation were used for each version of the BDV12 method because there was not enough data gathered in the Miami formation during this research effort to develop a new C-coefficient, and the average core REC in the mobilized segment (56%) elevation range was similar to the percentage of rock present at the I-396 TP-C location based on the MWD assessment ( $REC_{MWD} = 64\%$ ) covered in Chapter 4. Equation 5-16 used the original C-coefficient in the Fort Thompson formation and REC. However, as discussed, the REC for this site was not reflective of the untested volume in the Fort Thompson formation (El. -20 to -132.5 ft) and therefore RQD was used in the Fort Thompson formation for Equations 5-17 and 5-18. Equation 5-17 used the original  $C = 1.643$  and Equation 5-18 used a new  $C = 1.500$ . The new C-coefficient was developed using eight of the ten mobilized segments at the I-395/Signature Bridge sites (Figure 5-10). One of the two mobilized segments that was not considered was located in the Miami formation and the other mobilized segment (Test Shaft 7, SG6 to LTA) was considered an outlier as the mobilized segment indicated much higher strength compared to the core samples collected in the elevation range (Note: the MWD assessments confirmed the higher strength segment was valid, it was just a rare occurrence on the site). The new  $C = 1.500$  was very similar to the original  $C = 1.643$  found in BDV31-977-12 for ACIP piles in South Florida limestone. If the outlying segment were included in the development, the new C would have equaled 1.711. Interestingly, the original C-coefficient is close to the average of both new C-coefficients (1.606). The new  $C = 1.500$  was selected for analysis rather than  $C = 1.711$  because it provides a more conservative estimate.

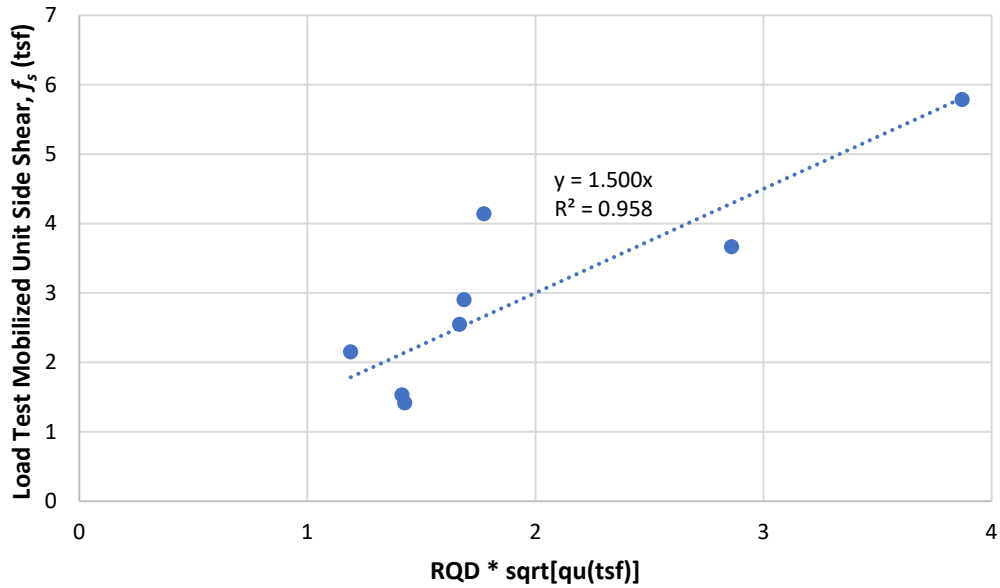


Figure 5-10. Developing a new C-coefficient based on site specific load test and core data.

With each of the  $q_u$  design methods determined, the measured side shear was plotted versus the predicted side shear, presented in Figure 5-11. The tabular results are presented in Tables 5-13 and 5-14, and the bias statistics for each method are provided in Table 5-15.

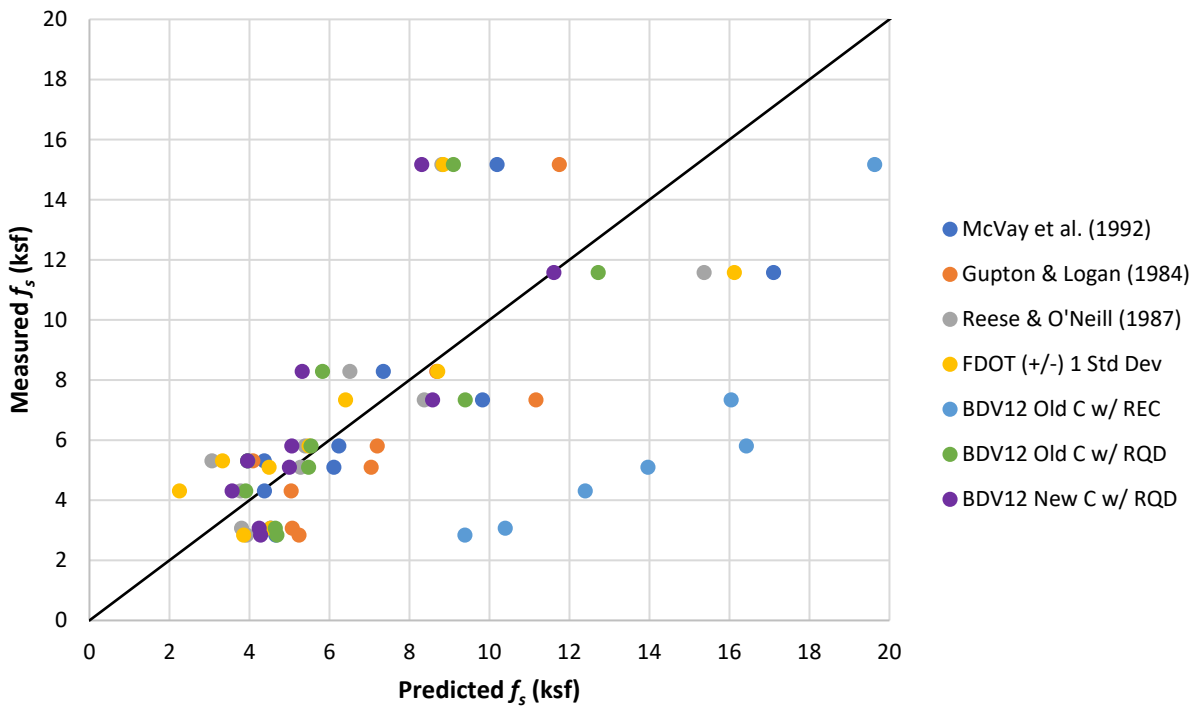


Figure 5-11. ACIP pile measured vs. predicted side shear capacity for multiple  $q_u$  design methods.

Table 5-13. Side shear estimates and bias per mobilized layer using  $q_u$  design methods.

Location	Segment	Load Test $f_s$ (ksf)	McVay et al. (1992)		Gupton & Logan (1984)		Reese & O'Neill (1987)		FDOT (+/-) $1\sigma$	
			$f_s$ (ksf)	Bias	$f_s$ (ksf)	Bias	$f_s$ (ksf)	Bias	$f_s$ (ksf)	Bias
I395 TP-C	GSE to SG23	5.30	4.38	1.21	4.09	1.30	3.07	1.73	3.33	1.59
	SG19 to SG17	2.83	4.66	0.61	5.24	0.54	3.93	0.72	3.86	0.73
	SG17 to SG14	7.33	9.83	0.75	11.17	0.66	8.38	0.88	6.41	1.14
	SG10 to SG8	3.06	4.53	0.68	5.07	0.60	3.80	0.80	4.53	0.68
	SG8 to LTA	4.30	4.38	0.98	5.05	0.85	3.78	1.14	2.25	1.91
	SG3 to SG2	8.28	7.35	1.13	8.69	0.95	6.51	1.27	8.71	0.95
	SG2 to SG1	11.57	17.11	0.68	20.50	0.56	15.37	0.75	16.13	0.72
	LTA to SG3	5.80	6.24	0.93	7.20	0.81	5.40	1.07	5.49	1.06
SB TP-D	SG9 to SG6	5.09	6.12	0.83	7.04	0.72	5.28	0.96	4.49	1.13
	SG6 to LTA	15.16	10.19	1.49	11.75	1.29	8.81	1.72	8.85	1.71

Table 5-14. Side shear estimates and bias per mobilized layer using  $q_u$  design methods continued.

Location	Segment	Load Test $f_s$ (ksf)	BDV12		BDV12 - Old C		BDV12 - New C	
			$f_s$ (ksf)	Bias	$f_s$ (ksf)	Bias	$f_s$ (ksf)	Bias
I395 TP-C	GSE to SG23	5.30	4.38	1.21	4.09	1.30	3.07	1.73
	SG19 to SG17	2.83	4.66	0.61	5.24	0.54	3.93	0.72
	SG17 to SG14	7.33	9.83	0.75	11.17	0.66	8.38	0.88
	SG10 to SG8	3.06	4.53	0.68	5.07	0.60	3.80	0.80
	SG8 to LTA	4.30	4.38	0.98	5.05	0.85	3.78	1.14
	SG3 to SG2	8.28	7.35	1.13	8.69	0.95	6.51	1.27
	SG2 to SG1	11.57	17.11	0.68	20.50	0.56	15.37	0.75
	LTA to SG3	5.80	6.24	0.93	7.20	0.81	5.40	1.07
SB TP-D	SG9 to SG6	5.09	6.12	0.83	7.04	0.72	5.28	0.96
	SG6 to LTA	15.16	10.19	1.49	11.75	1.29	8.81	1.72

Table 5-15. Bias statistics for  $q_u$  design methods.

Design Method	Mean	Std Dev	CV <sub>R</sub>
McVay et al. (1992)	0.93	0.27	0.29
Gupton & Logan (1984)	0.83	0.26	0.32
Reese & O'Neill (1987)	1.10	0.35	0.32
FDOT (+/-) 1 Std Dev	1.16	0.41	0.36
BDV12 Old C w/ REC	0.51	0.31	0.61
BDV12 Old C w/ RQD	1.04	0.33	0.31
BDV12 New C w/ RQD	1.13	0.35	0.31

### 5.5 Core $q_u$ LRFD $\phi$ Assessment

Once the bias statistics were derived, LRFD  $\phi$  assessment took place for each reliability index:  $\beta = 2, 2.33, 2.5, 3, 3.5,$  and  $4$ . The dead-to-live load ratio ( $Q_D/Q_L$ ) was set to three for LRFD calibration. Tables 5-16 through 5-21 provide the LRFD  $\phi$  and efficiency ( $\phi / \lambda$ ) for each  $\beta$  using the seven  $q_u$  design methods and three LRFD methods. Figures 5-12 through 5-14 provide the LRFD  $\phi$  vs.  $\beta$  curves for each LRFD method, FOSM (Pre-Styler), FOSM (Styler), and Monte Carlo, respectively.

Table 5-16. ACIP pile LRFD analysis – South Florida limestone for  $q_u$  design methods –  $\beta = 2$ .

Design Method	Core $q_u$ - $\beta = 2$					
	FOSM - Pre-Styler		FOSM - Styler		Monte Carlo	
	$\phi$	$\phi / \lambda$	$\phi$	$\phi / \lambda$	$\phi$	$\phi / \lambda$
McVay et al. (1992)	0.56	61%	0.62	66%	0.60	64%
Gupton & Logan (1984)	0.47	57%	0.52	62%	0.50	60%
Reese & O'Neill (1987)	0.63	57%	0.69	62%	0.67	60%
FDOT (+/-) 1 Std Dev	0.62	53%	0.67	58%	0.64	55%
BDV12 Old C w/ REC	0.17	33%	0.17	35%	0.16	33%
BDV12 Old C w/ RQD	0.60	58%	0.66	63%	0.64	61%
BDV12 New C w/ RQD	0.66	58%	0.72	64%	0.70	62%

Table 5-17. ACIP pile LRFD analysis – South Florida limestone for  $q_u$  design methods –  $\beta = 2.33$ .

Design Method	Core $q_u$ - $\beta = 2.33$					
	FOSM - Pre-Styler		FOSM - Styler		Monte Carlo	
	$\phi$	$\phi / \lambda$	$\phi$	$\phi / \lambda$	$\phi$	$\phi / \lambda$
McVay et al. (1992)	0.50	54%	0.56	60%	0.54	58%
Gupton & Logan (1984)	0.42	51%	0.46	56%	0.45	54%
Reese & O'Neill (1987)	0.56	51%	0.62	56%	0.59	54%
FDOT (+/-) 1 Std Dev	0.54	47%	0.59	51%	0.57	49%
BDV12 Old C w/ REC	0.14	27%	0.14	29%	0.13	26%
BDV12 Old C w/ RQD	0.53	51%	0.59	57%	0.57	55%
BDV12 New C w/ RQD	0.58	52%	0.65	57%	0.62	55%



Table 5-18. ACIP pile LRFD analysis – South Florida limestone for  $q_u$  design methods –  $\beta = 2.5$ .

Design Method	Core $q_u - \beta = 2.5$					
	FOSM - Pre-Styler		FOSM - Styler		Monte Carlo	
	$\phi$	$\phi / \lambda$	$\phi$	$\phi / \lambda$	$\phi$	$\phi / \lambda$
McVay et al. (1992)	0.47	51%	0.53	57%	0.51	55%
Gupton & Logan (1984)	0.39	47%	0.44	53%	0.42	51%
Reese & O'Neill (1987)	0.52	47%	0.58	53%	0.56	51%
FDOT (+/-) 1 Std Dev	0.50	43%	0.56	48%	0.53	46%
BDV12 Old C w/ REC	0.12	24%	0.13	26%	0.12	24%
BDV12 Old C w/ RQD	0.50	48%	0.56	54%	0.54	51%
BDV12 New C w/ RQD	0.55	49%	0.62	54%	0.59	52%

Table 5-19. ACIP pile LRFD analysis – South Florida limestone for  $q_u$  design methods –  $\beta = 3$ .

Design Method	Core $q_u - \beta = 3$					
	FOSM - Pre-Styler		FOSM - Styler		Monte Carlo	
	$\phi$	$\phi / \lambda$	$\phi$	$\phi / \lambda$	$\phi$	$\phi / \lambda$
McVay et al. (1992)	0.39	42%	0.46	49%	0.44	47%
Gupton & Logan (1984)	0.32	39%	0.37	45%	0.36	43%
Reese & O'Neill (1987)	0.43	39%	0.50	45%	0.47	43%
FDOT (+/-) 1 Std Dev	0.41	35%	0.47	40%	0.44	38%
BDV12 Old C w/ REC	0.09	18%	0.10	20%	0.09	18%
BDV12 Old C w/ RQD	0.42	40%	0.48	46%	0.46	44%
BDV12 New C w/ RQD	0.46	40%	0.53	46%	0.50	44%

Table 5-20. ACIP pile LRFD analysis – South Florida limestone for  $q_u$  design methods –  $\beta = 3.5$ .

Design Method	Core $q_u - \beta = 3.5$					
	FOSM - Pre-Styler		FOSM - Styler		Monte Carlo	
	$\phi$	$\phi / \lambda$	$\phi$	$\phi / \lambda$	$\phi$	$\phi / \lambda$
McVay et al. (1992)	0.33	35%	0.39	42%	0.38	40%
Gupton & Logan (1984)	0.27	32%	0.32	38%	0.30	36%
Reese & O'Neill (1987)	0.36	32%	0.42	38%	0.40	36%
FDOT (+/-) 1 Std Dev	0.34	29%	0.39	33%	0.37	32%
BDV12 Old C w/ REC	0.07	13%	0.07	15%	0.07	13%
BDV12 Old C w/ RQD	0.34	33%	0.41	39%	0.39	37%
BDV12 New C w/ RQD	0.38	33%	0.45	40%	0.43	38%

Table 5-21. ACIP pile LRFD analysis – South Florida limestone for  $q_u$  design methods –  $\beta = 4$ .

Design Method	Core $q_u - \beta = 4$					
	FOSM - Pre-Styler		FOSM - Styler		Monte Carlo	
	$\phi$	$\phi / \lambda$	$\phi$	$\phi / \lambda$	$\phi$	$\phi / \lambda$
McVay et al. (1992)	0.28	30%	0.34	36%	0.32	35%
Gupton & Logan (1984)	0.22	27%	0.27	32%	0.26	31%
Reese & O'Neill (1987)	0.30	27%	0.36	32%	0.34	31%
FDOT (+/-) 1 Std Dev	0.27	24%	0.32	28%	0.32	27%
BDV12 Old C w/ REC	0.05	10%	0.06	11%	0.05	10%
BDV12 Old C w/ RQD	0.29	27%	0.35	33%	0.33	32%
BDV12 New C w/ RQD	0.31	28%	0.38	34%	0.37	32%

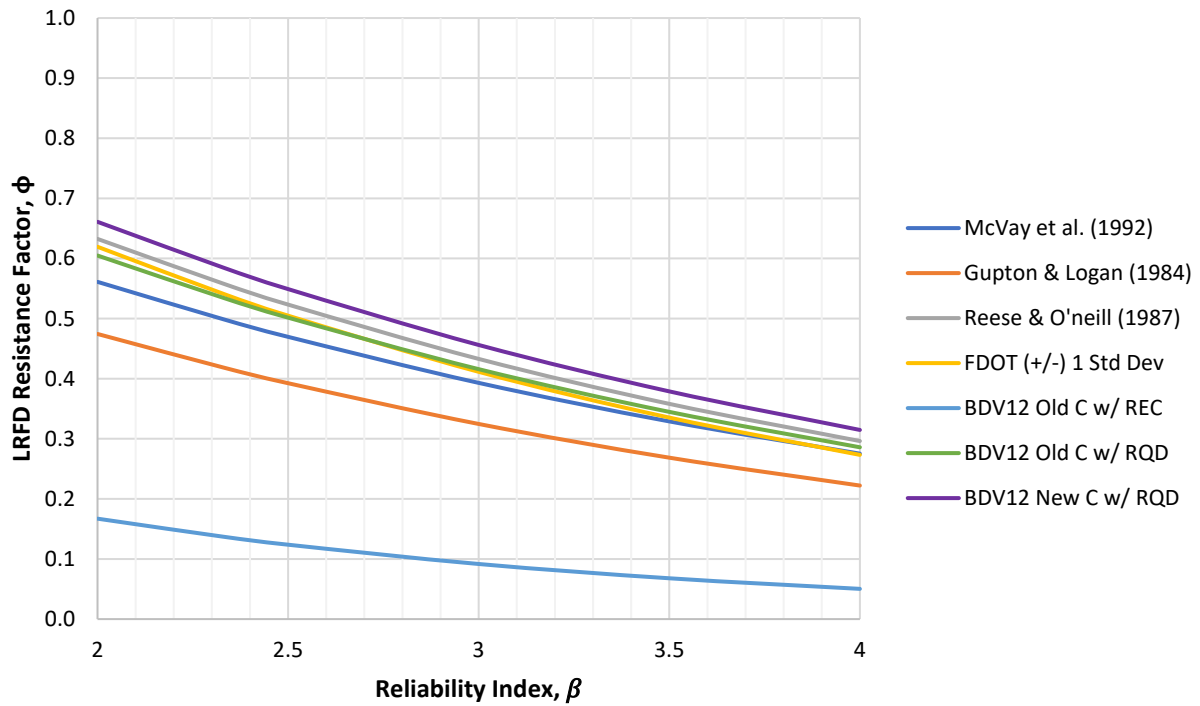


Figure 5-12. FOSM (Pre-Styler) LRFD  $\phi$  vs.  $\beta$  for multiple  $q_u$  design methods.

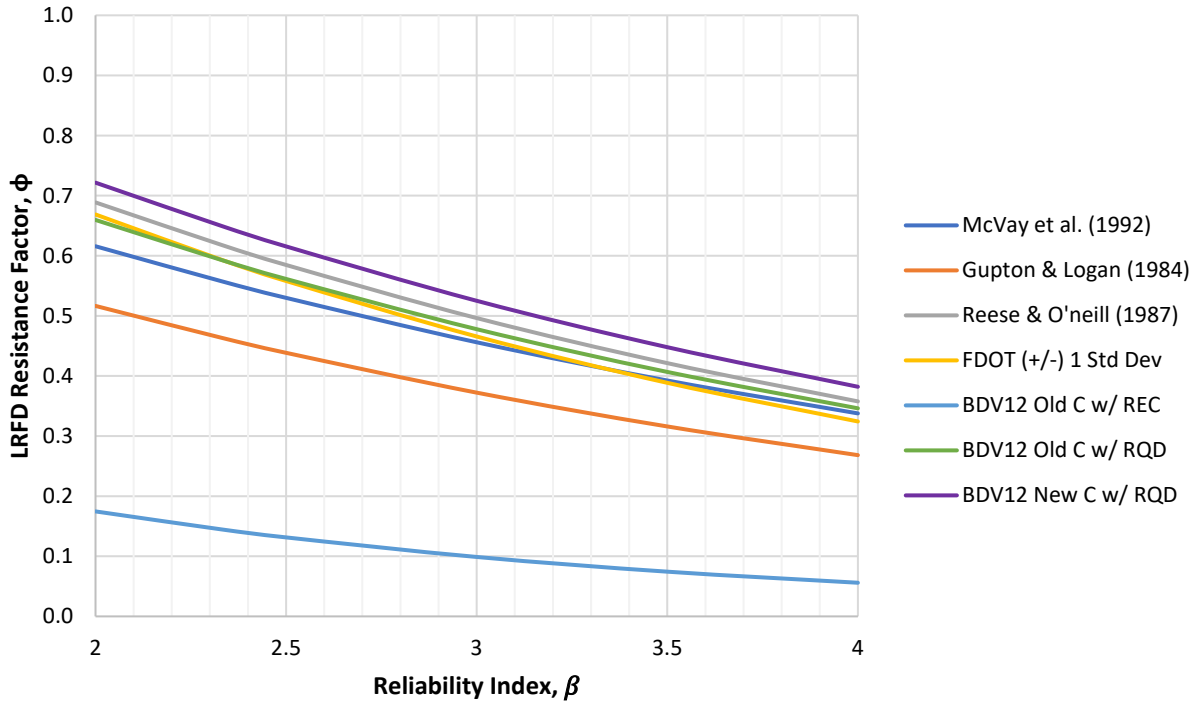


Figure 5-13. FOSM (Styler) LRFD  $\phi$  vs.  $\beta$  for multiple  $q_u$  design methods.

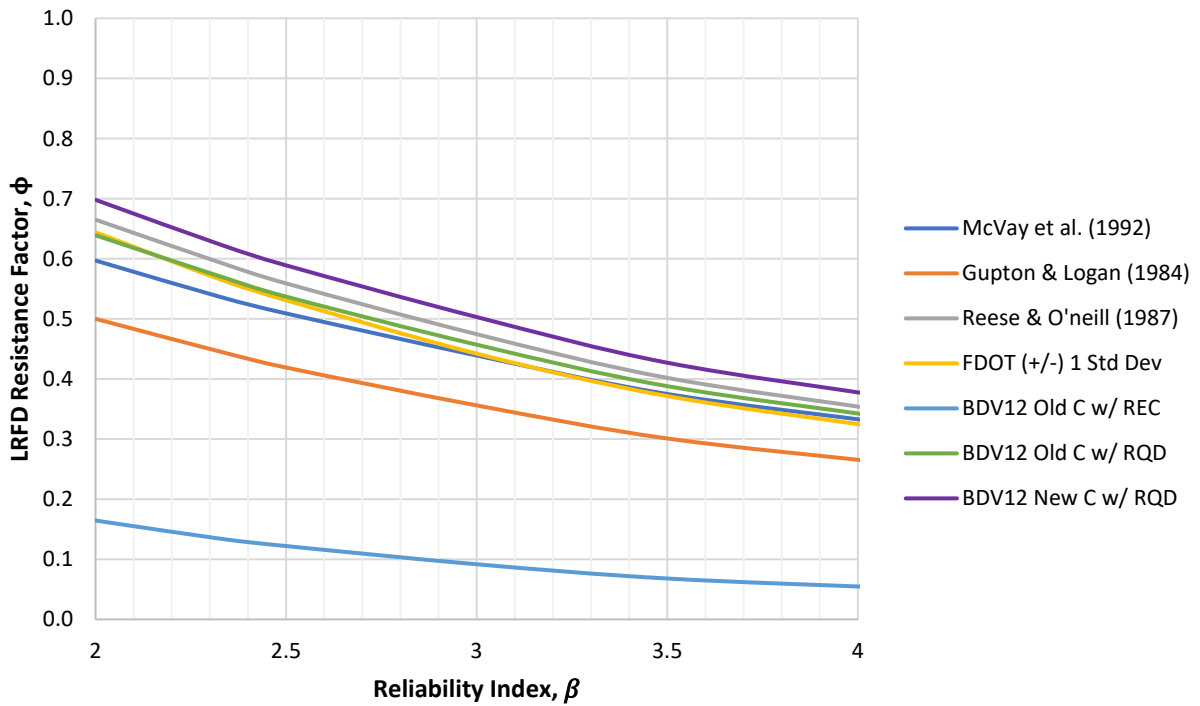


Figure 5-14. Monte Carlo LRFD  $\phi$  vs.  $\beta$  for multiple  $q_u$  design methods.

From Tables 5-16 through 5-21 and Figures 5-12 through 5-14, it is observed again that the FOSM (Styler) and Monte Carlo methods produced similar results. Over the full  $\beta$  range the average percent difference between the two methods ranged from 3.5% to 5.8%. The FOSM (Pre-Styler) method was the most conservative and over the full  $\beta$  range the average percent difference compared to the FOSM (Styler) method ranged from 8.3% to 18.6%, with the percent difference increasing as  $\beta$  increased. Again, the FOSM (Styler) method was used for comparison because this was the method used in BDV31-977-12 (McVay et al., 2016). Table 5-22 provides a comparison between the findings of this research effort with those included in BDV31-977-12. For the results from BDV31-977-12, two values are provided for  $\phi$  and  $(\phi / \lambda)$ . This is because in BDV31-977-12, the  $\phi$  assessments were separated by the limestone formation encountered. In Table 5-22, the Miami formation results are presented on the left side and the Fort Thompson formation results are presented on the right side. During this research effort, only one mobilized segment occurred in the Miami formation and therefore both formations were analyzed together. Also, only  $\beta = 2.33$  was analyzed in the prior research effort and therefore, this is the only comparison that can be made. From the results in Table 5-22, it can be seen that the new assessment produced higher resistance factors compared to the prior assessment. This was likely a result of higher quality load test data provided for this investigation, and an increased number of core samples available at the site compared to the prior effort. In the prior report, it was stated that many of the load tests were unable to differentiate rock and soil layers and skin and tip resistances due to limited pile instrumentation, and the core samples were collected over a much larger area in which averaging occurred per formation (Miami vs. Fort Thompson). The mobilized layers considered for this effort were predominately limestone and most mobilized segments occurred above the bidirectional load test assembly (i.e., load cell) which produced isolated shear that allowed the investigation to focus on side shear in limestone layers. Furthermore, this effort had the advantage of using MWD to assist in properly adjusting the incomplete  $q_u$  distribution which significantly improved the resistance factors compared to not adjusting the incomplete distribution. It should be noted that the prior effort stated in the conclusions of the Final Report that MWD could be used to improve the resistance factors, which was found to be correct in this effort.

Table 5-22. Comparison of  $q_u$  design methods  $\phi$  and  $\phi/\lambda$  from BDV31-977-125 and BDV31-977-12.

Design Method	Core $q_u$ - $\beta = 2.33$			
	FOSM - Styler		BDV31-977-12	
	$\phi$	$\phi / \lambda$	$\phi$	$\phi / \lambda$
McVay et al. (1992)	0.56	60%	N/A	N/A
Gupton & Logan (1984)	0.46	56%	0.34 / 0.32	41% / 38%
Reese & O'Neill (1987)	0.62	56%	0.46 / 0.42	41% / 38%
FDOT (+/-) 1 Std Dev	0.59	51%	0.47 / 0.33	45% / 51%
BDV12 Old C w/ REC	0.14	29%		
BDV12 Old C w/ RQD	0.59	57%	0.48 / 0.55	56% / 55%
BDV12 New C w/ RQD	0.65	57%		

## 6 LRFD Phi Assessment of MWD Specific Energy for ACIP Pile Capacity

The focus of this chapter is the assessment of LRFD resistance factors,  $\phi$ , for Auger Cast-in-Place (ACIP) piles constructed in south Florida limestone using data collected from measuring while drilling (MWD). The LRFD resistance factors were assessed using three different methods which includes the original FOSM approach (FOSM Pre-Styler), the revised FOSM approach (FOSM Styler), and Monte Carlo simulations (Monte Carlo) as discussed in Chapter 5. Also similar to Chapter 5, each LRFD method was assessed using six different Reliability Indices,  $\beta$ , ranging from 2 to 4, with the dead-to-live load ratio ( $Q_D/Q_L$ ) set to three for LRFD calibration based on McVay et al. (2000). All other component terms used in calculating  $\phi$  are listed under Equation 1 in Chapter 5.

For the investigation, two MWD approaches were considered. The first approach (MWD  $q_u$ ) used MWD data collected during production pile drilling to simulate MWD borings performed within a short distance ( $< 100$  ft) from the mobilized load test locations. This allowed the investigation to quantify the effects of spatial variability over short distances when sufficient strength data are collected within the vicinity of ACIP piles. The second approach (MWD  $f_s$ ) only used MWD data collected in the footprint of mobilized ACIP piles to show the benefits of eliminating spatial variability from pile capacity estimates, leaving only the method error as a source of uncertainty. The second approach also displays the superior QA/QC that can be achieved when MWD is performed in the footprint of each pile. The first approach considered four  $q_u$  design equations. The second approach considered ACIP pile rock auger MWD data, MWD rock auger data from ACIP piles and drilled shafts combined, and then considered the MWD QA/QC approach for bored piles as a whole, which included MWD data for ACIP pile and drilled shaft rock augers and drilled shaft rock buckets combined. Therefore, seven MWD side shear methods were investigated using three different LRFD methods and 6 reliability indices. In total, this amounts to 126 MWD LRFD resistance factor assessments and 324 LRFD assessments when combined with the 198 assessments performed in Chapter 5.

### 6.1 MWD $q_u$

From FDOT Project BDV31-820-006 (McVay and Rodgers, 2019), it was discovered that measuring while drilling (MWD) was capable of producing a near continuous profile of unconfined compression strength during rock coring and while drilling with a tri-cone roller bit for site investigation. In the prior study it was also found that the newly developed MWD site characterization technique was in near-perfect agreement with recovered rock core specimens tested in the laboratory and increased the number of strength assessments obtained by an order of magnitude. This introduced a new method of site characterization that has the potential to revolutionize the design of ACIP piles and drilled shafts. To date, MWD site characterization and bored pile MWD QA/QC have not been completed on the same site. However, both methods produce near continuous strength ( $q_u$  or  $f_s$ ) profiles that can be directly compared. Therefore, the  $q_u$  data collected during ACIP production pile drilling can be used to simulate the MWD site characterization approach, which allowed the method to be considered for the LRFD analyses. Consequently, the MWD  $q_u$  data obtained from monitoring production piles in proximity of the mobilized ACIP piles at I-395 and Signature Bridge were used to simulate the new method of site characterization and ACIP pile LRFD design.

### 6.1.1 MWD $q_u$ Design Equations

The  $q_u$  design equations considered for the MWD LRFD analysis included McVay et al. (1992) with the Florida Geomaterials equation used to simplify the equation as discussed in Rodgers et al. (2019), Gupton and Logan (1984), Reese and O'Neill (1987), and the FDOT's Soils and Foundation Handbook (SFH) recommended method which is McVay et al. (1992) with plus or minus one standard deviation from the mean  $q_u$  removed. The FDOT method was also simplified using the Florida Geomaterials equation. Each of the methods used in the analysis were selected because they performed the best in a prior investigation (BDV31-977-20; McVay and Rodgers, 2016) for drilled shafts socketed into Florida limestone, where 10 different leading design equations were investigated.

During the MWD LRFD investigation, the side shear for each mobilized segment was calculated using each design equation with MWD  $q_u$  data collected within each respective mobilized segments elevation range during production pile drilling. As stated, each of the production piles considered were located within 100 ft of the load test locations. Therefore, spatial error existed in the prediction but far less than the conventional boring estimates covered in Chapter 5 which employed data hundreds to thousands of feet away from the load test locations. The production piles considered for the I-395 Test Pile C analysis included ten piles from Pile Group C1 and eight piles from Group C2, and 16 piles from Signature Bridge Group D were considered for the Signature Bridge Test Pile D analysis (Note: the same piles analyzed in Chapters 3 and 4 were used). SR-836 Test Pile A was not included in the MWD  $q_u$  assessment because production piles within close proximity to Test Pile A had not been completed at the time of the analysis.

As discussed in Chapter 4, using the specific energy threshold, MWD was capable of estimating the percentage of rock present within each elevation range of interest. Consequently, each of the side shear equations was multiplied by the percentage of rock ( $REC_{MWD}$ ) estimated by MWD within each respective mobilized segment's elevation range to adjust the average side shear based on the in situ conditions. This is similar to FDOT's SFH standard approach of adjusting side shear based on core recoveries as discussed in Chapter 5. The measured side shear from load testing is plotted vs. the predicted side shear from MWD in Figure 6-1, the tabular results are presented in Table 6-1, and the bias statistics for each method are provided in Table 6-2.

McVay et al. (1992)

$$f_s = 1/2 * \sqrt{q_u} * \sqrt{q_t} * REC_{MWD} \rightarrow (FL\ Geomaterials\ EQN\ used\ to\ estimate\ q_t) \quad (6-1)$$

$$q_t = 0.436 \times q_u^{0.825} \rightarrow (FL\ Geomaterials\ EQN) \quad (6-2)$$

$$f_s = 0.3302 \times q_u^{0.9125} \times 144 \frac{in^2}{ft^2} / 1,000 \frac{lb_f}{kip} \rightarrow (Simplified\ EQN) \quad (6-3)$$

Gupton and Logan (1984)

$$f_s = 0.2 * q_u * REC_{MWD} * 2 (ksf/tsf) \quad (6-4)$$

Reese and O'Neill (1987)

$$f_s = 0.15 * q_u * REC_{MWD} * 2 \text{ (ksf/tsf)} \quad (6-5)$$

FDOT SFH Method

$$f_s = 1/2 * \sqrt{q_u} * \sqrt{q_t} * REC_{MWD} \quad (6-1)$$

where,

- the FL Geomaterials equation was used to estimate  $q_t$  as shown in Eq. 6-2 and 6-3, and
- $q_u \pm 1$  standard deviation from the mean  $q_u$  was removed.

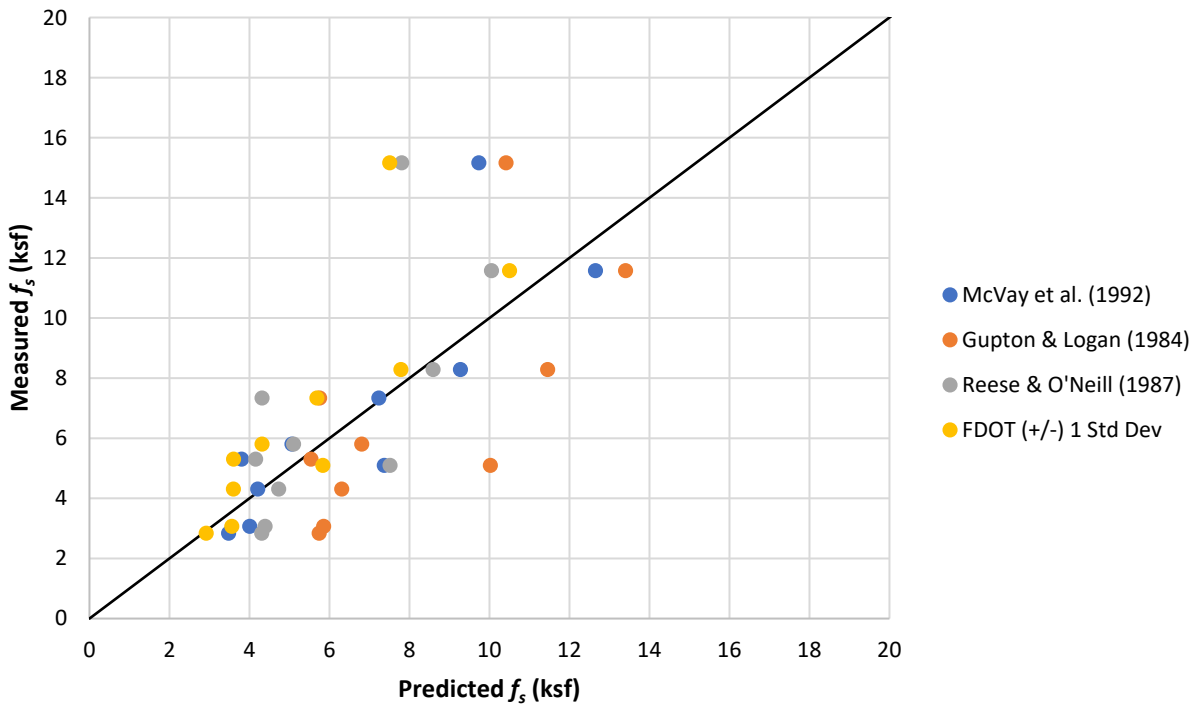


Figure 6-1. ACIP pile measured vs. predicted side shear capacity for MWD  $q_u$  design methods.

Table 6-1. Side shear estimates and bias per mobilized layer using MWD  $q_u$  design methods.

Location	Segment	Load Test $f_s$ (ksf)	McVay et al. (1992)		Gupton & Logan (1984)		Reese & O'Neill (1987)		FDOT (+/-) $1\sigma$	
			$f_s$ (ksf)	Bias	$f_s$ (ksf)	Bias	$f_s$ (ksf)	Bias	$f_s$ (ksf)	Bias
1395 TP-C	GSE to SG23	5.30	3.80	1.39	5.54	0.96	4.16	1.27	3.61	1.47
	SG19 to SG17	2.83	3.48	0.81	5.75	0.49	4.31	0.66	2.92	0.97
	SG17 to SG14	7.33	7.24	1.01	5.76	1.27	4.32	1.70	5.69	1.29
	SG10 to SG8	3.06	4.01	0.76	5.86	0.52	4.39	0.70	3.56	0.86
	SG8 to LTA	4.30	4.21	1.02	6.31	0.68	4.73	0.91	3.60	1.19
	SG3 to SG2	8.28	9.28	0.89	11.46	0.72	8.59	0.96	7.79	1.06
	SG2 to SG1	11.57	12.66	0.91	13.41	0.86	10.06	1.15	10.51	1.10
	LTA to SG3	5.80	5.07	1.14	6.81	0.85	5.11	1.14	4.32	1.34
SB TP-D	SG9 to SG6	5.09	7.37	0.69	10.03	0.51	7.52	0.68	5.84	0.87
	SG6 to LTA	15.16	9.74	1.56	10.42	1.46	7.81	1.94	7.51	2.02

Table 6-2. Bias statistics for MWD  $q_u$  design methods.

Design Method	Mean	Std Dev	CV <sub>R</sub>
McVay et al. (1992)	1.02	0.26	0.26
Gupton & Logan (1984)	0.83	0.31	0.37
Reese & O'Neill (1987)	1.11	0.41	0.37
FDOT (+/-) 1 Std Dev	1.22	0.33	0.27

## 6.2 MWD $q_u$ LRFD $\phi$ Assessment

Once the bias statistics were derived, LRFD  $\phi$  assessment took place for each reliability index:  $\beta = 2, 2.33, 2.5, 3, 3.5,$  and  $4$ . Tables 6-3 through 6-8 provide the LRFD  $\phi$  and efficiency ( $\phi / \lambda$ ) for each  $\beta$  using the four MWD  $q_u$  design methods and three LRFD methods. Figures 6-2 through 6-4 provide the LRFD  $\phi$  vs.  $\beta$  curves for each LRFD method, FOSM (Pre-Styler), FOSM (Styler), and Monte Carlo, respectively.

Table 6-3. ACIP pile LRFD analysis – South Florida limestone for MWD  $q_u$  methods –  $\beta = 2$ .

Design Method	MWD $q_u - \beta = 2$					
	FOSM – Pre-Styler		FOSM – Styler		Monte Carlo	
	$\phi$	$\phi / \lambda$	$\phi$	$\phi / \lambda$	$\phi$	$\phi / \lambda$
McVay et al. (1992)	0.65	64%	0.72	71%	0.70	69%
Gupton & Logan (1984)	0.43	52%	0.47	56%	0.45	54%
Reese & O'Neill (1987)	0.58	52%	0.62	56%	0.60	54%
FDOT (+/-) 1 Std Dev	0.76	62%	0.84	69%	0.82	67%



Table 6-4. ACIP pile LRFD analysis – South Florida limestone for MWD  $q_u$  methods –  $\beta = 2.33$ .

Design Method	MWD $q_u - \beta = 2.33$					
	FOSM – Pre-Styler		FOSM – Styler		Monte Carlo	
	$\phi$	$\phi / \lambda$	$\phi$	$\phi / \lambda$	$\phi$	$\phi / \lambda$
McVay et al. (1992)	0.58	57%	0.66	64%	0.64	62%
Gupton & Logan (1984)	0.38	45%	0.41	49%	0.39	47%
Reese & O’Neill (1987)	0.50	45%	0.55	49%	0.52	47%
FDOT (+/-) 1 Std Dev	0.68	56%	0.76	63%	0.74	60%

Table 6-5. ACIP pile LRFD analysis – South Florida limestone for MWD  $q_u$  methods –  $\beta = 2.5$ .

Design Method	MWD $q_u - \beta = 2.5$					
	FOSM – Pre-Styler		FOSM – Styler		Monte Carlo	
	$\phi$	$\phi / \lambda$	$\phi$	$\phi / \lambda$	$\phi$	$\phi / \lambda$
McVay et al. (1992)	0.55	54%	0.63	62%	0.61	59%
Gupton & Logan (1984)	0.35	42%	0.39	46%	0.37	44%
Reese & O’Neill (1987)	0.47	42%	0.52	46%	0.49	44%
FDOT (+/-) 1 Std Dev	0.64	53%	0.73	60%	0.70	57%

Table 6-6. ACIP pile LRFD analysis – South Florida limestone for MWD  $q_u$  methods –  $\beta = 3$ .

Design Method	MWD $q_u - \beta = 3$					
	FOSM – Pre-Styler		FOSM – Styler		Monte Carlo	
	$\phi$	$\phi / \lambda$	$\phi$	$\phi / \lambda$	$\phi$	$\phi / \lambda$
McVay et al. (1992)	0.47	46%	0.55	54%	0.53	52%
Gupton & Logan (1984)	0.28	34%	0.32	39%	0.30	37%
Reese & O’Neill (1987)	0.38	34%	0.43	38%	0.41	36%
FDOT (+/-) 1 Std Dev	0.54	44%	0.63	52%	0.61	50%

Table 6-7. ACIP pile LRFD analysis – South Florida limestone for MWD  $q_u$  methods –  $\beta = 3.5$ .

Design Method	MWD $q_u - \beta = 3.5$					
	FOSM – Pre-Styler		FOSM – Styler		Monte Carlo	
	$\phi$	$\phi / \lambda$	$\phi$	$\phi / \lambda$	$\phi$	$\phi / \lambda$
McVay et al. (1992)	0.39	39%	0.48	47%	0.46	45%
Gupton & Logan (1984)	0.23	28%	0.27	32%	0.25	30%
Reese & O’Neill (1987)	0.31	28%	0.35	32%	0.35	31%
FDOT (+/-) 1 Std Dev	0.45	37%	0.55	45%	0.52	43%

Table 6-8. ACIP pile LRFD analysis – South Florida limestone for MWD  $q_u$  methods –  $\beta = 4$ .

Design Method	MWD $q_u - \beta = 4$					
	FOSM – Pre-Styler		FOSM – Styler		Monte Carlo	
	$\phi$	$\phi / \lambda$	$\phi$	$\phi / \lambda$	$\phi$	$\phi / \lambda$
McVay et al. (1992)	0.33	33%	0.42	41%	0.40	39%
Gupton & Logan (1984)	0.19	22%	0.22	27%	0.21	25%
Reese & O’Neill (1987)	0.25	22%	0.29	26%	0.28	25%
FDOT (+/-) 1 Std Dev	0.38	31%	0.47	39%	0.46	38%

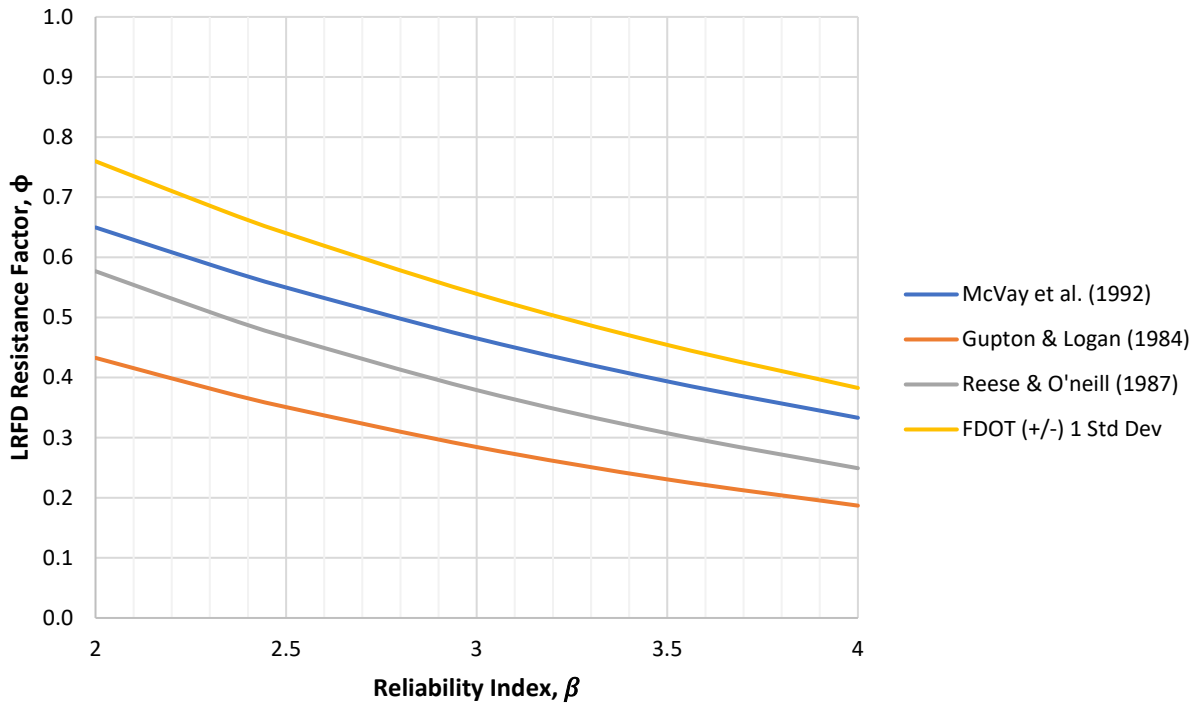


Figure 6-2. FOSM (Pre-Styler) LRFD  $\phi$  vs.  $\beta$  for multiple MWD  $q_u$  design methods.

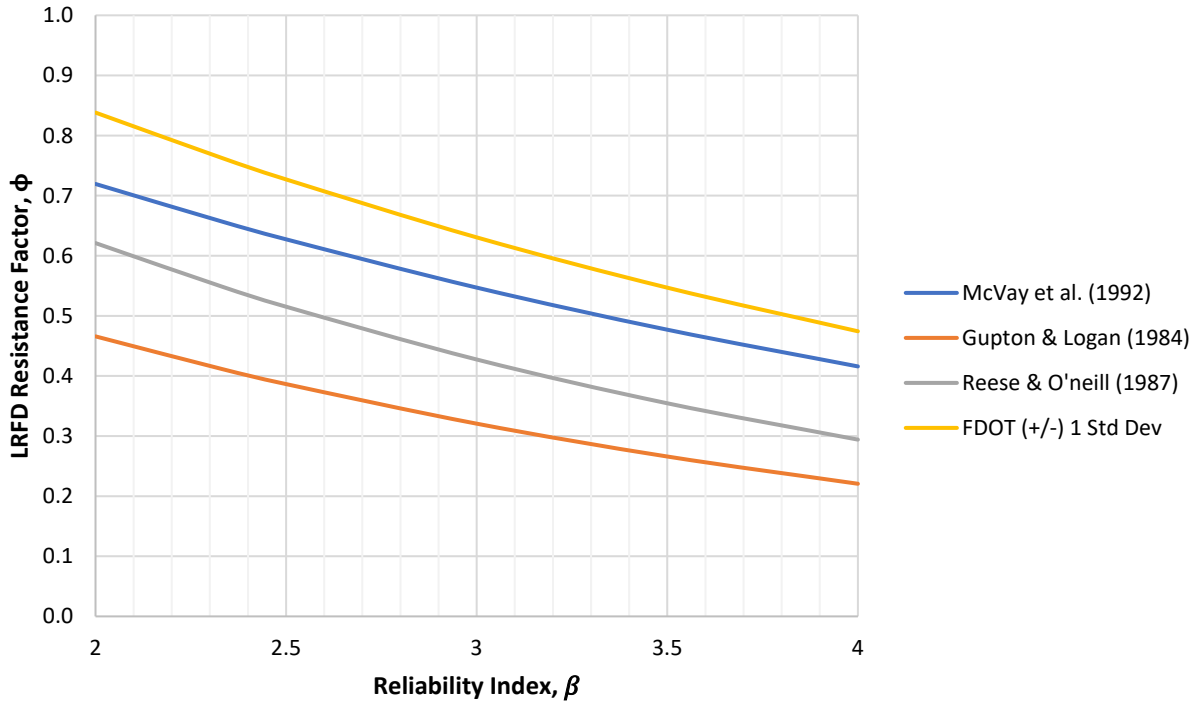


Figure 6-3. FOSM (Styler) LRFD  $\phi$  vs.  $\beta$  for multiple MWD  $q_u$  design methods.

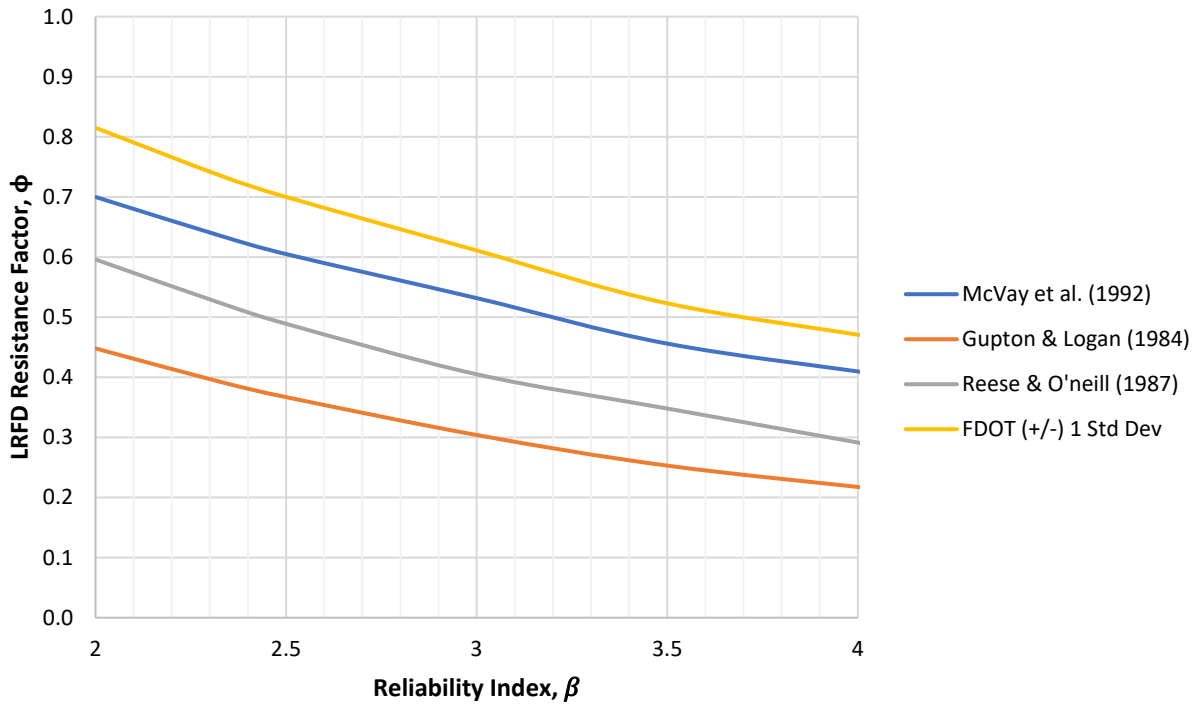


Figure 6-4. Monte Carlo LRFD  $\phi$  vs.  $\beta$  for multiple MWD  $q_u$  design methods.

From Tables 6-3 through 6-8 and Figures 6-2 through 6-4, it is observed that the FOSM (Styler) and Monte Carlo methods produced similar results. Over the full  $\beta$  range the average percent difference between the two methods ranged from 3.3% to 4.3%. The FOSM (Pre-Styler) method was the most conservative and over the full  $\beta$  range the average percent difference compared to the FOSM (Styler) method ranged from 8.9% to 19.8%, with the percent difference increasing as  $\beta$  increased. Table 6-9 provides a comparison between the findings of this research effort with those included in BDV31-977-12 (McVay et al., 2016). For the results from BDV31-977-12, two values are provided for  $\phi$  and  $(\phi / \lambda)$ . This is because in BDV31-977-12, the  $\phi$  assessments were separated by the limestone formation encountered. In Table 6-9, the Miami formation results are presented on the left side and the Fort Thompson formation results are presented on the right side. During this research effort, only one mobilized segment occurred in the Miami formation and therefore both formations were analyzed together. Also, only  $\beta = 2.33$  was analyzed in the prior research effort and therefore, this is the only comparison that could be made. From the results in Table 6-9, it can be seen that the MWD  $q_u$  approach produced higher resistance factors compared to the Core  $q_u$  approach at the same site and the prior assessment completed in BDV31-977-12 when using the FDOT's SFH recommended method (McVay et al. / FDOT). However, the resistance factors for the Gupton and Logan and Reese and O'Neill methods were reduced for the MWD  $q_u$  approach. This was due to an increased resistance coefficient of variability ( $CV_R$ ) for both design methods. This can be observed in Table 6-10 that compares the bias statistics between the MWD  $q_u$  and Core  $q_u$  methods. The increased  $CV_R$  is due to a much wider range of strengths considered for the MWD  $q_u$  approach. As discussed in Chapter 5, the Core  $q_u$  side shear was adjusted for each method using the RQD within each investigated elevation range to account for an incomplete strength distribution. The adjustment inherently reduced the range of Core  $q_u$  side shear strengths compared to the MWD  $q_u$  side shear strengths and reduced the variability of the capacity estimates. This is observed in Table 6-10 when comparing the range of the bias (max and min) for each method. The range of the bias, and inherently the  $CV_R$ , were reduced for the McVay and FDOT method whereas, the range of the bias and  $CV_R$  were increased for the Gupton and Logan and Reese and O'Neill methods. This indicates that the FDOT's recommended method performs better when a complete distribution of strength statistics is provided for pile capacity estimates and further supports the use of MWD which was capable of providing the complete strength distribution. It should be noted that the FDOT method also reduces the range of  $q_u$  considered for side shear capacity estimates. This ultimately provides a more conservative approach than McVay et al. that considers all  $q_u$  data. In all cases, including the SPT and BDV12 methods discussed in Chapter 5, McVay et al. coupled with MWD produced the most efficient results (highest % of available side shear for design) as indicated by the  $\phi/\lambda$ , and the second highest  $\phi$ -factor (the FDOT method coupled with MWD  $q_u$  produced the highest  $\phi$ -factor). This suggests the equation form is more effective than the comparative methods when the full range of strengths and variability are considered and provides better guidance for LRFD resistance factors for ACIP piles socketed into Florida limestone when using  $q_u$  data in design.

Table 6-9. Comparison of  $q_u$  methods  $\phi$  and  $\phi/\lambda$  from BDV31-977-125 and BDV31-977-12.

Design Method	Core $q_u - \beta = 2.33$					
	MWD $q_u$		Core $q_u$		BDV31-977-12	
	$\phi$	$\phi / \lambda$	$\phi$	$\phi / \lambda$	$\phi$	$\phi / \lambda$
McVay et al. (1992)	0.66	64%	0.56	60%	N/A	N/A
Gupton & Logan (1984)	0.41	49%	0.46	56%	0.34 / 0.32	41% / 38%
Reese & O'Neill (1987)	0.55	49%	0.62	56%	0.46 / 0.42	41% / 38%
FDOT (+/-) 1 Std Dev	0.76	63%	0.59	51%	0.47 / 0.33	45% / 51%

Table 6-10. Comparing bias statistics between the MWD  $q_u$  and Core  $q_u$  design methods.

Design Method		Mean	Std Dev	CV <sub>R</sub>	Min	Max
Core $q_u$	McVay et al. (1992)	0.93	0.27	0.29	0.61	1.49
	Gupton & Logan (1984)	0.83	0.26	0.32	0.54	1.30
	Reese & O'Neill (1987)	1.10	0.35	0.32	0.72	1.73
	FDOT (+/-) 1 Std Dev	1.16	0.41	0.36	0.68	1.91
MWD $q_u$	McVay et al. (1992)	1.02	0.26	0.26	0.69	1.56
	Gupton & Logan (1984)	0.83	0.31	0.37	0.49	1.46
	Reese & O'Neill (1987)	1.11	0.41	0.37	0.66	1.94
	FDOT (+/-) 1 Std Dev	1.22	0.33	0.27	0.86	2.02

### 6.3 MWD $f_s$

For the final LRFD analysis, MWD conducted in the footprint of load tested ACIP piles and drilled shafts was considered. The method is intended to be used for future bored pile QA/QC to ensure as-built deep foundations meet or exceed the demands of the engineering design. The method provides superior capacity estimation as the MWD test is conducted at full-scale in the footprint of each deep foundation which removes spatial variability as a source of uncertainty.

From FDOT projects BDV31-977-20 (McVay and Rodgers, 2016), BDV31-977-91 (McVay and Rodgers, 2020), and the current research effort for ACIP piles in south Florida, the MWD QA/QC procedure has been conducted in five locations (Figure 6-5) throughout the state of Florida with mobilized load test data available for direct comparison. This includes drilled shafts that used rock augers at Little River in Quincy, Overland Bridge in Jacksonville, and Kanapaha in Gainesville; drilled shafts that used rock drilling buckets at Selmon Expressway in Tampa; and ACIP piles that used rock augers in Miami (current research). From each of these efforts a total of 36 data points has been collected that compare the estimated side shear from specific energy obtained through MWD and the mobilized side shear recorded during full-scale load tests. Of the 36 data points, 11 were obtained from monitoring drilled shafts with rock augers, 12 were obtained from monitoring drilled shafts with rock drilling buckets, and 13 were obtained from monitoring ACIP piles with rock augers. Because the method directly relates MWD specific energy to unit side shear, conventional design equations are not used. Instead, developed

regression equations are used to estimate side shear based on the average specific energy recorded over each mobilized load test segment as indicated in Figure 6-6. Also observed in Figure 6-6 is that ACIP piles and drilled shafts share a similar relationship for rock augers, but a different relationship is found for drilled shaft rock buckets. This is due to the largely different drilling tool geometries when comparing rock augers to rock buckets whereas the rock augers for ACIP piles and drilled shafts are quite similar and therefore produce a similar relationship between specific energy and rock strength. Using the developed relationships in Figure 6-6, predicted side shear from MWD is compared to the measured side shear from mobilized load tests in Figure 6-7. Table 6-11 provides the side shear estimates and bias per mobilized layer using the MWD QA/QC method and Table 6-12 provides the bias statistics.



Figure 6-5. Locations of all Florida MWD bored pile QA/QC investigations.

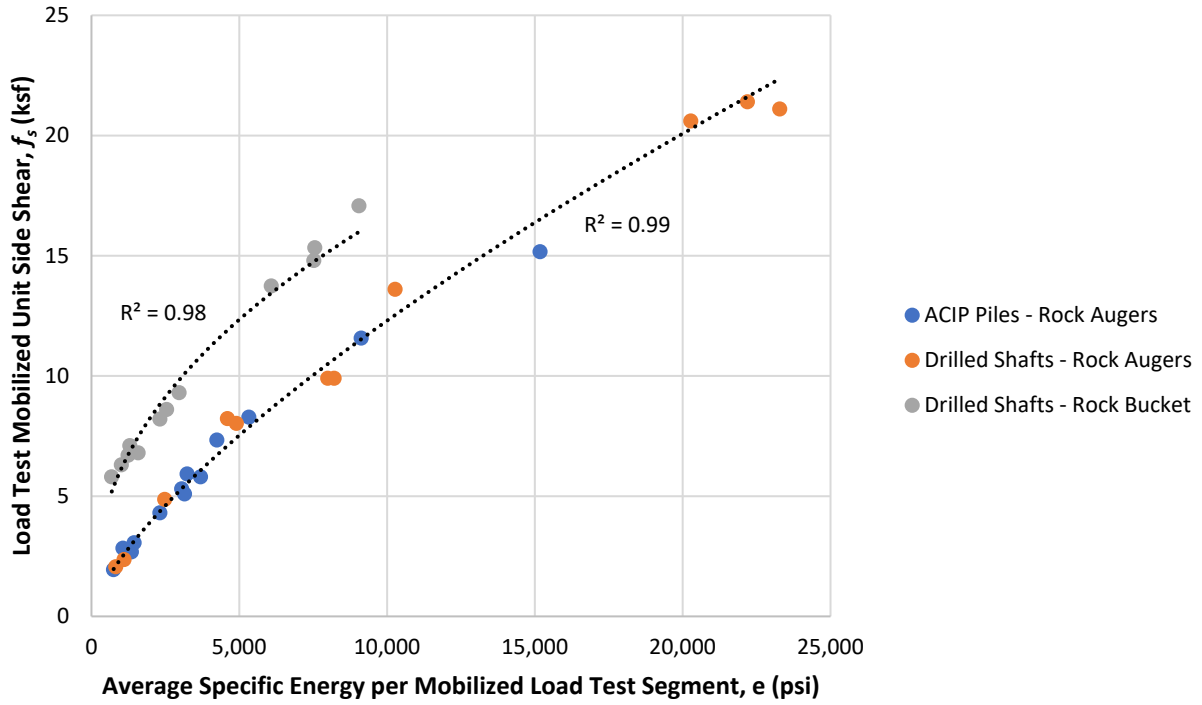


Figure 6-6. Mobilized unit side shear vs. average specific energy.

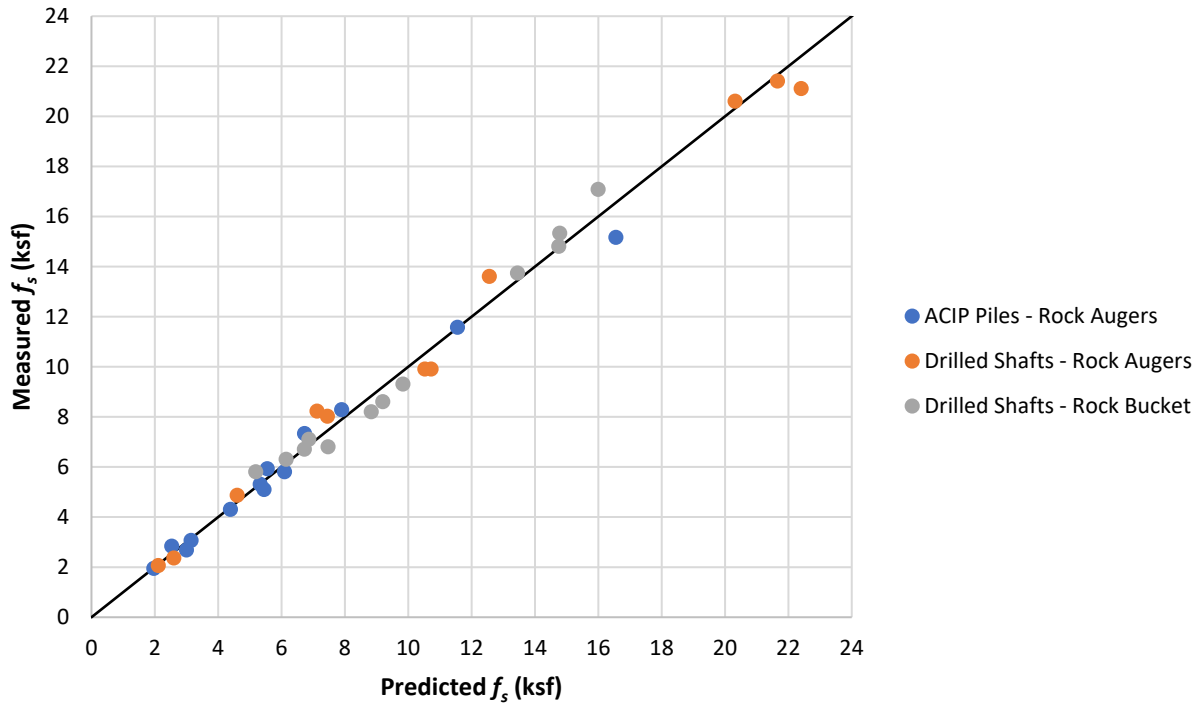


Figure 6-7. ACIP pile measured vs. predicted side shear capacity for MWD  $f_s$  design methods.

Table 6-11. Side shear estimates and bias per mobilized layer using the MWD QA/QC method.

Bored Pile Type	Drilling Tool	Location	Segment	Load Test	MWD			
				$f_s$ (ksf)	$f_s$ (ksf)	Bias		
ACIP Piles	Rock Auger	I395 TP-C	GSE to SG23	5.30	5.33	0.99		
			SG19 to SG17	2.83	2.54	1.11		
			SG17 to SG14	7.33	6.73	1.09		
			SG10 to SG8	3.06	3.15	0.97		
			SG8 to LTA	4.30	4.39	0.98		
			SG3 to SG2	8.28	7.90	1.05		
			SG2 to SG1	11.57	11.56	1.00		
			LTA to SG3	5.80	6.10	0.95		
			I395 TP-D	SG9 to SG6	5.09	5.45	0.93	
				SG6 to LTA	15.16	16.56	0.92	
			SR-836 TP-A	SR-836 TP-A	GSE to SG13	1.94	1.97	0.98
					SG13 to SG11	2.68	3.00	0.89
SG11 to LTA	5.92	5.55			1.07			
Drilled Shafts	Rock Auger	Little River	SG8 to SG7	9.90	10.73	0.92		
			SG7 to SG6	21.10	22.41	0.94		
			SG6 to LTA	20.60	20.32	1.01		
			LTA to SG5	21.40	21.66	0.99		
			SG5 to SG4	13.60	12.56	1.08		
			SG4 to SG3	9.90	10.53	0.94		
			Kanapaha	Kanapaha	SG1 to SG2	8.02	7.45	1.08
					SG2 to SG3	8.22	7.12	1.15
					SG4 to Tip	4.86	4.60	1.06
					East Shaft	2.36	2.60	0.91
			Overland	Overland	Segment 2	2.06	2.12	0.97
			Drilled Shafts	Rock Bucket	Selmon Expy TS-2	Segment 15	15.33	14.79
Segment 16	17.07	16.00				1.07		
Segment 17	13.74	13.45				1.02		
Toe Segment	14.80	14.76				1.00		
Selmon Expy TS-3	Selmon Expy TS-3	Segment 12			8.60	9.20	0.93	
		Segment 13			6.70	6.73	1.00	
		Toe Segment			8.20	8.83	0.93	
Selmon Expy TS-4	Selmon Expy TS-4	Segment 5			5.80	5.19	1.12	
		Segment 10			6.30	6.15	1.02	
		Segment 11			7.10	6.87	1.03	
		Segment 12			6.80	7.47	0.91	
		Segment 16			9.30	9.84	0.95	



Table 6-12. Bias statistics for MWD QA/QC method.

Design Method	Mean	Std Dev	CV <sub>R</sub>
ACIP Pile - Rock Augers	1.00	0.06	0.06
Rock Augers	1.00	0.07	0.07
Rock Buckets	1.00	0.07	0.07

#### 6.4 MWD $f_s$ LRFD $\phi$ Assessment

Once the bias statistics were derived, LRFD  $\phi$  assessment took place for each reliability index:  $\beta = 2, 2.33, 2.5, 3, 3.5,$  and  $4$ , using a dead-to-live load ratio ( $Q_D/Q_L$ ) set to three for LRFD calibration. Tables 6-13 through 6-18 provide the LRFD  $\phi$  and efficiency ( $\phi / \lambda$ ) for each  $\beta$  using the three MWD  $f_s$  methods and three LRFD methods. Figures 6-8 through 6-10 provide the LRFD  $\phi$  vs.  $\beta$  curves for each LRFD method, FOSM (Pre-Styler), FOSM (Styler), and Monte Carlo, respectively.

Table 6-13. ACIP pile LRFD analysis – South Florida limestone for MWD  $f_s$  methods –  $\beta = 2$ .

Design Method	MWD $f_s - \beta = 2$					
	FOSM - Pre-Styler		FOSM - Styler		Monte Carlo	
	$\phi$	$\phi / \lambda$	$\phi$	$\phi / \lambda$	$\phi$	$\phi / \lambda$
ACIP Piles	0.81	81%	0.98	98%	0.97	98%
ACIP & DS Rock Augers	0.81	81%	0.98	98%	0.97	97%
ACIP & DS All Data	0.81	81%	0.98	98%	0.98	98%

Table 6-14. ACIP pile LRFD analysis – South Florida limestone for MWD  $f_s$  methods –  $\beta = 2.33$ .

Design Method	MWD $f_s - \beta = 2.33$					
	FOSM - Pre-Styler		FOSM - Styler		Monte Carlo	
	$\phi$	$\phi / \lambda$	$\phi$	$\phi / \lambda$	$\phi$	$\phi / \lambda$
ACIP Piles	0.75	75%	0.94	94%	0.93	94%
ACIP & DS Rock Augers	0.75	75%	0.94	94%	0.93	93%
ACIP & DS All Data	0.75	75%	0.94	94%	0.94	94%

Table 6-15. ACIP pile LRFD analysis – South Florida limestone for MWD  $f_s$  methods –  $\beta = 2.5$ .

Design Method	MWD $f_s - \beta = 2.5$					
	FOSM - Pre-Styler		FOSM - Styler		Monte Carlo	
	$\phi$	$\phi / \lambda$	$\phi$	$\phi / \lambda$	$\phi$	$\phi / \lambda$
ACIP Piles	0.72	72%	0.92	92%	0.91	92%
ACIP & DS Rock Augers	0.72	72%	0.92	92%	0.91	91%
ACIP & DS All Data	0.72	72%	0.92	92%	0.92	92%

Table 6-16. ACIP pile LRFD analysis – South Florida limestone for MWD  $f_s$  methods –  $\beta = 3$ .

Design Method	MWD $f_s - \beta = 3$					
	FOSM - Pre-Styler		FOSM - Styler		Monte Carlo	
	$\phi$	$\phi / \lambda$	$\phi$	$\phi / \lambda$	$\phi$	$\phi / \lambda$
ACIP Piles	0.64	65%	0.86	87%	0.86	86%
ACIP & DS Rock Augers	0.64	64%	0.86	86%	0.86	86%
ACIP & DS All Data	0.65	65%	0.87	87%	0.86	86%

Table 6-17. ACIP pile LRFD analysis – South Florida limestone for MWD  $f_s$  methods –  $\beta = 3.5$ .

Design Method	MWD $f_s - \beta = 3.5$					
	FOSM - Pre-Styler		FOSM - Styler		Monte Carlo	
	$\phi$	$\phi / \lambda$	$\phi$	$\phi / \lambda$	$\phi$	$\phi / \lambda$
ACIP Piles	0.57	58%	0.81	82%	0.80	81%
ACIP & DS Rock Augers	0.57	57%	0.81	81%	0.80	80%
ACIP & DS All Data	0.58	58%	0.81	81%	0.81	81%

Table 6-18. ACIP pile LRFD analysis – South Florida limestone for MWD  $f_s$  methods –  $\beta = 4$ .

Design Method	MWD $f_s - \beta = 4$					
	FOSM - Pre-Styler		FOSM - Styler		Monte Carlo	
	$\phi$	$\phi / \lambda$	$\phi$	$\phi / \lambda$	$\phi$	$\phi / \lambda$
ACIP Piles	0.51	51%	0.76	77%	0.74	74%
ACIP & DS Rock Augers	0.51	51%	0.76	76%	0.73	73%
ACIP & DS All Data	0.51	51%	0.76	76%	0.74	74%

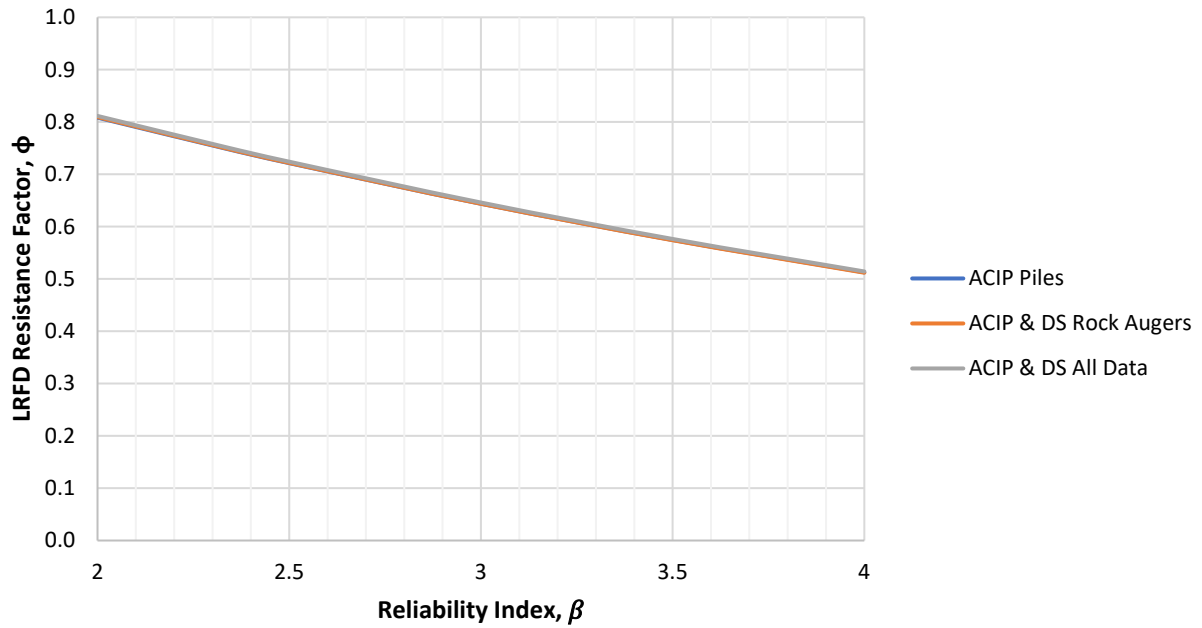


Figure 6-8. FOSM (Pre-Styler) LRFD  $\phi$  vs.  $\beta$  for MWD  $f_s$  design methods.

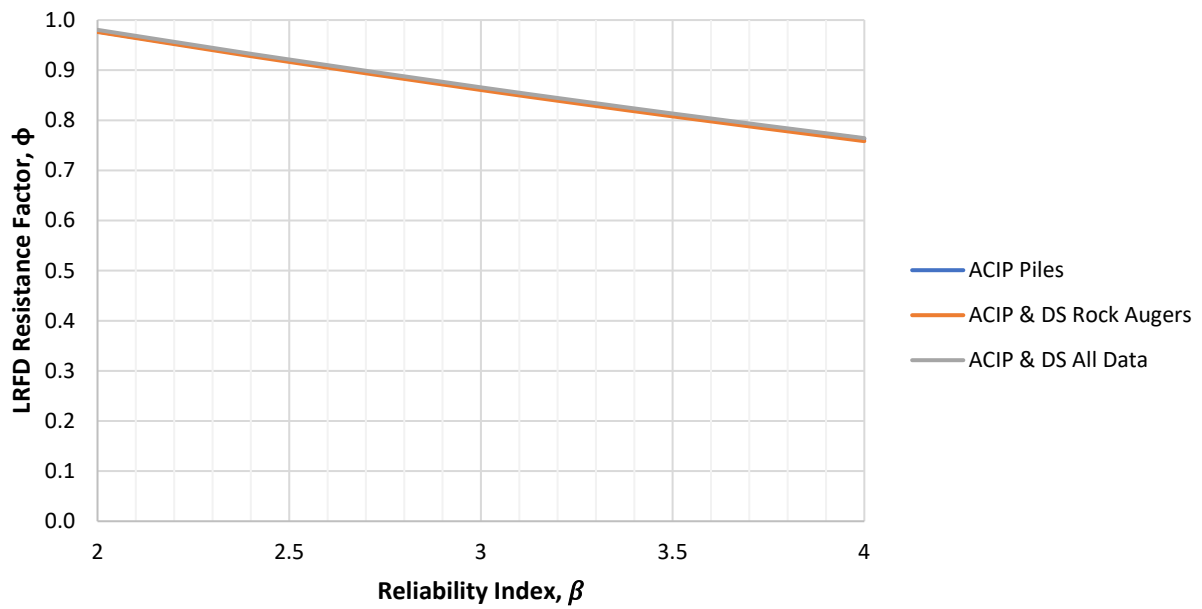


Figure 6-9. FOSM (Styler) LRFD  $\phi$  vs.  $\beta$  for MWD  $f_s$  design methods.

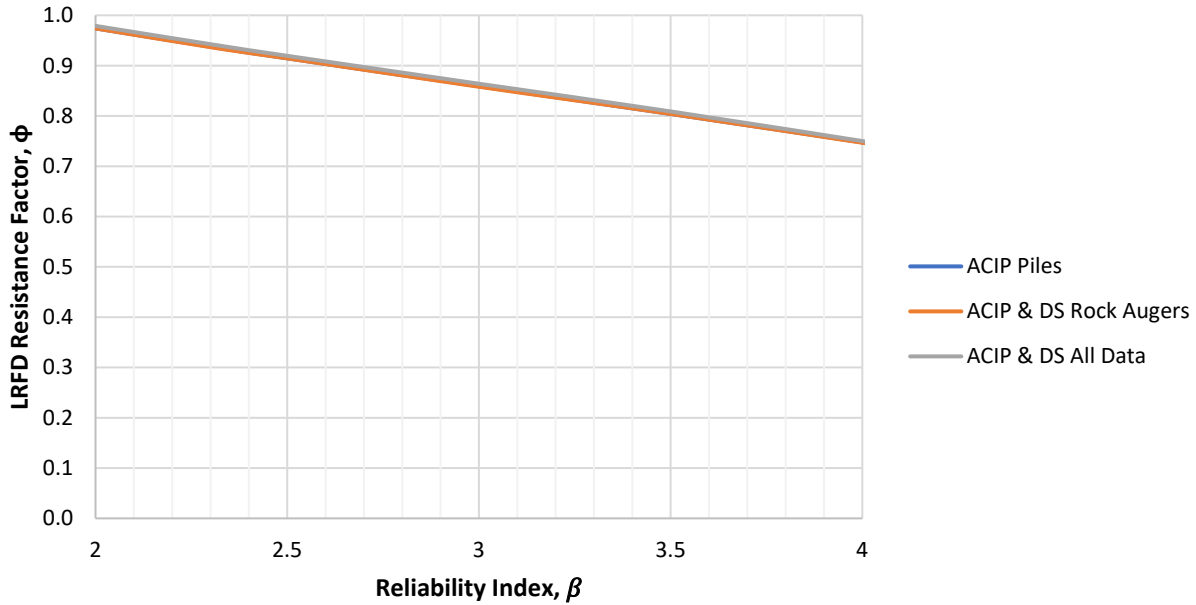


Figure 6-10. Monte Carlo LRFD  $\phi$  vs.  $\beta$  for MWD  $f_s$  design methods.

From Tables 6-13 through 6-18 and Figures 6-8 through 6-10, it is observed that the FOSM (Styler) and Monte Carlo methods produced similar results. Over the full  $\beta$  range the average percent difference between the two methods ranged from 0.2% to 3.6%. The FOSM (Pre-Styler) method was the most conservative and over the full  $\beta$  range the average percent difference compared to the FOSM (Styler) method ranged from 18.8% to 39.1%, with the percent difference increasing as  $\beta$  increased. Also observed, when spatial variability is removed as a source of uncertainty, the resistance factors are significantly improved. For  $\beta = 2.33$  (redundant piles/shafts) using FOSM (Styler),  $\phi = 0.94$  when considering all 36 MWD-load test comparisons, which is 0.18 higher than the highest  $\phi$  found using the MWD  $q_u$  approach which did not eliminate spatial variability, 0.29 higher than the highest  $\phi$  found using the Core  $q_u$  approach, and 0.71 higher than the highest  $\phi$  found using the SPT approach. These results exemplify the benefits of MWD for the design and construction of ACIP piles and drilled shafts socketed into Florida limestone. From the bias statistics provided in Table 6-12, in all cases the mean bias was equal to 1.00 with a  $CV_R$  less than or equal to 0.07 which indicates minimal variability in the predicted and measured resistance. Furthermore, both MWD methods discussed in this deliverable performed better than the conventional methods, Core  $q_u$  and SPT. Finally, as indicated by the results, using SPT data is not ideal for ACIP pile design when the piles are to be socketed into Florida limestone, regardless of the design equation.

## 7 Conclusions

Based on the results of this study, the following conclusions can be drawn.

- Two ACIP analysis spreadsheets were successfully developed that transform time-referenced AME data into depth-referenced data that provide compatibility with Teale's specific energy equation for in situ MWD assessment. The CEI version of the spreadsheet QA/QC assessment focuses on specific energy and total energy and the UF researcher version of the spreadsheet was capable of assessing unconfined compression strength, pile side shear, and pile capacity. Each version of the spreadsheet will provide superior ACIP pile QA/QC during future installations in South Florida limestone. Additionally, both spreadsheets provided a drilling depth versus time profile that identifies where time was spent during installation for future pile drilling optimization.
- MWD generated 299 times more rock strength data than rock core sampling within the same investigated area and elevation range. This illustrates the superior high resolution profiling MWD can provide during a site investigation and the additional subsurface information that can be gathered from monitoring every pile on a site. The results indicate that MWD has the ability to provide a much better understanding of the subsurface conditions, strength distribution, and layering present at a site.
- The laboratory-tested core strengths compared well with MWD in the top 35 feet, but as the coring depths became deeper (35 feet and below), MWD indicated much lower  $q_u$  strengths compared to the laboratory core samples. This indicates that rock coring at greater depths in South Florida may be prone to operating outside of the operational limits, which diminishes core recoveries (REC) and the rock quality designation (RQD), reduces the number of core samples available for laboratory testing, and skews the mean strength toward the higher end. All of which indicated MWD coring should be conducted in South Florida limestone. This would ultimately improve the site characterization and inherently improve the LRFD  $\phi$  assessment.
- Using RQD to adjust the rock core strength distribution at lower depths (below 35 feet) improved the LRFD  $\phi$  assessment compared to using REC, which is common practice. This is because using RQD under the conditions discussed properly accounted for the untested volume of rock at the site whereas REC overestimated the untested volume of rock by more than a factor of two. When the lower-depth core strength distribution was adjusted using RQD, the results compared well with the MWD  $q_u$  assessments and load-tested side shear strengths, which further supports this conclusion.
- Load testing suggested that residual stresses are developed in South Florida limestone for ACIP piles. In all load tests conducted, residual stresses were observed that greatly complicated the load test reduction. Consequently, residual stresses must be quantified and properly accounted for prior to future ACIP Pile MWD correlations being developed at higher resolution (i.e., five-foot instrumented segments).
- LRFD  $\phi$  assessment was performed using site-specific data with LRFD methods FOSM (Pre-Styler), FOSM (Styler), and Monte Carlo simulations (50,000 trials per assessment). Methods that employed rock cores indicated similar results as drilled shafts but higher  $\phi$  values than the original ACIP pile results presented in FDOT project BDV31-977-12. Methods that employed SPT data produced the lowest  $\phi$  values, similar to the original ACIP pile report. This is attributed to poor correlation between SPT blow counts and

rock strength and suggests SPT design methods are not ideal for ACIP piles socketed into South Florida limestone. Conversely, the MWD methods resulted in higher  $\phi$  values compared to the conventional methods due to the excellent correlation that exists between specific energy, unconfined compression strength, side shear strength, and pile capacity. When MWD was conducted in the footprint of the piles (QA/QC procedure), the highest  $\phi$  values were achieved because spatial variability was eliminated. However, this approach requires multiple load tests with full mobilization and site specific correlations to be developed before the highest  $\phi$  values can be considered.

- MWD is viable for ACIP pile QA/QC. From this report it was found that MWD specific energy was in agreement with the layering identified by the SPT borings, MWD agreed with the load test results as an excellent correlation was developed between unit side shear and specific energy, MWD was in agreement with the rock core strength range and layering, MWD data were able to provide accurate test pile models that showed the same behavior as the actual load tested piles, and observed in the QA/QC pile summaries. MWD indicated the strength of rock decreased moving east-to-west which agrees with the trends of rock cores and load tests. Additionally, the drilling profiles also showed the same trends as the estimated pile capacities and indicated stronger rock takes longer to drill which is the expected trend. From the LRFD  $\phi$  analyses, both MWD methods produced the highest LRFD  $\phi$  values and performing MWD in the footprint of ACIP piles provides superior QA/QC as the effects of spatial variability are eliminated. Furthermore, MWD was able to assist in determining the proper strength distribution obtained from traditional rock core sampling. All of these supporting observations indicate the MWD correlation and procedures developed for ACIP pile capacity QA/QC are valid for the in situ assessment of rock strength and pile capacity.

## 8 Recommendations

The following recommendations are based on this study's findings:

- Conduct more MWD research for South Florida ACIP piles as more data is needed to further validate the results of this research effort.
- Collect more MWD data in the footprint of load tested ACIP piles to increase the data set acquired during this research.
- Investigate using MWD coring practices in South Florida to assist with recovering more samples in formations that are difficult to core. As indicated by the results of this work, coring at greater depths in South Florida limestone is problematic using conventional coring techniques. As a result of the conventional coring deficiencies, the strength distribution is misleading and indicates the formation is predominantly stronger rock which was found to be incorrect when compared to MWD and the load test results. Additionally, MWD will provide a significant increase strength data available for design which inherently increases the LRFD  $\phi$  derived and reduces the cost per shaft.
- Sampling frequencies should be increased for South Florida AME equipment in order to obtain more than one time-based sampled measurement per recorded depth increment (i.e., the distance between depth-referenced measurements used for strength analysis). Currently, one sample per second is recorded. Increasing the sampling frequency would provide multiple time-based measurements per depth-referenced measurement and provide a more accurate averaged value for every data point. As indicated by this research, the current sampling frequency was found to be adequate when drilling in stronger layers of limestone as the drilling rate tends to slow down in the stronger layers. However, future ACIP pile MWD efforts should focus on delineating lower strength limestone and soil which will require a higher sampling frequency to ensure multiple readings are provided per recorded depth increment, regardless of the geomaterial encountered. Furthermore, UF researchers anticipate that monitoring vibration as an additional drilling parameter will assist in the delineation of soil and rock in future MWD efforts, which will likely require a minimum sampling frequency of 100 Hz. Alternatively, a controlled penetration could be specified for ACIP pile drilling to ensure at least one time-based data point is recorded per depth-referenced measurement.
- Develop an ACIP pile MWD analysis program that is capable of handling higher sampling frequencies than the current spreadsheet developed during this research effort. The current analysis spreadsheet was capable of handling the large data sets that were generated using a 1-Hz sampling frequency (typically 10,000 data points or less for each monitored drilling parameter). However, the spreadsheet file sizes generated are quite large ( $\approx 40$  MB) and increasing the sampling frequency only adds to the file size. UF researchers attempted to develop a high sampling frequency version of the spreadsheet (1 million data points for each drilling parameter) to accommodate the recommended higher sampling frequencies but unfortunately the file size and processing demands repeatedly resulted in the program crashing. Consequently, if software is developed to accommodate the recommended increased sampling frequency, an excel based format is not recommended. The proposed software should be developed based on the programming that was developed for the ACIP pile spreadsheet, as the current analysis program performed exceptionally well with the given data set sizes.

- Residual stresses that develop in South Florida ACIP piles should be further investigated. As discussed, residual stresses were identified in every load tested pile by the UF research team as well as the load test consultant who originally reduced the load test. Ignoring the effect of residual stresses in future South Florida piles will lead to inaccurate strength layering and design related issues. As well, residual stress needs to be resolved to get accurate high resolution load test layering and to build correlation with MWD.
- Finally, in regard to load testing in South Florida limestone, strain gauge readings should be taken immediately before (and after) every event of the piling work and not just during the actual load test. Continuous measurements would be the ideal approach; however, continuous measurements may not be feasible, currently. Therefore, readings should be conducted at the following times:
  1. After installation of the gauges while the reinforcement cage is laying on the ground (to ensure all gauges are functioning);
  2. For ACP testing, when the cage has been placed into the grouted hole and the gauges have adjusted to the ground or initial grout temperature (within one hour); for drilled shafts when the pour has just been completed;
  3. Immediately before starting the load test.

After load test analysis is complete, the reported side shear in each level should be converted to load and compared to the applied load. This will ensure the measured loads within the pile do not exceed the applied load. This should be done for each load step. Additionally, strain gauge data that was used to generate T-Z curves should be multiplied by segment length to obtain segment deformations that are then summed over the full pile length and compared with pile top movement, LTA movement, and tell-tale movement. The error should be within 10%. If measurements are not taken at these recommended intervals and residual stresses are present within the pile or the segment deformation error is greater than 10%, the load test data should be reanalyzed in larger layers using stable strain gauge locations, as was completed during this research. However, taking this approach will result in a loss of load test layer resolution.



## References

- Allen, T. M., (2005), *Development of Geotechnical Resistance Factors and Downdrag Load Factors for LRFD Foundation Strength Limit State Design*, Publication No. FHWA-NHI05-052, Federal Highway Administration, Washington, D.C., 41 pp.
- Barker, R. M., Duncan, J. M., Rojiani, K. B., Ooi, P. S. K., Tan, C. K., and Kim, S. G., (1991), *Manuals for the Design of Bridge Foundations: Shallow Foundations, Driven Piles, Retaining Walls and Abutments, Drilled Shafts, Estimating Tolerable Movements, and Load Factor Design Specifications and Commentary*, NCHRP Report 343, TRB, National Research Council, Washington, D.C.
- Crapps, D. K., (1986). *Design, construction and inspection of drilled shafts in limerock and limestone*, Proc. Annual Meeting of Florida Section, ASCE.
- Frizzi, R.P. and Meyer, M.E. (2000). "Augercast Piles: South Florida Experience," Geotechnical Special Publication No. 100, N. D. Dennis, R. Castelli, and M. W. O'Neill (Eds.), ASCE, August, pp. 382–396.
- Gupton, C, and Logan, T. (1984). "Design guidelines for drilled shafts in weak rocks of south Florida," Proc. South Florida Annual ASCE Meeting, ASCE.
- ISO/IEC. (2016). *Geotechnical Investigation and Testing – Field Testing – Part 15: Measuring While Drilling*, ISO 22476-15:2016, International Standards Organization. Geneva, Switzerland.
- McVay, M., Townsend, F., and Williams, R. (1992). "Design of socketed drilled shafts in limestone." *Journal of Geotechnical Engineering*, 118(10): 1626–1637. doi: 10.1061/(ASCE)0733-9410(1992)118:10(1626).
- McVay, M., Birgisson, B., Zhang, L., Perez, A., and Putcha, S. (2000). "Load and resistance factor design (LRFD) for driven piles using dynamic methods—a Florida perspective." *Geotech. Test. J.*, 23(1), 55–66.
- McVay, M., Klammler, H., Faraone, M., Dase, K., and Jenneisch, C. (2012) "Development of Variable LRFD  $\phi$  Factors for Deep Foundation Design Due to Site Variability". Final Report. Florida Department of Transportation (FDOT) Contract No. BDK75-977-23.
- McVay, M., and Rodgers, M. (2016). "Drilled Shaft Resistance Based on Diameter, Torque, and Crowd (Drilling Resistance vs. Rock Strength) Phase II". Final Report. Florida Department of Transportation (FDOT) Contract No. BDV31-977-20.
- McVay, M., Wasman, S., Huang, L., and Crawford, S. (2016). "Load and Resistance Factors for Augercast In Place Piles". Final Report. Florida Department of Transportation (FDOT) Contract No. BDV31-977-12.

- McVay, M., and Rodgers, M. (2019). “Measuring While Drilling for Florida Site Investigation (FLMWD)”. Final Report. Florida Department of Transportation (FDOT) Contract No. BDV31-820-006.
- McVay, M., and Rodgers, M. (2020). “Implementation of Measuring While Drilling Shafts in Florida (FLMWDS). Final Report. Florida Department of Transportation (FDOT) Contract No. BDV31-977-91. <https://trid.trb.org/view/1736641>
- Paikowsky, S. G., (2004). *Load and resistance factor design (LRFD) for deep foundations*, NCHRP Report 507, Transportation Research Board, Washington D.C.
- Ramos, H.R., Antorena, J.A., and McDaniel, T.G. (1994). *Correlations between the Standard Penetration Test (SPT) and the Measured Shear Strength of Florida Natural Rock*, Proc. Int. Conf. on Design and Construction of Deep Foundations, FHWA, pp. 699-711.
- Reese, L. C, and O'Neill, M. W. (1987). *Drilled shafts: construction procedures and design methods*, Design manual, U.S. Department of Transportation, Federal Highway Administration, McLean, Va.
- Rodgers M., McVay M., Ferraro C., Horhota D., Tibbetts C., Crawford S. (2017). “Measuring Rock Strength While Drilling Shafts Socketed into Florida Limestone.” *ASCE Journal of Geotechnical and Geoenvironmental Engineering*. 144(3). doi:10.1061/(ASCE)GT.1943-5606.0001847.
- Rodgers M., McVay M., Horhota D., Hernando J. (2018). “Assessment of Rock Strength from Measuring While Drilling Shafts in Florida Limestone.” *Canadian Geotechnical Journal*. 55(8): 1154-1167. doi:10.1139/cgj-2017-0321.
- Rodgers M., McVay M., Horhota D., Sinnreich J., Hernando J. (2019). “Assessment of Shear Strength from Measuring While Drilling Shafts in Florida Limestone.” *Canadian Geotechnical Journal*. doi:10.1139/cgj-2017-0629.
- Rodgers M., McVay M., Horhota D., Hernando J., Paris J. (2020). “Measuring While Drilling in Florida Limestone for Geotechnical Site Investigation.” *Canadian Geotechnical Journal*. doi.org/10.1139/cgj-2019-0094.
- Rodgers M., McVay M., Horhota D., Hernando J., Paris J. (2021). “Operational Limits of Measuring While Drilling in Florida Limestone for Geotechnical Site Characterization.” *ASCE Journal of Geotechnical and Geoenvironmental Engineering*. 144(3). doi: 10.1061/(ASCE)GT.1943-5606.0002688.
- Sinnreich, J. (2012). “Strain Gage Analysis for Nonlinear Pile Stiffness.” *Geotechnical Testing Journal*. 35(2):1-8. DOI: 10.1520/GTJ103412.
- Styler, M. A. (2006). *Development and implementation of the Diggs format to perform LRFD resistance factor calibration of driven concrete piles in Florida*, Master Thesis, Department of Civil and Coastal Engineering, University of Florida.
- Teale, R. (1965). “The concept of specific energy in rock drilling.” *International Journal of Rock Mechanics and Mining Sciences*. 2(1): 57–73.

Withiam, J. L., Voytko, E.P., Barker, R.M., Duncan, M.J., Kelly, B.C., Musser, S.C. and Elias, V., (1997). *Load and Resistance Factor Design (LRFD) of Highway Bridge Substructures*, U.S. DOT Federal Highway Administration, Washington D.C.

## Appendix A – ACIP Pile QA/QC Summary Reports

Project		Location		Engineer		Pile ID	
I-395		Miami, Florida		Rodgers, McVay, Kelch		B1	
Station		Offset (ft)		Drill Rig		Drill Bit Diameter (in)	
100+00.01		10.00		Drill Rig B		30	
Top of Pile Elevation (ft)		Bottom of Pile Elevation (ft)		Depth Increment Analyzed (cm)		ISO-MWD Assessment	
13.4		-80.60		1		Class 1	
Specific Energy Above Threshold, e (psi)				ACIP Pile Capacity QA/QC			
Specific Energy Threshold (psi)		1,250		Pile Length (ft)		94.00	
Mean		2,418		Total Rock Socket Length (ft)		50.6	
Median		1,949		Average Pile Side Shear, $f_s$ (ksf)		2.58	
Standard Deviation		2,425		Unfactored Pile Capacity (kips)		1,904	
Coefficient of Variation (CV)		1.00		Factored Pile Capacity (kips)		1,142	
Maximum		59,253		Factored Design Load (kips)		1,070	
Minimum		1,253		C/D Ratio for LRFD $\Phi = 0.6$		1.07	
Number of Data Points		1,541		Design Requirement Inspection		<b>Passed</b>	
Unconfined Compressive Strength Above Threshold, $q_u$ (psi)				Pile Installation Summary			
$q_u$ Threshold (psi)		88		Drilling Time (min)		23.3	
Mean		159		ReDrill Time (min)		11.4	
Median		134		Idle Rotation Time (min)		1.6	
Standard Deviation		110		Idle Time (min)		9.1	
Coefficient of Variation (CV)		0.69		Withdrawal Time (min)		5.4	
Maximum		2,134		Penetration w/o Rotation Time (min)		0.5	
Minimum		88		Total Time (min)		51.3	
Number of Data Points		1,541		Drilling Efficiency (%)		45%	

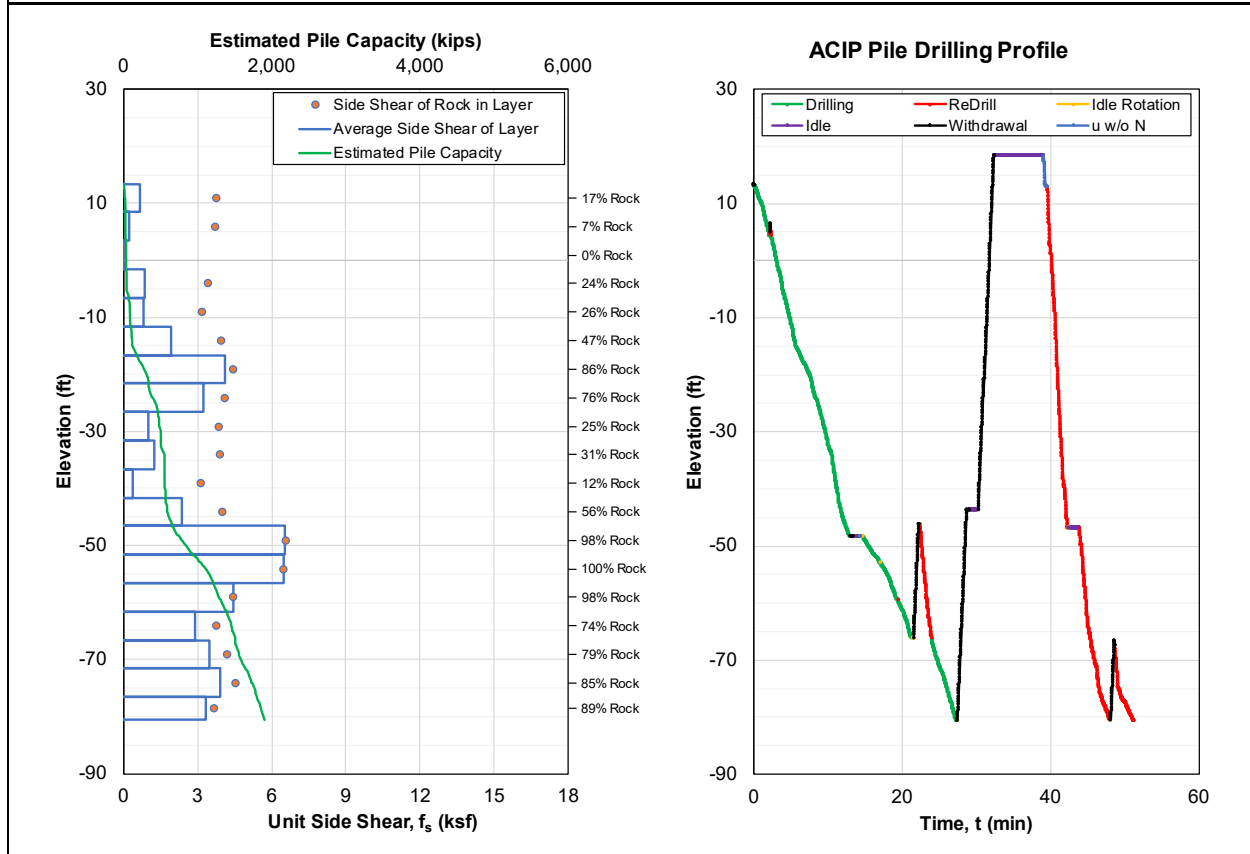


Figure A-1. ACIP pile capacity QA/QC report for Group B Pile 1.

Project	Location	Engineer	Pile ID
I-395	Miami, Florida	Rodgers, McVay, Kelch	B2
Station	Offset (ft)	Drill Rig	Drill Bit Diameter (in)
100+00.01	10.00	Drill Rig B	30
Top of Pile Elevation (ft)	Bottom of Pile Elevation (ft)	Depth Increment Analyzed (cm)	ISO-MWD Assessment
13.4	-80.60	1	Class 1

Specific Energy Above Threshold, e (psi)	
Specific Energy Threshold (psi)	1,250
Mean	2,569
Median	2,077
Standard Deviation	1,796
Coefficient of Variation (CV)	0.70
Maximum	27,340
Minimum	1,256
Number of Data Points	1,525

Unconfined Compressive Strength Above Threshold, q <sub>u</sub> (psi)	
q <sub>u</sub> Threshold (psi)	88
Mean	169
Median	142
Standard Deviation	97
Coefficient of Variation (CV)	0.57
Maximum	1,248
Minimum	88
Number of Data Points	1,525

ACIP Pile Capacity QA/QC	
Pile Length (ft)	94.00
Total Rock Socket Length (ft)	50.0
Average Pile Side Shear, f <sub>s</sub> (ksf)	2.71
Unfactored Pile Capacity (kips)	2,001
Factored Pile Capacity (kips)	1,201
Factored Design Load (kips)	1,070
C/D Ratio for LRFD $\Phi = 0.6$	1.12
Design Requirement Inspection	<b>Passed</b>

Pile Installation Summary	
Drilling Time (min)	21.9
ReDrill Time (min)	5.4
Idle Rotation Time (min)	0.6
Idle Time (min)	1.0
Withdrawal Time (min)	2.0
Penetration w/o Rotation Time (min)	0.0
Total Time (min)	30.8
Drilling Efficiency (%)	71%

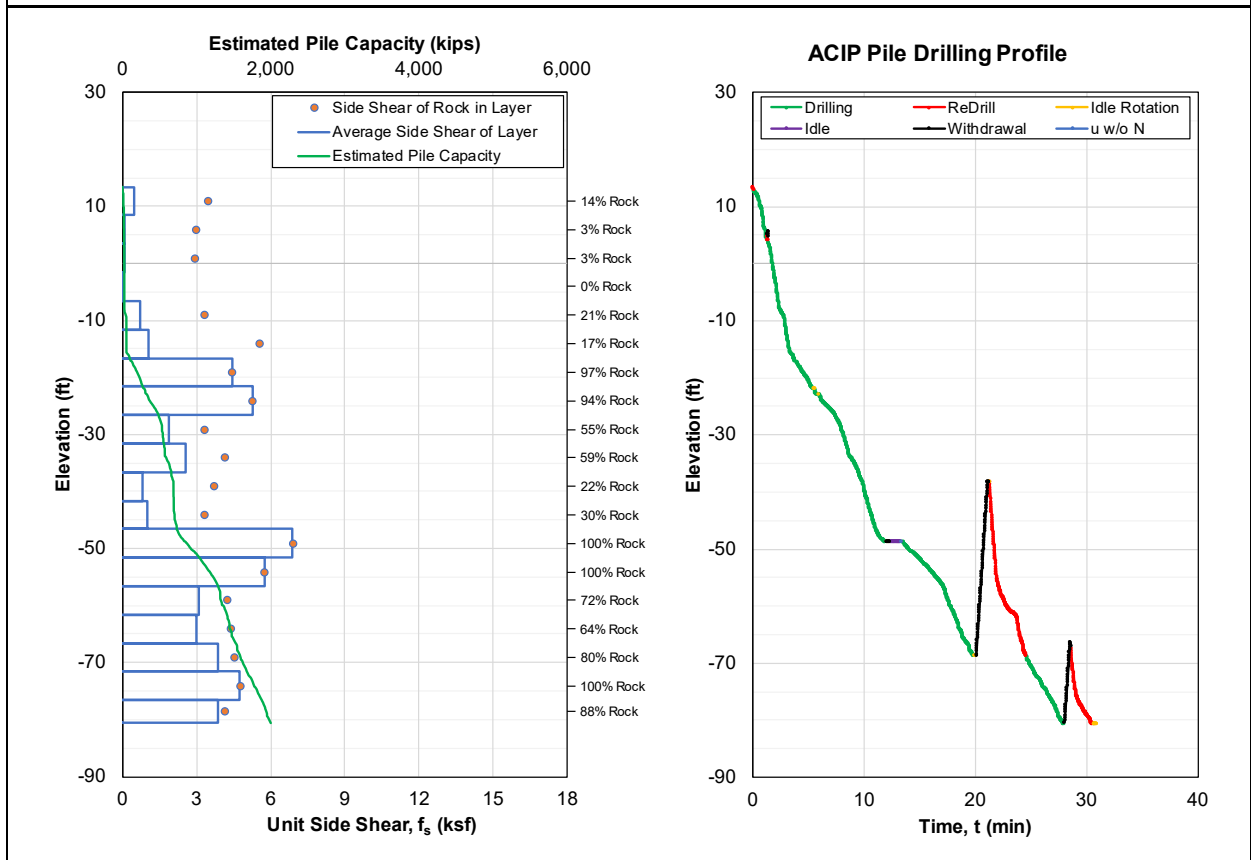


Figure A-2. ACIP pile capacity QA/QC report for Group B Pile 2.

Project	Location	Engineer	Pile ID
I-395	Miami, Florida	Rodgers, McVay, Kelch	B3
Station	Offset (ft)	Drill Rig	Drill Bit Diameter (in)
100+00.01	10.00	Drill Rig B	30
Top of Pile Elevation (ft)	Bottom of Pile Elevation (ft)	Depth Increment Analyzed (cm)	ISO-MWD Assessment
13.46	-80.80	1	Class 1

Specific Energy Above Threshold, e (psi)	
Specific Energy Threshold (psi)	1,250
Mean	2,682
Median	2,104
Standard Deviation	2,879
Coefficient of Variation (CV)	1.07
Maximum	63,983
Minimum	1,251
Number of Data Points	1,729

Unconfined Compressive Strength Above Threshold, q <sub>u</sub> (psi)	
q <sub>u</sub> Threshold (psi)	88
Mean	174
Median	144
Standard Deviation	129
Coefficient of Variation (CV)	0.74
Maximum	2,245
Minimum	88
Number of Data Points	1,729

ACIP Pile Capacity QA/QC	
Pile Length (ft)	94.26
Total Rock Socket Length (ft)	56.7
Average Pile Side Shear, f <sub>s</sub> (ksf)	3.12
Unfactored Pile Capacity (kips)	2,312
Factored Pile Capacity (kips)	1,387
Factored Design Load (kips)	1,070
C/D Ratio for LRFD $\Phi = 0.6$	1.30
Design Requirement Inspection	<b>Passed</b>

Pile Installation Summary	
Drilling Time (min)	24.8
ReDrill Time (min)	13.8
Idle Rotation Time (min)	2.2
Idle Time (min)	39.7
Withdrawal Time (min)	7.4
Penetration w/o Rotation Time (min)	0.7
Total Time (min)	88.6
Drilling Efficiency (%)	28%

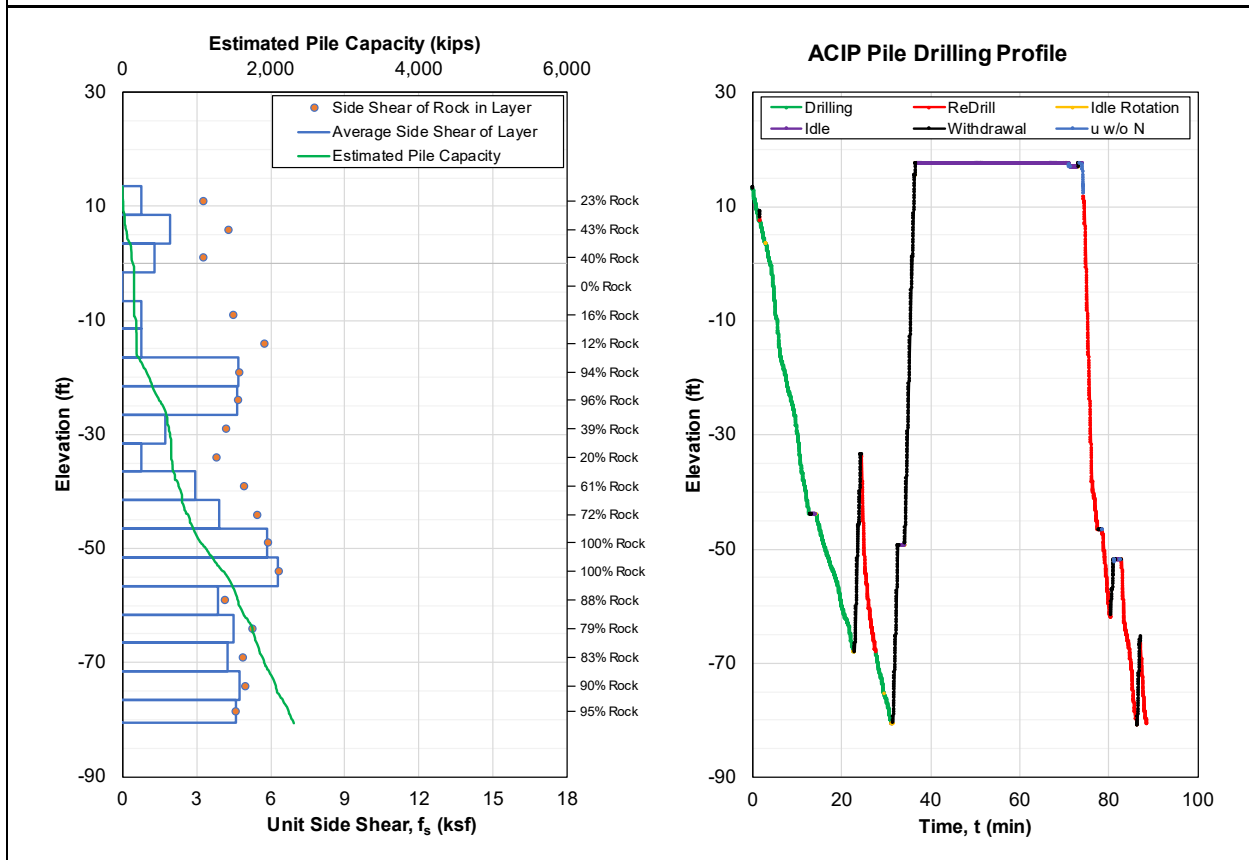


Figure A-3. ACIP pile capacity QA/QC report for Group B Pile 3.

Project	Location	Engineer	Pile ID
I-395	Miami, Florida	Rodgers, McVay, Kelch	B4
Station	Offset (ft)	Drill Rig	Drill Bit Diameter (in)
100+00.01	10.00	Drill Rig B	30
Top of Pile Elevation (ft)	Bottom of Pile Elevation (ft)	Depth Increment Analyzed (cm)	ISO-MWD Assessment
13.42	-80.61	1	Class 1

Specific Energy Above Threshold, e (psi)	
Specific Energy Threshold (psi)	1,250
Mean	3,231
Median	2,516
Standard Deviation	2,927
Coefficient of Variation (CV)	0.91
Maximum	36,795
Minimum	1,251
Number of Data Points	1,689

ACIP Pile Capacity QA/QC	
Pile Length (ft)	94.03
Total Rock Socket Length (ft)	55.4
Average Pile Side Shear, $f_s$ (ksf)	3.57
Unfactored Pile Capacity (kips)	2,635
Factored Pile Capacity (kips)	1,581
Factored Design Load (kips)	1,070
C/D Ratio for LRFD $\Phi = 0.6$	1.48
Design Requirement Inspection	<b>Passed</b>

Unconfined Compressive Strength Above Threshold, $q_u$ (psi)	
$q_u$ Threshold (psi)	88
Mean	206
Median	170
Standard Deviation	145
Coefficient of Variation (CV)	0.70
Maximum	1,542
Minimum	88
Number of Data Points	1,689

Pile Installation Summary	
Drilling Time (min)	28.4
ReDrill Time (min)	6.1
Idle Rotation Time (min)	1.3
Idle Time (min)	1.0
Withdrawal Time (min)	2.1
Penetration w/o Rotation Time (min)	0.1
Total Time (min)	39.1
Drilling Efficiency (%)	73%

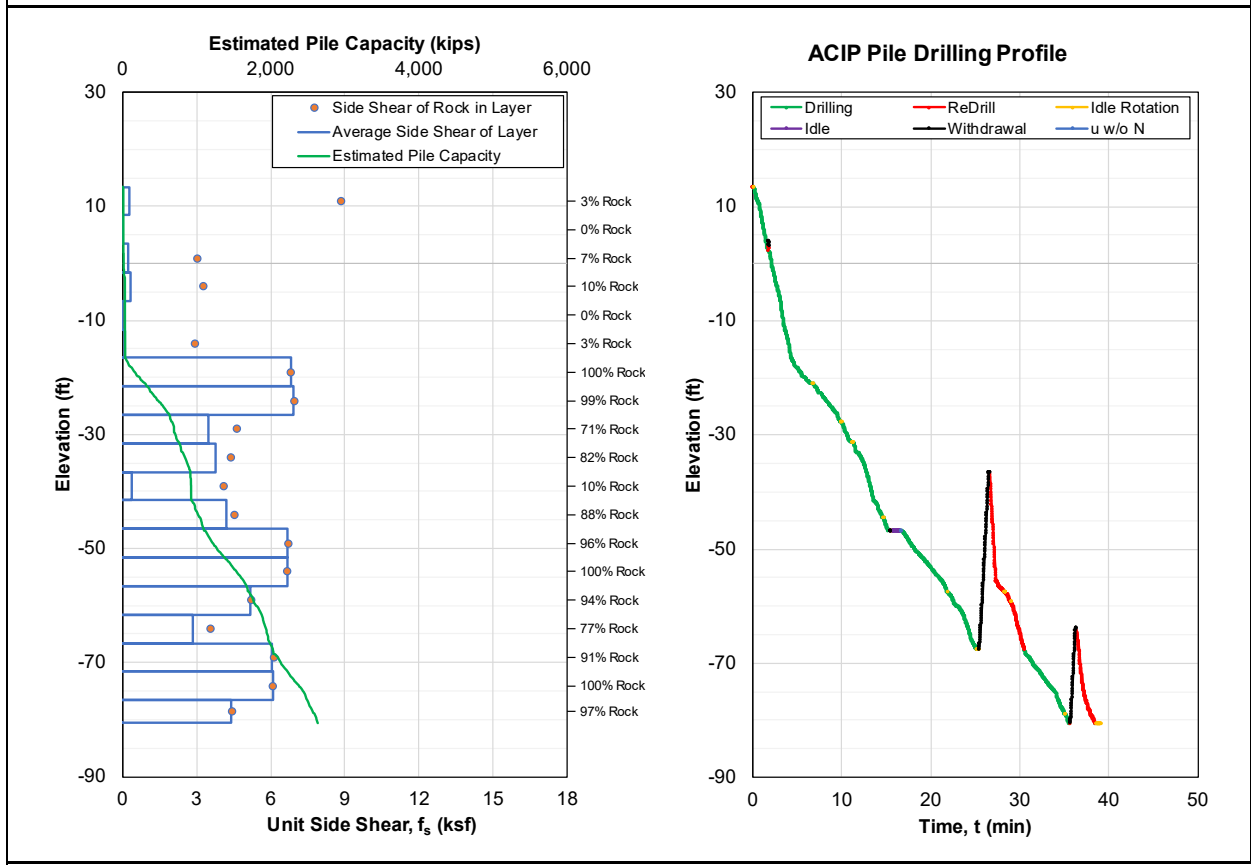


Figure A-4. ACIP pile capacity QA/QC report for Group B Pile 4.

Project	Location	Engineer	Pile ID
I-395	Miami, Florida	Rodgers, McVay, Kelch	B5
Station	Offset (ft)	Drill Rig	Drill Bit Diameter (in)
100+00.01	10.00	Drill Rig B	30
Top of Pile Elevation (ft)	Bottom of Pile Elevation (ft)	Depth Increment Analyzed (cm)	ISO-MWD Assessment
13.51	-80.52	1	Class 1

Specific Energy Above Threshold, e (psi)	
Specific Energy Threshold (psi)	1,250
Mean	3,000
Median	2,341
Standard Deviation	2,918
Coefficient of Variation (CV)	0.97
Maximum	63,139
Minimum	1,257
Number of Data Points	1,741

ACIP Pile Capacity QA/QC	
Pile Length (ft)	94.03
Total Rock Socket Length (ft)	57.1
Average Pile Side Shear, $f_s$ (ksf)	3.46
Unfactored Pile Capacity (kips)	2,556
Factored Pile Capacity (kips)	1,534
Factored Design Load (kips)	1,070
C/D Ratio for LRFD $\Phi = 0.6$	1.43
Design Requirement Inspection	<b>Passed</b>

Unconfined Compressive Strength Above Threshold, $q_u$ (psi)	
$q_u$ Threshold (psi)	88
Mean	192
Median	159
Standard Deviation	138
Coefficient of Variation (CV)	0.72
Maximum	2,226
Minimum	88
Number of Data Points	1,741

Pile Installation Summary	
Drilling Time (min)	25.7
ReDrill Time (min)	11.1
Idle Rotation Time (min)	1.9
Idle Time (min)	79.8
Withdrawal Time (min)	5.7
Penetration w/o Rotation Time (min)	0.5
Total Time (min)	124.6
Drilling Efficiency (%)	21%

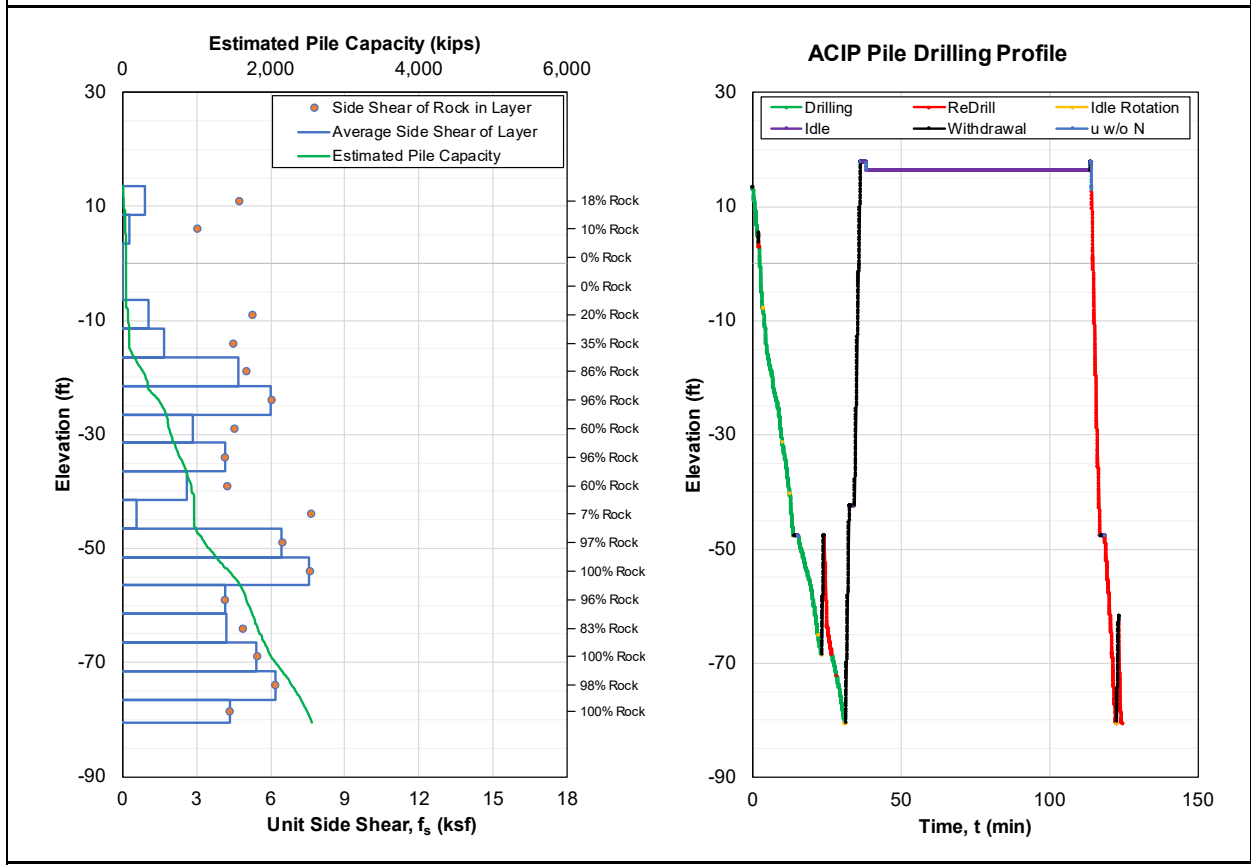


Figure A-5. ACIP pile capacity QA/QC report for Group B Pile 5.



Project	Location	Engineer	Pile ID
I-395	Miami, Florida	Rodgers, McVay, Kelch	B6
Station	Offset (ft)	Drill Rig	Drill Bit Diameter (in)
100+00.01	10.00	Drill Rig B	30
Top of Pile Elevation (ft)	Bottom of Pile Elevation (ft)	Depth Increment Analyzed (cm)	ISO-MWD Assessment
13.52	-80.51	1	Class 1

Specific Energy Above Threshold, e (psi)	
Specific Energy Threshold (psi)	1,250
Mean	2,571
Median	2,116
Standard Deviation	2,695
Coefficient of Variation (CV)	1.05
Maximum	88,045
Minimum	1,250
Number of Data Points	1,701

Unconfined Compressive Strength Above Threshold, q <sub>u</sub> (psi)	
q <sub>u</sub> Threshold (psi)	88
Mean	168
Median	145
Standard Deviation	112
Coefficient of Variation (CV)	0.66
Maximum	2,760
Minimum	88
Number of Data Points	1,701

ACIP Pile Capacity QA/QC	
Pile Length (ft)	94.03
Total Rock Socket Length (ft)	55.8
Average Pile Side Shear, f <sub>s</sub> (ksf)	3.00
Unfactored Pile Capacity (kips)	2,217
Factored Pile Capacity (kips)	1,330
Factored Design Load (kips)	1,070
C/D Ratio for LRFD $\Phi = 0.6$	1.24
Design Requirement Inspection	<b>Passed</b>

Pile Installation Summary	
Drilling Time (min)	24.6
ReDrill Time (min)	10.5
Idle Rotation Time (min)	1.6
Idle Time (min)	24.5
Withdrawal Time (min)	5.8
Penetration w/o Rotation Time (min)	0.5
Total Time (min)	67.5
Drilling Efficiency (%)	36%

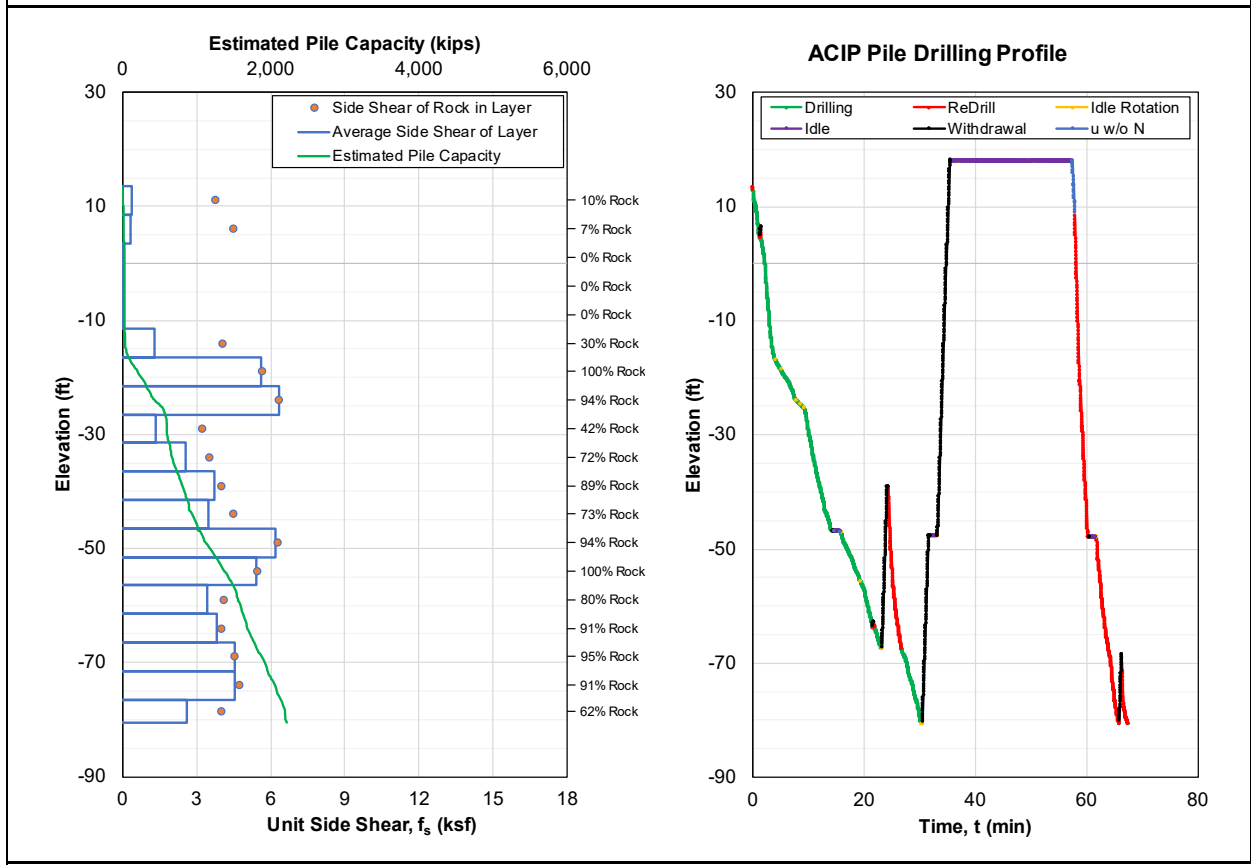


Figure A-6. ACIP pile capacity QA/QC report for Group B Pile 6.

Project	Location	Engineer	Pile ID
I-395	Miami, Florida	Rodgers, McVay, Kelch	B7
Station	Offset (ft)	Drill Rig	Drill Bit Diameter (in)
100+00.01	10.00	Drill Rig B	30
Top of Pile Elevation (ft)	Bottom of Pile Elevation (ft)	Depth Increment Analyzed (cm)	ISO-MWD Assessment
13.54	-80.49	1	Class 1

Specific Energy Above Threshold, e (psi)	
Specific Energy Threshold (psi)	1,250
Mean	2,643
Median	2,162
Standard Deviation	2,053
Coefficient of Variation (CV)	0.78
Maximum	41,558
Minimum	1,250
Number of Data Points	1,925

Unconfined Compressive Strength Above Threshold, q <sub>u</sub> (psi)	
q <sub>u</sub> Threshold (psi)	88
Mean	173
Median	148
Standard Deviation	104
Coefficient of Variation (CV)	0.60
Maximum	1,678
Minimum	88
Number of Data Points	1,925

ACIP Pile Capacity QA/QC	
Pile Length (ft)	94.03
Total Rock Socket Length (ft)	63.2
Average Pile Side Shear, f <sub>s</sub> (ksf)	3.49
Unfactored Pile Capacity (kips)	2,581
Factored Pile Capacity (kips)	1,549
Factored Design Load (kips)	1,070
C/D Ratio for LRFD $\Phi = 0.6$	1.45
Design Requirement Inspection	<b>Passed</b>

Pile Installation Summary	
Drilling Time (min)	28.1
ReDrill Time (min)	10.9
Idle Rotation Time (min)	6.4
Idle Time (min)	38.2
Withdrawal Time (min)	6.0
Penetration w/o Rotation Time (min)	0.7
Total Time (min)	90.2
Drilling Efficiency (%)	31%

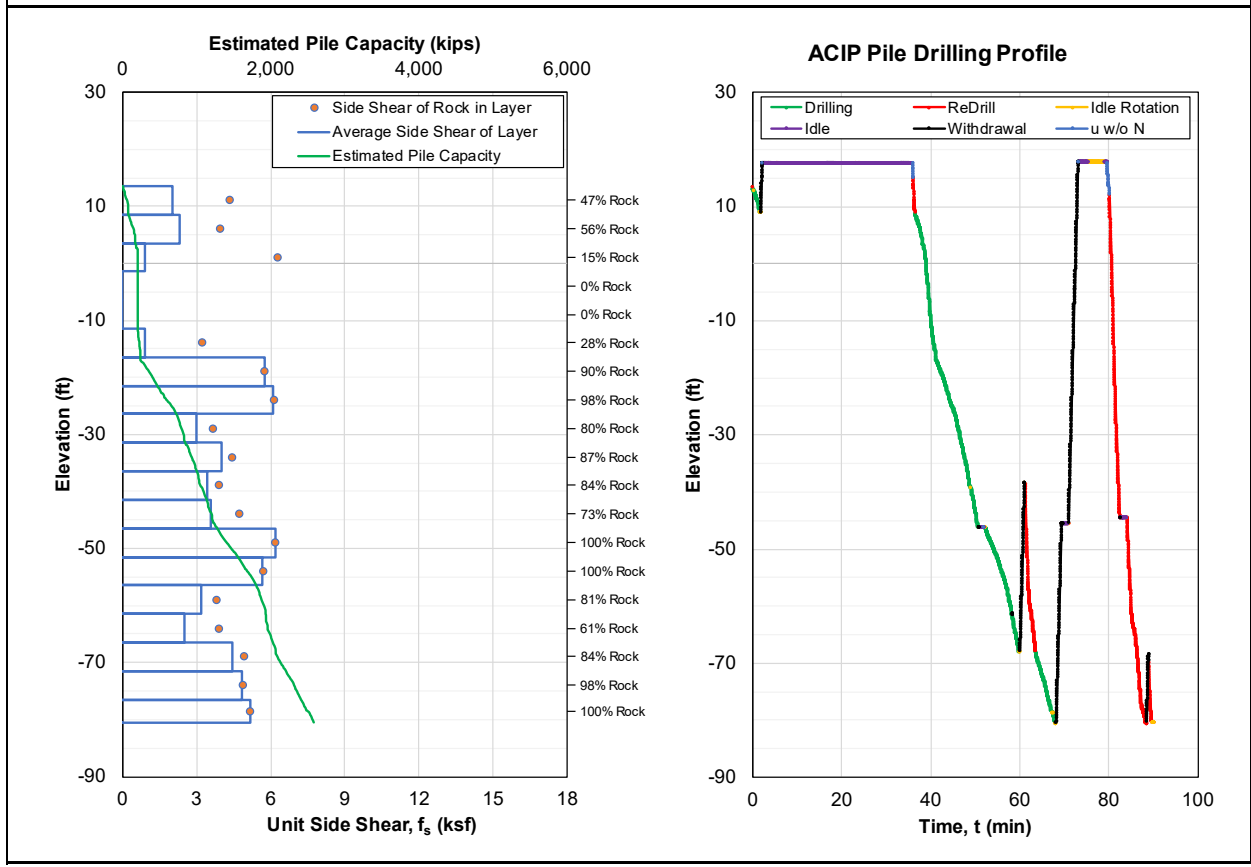


Figure A-7. ACIP pile capacity QA/QC report for Group B Pile 7.

Project	Location	Engineer	Pile ID
I-395	Miami, Florida	Rodgers, McVay, Kelch	B8
Station	Offset (ft)	Drill Rig	Drill Bit Diameter (in)
100+00.01	10.00	Drill Rig B	30
Top of Pile Elevation (ft)	Bottom of Pile Elevation (ft)	Depth Increment Analyzed (cm)	ISO-MWD Assessment
13.58	-80.42	1	Class 1

Specific Energy Above Threshold, e (psi)	
Specific Energy Threshold (psi)	1,250
Mean	3,010
Median	2,301
Standard Deviation	3,385
Coefficient of Variation (CV)	1.12
Maximum	75,003
Minimum	1,254
Number of Data Points	1,931

ACIP Pile Capacity QA/QC	
Pile Length (ft)	94.00
Total Rock Socket Length (ft)	63.4
Average Pile Side Shear, $f_s$ (ksf)	3.83
Unfactored Pile Capacity (kips)	2,826
Factored Pile Capacity (kips)	1,696
Factored Design Load (kips)	1,070
C/D Ratio for LRFD $\Phi = 0.6$	1.58
Design Requirement Inspection	<b>Passed</b>

Unconfined Compressive Strength Above Threshold, $q_u$ (psi)	
$q_u$ Threshold (psi)	88
Mean	192
Median	156
Standard Deviation	148
Coefficient of Variation (CV)	0.77
Maximum	2,490
Minimum	88
Number of Data Points	1,931

Pile Installation Summary	
Drilling Time (min)	30.5
ReDrill Time (min)	8.1
Idle Rotation Time (min)	1.9
Idle Time (min)	13.2
Withdrawal Time (min)	3.3
Penetration w/o Rotation Time (min)	0.0
Total Time (min)	57.0
Drilling Efficiency (%)	54%

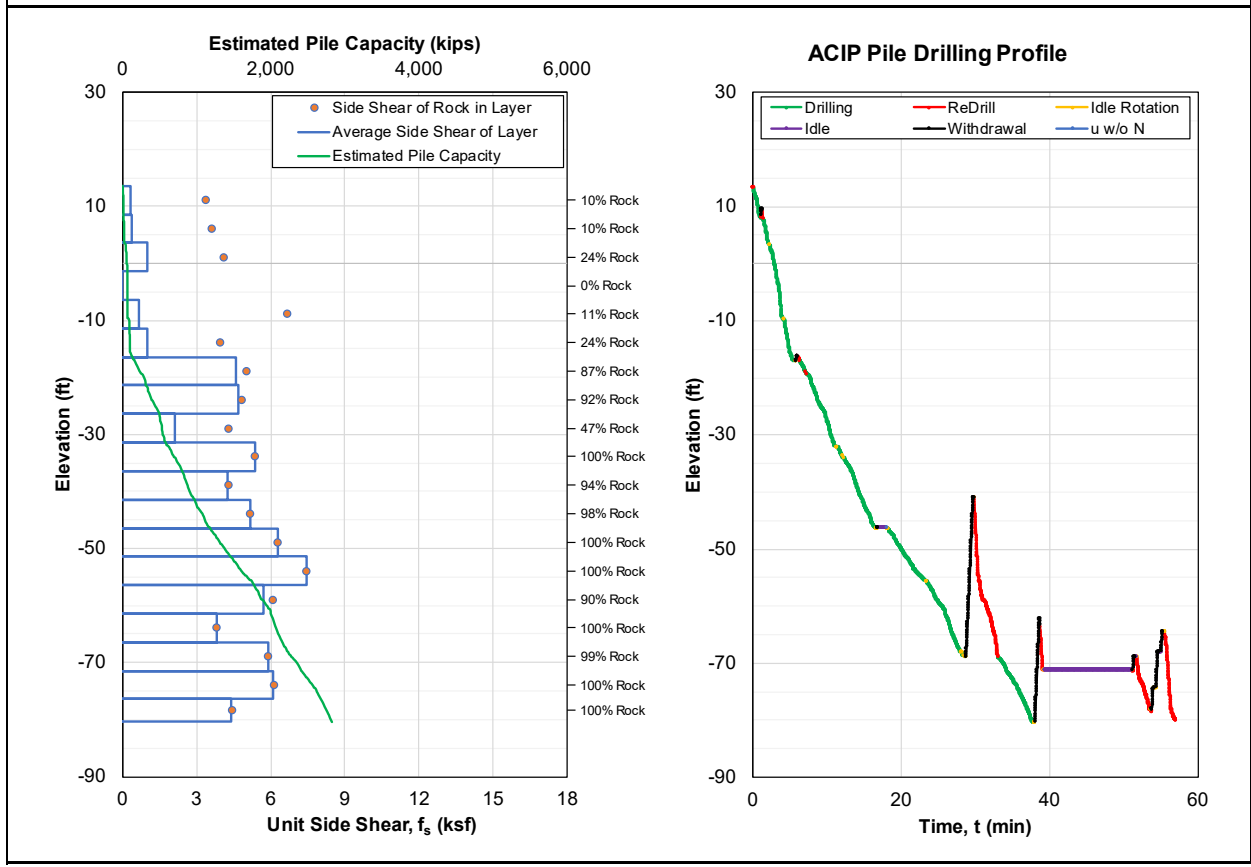


Figure A-8. ACIP pile capacity QA/QC report for Group B Pile 8.

Project	Location	Engineer	Pile ID
I-395	Miami, Florida	Rodgers, McVay, Kelch	B9
Station	Offset (ft)	Drill Rig	Drill Bit Diameter (in)
100+00.01	10.00	Drill Rig B	30
Top of Pile Elevation (ft)	Bottom of Pile Elevation (ft)	Depth Increment Analyzed (cm)	ISO-MWD Assessment
13.52	-80.51	1	Class 1

Specific Energy Above Threshold, e (psi)	
Specific Energy Threshold (psi)	1,250
Mean	2,777
Median	2,239
Standard Deviation	3,076
Coefficient of Variation (CV)	1.11
Maximum	74,880
Minimum	1,251
Number of Data Points	1,787

ACIP Pile Capacity QA/QC	
Pile Length (ft)	94.03
Total Rock Socket Length (ft)	58.6
Average Pile Side Shear, $f_s$ (ksf)	3.34
Unfactored Pile Capacity (kips)	2,464
Factored Pile Capacity (kips)	1,478
Factored Design Load (kips)	1,070
C/D Ratio for LRFD $\Phi = 0.6$	1.38
Design Requirement Inspection	<b>Passed</b>

Unconfined Compressive Strength Above Threshold, $q_u$ (psi)	
$q_u$ Threshold (psi)	88
Mean	179
Median	152
Standard Deviation	131
Coefficient of Variation (CV)	0.73
Maximum	2,488
Minimum	88
Number of Data Points	1,787

Pile Installation Summary	
Drilling Time (min)	27.7
ReDrill Time (min)	13.2
Idle Rotation Time (min)	1.9
Idle Time (min)	9.1
Withdrawal Time (min)	6.1
Penetration w/o Rotation Time (min)	0.4
Total Time (min)	58.4
Drilling Efficiency (%)	48%

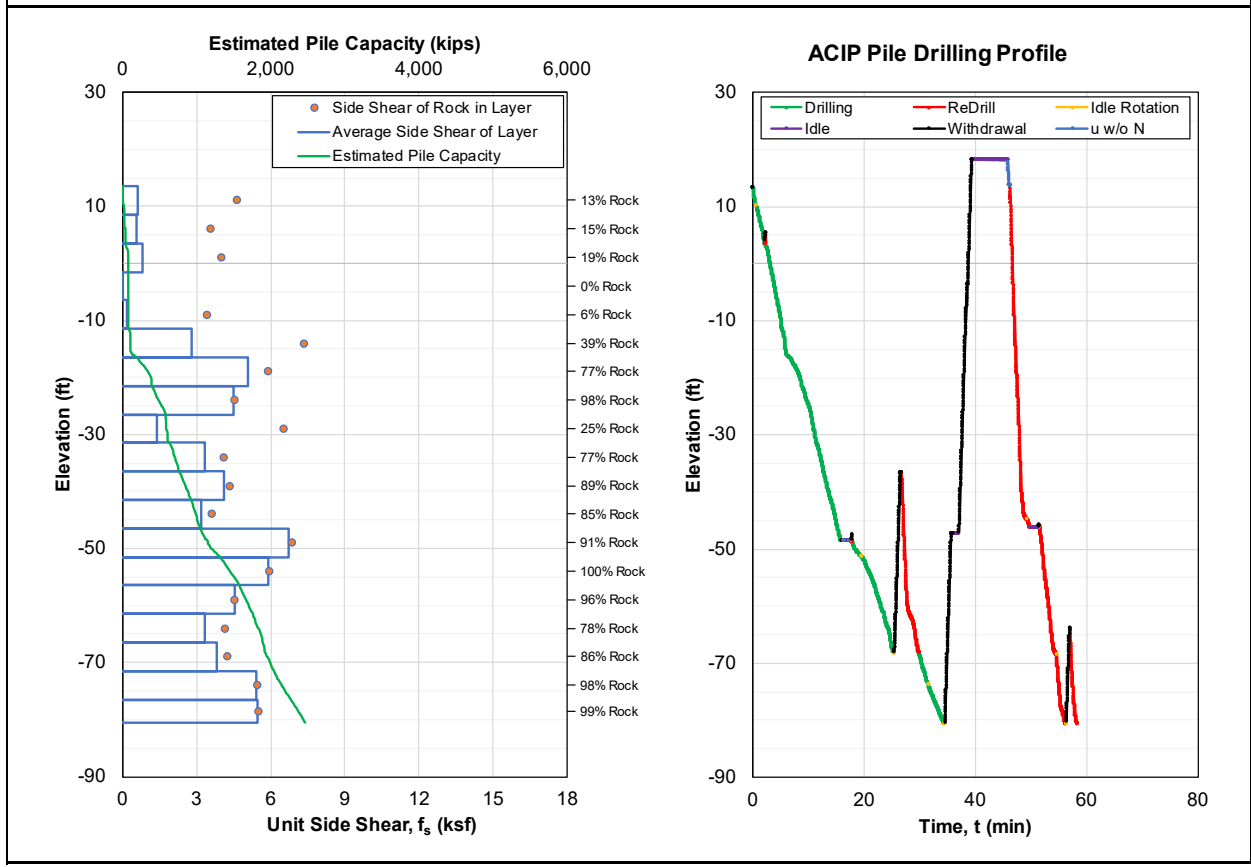


Figure A-9. ACIP pile capacity QA/QC report for Group B Pile 9.

Project	Location	Engineer	Pile ID
I-395	Miami, Florida	Rodgers, McVay, Kelch	B10
Station	Offset (ft)	Drill Rig	Drill Bit Diameter (in)
100+00.01	10.00	Drill Rig B	30
Top of Pile Elevation (ft)	Bottom of Pile Elevation (ft)	Depth Increment Analyzed (cm)	ISO-MWD Assessment
13.5	-80.56	1	Class 1

Specific Energy Above Threshold, e (psi)	
Specific Energy Threshold (psi)	1,250
Mean	2,943
Median	2,371
Standard Deviation	2,415
Coefficient of Variation (CV)	0.82
Maximum	30,234
Minimum	1,252
Number of Data Points	1,883

ACIP Pile Capacity QA/QC	
Pile Length (ft)	94.06
Total Rock Socket Length (ft)	61.8
Average Pile Side Shear, $f_s$ (ksf)	3.71
Unfactored Pile Capacity (kips)	2,743
Factored Pile Capacity (kips)	1,646
Factored Design Load (kips)	1,070
C/D Ratio for LRFD $\Phi = 0.6$	1.54
Design Requirement Inspection	<b>Passed</b>

Unconfined Compressive Strength Above Threshold, $q_u$ (psi)	
$q_u$ Threshold (psi)	88
Mean	190
Median	161
Standard Deviation	123
Coefficient of Variation (CV)	0.65
Maximum	1,342
Minimum	88
Number of Data Points	1,883

Pile Installation Summary	
Drilling Time (min)	29.3
ReDrill Time (min)	12.5
Idle Rotation Time (min)	2.8
Idle Time (min)	44.1
Withdrawal Time (min)	5.8
Penetration w/o Rotation Time (min)	0.4
Total Time (min)	94.8
Drilling Efficiency (%)	31%

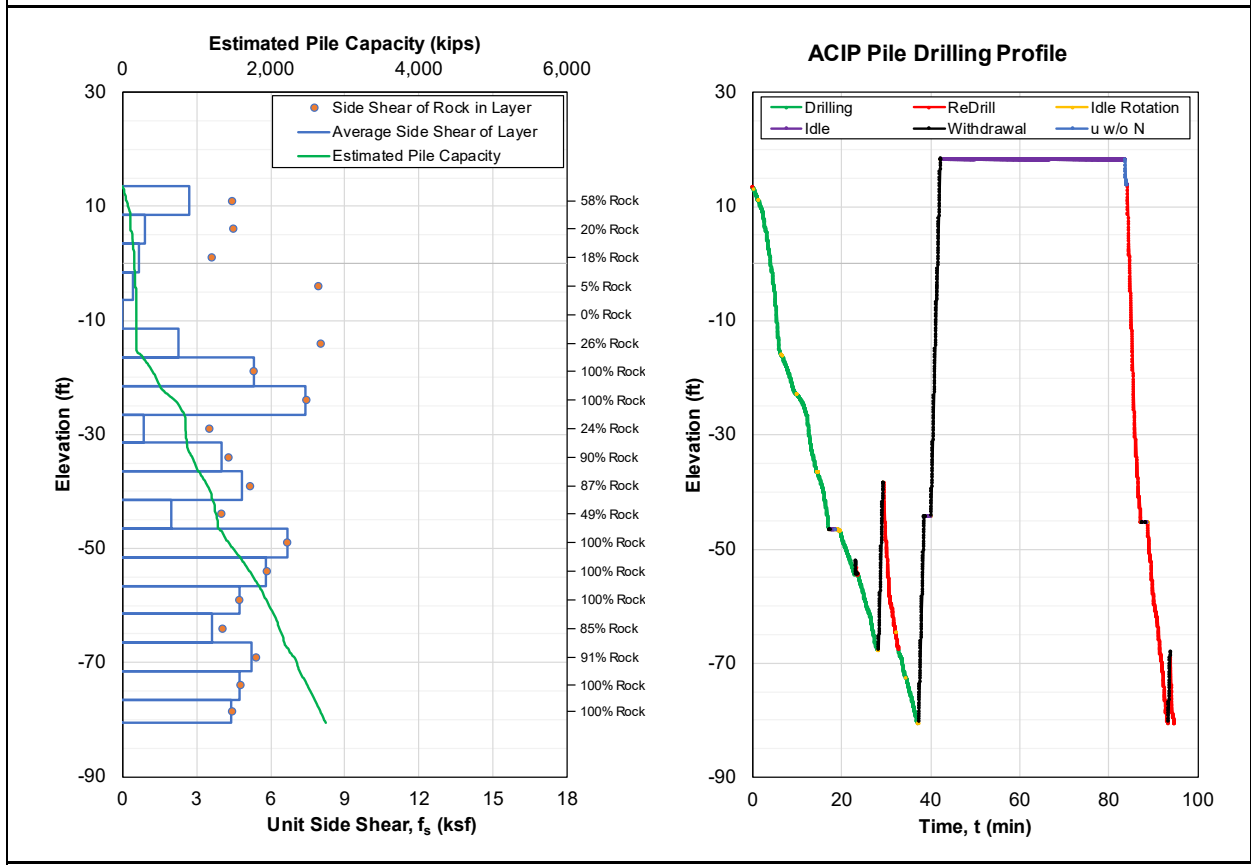


Figure A-10. ACIP pile capacity QA/QC report for Group B Pile 10.

Project	Location	Engineer	Pile ID
I-395	Miami, Florida	Rodgers, McVay, Kelch	B11
Station	Offset (ft)	Drill Rig	Drill Bit Diameter (in)
100+00.01	10.00	Drill Rig B	30
Top of Pile Elevation (ft)	Bottom of Pile Elevation (ft)	Depth Increment Analyzed (cm)	ISO-MWD Assessment
13.58	-80.51	1	Class 1

Specific Energy Above Threshold, e (psi)	
Specific Energy Threshold (psi)	1,250
Mean	2,830
Median	2,120
Standard Deviation	3,161
Coefficient of Variation (CV)	1.12
Maximum	59,220
Minimum	1,252
Number of Data Points	1,889

ACIP Pile Capacity QA/QC	
Pile Length (ft)	94.09
Total Rock Socket Length (ft)	62.0
Average Pile Side Shear, $f_s$ (ksf)	3.55
Unfactored Pile Capacity (kips)	2,624
Factored Pile Capacity (kips)	1,574
Factored Design Load (kips)	1,070
C/D Ratio for LRFD $\Phi = 0.6$	1.47
Design Requirement Inspection	<b>Passed</b>

Unconfined Compressive Strength Above Threshold, $q_u$ (psi)	
$q_u$ Threshold (psi)	88
Mean	181
Median	145
Standard Deviation	143
Coefficient of Variation (CV)	0.79
Maximum	2,133
Minimum	88
Number of Data Points	1,889

Pile Installation Summary	
Drilling Time (min)	27.0
ReDrill Time (min)	15.0
Idle Rotation Time (min)	26.6
Idle Time (min)	18.9
Withdrawal Time (min)	6.1
Penetration w/o Rotation Time (min)	0.2
Total Time (min)	93.6
Drilling Efficiency (%)	29%

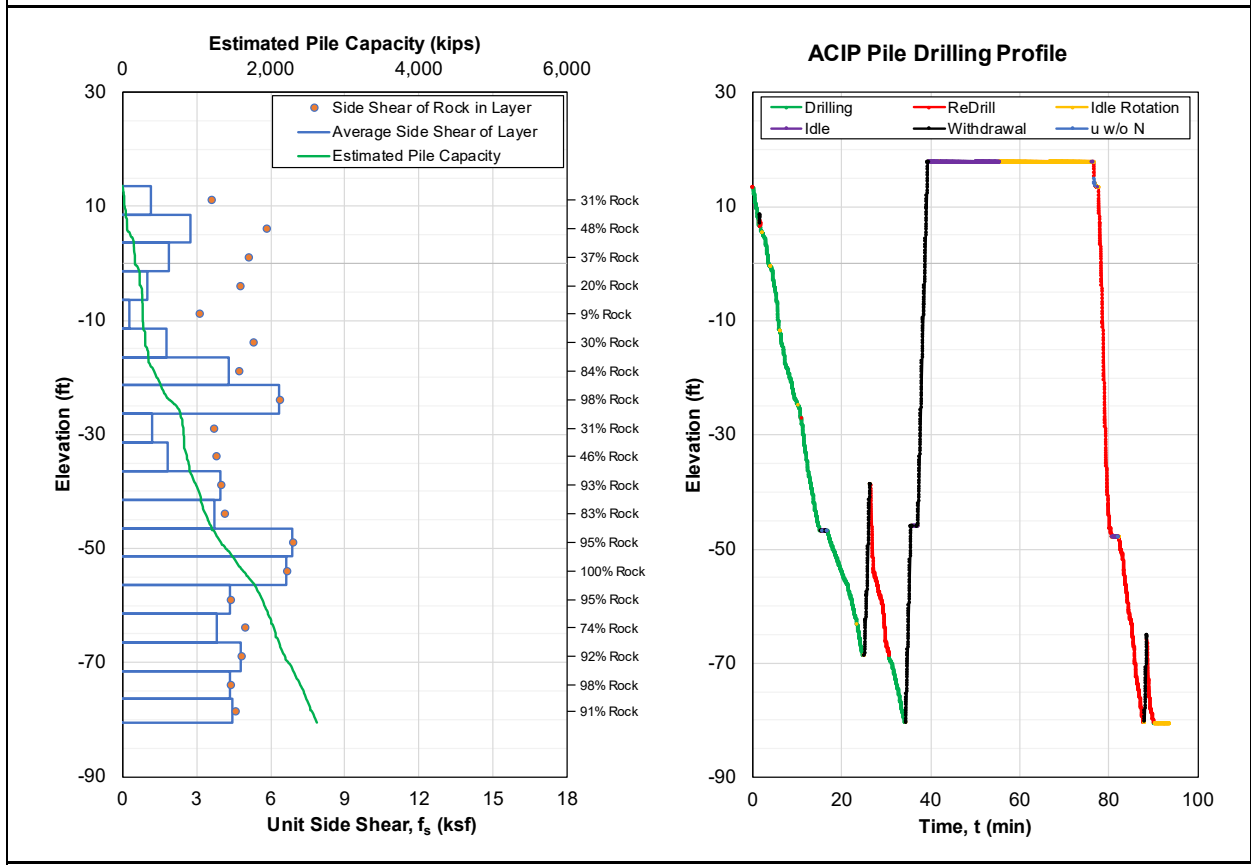


Figure A-11. ACIP pile capacity QA/QC report for Group B Pile 11.

Project	Location	Engineer	Pile ID
I-395	Miami, Florida	Rodgers, McVay, Kelch	B12
Station	Offset (ft)	Drill Rig	Drill Bit Diameter (in)
100+00.01	10.00	Drill Rig B	30
Top of Pile Elevation (ft)	Bottom of Pile Elevation (ft)	Depth Increment Analyzed (cm)	ISO-MWD Assessment
13.51	-80.49	1	Class 1

Specific Energy Above Threshold, e (psi)	
Specific Energy Threshold (psi)	1,250
Mean	3,054
Median	2,307
Standard Deviation	3,107
Coefficient of Variation (CV)	1.02
Maximum	41,392
Minimum	1,252
Number of Data Points	1,488

Unconfined Compressive Strength Above Threshold, q <sub>u</sub> (psi)	
q <sub>u</sub> Threshold (psi)	88
Mean	194
Median	157
Standard Deviation	148
Coefficient of Variation (CV)	0.76
Maximum	1,674
Minimum	88
Number of Data Points	1,488

ACIP Pile Capacity QA/QC	
Pile Length (ft)	94.00
Total Rock Socket Length (ft)	48.8
Average Pile Side Shear, f <sub>s</sub> (ksf)	2.98
Unfactored Pile Capacity (kips)	2,203
Factored Pile Capacity (kips)	1,322
Factored Design Load (kips)	1,070
C/D Ratio for LRFD $\Phi = 0.6$	1.24
Design Requirement Inspection	<b>Passed</b>

Pile Installation Summary	
Drilling Time (min)	25.0
ReDrill Time (min)	11.9
Idle Rotation Time (min)	2.5
Idle Time (min)	35.9
Withdrawal Time (min)	6.4
Penetration w/o Rotation Time (min)	0.4
Total Time (min)	82.1
Drilling Efficiency (%)	31%

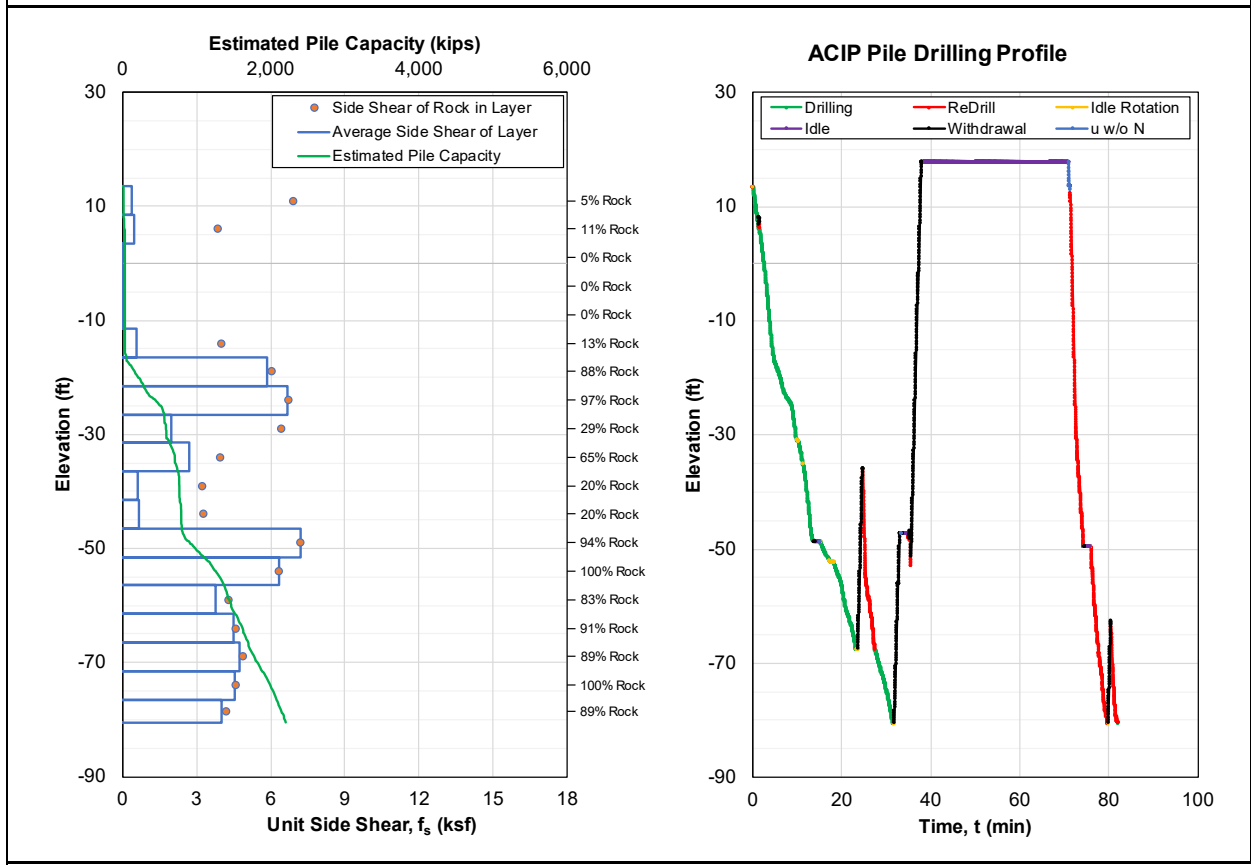


Figure A-12. ACIP pile capacity QA/QC report for Group B Pile 12.

Project	Location	Engineer	Pile ID
I-395	Miami, Florida	Rodgers, McVay, Kelch	B13
Station	Offset (ft)	Drill Rig	Drill Bit Diameter (in)
100+00.01	10.00	Drill Rig B	30
Top of Pile Elevation (ft)	Bottom of Pile Elevation (ft)	Depth Increment Analyzed (cm)	ISO-MWD Assessment
13.55	-80.51	1	Class 1

Specific Energy Above Threshold, e (psi)	
Specific Energy Threshold (psi)	1,250
Mean	2,928
Median	2,121
Standard Deviation	5,313
Coefficient of Variation (CV)	1.81
Maximum	185,070
Minimum	1,253
Number of Data Points	1,905

ACIP Pile Capacity QA/QC	
Pile Length (ft)	94.06
Total Rock Socket Length (ft)	62.5
Average Pile Side Shear, $f_s$ (ksf)	3.62
Unfactored Pile Capacity (kips)	2,674
Factored Pile Capacity (kips)	1,604
Factored Design Load (kips)	1,070
C/D Ratio for LRFD $\Phi = 0.6$	1.50
Design Requirement Inspection	<b>Passed</b>

Unconfined Compressive Strength Above Threshold, $q_u$ (psi)	
$q_u$ Threshold (psi)	88
Mean	184
Median	145
Standard Deviation	172
Coefficient of Variation (CV)	0.94
Maximum	4,359
Minimum	88
Number of Data Points	1,905

Pile Installation Summary	
Drilling Time (min)	27.7
ReDrill Time (min)	14.8
Idle Rotation Time (min)	11.0
Idle Time (min)	41.8
Withdrawal Time (min)	6.6
Penetration w/o Rotation Time (min)	0.5
Total Time (min)	102.4
Drilling Efficiency (%)	27%

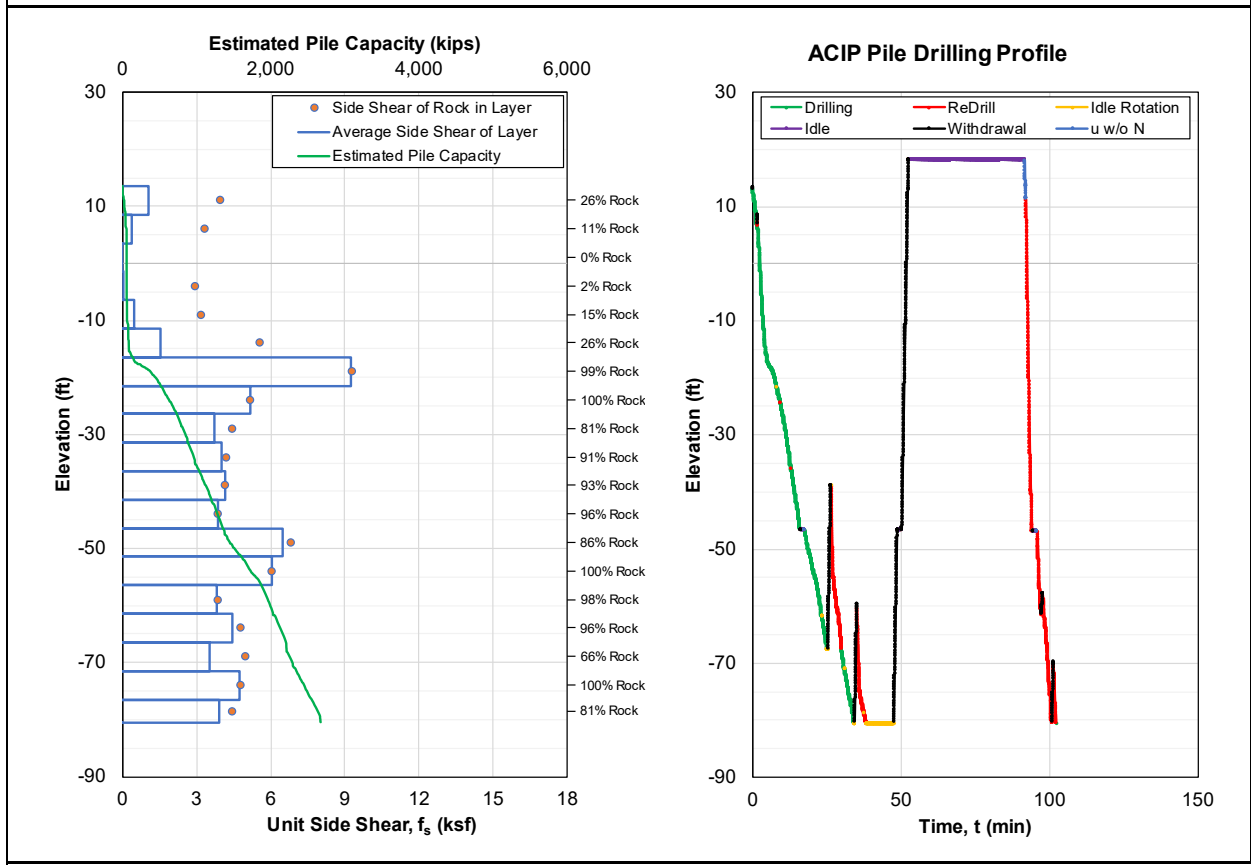


Figure A-13. ACIP pile capacity QA/QC report for Group B Pile 13.



Project	Location	Engineer	Pile ID
I-395	Miami, Florida	Rodgers, McVay, Kelch	B14
Station	Offset (ft)	Drill Rig	Drill Bit Diameter (in)
100+00.01	10.00	Drill Rig B	30
Top of Pile Elevation (ft)	Bottom of Pile Elevation (ft)	Depth Increment Analyzed (cm)	ISO-MWD Assessment
13.55	-80.48	1	Class 1

Specific Energy Above Threshold, e (psi)	
Specific Energy Threshold (psi)	1,250
Mean	2,992
Median	2,071
Standard Deviation	4,469
Coefficient of Variation (CV)	1.49
Maximum	131,557
Minimum	1,250
Number of Data Points	1,508

ACIP Pile Capacity QA/QC	
Pile Length (ft)	94.03
Total Rock Socket Length (ft)	49.5
Average Pile Side Shear, $f_s$ (ksf)	2.93
Unfactored Pile Capacity (kips)	2,164
Factored Pile Capacity (kips)	1,299
Factored Design Load (kips)	1,070
C/D Ratio for LRFD $\Phi = 0.6$	1.21
Design Requirement Inspection	<b>Passed</b>

Unconfined Compressive Strength Above Threshold, $q_u$ (psi)	
$q_u$ Threshold (psi)	88
Mean	188
Median	142
Standard Deviation	166
Coefficient of Variation (CV)	0.88
Maximum	3,547
Minimum	88
Number of Data Points	1,508

Pile Installation Summary	
Drilling Time (min)	22.6
ReDrill Time (min)	9.7
Idle Rotation Time (min)	1.7
Idle Time (min)	39.4
Withdrawal Time (min)	5.6
Penetration w/o Rotation Time (min)	0.4
Total Time (min)	79.3
Drilling Efficiency (%)	28%

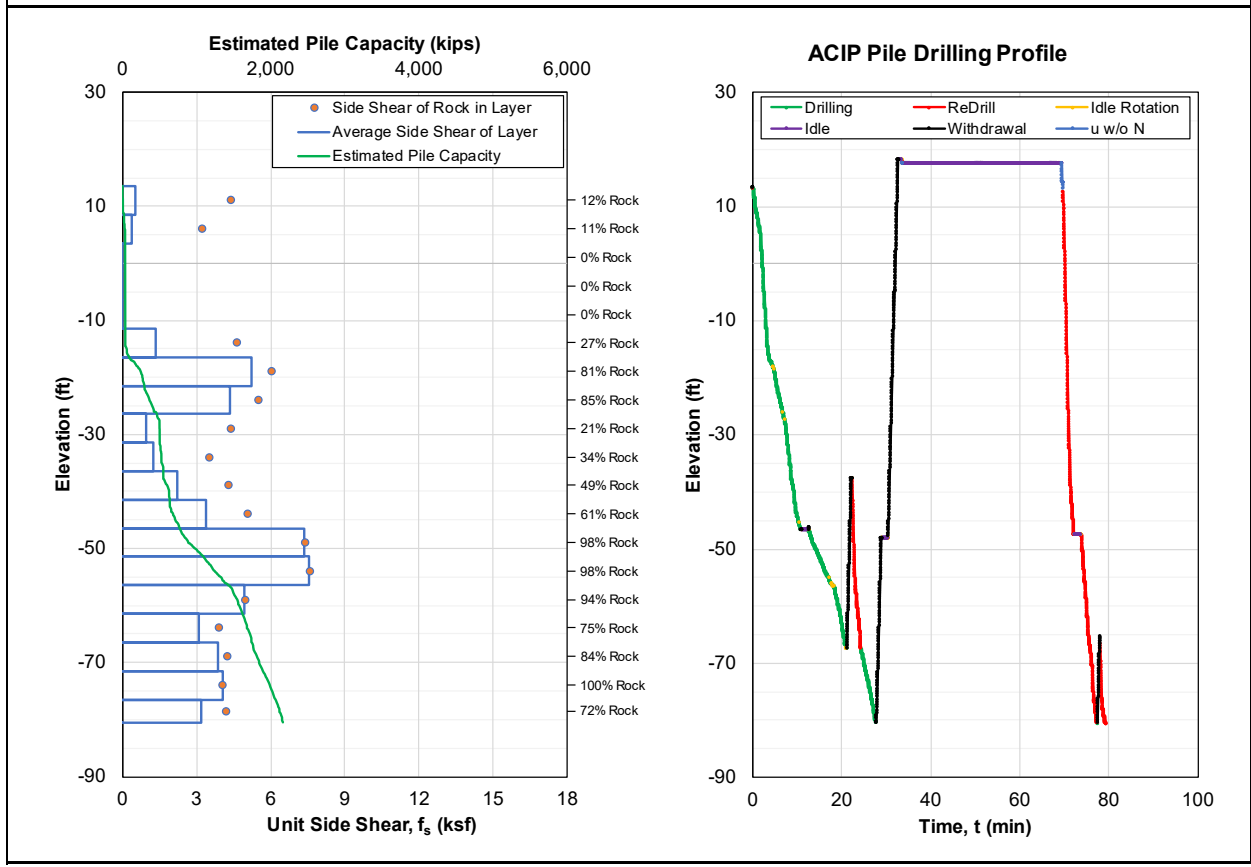


Figure A-14. ACIP pile capacity QA/QC report for Group B Pile 14.

Project	Location	Engineer	Pile ID
I-395	Miami, Florida	Rodgers, McVay, Kelch	B15
Station	Offset (ft)	Drill Rig	Drill Bit Diameter (in)
100+00.01	10.00	Drill Rig B	30
Top of Pile Elevation (ft)	Bottom of Pile Elevation (ft)	Depth Increment Analyzed (cm)	ISO-MWD Assessment
13.53	-80.63	1	Class 1

Specific Energy Above Threshold, e (psi)	
Specific Energy Threshold (psi)	1,250
Mean	3,082
Median	2,263
Standard Deviation	4,249
Coefficient of Variation (CV)	1.38
Maximum	106,269
Minimum	1,252
Number of Data Points	1,753

ACIP Pile Capacity QA/QC	
Pile Length (ft)	94.16
Total Rock Socket Length (ft)	57.5
Average Pile Side Shear, $f_s$ (ksf)	3.49
Unfactored Pile Capacity (kips)	2,584
Factored Pile Capacity (kips)	1,551
Factored Design Load (kips)	1,070
C/D Ratio for LRFD $\Phi = 0.6$	1.45
Design Requirement Inspection	<b>Passed</b>

Unconfined Compressive Strength Above Threshold, $q_u$ (psi)	
$q_u$ Threshold (psi)	88
Mean	194
Median	154
Standard Deviation	167
Coefficient of Variation (CV)	0.86
Maximum	3,108
Minimum	88
Number of Data Points	1,753

Pile Installation Summary	
Drilling Time (min)	28.1
ReDrill Time (min)	14.7
Idle Rotation Time (min)	2.8
Idle Time (min)	34.7
Withdrawal Time (min)	6.3
Penetration w/o Rotation Time (min)	0.3
Total Time (min)	86.9
Drilling Efficiency (%)	32%

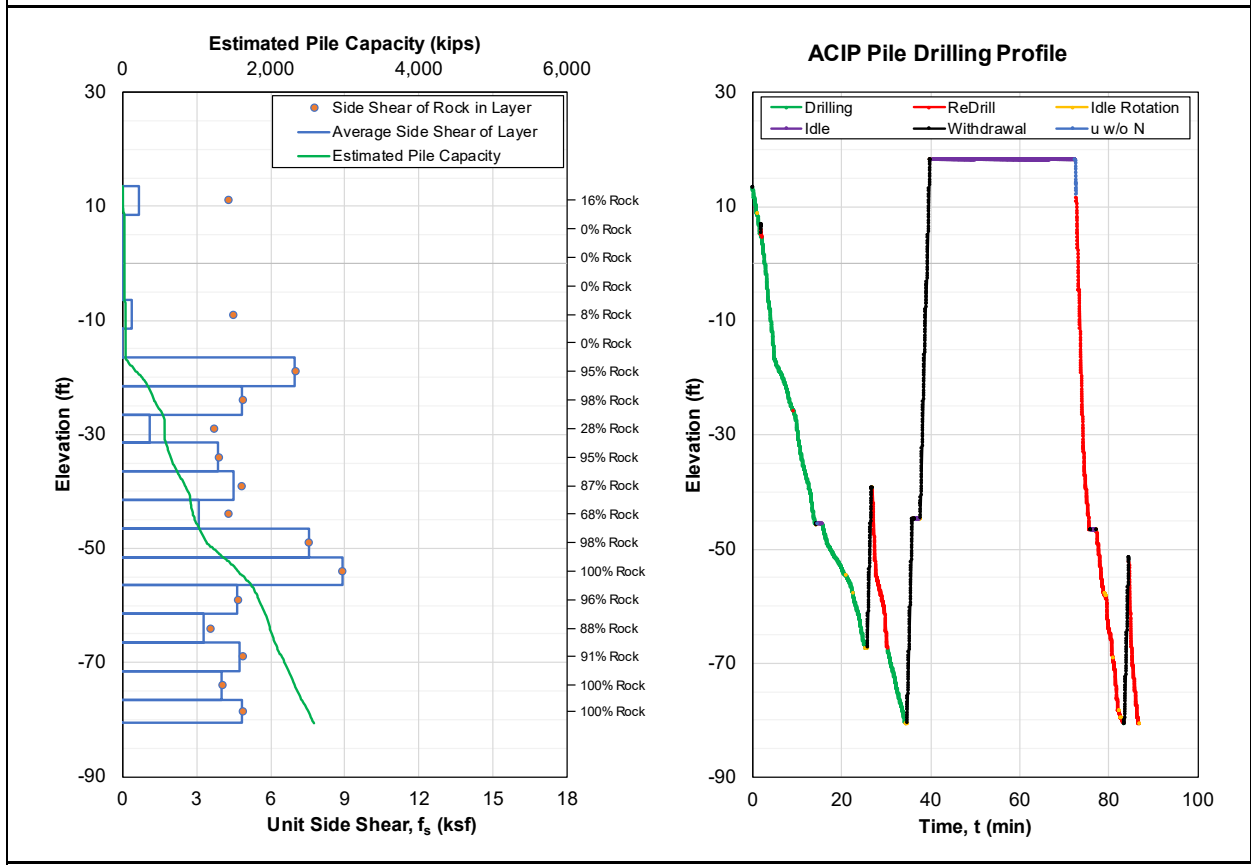


Figure A-15. ACIP pile capacity QA/QC report for Group B Pile 15.

Project	Location	Engineer	Pile ID
I-395	Miami, Florida	Rodgers, McVay, Kelch	B16
Station	Offset (ft)	Drill Rig	Drill Bit Diameter (in)
100+00.01	10.00	Drill Rig B	30
Top of Pile Elevation (ft)	Bottom of Pile Elevation (ft)	Depth Increment Analyzed (cm)	ISO-MWD Assessment
13.55	-80.54	1	Class 1

Specific Energy Above Threshold, e (psi)	
Specific Energy Threshold (psi)	1,250
Mean	2,841
Median	2,303
Standard Deviation	2,394
Coefficient of Variation (CV)	0.84
Maximum	49,698
Minimum	1,252
Number of Data Points	1,704

Unconfined Compressive Strength Above Threshold, q <sub>u</sub> (psi)	
q <sub>u</sub> Threshold (psi)	88
Mean	185
Median	157
Standard Deviation	115
Coefficient of Variation (CV)	0.62
Maximum	1,897
Minimum	88
Number of Data Points	1,704

ACIP Pile Capacity QA/QC	
Pile Length (ft)	94.09
Total Rock Socket Length (ft)	55.9
Average Pile Side Shear, f <sub>s</sub> (ksf)	3.27
Unfactored Pile Capacity (kips)	2,419
Factored Pile Capacity (kips)	1,451
Factored Design Load (kips)	1,070
C/D Ratio for LRFD $\Phi = 0.6$	1.36
Design Requirement Inspection	<b>Passed</b>

Pile Installation Summary	
Drilling Time (min)	25.7
ReDrill Time (min)	13.4
Idle Rotation Time (min)	2.5
Idle Time (min)	14.0
Withdrawal Time (min)	5.7
Penetration w/o Rotation Time (min)	0.4
Total Time (min)	61.6
Drilling Efficiency (%)	42%

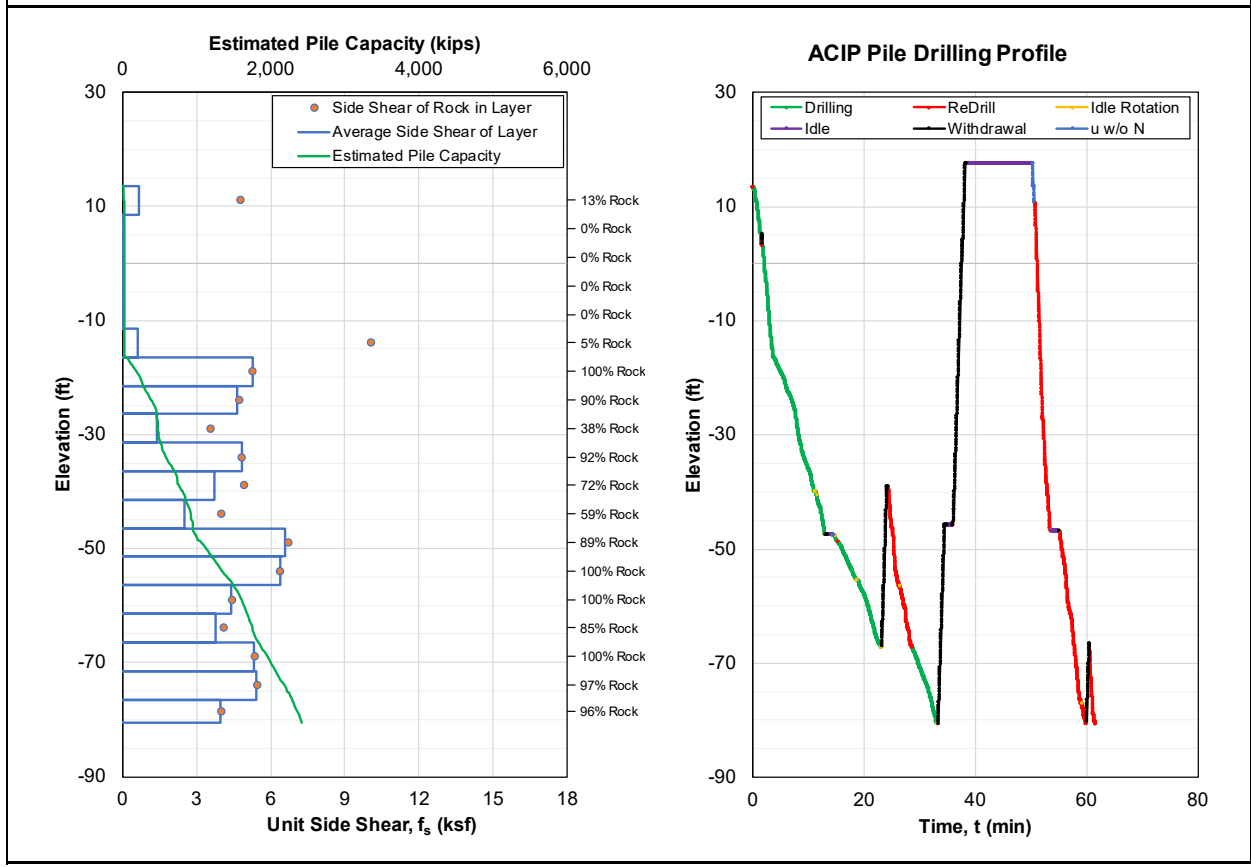


Figure A-16. ACIP pile capacity QA/QC report for Group B Pile 16.

Project	Location	Engineer	Pile ID
I-395	Miami, Florida	Rodgers, McVay, Kelch	C1-1
Station	Offset (ft)	Drill Rig	Drill Bit Diameter (in)
100+00.01	10.00	Drill Rig A	30
Top of Pile Elevation (ft)	Bottom of Pile Elevation (ft)	Depth Increment Analyzed (cm)	ISO-MWD Assessment
10.08	-111.41	1	Class 1

Specific Energy Above Threshold, e (psi)	
Specific Energy Threshold (psi)	1,250
Mean	3,495
Median	1,935
Standard Deviation	14,068
Coefficient of Variation (CV)	4.03
Maximum	380,290
Minimum	1,255
Number of Data Points	3,118

ACIP Pile Capacity QA/QC	
Pile Length (ft)	121.49
Total Rock Socket Length (ft)	102.3
Average Pile Side Shear, $f_s$ (ksf)	4.81
Unfactored Pile Capacity (kips)	4,590
Factored Pile Capacity (kips)	2,754
Factored Design Load (kips)	920
C/D Ratio for LRFD $\Phi = 0.6$	2.99
Design Requirement Inspection	<b>Passed</b>

Unconfined Compressive Strength Above Threshold, $q_u$ (psi)	
$q_u$ Threshold (psi)	88
Mean	196
Median	133
Standard Deviation	293
Coefficient of Variation (CV)	1.50
Maximum	6,625
Minimum	88
Number of Data Points	3,118

Pile Installation Summary	
Drilling Time (min)	26.1
ReDrill Time (min)	0.5
Idle Rotation Time (min)	1.6
Idle Time (min)	3.8
Withdrawal Time (min)	0.2
Penetration w/o Rotation Time (min)	0.1
Total Time (min)	32.3
Drilling Efficiency (%)	81%

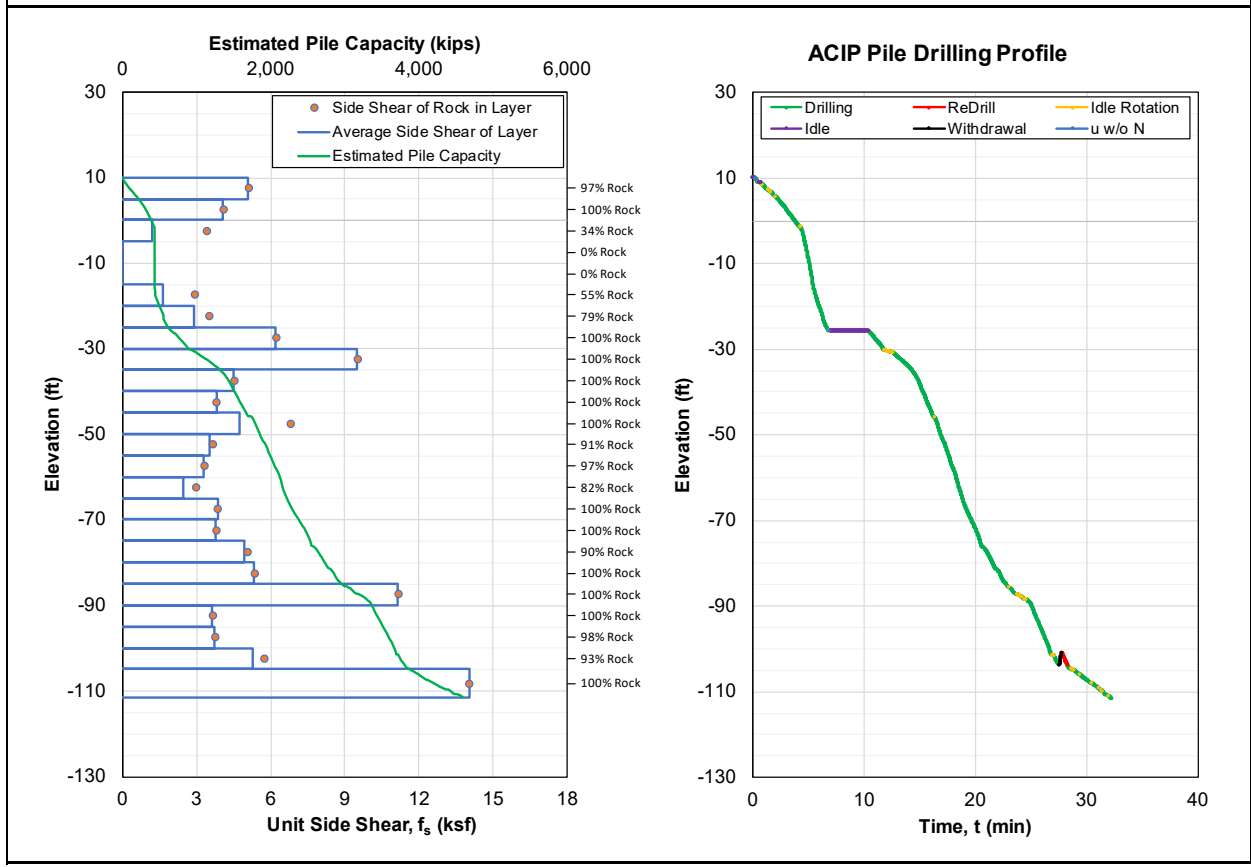


Figure A-17. ACIP pile capacity QA/QC report for Group C-1 Pile 1.

Project	Location	Engineer	Pile ID
I-395	Miami, Florida	Rodgers, McVay, Kelch	C1-2
Station	Offset (ft)	Drill Rig	Drill Bit Diameter (in)
100+00.01	10.00	Drill Rig A	30
Top of Pile Elevation (ft)	Bottom of Pile Elevation (ft)	Depth Increment Analyzed (cm)	ISO-MWD Assessment
10.81	-110.65	1	Class 1

Specific Energy Above Threshold, e (psi)	
Specific Energy Threshold (psi)	1,250
Mean	3,021
Median	2,095
Standard Deviation	3,469
Coefficient of Variation (CV)	1.15
Maximum	67,331
Minimum	1,251
Number of Data Points	2,713

ACIP Pile Capacity QA/QC	
Pile Length (ft)	121.46
Total Rock Socket Length (ft)	89.0
Average Pile Side Shear, $f_s$ (ksf)	4.13
Unfactored Pile Capacity (kips)	3,943
Factored Pile Capacity (kips)	2,366
Factored Design Load (kips)	920
C/D Ratio for LRFD $\Phi = 0.6$	2.57
Design Requirement Inspection	<b>Passed</b>

Unconfined Compressive Strength Above Threshold, $q_u$ (psi)	
$q_u$ Threshold (psi)	88
Mean	191
Median	143
Standard Deviation	159
Coefficient of Variation (CV)	0.84
Maximum	2,322
Minimum	88
Number of Data Points	2,713

Pile Installation Summary	
Drilling Time (min)	24.3
ReDrill Time (min)	0.1
Idle Rotation Time (min)	1.1
Idle Time (min)	1.3
Withdrawal Time (min)	0.0
Penetration w/o Rotation Time (min)	0.1
Total Time (min)	26.9
Drilling Efficiency (%)	91%

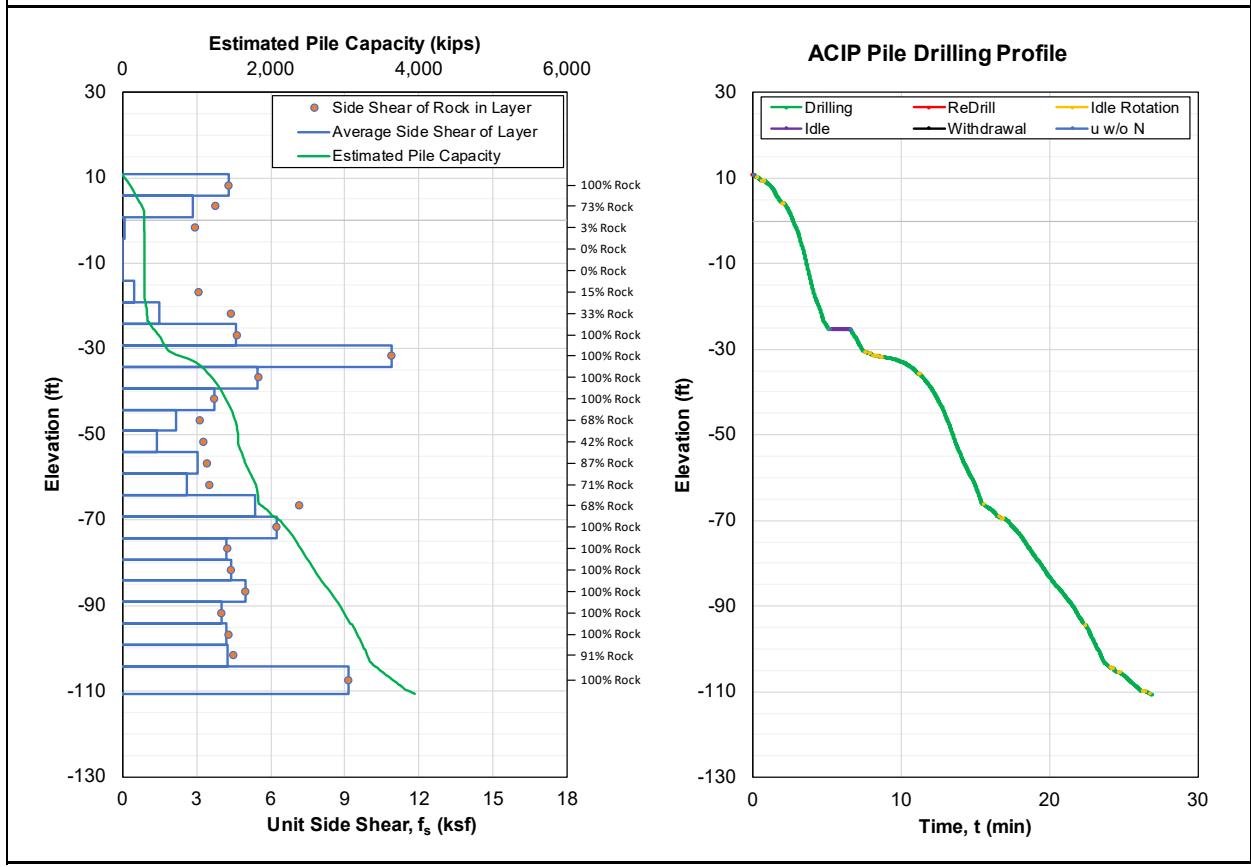


Figure A-18. ACIP pile capacity QA/QC report for Group C-1 Pile 2.

Project	Location	Engineer	Pile ID
I-395	Miami, Florida	Rodgers, McVay, Kelch	C1-3
Station	Offset (ft)	Drill Rig	Drill Bit Diameter (in)
100+00.01	10.00	Drill Rig A	30
Top of Pile Elevation (ft)	Bottom of Pile Elevation (ft)	Depth Increment Analyzed (cm)	ISO-MWD Assessment
10.74	-110.75	1	Class 1

Specific Energy Above Threshold, e (psi)	
Specific Energy Threshold (psi)	1,250
Mean	3,718
Median	2,362
Standard Deviation	5,535
Coefficient of Variation (CV)	1.49
Maximum	114,248
Minimum	1,251
Number of Data Points	2,486

Unconfined Compressive Strength Above Threshold, q <sub>u</sub> (psi)	
q <sub>u</sub> Threshold (psi)	88
Mean	225
Median	160
Standard Deviation	216
Coefficient of Variation (CV)	0.96
Maximum	3,251
Minimum	88
Number of Data Points	2,486

ACIP Pile Capacity QA/QC	
Pile Length (ft)	121.49
Total Rock Socket Length (ft)	81.6
Average Pile Side Shear, f <sub>s</sub> (ksf)	4.38
Unfactored Pile Capacity (kips)	4,178
Factored Pile Capacity (kips)	2,507
Factored Design Load (kips)	920
C/D Ratio for LRFD $\Phi = 0.6$	2.72
Design Requirement Inspection	<b>Passed</b>

Pile Installation Summary	
Drilling Time (min)	27.4
ReDrill Time (min)	0.0
Idle Rotation Time (min)	5.4
Idle Time (min)	1.1
Withdrawal Time (min)	3.2
Penetration w/o Rotation Time (min)	0.1
Total Time (min)	37.2
Drilling Efficiency (%)	74%

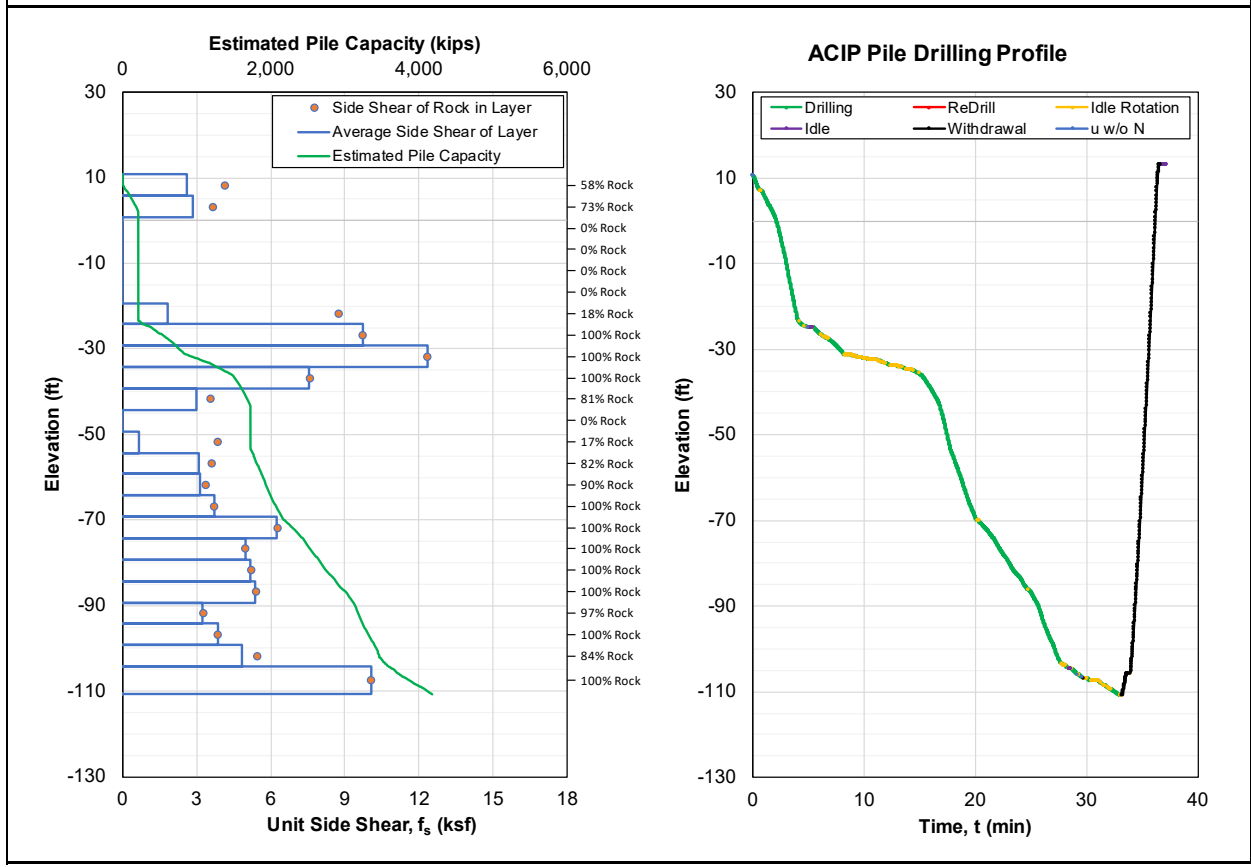


Figure A-19. ACIP pile capacity QA/QC report for Group C-1 Pile 3.

Project	Location	Engineer	Pile ID
I-395	Miami, Florida	Rodgers, McVay, Kelch	C1-4
Station	Offset (ft)	Drill Rig	Drill Bit Diameter (in)
100+00.01	10.00	Drill Rig A	30
Top of Pile Elevation (ft)	Bottom of Pile Elevation (ft)	Depth Increment Analyzed (cm)	ISO-MWD Assessment
10.74	-110.72	1	Class 1

Specific Energy Above Threshold, e (psi)	
Specific Energy Threshold (psi)	1,250
Mean	3,598
Median	1,970
Standard Deviation	7,561
Coefficient of Variation (CV)	2.10
Maximum	180,071
Minimum	1,251
Number of Data Points	2,997

Unconfined Compressive Strength Above Threshold, q <sub>u</sub> (psi)	
q <sub>u</sub> Threshold (psi)	88
Mean	210
Median	135
Standard Deviation	254
Coefficient of Variation (CV)	1.21
Maximum	4,289
Minimum	88
Number of Data Points	2,997

ACIP Pile Capacity QA/QC	
Pile Length (ft)	121.46
Total Rock Socket Length (ft)	98.3
Average Pile Side Shear, f <sub>s</sub> (ksf)	4.94
Unfactored Pile Capacity (kips)	4,710
Factored Pile Capacity (kips)	2,826
Factored Design Load (kips)	920
C/D Ratio for LRFD $\Phi = 0.6$	3.07
Design Requirement Inspection	<b>Passed</b>

Pile Installation Summary	
Drilling Time (min)	27.3
ReDrill Time (min)	0.3
Idle Rotation Time (min)	14.4
Idle Time (min)	37.2
Withdrawal Time (min)	0.8
Penetration w/o Rotation Time (min)	0.0
Total Time (min)	80.0
Drilling Efficiency (%)	34%

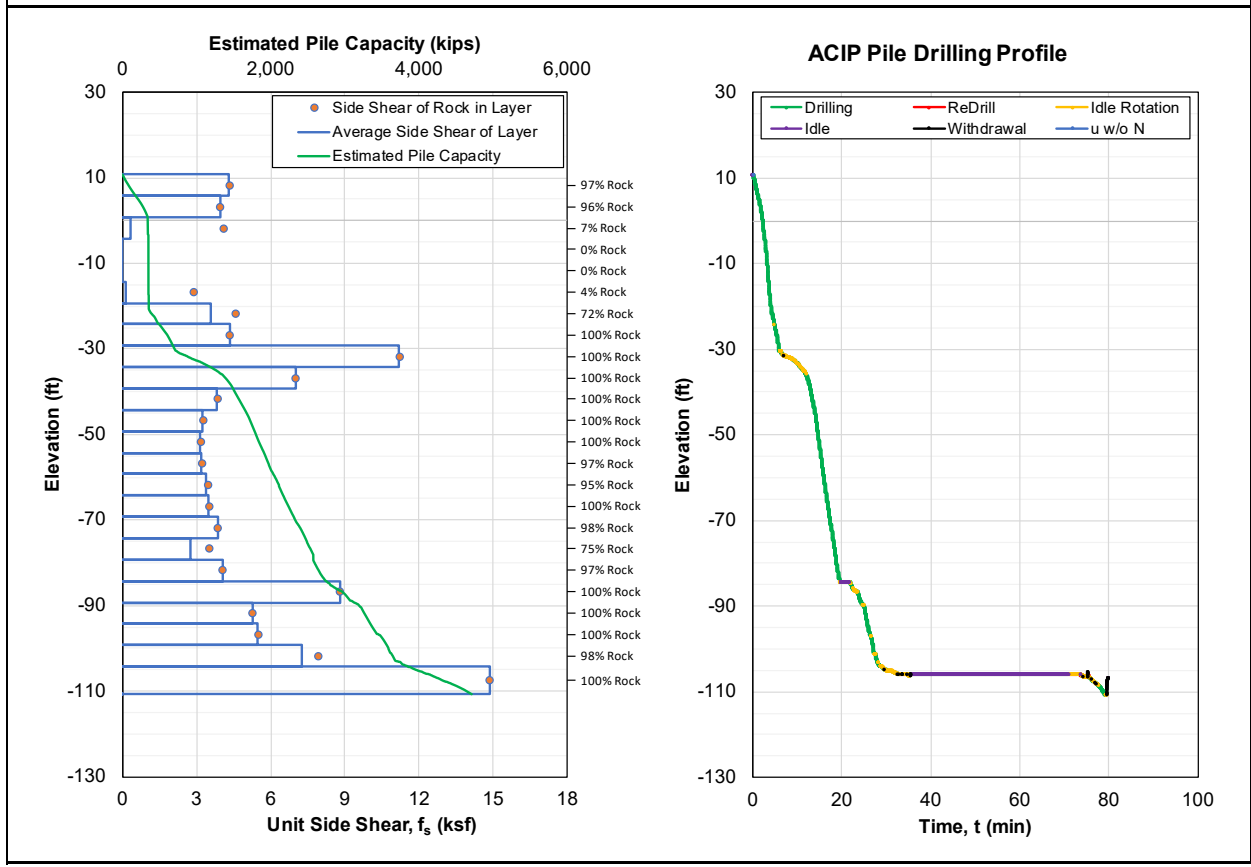


Figure A-20. ACIP pile capacity QA/QC report for Group C-1 Pile 4.

Project	Location	Engineer	Pile ID
I-395	Miami, Florida	Rodgers, McVay, Kelch	C1-5
Station	Offset (ft)	Drill Rig	Drill Bit Diameter (in)
100+00.01	10.00	Drill Rig A	30
Top of Pile Elevation (ft)	Bottom of Pile Elevation (ft)	Depth Increment Analyzed (cm)	ISO-MWD Assessment
10.29	-111.20	1	Class 1

Specific Energy Above Threshold, e (psi)	
Specific Energy Threshold (psi)	1,250
Mean	2,845
Median	1,907
Standard Deviation	5,723
Coefficient of Variation (CV)	2.01
Maximum	182,028
Minimum	1,253
Number of Data Points	2,618

ACIP Pile Capacity QA/QC	
Pile Length (ft)	121.49
Total Rock Socket Length (ft)	85.9
Average Pile Side Shear, $f_s$ (ksf)	3.73
Unfactored Pile Capacity (kips)	3,560
Factored Pile Capacity (kips)	2,136
Factored Design Load (kips)	920
C/D Ratio for LRFD $\Phi = 0.6$	2.32
Design Requirement Inspection	<b>Passed</b>

Unconfined Compressive Strength Above Threshold, $q_u$ (psi)	
$q_u$ Threshold (psi)	88
Mean	178
Median	131
Standard Deviation	177
Coefficient of Variation (CV)	1.00
Maximum	4,317
Minimum	88
Number of Data Points	2,618

Pile Installation Summary	
Drilling Time (min)	21.2
ReDrill Time (min)	6.9
Idle Rotation Time (min)	0.8
Idle Time (min)	15.8
Withdrawal Time (min)	0.0
Penetration w/o Rotation Time (min)	0.1
Total Time (min)	44.7
Drilling Efficiency (%)	47%

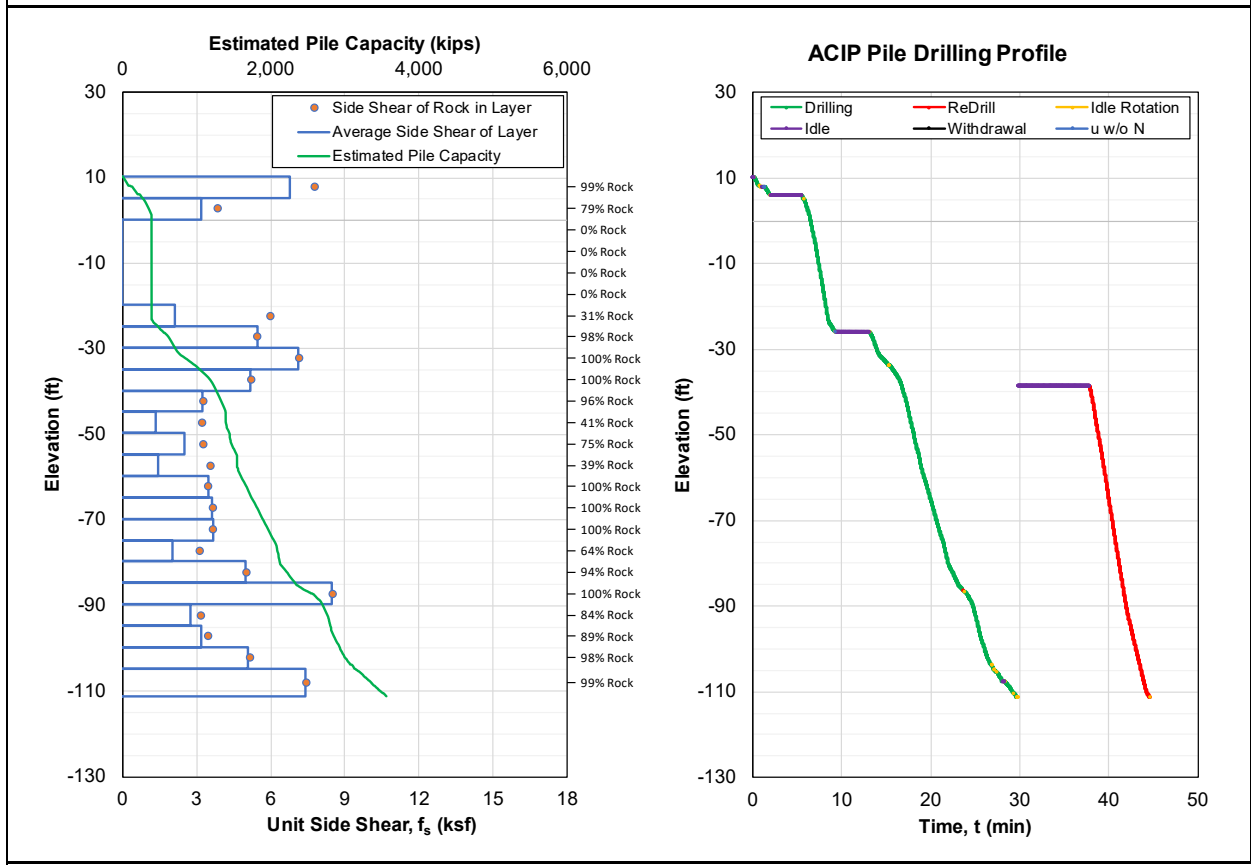


Figure A-21. ACIP pile capacity QA/QC report for Group C-1 Pile 5.



Project	Location	Engineer	Pile ID
I-395	Miami, Florida	Rodgers, McVay, Kelch	C1-6
Station	Offset (ft)	Drill Rig	Drill Bit Diameter (in)
100+00.01	10.00	Drill Rig A	30
Top of Pile Elevation (ft)	Bottom of Pile Elevation (ft)	Depth Increment Analyzed (cm)	ISO-MWD Assessment
10.94	-110.52	1	Class 1

Specific Energy Above Threshold, e (psi)	
Specific Energy Threshold (psi)	1,250
Mean	3,318
Median	1,955
Standard Deviation	6,775
Coefficient of Variation (CV)	2.04
Maximum	198,152
Minimum	1,251
Number of Data Points	2,768

ACIP Pile Capacity QA/QC	
Pile Length (ft)	121.46
Total Rock Socket Length (ft)	90.8
Average Pile Side Shear, $f_s$ (ksf)	4.34
Unfactored Pile Capacity (kips)	4,137
Factored Pile Capacity (kips)	2,482
Factored Design Load (kips)	920
C/D Ratio for LRFD $\Phi = 0.6$	2.70
Design Requirement Inspection	<b>Passed</b>

Unconfined Compressive Strength Above Threshold, $q_u$ (psi)	
$q_u$ Threshold (psi)	88
Mean	198
Median	134
Standard Deviation	228
Coefficient of Variation (CV)	1.15
Maximum	4,540
Minimum	88
Number of Data Points	2,768

Pile Installation Summary	
Drilling Time (min)	23.5
ReDrill Time (min)	0.2
Idle Rotation Time (min)	1.5
Idle Time (min)	0.0
Withdrawal Time (min)	0.1
Penetration w/o Rotation Time (min)	0.0
Total Time (min)	25.3
Drilling Efficiency (%)	93%

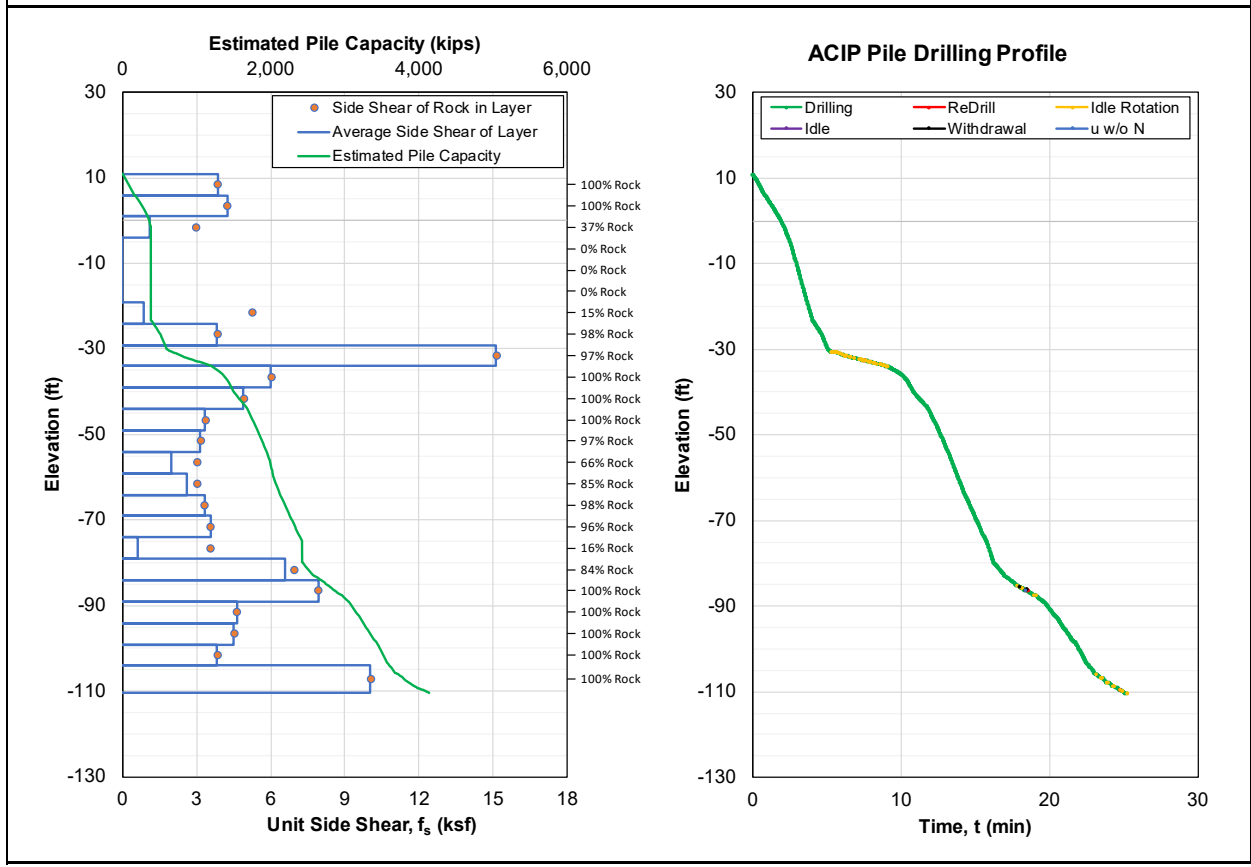


Figure A-22. ACIP pile capacity QA/QC report for Group C-1 Pile 6.

Project	Location	Engineer	Pile ID
I-395	Miami, Florida	Rodgers, McVay, Kelch	C1-7
Station	Offset (ft)	Drill Rig	Drill Bit Diameter (in)
100+00.01	10.00	Drill Rig A	30
Top of Pile Elevation (ft)	Bottom of Pile Elevation (ft)	Depth Increment Analyzed (cm)	ISO-MWD Assessment
10.46	-111.00	1	Class 1

Specific Energy Above Threshold, e (psi)	
Specific Energy Threshold (psi)	1,250
Mean	2,755
Median	2,078
Standard Deviation	4,851
Coefficient of Variation (CV)	1.76
Maximum	171,051
Minimum	1,251
Number of Data Points	3,025

ACIP Pile Capacity QA/QC	
Pile Length (ft)	121.46
Total Rock Socket Length (ft)	99.2
Average Pile Side Shear, $f_s$ (ksf)	4.23
Unfactored Pile Capacity (kips)	4,031
Factored Pile Capacity (kips)	2,419
Factored Design Load (kips)	920
C/D Ratio for LRFD $\Phi = 0.6$	2.63
Design Requirement Inspection	<b>Passed</b>

Unconfined Compressive Strength Above Threshold, $q_u$ (psi)	
$q_u$ Threshold (psi)	88
Mean	173
Median	142
Standard Deviation	167
Coefficient of Variation (CV)	0.96
Maximum	4,159
Minimum	88
Number of Data Points	3,025

Pile Installation Summary	
Drilling Time (min)	23.0
ReDrill Time (min)	0.1
Idle Rotation Time (min)	1.4
Idle Time (min)	1.0
Withdrawal Time (min)	0.1
Penetration w/o Rotation Time (min)	0.0
Total Time (min)	25.5
Drilling Efficiency (%)	90%

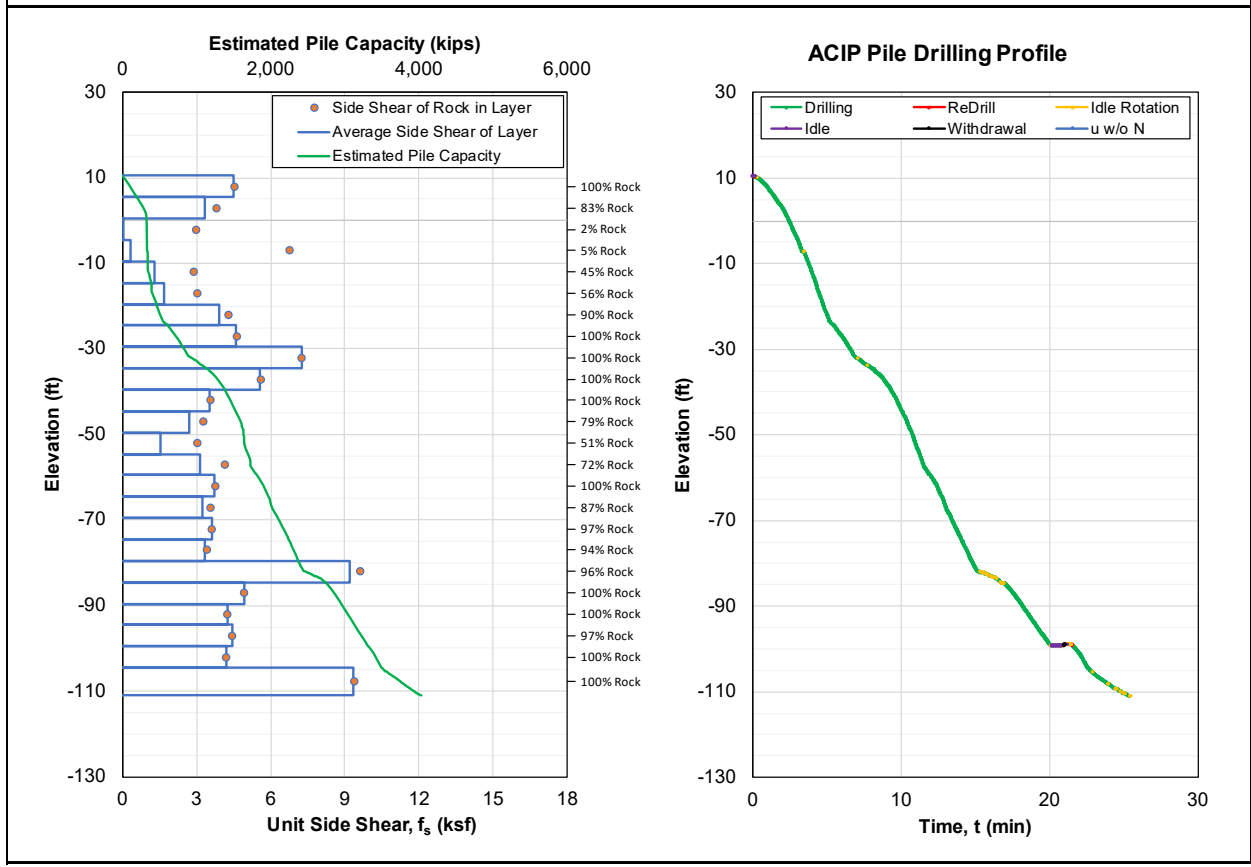


Figure A-23. ACIP pile capacity QA/QC report for Group C-1 Pile 7.

Project	Location	Engineer	Pile ID
I-395	Miami, Florida	Rodgers, McVay, Kelch	C1-8
Station	Offset (ft)	Drill Rig	Drill Bit Diameter (in)
100+00.01	10.00	Drill Rig A	30
Top of Pile Elevation (ft)	Bottom of Pile Elevation (ft)	Depth Increment Analyzed (cm)	ISO-MWD Assessment
10.68	-110.84	1	Class 1

Specific Energy Above Threshold, e (psi)	
Specific Energy Threshold (psi)	1,250
Mean	3,001
Median	2,013
Standard Deviation	5,542
Coefficient of Variation (CV)	1.85
Maximum	175,526
Minimum	1,251
Number of Data Points	2,416

Unconfined Compressive Strength Above Threshold, q <sub>u</sub> (psi)	
q <sub>u</sub> Threshold (psi)	88
Mean	185
Median	138
Standard Deviation	190
Coefficient of Variation (CV)	1.03
Maximum	4,224
Minimum	88
Number of Data Points	2,416

ACIP Pile Capacity QA/QC	
Pile Length (ft)	121.52
Total Rock Socket Length (ft)	79.3
Average Pile Side Shear, f <sub>s</sub> (ksf)	3.57
Unfactored Pile Capacity (kips)	3,408
Factored Pile Capacity (kips)	2,045
Factored Design Load (kips)	920
C/D Ratio for LRFD $\Phi = 0.6$	2.22
Design Requirement Inspection	<b>Passed</b>

Pile Installation Summary	
Drilling Time (min)	25.9
ReDrill Time (min)	0.0
Idle Rotation Time (min)	2.7
Idle Time (min)	0.5
Withdrawal Time (min)	0.0
Penetration w/o Rotation Time (min)	0.0
Total Time (min)	29.1
Drilling Efficiency (%)	89%

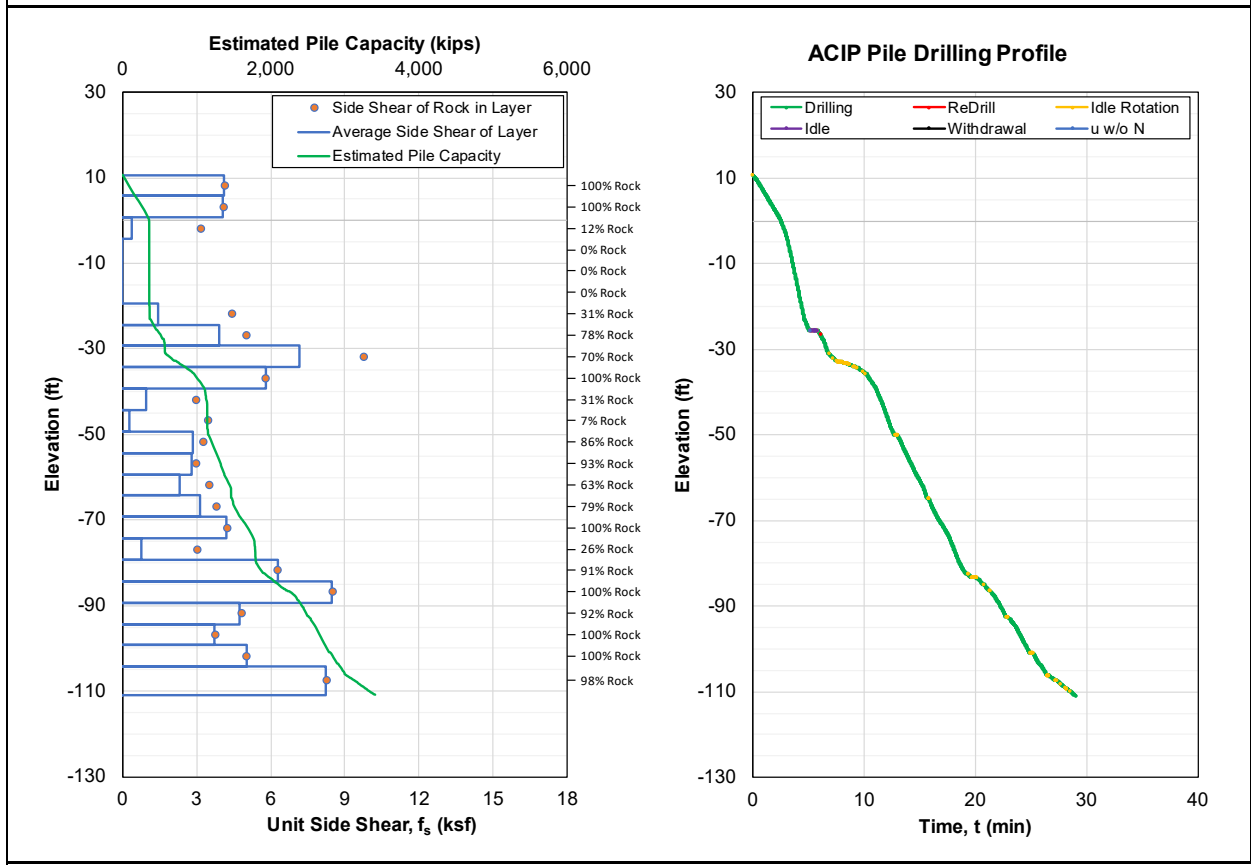


Figure A-24. ACIP pile capacity QA/QC report for Group C-1 Pile 8.

Project	Location	Engineer	Pile ID
I-395	Miami, Florida	Rodgers, McVay, Kelch	C1-9
Station	Offset (ft)	Drill Rig	Drill Bit Diameter (in)
100+00.01	10.00	Drill Rig A	30
Top of Pile Elevation (ft)	Bottom of Pile Elevation (ft)	Depth Increment Analyzed (cm)	ISO-MWD Assessment
10.86	-110.63	1	Class 1

Specific Energy Above Threshold, e (psi)	
Specific Energy Threshold (psi)	1,250
Mean	3,664
Median	2,222
Standard Deviation	9,971
Coefficient of Variation (CV)	2.72
Maximum	364,544
Minimum	1,252
Number of Data Points	2,485

ACIP Pile Capacity QA/QC	
Pile Length (ft)	121.49
Total Rock Socket Length (ft)	81.5
Average Pile Side Shear, $f_s$ (ksf)	4.16
Unfactored Pile Capacity (kips)	3,974
Factored Pile Capacity (kips)	2,384
Factored Design Load (kips)	920
C/D Ratio for LRFD $\Phi = 0.6$	2.59
Design Requirement Inspection	<b>Passed</b>

Unconfined Compressive Strength Above Threshold, $q_u$ (psi)	
$q_u$ Threshold (psi)	88
Mean	214
Median	151
Standard Deviation	258
Coefficient of Variation (CV)	1.21
Maximum	6,467
Minimum	88
Number of Data Points	2,485

Pile Installation Summary	
Drilling Time (min)	24.9
ReDrill Time (min)	0.1
Idle Rotation Time (min)	2.2
Idle Time (min)	0.3
Withdrawal Time (min)	0.2
Penetration w/o Rotation Time (min)	0.0
Total Time (min)	27.7
Drilling Efficiency (%)	90%

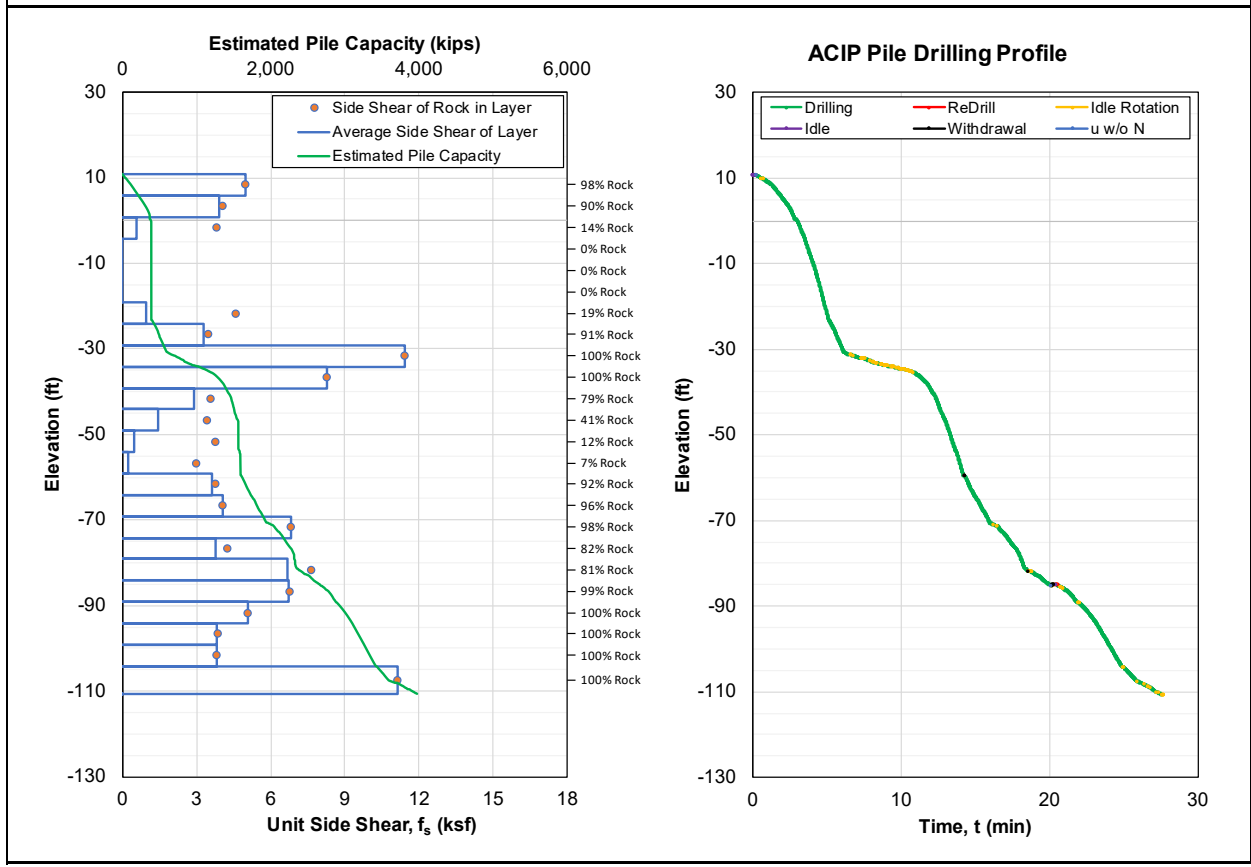


Figure A-25. ACIP pile capacity QA/QC report for Group C-1 Pile 9.

Project	Location	Engineer	Pile ID
I-395	Miami, Florida	Rodgers, McVay, Kelch	C1-10
Station	Offset (ft)	Drill Rig	Drill Bit Diameter (in)
100+00.01	10.00	Drill Rig A	30
Top of Pile Elevation (ft)	Bottom of Pile Elevation (ft)	Depth Increment Analyzed (cm)	ISO-MWD Assessment
11.01	-110.48	1	Class 1

Specific Energy Above Threshold, e (psi)	
Specific Energy Threshold (psi)	1,250
Mean	3,131
Median	1,931
Standard Deviation	5,092
Coefficient of Variation (CV)	1.63
Maximum	124,766
Minimum	1,250
Number of Data Points	2,502

ACIP Pile Capacity QA/QC	
Pile Length (ft)	121.49
Total Rock Socket Length (ft)	82.1
Average Pile Side Shear, $f_s$ (ksf)	3.83
Unfactored Pile Capacity (kips)	3,652
Factored Pile Capacity (kips)	2,191
Factored Design Load (kips)	920
C/D Ratio for LRFD $\Phi = 0.6$	2.38
Design Requirement Inspection	<b>Passed</b>

Unconfined Compressive Strength Above Threshold, $q_u$ (psi)	
$q_u$ Threshold (psi)	88
Mean	193
Median	133
Standard Deviation	194
Coefficient of Variation (CV)	1.01
Maximum	3,433
Minimum	88
Number of Data Points	2,502

Pile Installation Summary	
Drilling Time (min)	21.8
ReDrill Time (min)	0.0
Idle Rotation Time (min)	0.7
Idle Time (min)	0.3
Withdrawal Time (min)	0.0
Penetration w/o Rotation Time (min)	0.0
Total Time (min)	22.8
Drilling Efficiency (%)	96%

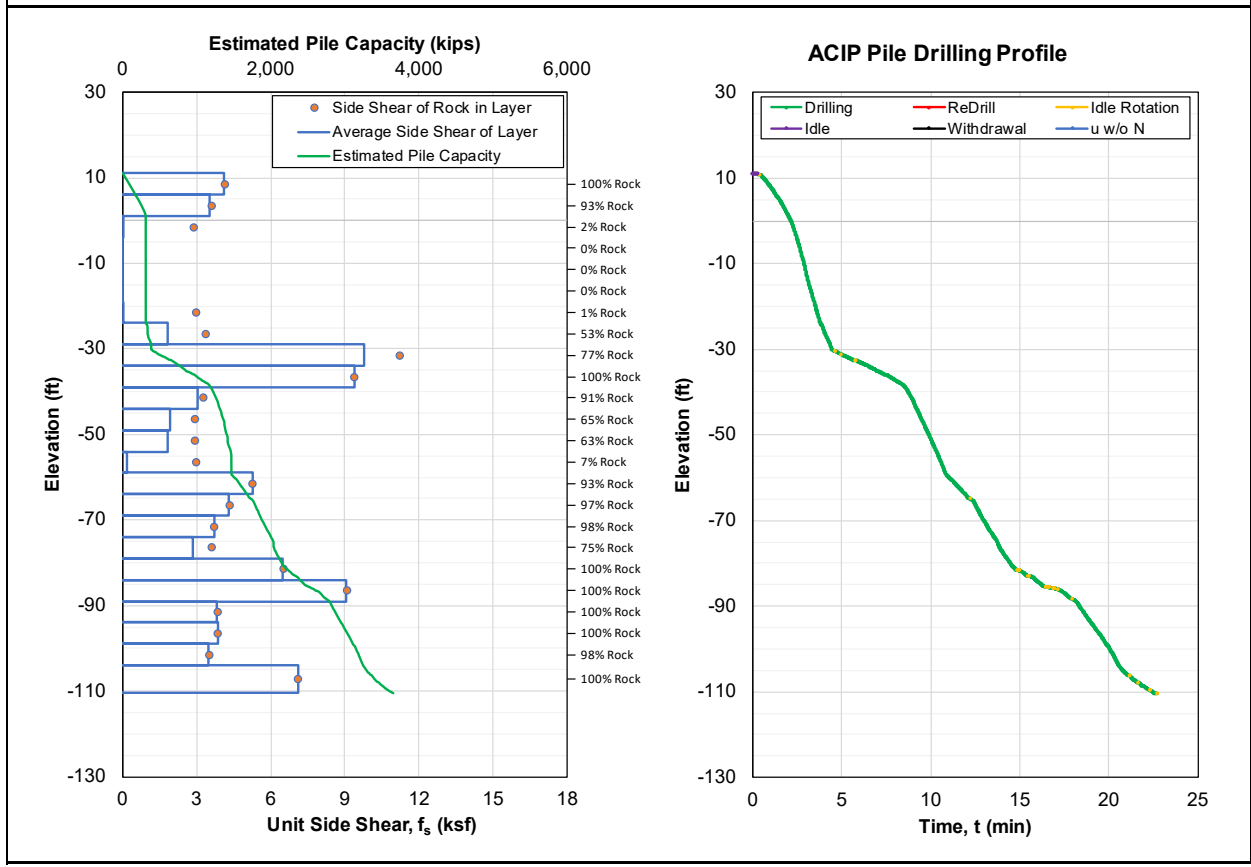


Figure A-26. ACIP pile capacity QA/QC report for Group C-1 Pile 10.

Project	Location	Engineer	Pile ID
I-395	Miami, Florida	Rodgers, McVay, Kelch	C2-1
Station	Offset (ft)	Drill Rig	Drill Bit Diameter (in)
100+00.01	10.00	Drill Rig A	30
Top of Pile Elevation (ft)	Bottom of Pile Elevation (ft)	Depth Increment Analyzed (cm)	ISO-MWD Assessment
10.52	-100.96	1	Class 1

Specific Energy Above Threshold, e (psi)	
Specific Energy Threshold (psi)	1,250
Mean	3,142
Median	1,758
Standard Deviation	6,454
Coefficient of Variation (CV)	2.05
Maximum	189,920
Minimum	1,256
Number of Data Points	2,480

ACIP Pile Capacity QA/QC	
Pile Length (ft)	111.48
Total Rock Socket Length (ft)	81.4
Average Pile Side Shear, $f_s$ (ksf)	4.09
Unfactored Pile Capacity (kips)	3,583
Factored Pile Capacity (kips)	2,150
Factored Design Load (kips)	980
C/D Ratio for LRFD $\Phi = 0.6$	2.19
Design Requirement Inspection	<b>Passed</b>

Unconfined Compressive Strength Above Threshold, $q_u$ (psi)	
$q_u$ Threshold (psi)	88
Mean	191
Median	121
Standard Deviation	210
Coefficient of Variation (CV)	1.10
Maximum	4,427
Minimum	88
Number of Data Points	2,480

Pile Installation Summary	
Drilling Time (min)	21.1
ReDrill Time (min)	0.1
Idle Rotation Time (min)	2.2
Idle Time (min)	0.1
Withdrawal Time (min)	0.0
Penetration w/o Rotation Time (min)	0.0
Total Time (min)	23.4
Drilling Efficiency (%)	90%

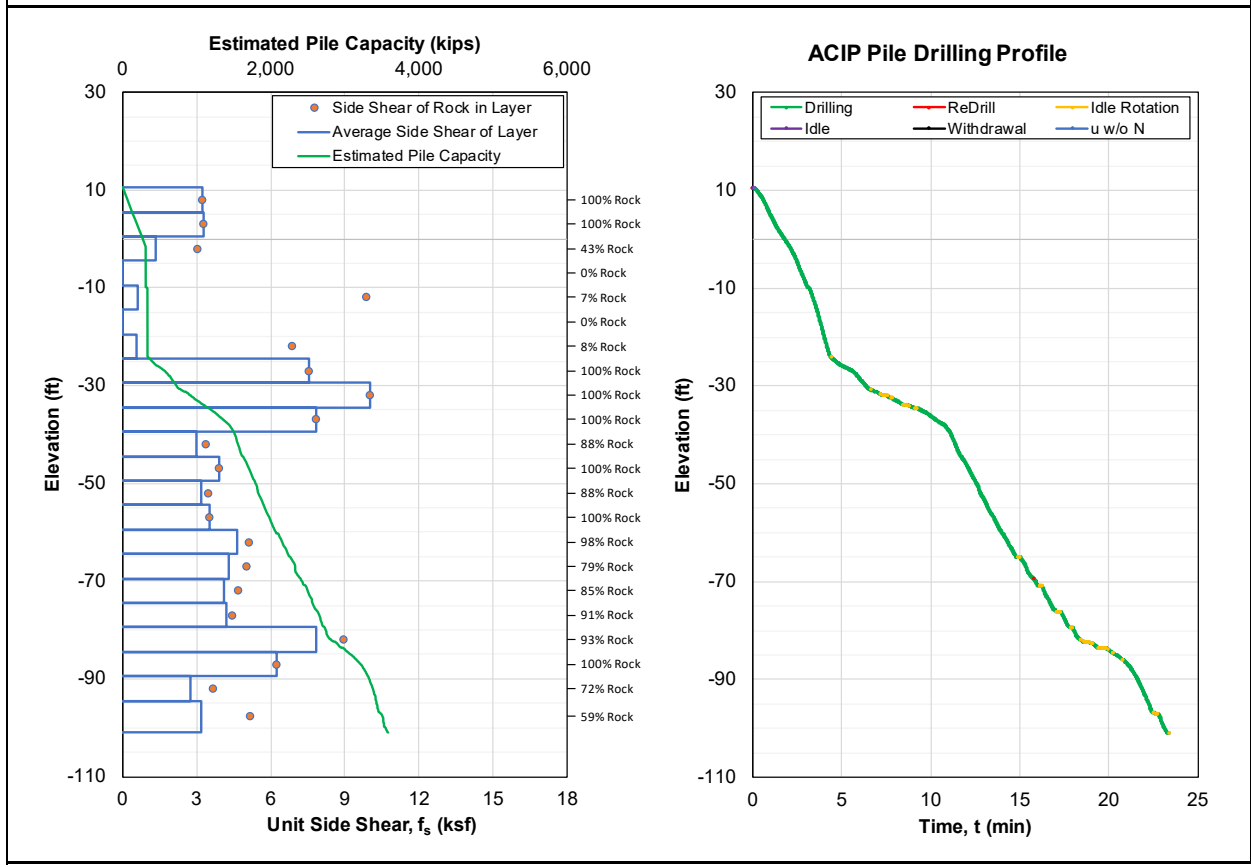


Figure A-27. ACIP pile capacity QA/QC report for Group C-2 Pile 1.

Project	Location	Engineer	Pile ID
I-395	Miami, Florida	Rodgers, McVay, Kelch	C2-2
Station	Offset (ft)	Drill Rig	Drill Bit Diameter (in)
100+00.01	10.00	Drill Rig A	30
Top of Pile Elevation (ft)	Bottom of Pile Elevation (ft)	Depth Increment Analyzed (cm)	ISO-MWD Assessment
10.54	-100.98	1	Class 1

Specific Energy Above Threshold, e (psi)	
Specific Energy Threshold (psi)	1,250
Mean	2,679
Median	1,802
Standard Deviation	3,413
Coefficient of Variation (CV)	1.27
Maximum	50,734
Minimum	1,251
Number of Data Points	1,902

Unconfined Compressive Strength Above Threshold, q <sub>u</sub> (psi)	
q <sub>u</sub> Threshold (psi)	88
Mean	170
Median	124
Standard Deviation	155
Coefficient of Variation (CV)	0.91
Maximum	1,923
Minimum	88
Number of Data Points	1,902

ACIP Pile Capacity QA/QC	
Pile Length (ft)	111.52
Total Rock Socket Length (ft)	62.4
Average Pile Side Shear, f <sub>s</sub> (ksf)	2.84
Unfactored Pile Capacity (kips)	2,486
Factored Pile Capacity (kips)	1,491
Factored Design Load (kips)	980
C/D Ratio for LRFD $\Phi = 0.6$	1.52
Design Requirement Inspection	<b>Passed</b>

Pile Installation Summary	
Drilling Time (min)	17.7
ReDrill Time (min)	0.0
Idle Rotation Time (min)	1.0
Idle Time (min)	0.4
Withdrawal Time (min)	0.0
Penetration w/o Rotation Time (min)	0.0
Total Time (min)	19.1
Drilling Efficiency (%)	93%

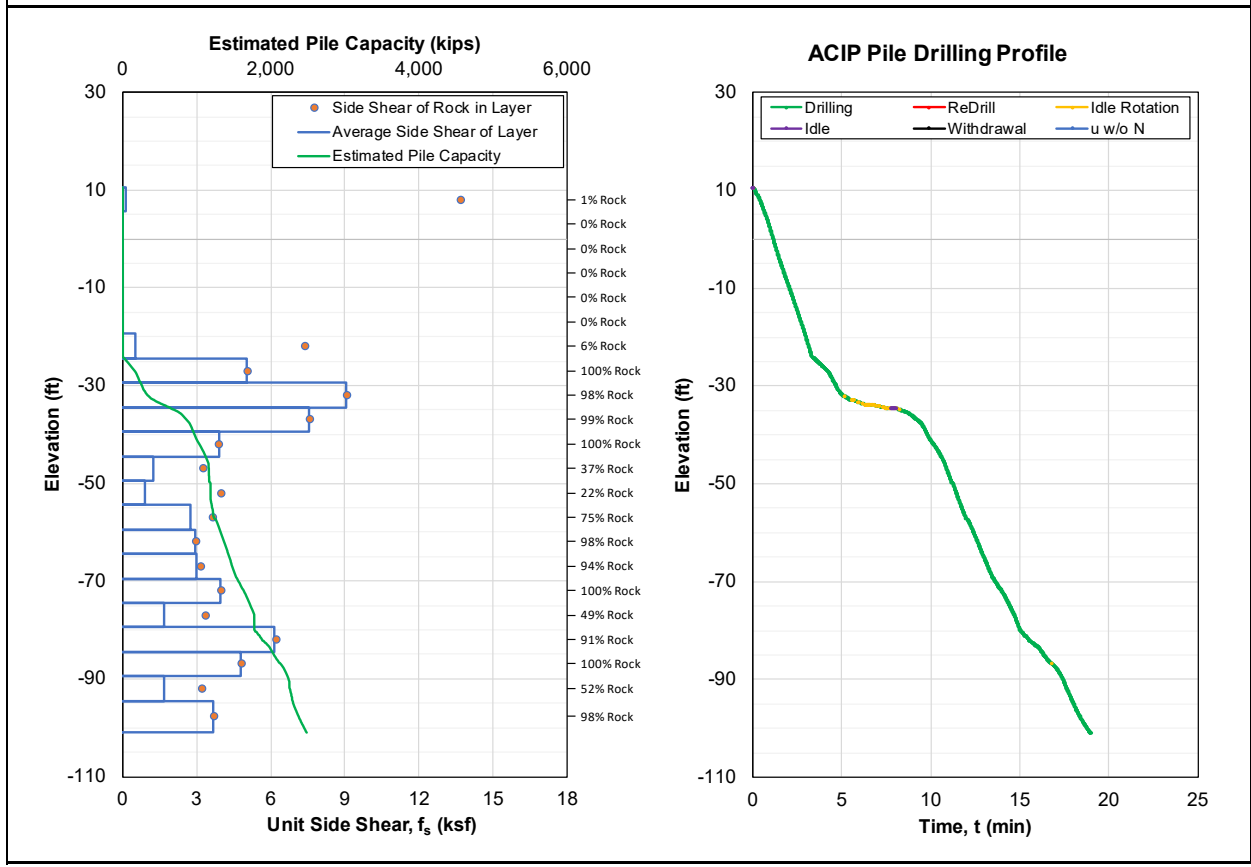


Figure A-28. ACIP pile capacity QA/QC report for Group C-2 Pile 2.

Project	Location	Engineer	Pile ID
I-395	Miami, Florida	Rodgers, McVay, Kelch	C2-3
Station	Offset (ft)	Drill Rig	Drill Bit Diameter (in)
100+00.01	10.00	Drill Rig A	30
Top of Pile Elevation (ft)	Bottom of Pile Elevation (ft)	Depth Increment Analyzed (cm)	ISO-MWD Assessment
10.63	-100.85	1	Class 1

Specific Energy Above Threshold, e (psi)	
Specific Energy Threshold (psi)	1,250
Mean	2,769
Median	1,941
Standard Deviation	3,703
Coefficient of Variation (CV)	1.34
Maximum	74,729
Minimum	1,252
Number of Data Points	3,048

Unconfined Compressive Strength Above Threshold, q <sub>u</sub> (psi)	
q <sub>u</sub> Threshold (psi)	88
Mean	175
Median	133
Standard Deviation	158
Coefficient of Variation (CV)	0.90
Maximum	2,484
Minimum	88
Number of Data Points	3,048

ACIP Pile Capacity QA/QC	
Pile Length (ft)	111.48
Total Rock Socket Length (ft)	100.0
Average Pile Side Shear, f <sub>s</sub> (ksf)	4.68
Unfactored Pile Capacity (kips)	4,100
Factored Pile Capacity (kips)	2,460
Factored Design Load (kips)	980
C/D Ratio for LRFD $\Phi = 0.6$	2.51
Design Requirement Inspection	<b>Passed</b>

Pile Installation Summary	
Drilling Time (min)	21.4
ReDrill Time (min)	1.6
Idle Rotation Time (min)	4.5
Idle Time (min)	80.4
Withdrawal Time (min)	0.7
Penetration w/o Rotation Time (min)	0.1
Total Time (min)	108.7
Drilling Efficiency (%)	20%

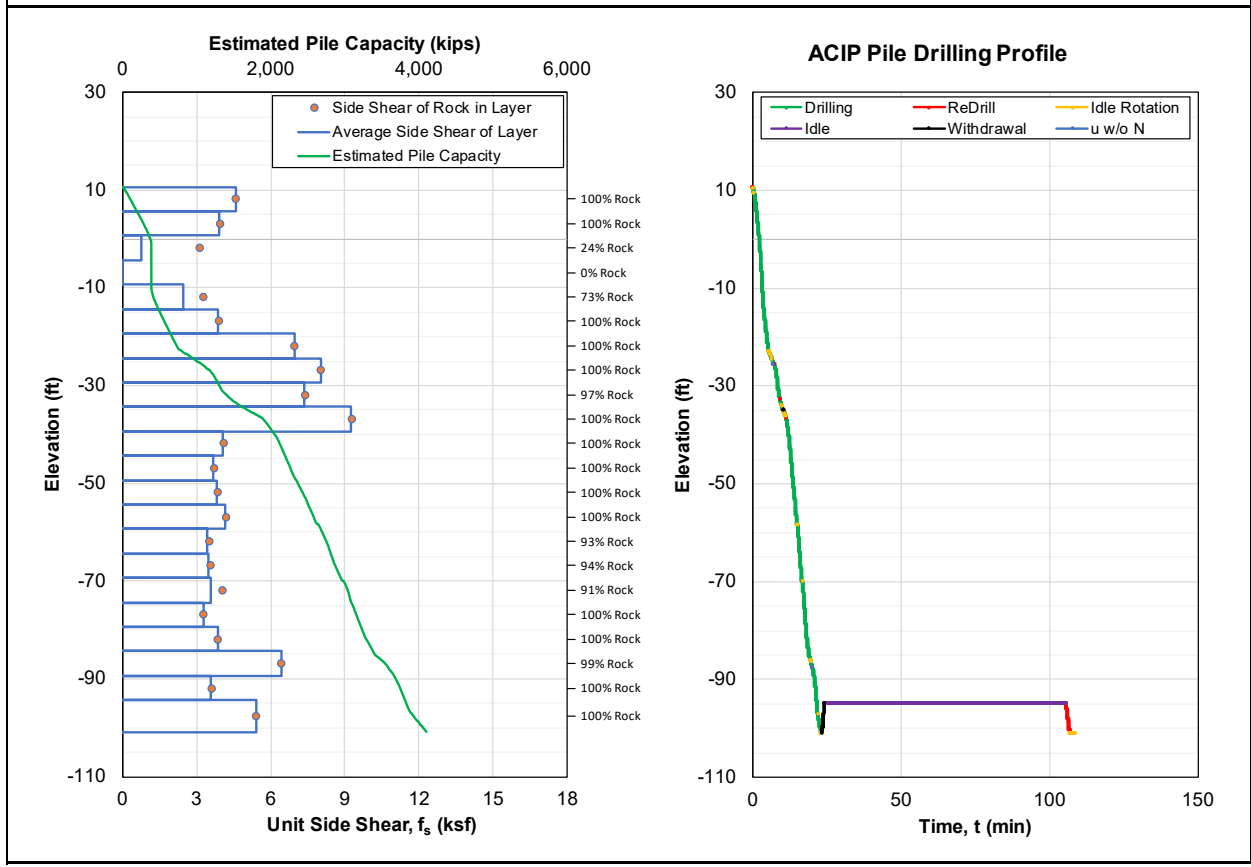


Figure A-29. ACIP pile capacity QA/QC report for Group C-2 Pile 3.



Project	Location	Engineer	Pile ID
I-395	Miami, Florida	Rodgers, McVay, Kelch	C2-4
Station	Offset (ft)	Drill Rig	Drill Bit Diameter (in)
100+00.01	10.00	Drill Rig A	30
Top of Pile Elevation (ft)	Bottom of Pile Elevation (ft)	Depth Increment Analyzed (cm)	ISO-MWD Assessment
10.66	-100.86	1	Class 1

Specific Energy Above Threshold, e (psi)	
Specific Energy Threshold (psi)	1,250
Mean	2,707
Median	1,862
Standard Deviation	3,700
Coefficient of Variation (CV)	1.37
Maximum	80,155
Minimum	1,252
Number of Data Points	2,474

Unconfined Compressive Strength Above Threshold, q <sub>u</sub> (psi)	
q <sub>u</sub> Threshold (psi)	88
Mean	172
Median	128
Standard Deviation	158
Coefficient of Variation (CV)	0.92
Maximum	2,599
Minimum	88
Number of Data Points	2,474

ACIP Pile Capacity QA/QC	
Pile Length (ft)	111.52
Total Rock Socket Length (ft)	81.2
Average Pile Side Shear, f <sub>s</sub> (ksf)	3.72
Unfactored Pile Capacity (kips)	3,260
Factored Pile Capacity (kips)	1,956
Factored Design Load (kips)	980
C/D Ratio for LRFD $\Phi = 0.6$	2.00
Design Requirement Inspection	<b>Passed</b>

Pile Installation Summary	
Drilling Time (min)	19.6
ReDrill Time (min)	0.0
Idle Rotation Time (min)	2.2
Idle Time (min)	0.1
Withdrawal Time (min)	0.0
Penetration w/o Rotation Time (min)	0.0
Total Time (min)	22.0
Drilling Efficiency (%)	89%

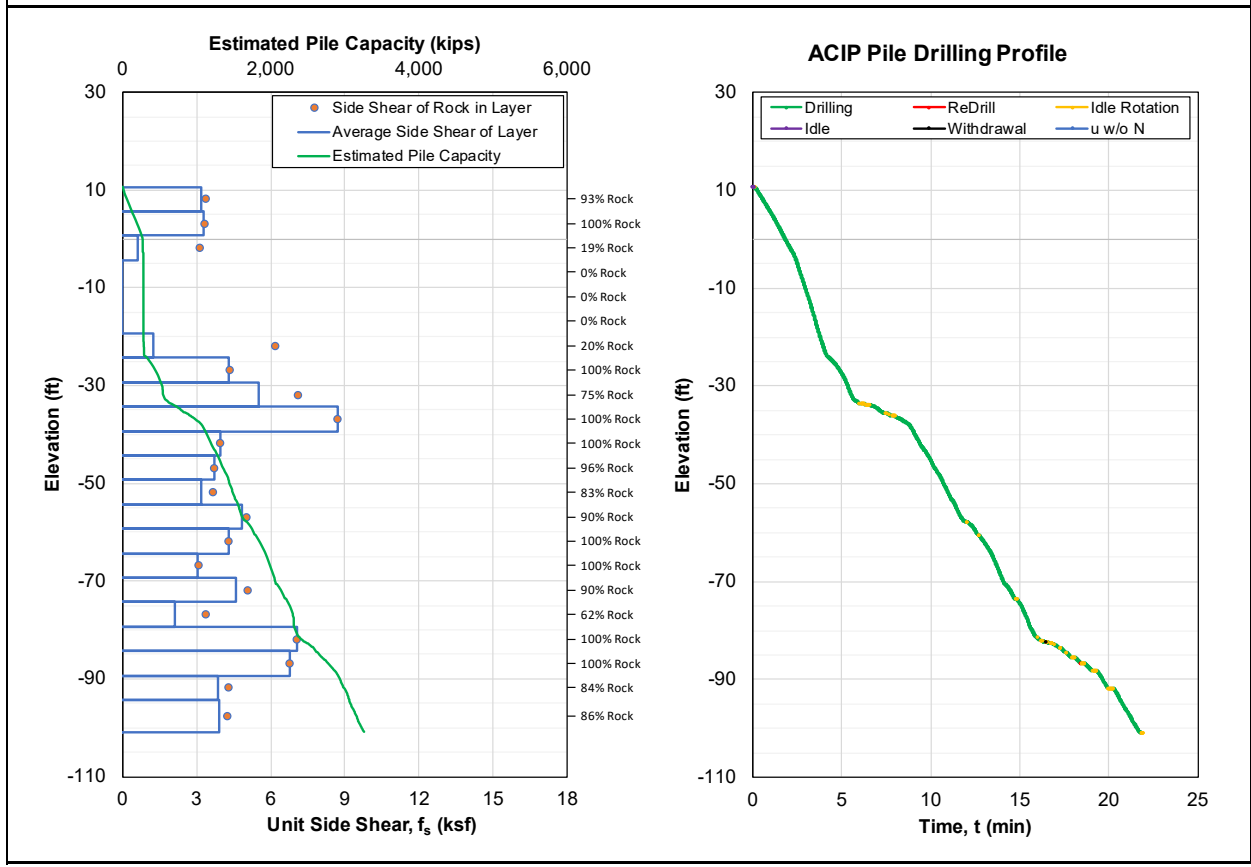


Figure A-30. ACIP pile capacity QA/QC report for Group C-2 Pile 4.

Project	Location	Engineer	Pile ID
I-395	Miami, Florida	Rodgers, McVay, Kelch	C2-5
Station	Offset (ft)	Drill Rig	Drill Bit Diameter (in)
100+00.01	10.00	Drill Rig A	30
Top of Pile Elevation (ft)	Bottom of Pile Elevation (ft)	Depth Increment Analyzed (cm)	ISO-MWD Assessment
10.85	-100.63	1	Class 1

Specific Energy Above Threshold, e (psi)	
Specific Energy Threshold (psi)	1,250
Mean	3,769
Median	2,136
Standard Deviation	7,152
Coefficient of Variation (CV)	1.90
Maximum	183,684
Minimum	1,253
Number of Data Points	2,565

ACIP Pile Capacity QA/QC	
Pile Length (ft)	111.48
Total Rock Socket Length (ft)	84.2
Average Pile Side Shear, $f_s$ (ksf)	4.87
Unfactored Pile Capacity (kips)	4,266
Factored Pile Capacity (kips)	2,559
Factored Design Load (kips)	980
C/D Ratio for LRFD $\Phi = 0.6$	2.61
Design Requirement Inspection	<b>Passed</b>

Unconfined Compressive Strength Above Threshold, $q_u$ (psi)	
$q_u$ Threshold (psi)	88
Mean	223
Median	146
Standard Deviation	243
Coefficient of Variation (CV)	1.09
Maximum	4,340
Minimum	88
Number of Data Points	2,565

Pile Installation Summary	
Drilling Time (min)	26.4
ReDrill Time (min)	0.1
Idle Rotation Time (min)	3.6
Idle Time (min)	0.1
Withdrawal Time (min)	0.0
Penetration w/o Rotation Time (min)	0.1
Total Time (min)	30.3
Drilling Efficiency (%)	87%

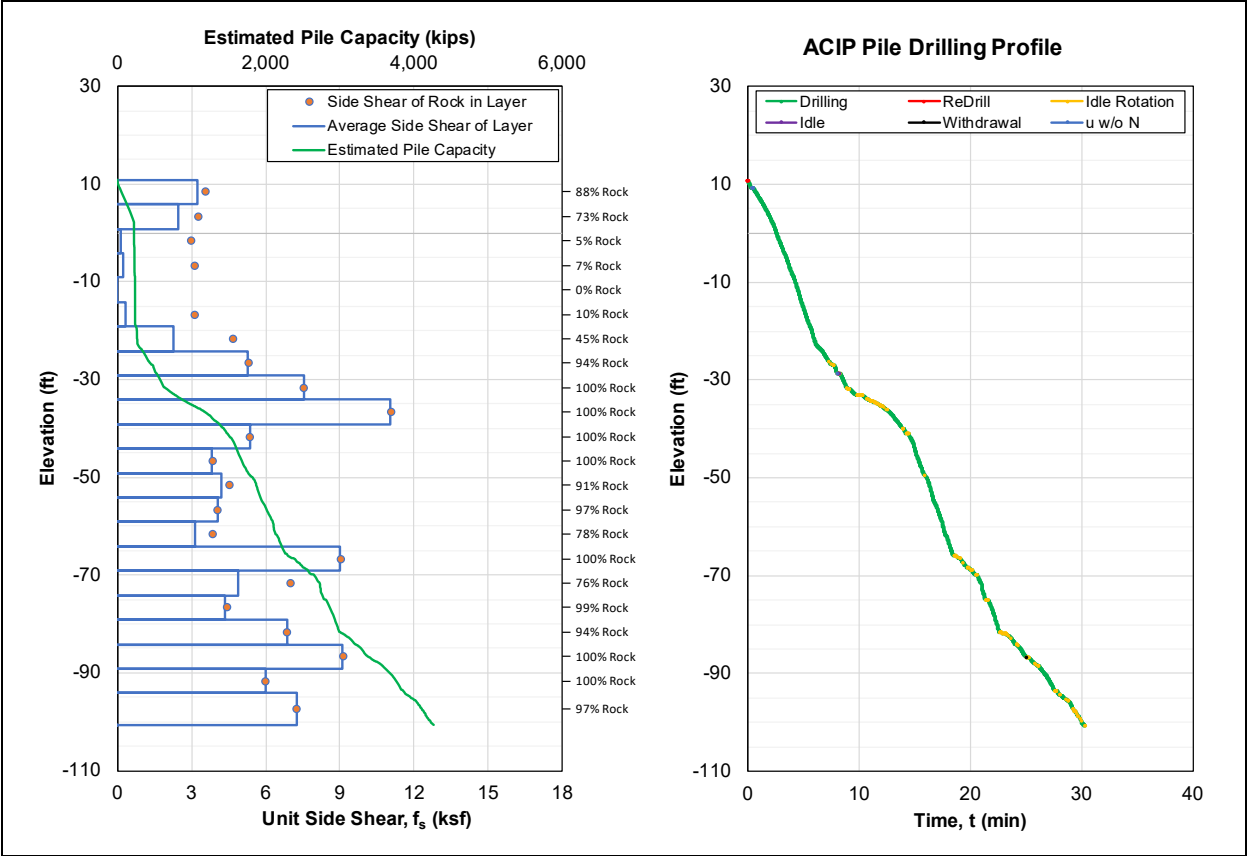


Figure A-31. ACIP pile capacity QA/QC report for Group C-2 Pile 5.

Project	Location	Engineer	Pile ID
I-395	Miami, Florida	Rodgers, McVay, Kelch	C2-6
Station	Offset (ft)	Drill Rig	Drill Bit Diameter (in)
100+00.01	10.00	Drill Rig A	30
Top of Pile Elevation (ft)	Bottom of Pile Elevation (ft)	Depth Increment Analyzed (cm)	ISO-MWD Assessment
11	-100.48	1	Class 1

Specific Energy Above Threshold, e (psi)	
Specific Energy Threshold (psi)	1,250
Mean	2,809
Median	1,754
Standard Deviation	8,330
Coefficient of Variation (CV)	2.97
Maximum	367,776
Minimum	1,251
Number of Data Points	2,319

Unconfined Compressive Strength Above Threshold, q <sub>u</sub> (psi)	
q <sub>u</sub> Threshold (psi)	88
Mean	171
Median	121
Standard Deviation	203
Coefficient of Variation (CV)	1.19
Maximum	6,500
Minimum	88
Number of Data Points	2,319

ACIP Pile Capacity QA/QC	
Pile Length (ft)	111.48
Total Rock Socket Length (ft)	76.1
Average Pile Side Shear, f <sub>s</sub> (ksf)	3.47
Unfactored Pile Capacity (kips)	3,038
Factored Pile Capacity (kips)	1,823
Factored Design Load (kips)	980
C/D Ratio for LRFD $\Phi = 0.6$	1.86
Design Requirement Inspection	<b>Passed</b>

Pile Installation Summary	
Drilling Time (min)	19.3
ReDrill Time (min)	0.0
Idle Rotation Time (min)	0.8
Idle Time (min)	0.1
Withdrawal Time (min)	0.0
Penetration w/o Rotation Time (min)	0.0
Total Time (min)	20.2
Drilling Efficiency (%)	96%

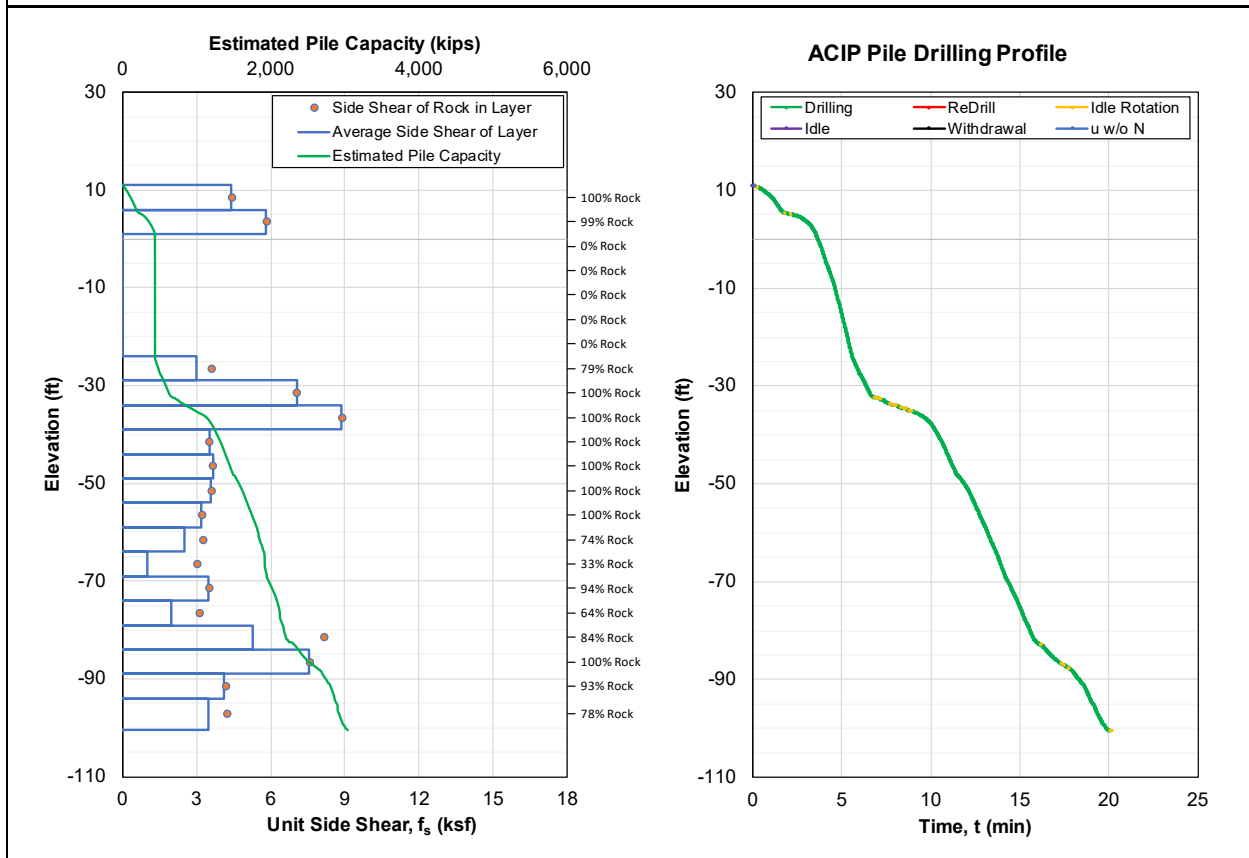


Figure A-32. ACIP pile capacity QA/QC report for Group C-2 Pile 6.

Project	Location	Engineer	Pile ID
I-395	Miami, Florida	Rodgers, McVay, Kelch	C2-7
Station	Offset (ft)	Drill Rig	Drill Bit Diameter (in)
100+00.01	10.00	Drill Rig A	30
Top of Pile Elevation (ft)	Bottom of Pile Elevation (ft)	Depth Increment Analyzed (cm)	ISO-MWD Assessment
10.84	-100.15	1	Class 1

Specific Energy Above Threshold, e (psi)	
Specific Energy Threshold (psi)	1,250
Mean	2,871
Median	2,012
Standard Deviation	3,607
Coefficient of Variation (CV)	1.26
Maximum	63,530
Minimum	1,257
Number of Data Points	2,827

Unconfined Compressive Strength Above Threshold, q <sub>u</sub> (psi)	
q <sub>u</sub> Threshold (psi)	88
Mean	181
Median	138
Standard Deviation	164
Coefficient of Variation (CV)	0.91
Maximum	2,235
Minimum	88
Number of Data Points	2,827

ACIP Pile Capacity QA/QC	
Pile Length (ft)	110.99
Total Rock Socket Length (ft)	92.7
Average Pile Side Shear, f <sub>s</sub> (ksf)	4.48
Unfactored Pile Capacity (kips)	3,907
Factored Pile Capacity (kips)	2,344
Factored Design Load (kips)	980
C/D Ratio for LRFD $\Phi = 0.6$	2.39
Design Requirement Inspection	<b>Passed</b>

Pile Installation Summary	
Drilling Time (min)	24.4
ReDrill Time (min)	0.1
Idle Rotation Time (min)	2.1
Idle Time (min)	0.1
Withdrawal Time (min)	0.0
Penetration w/o Rotation Time (min)	0.0
Total Time (min)	26.7
Drilling Efficiency (%)	91%

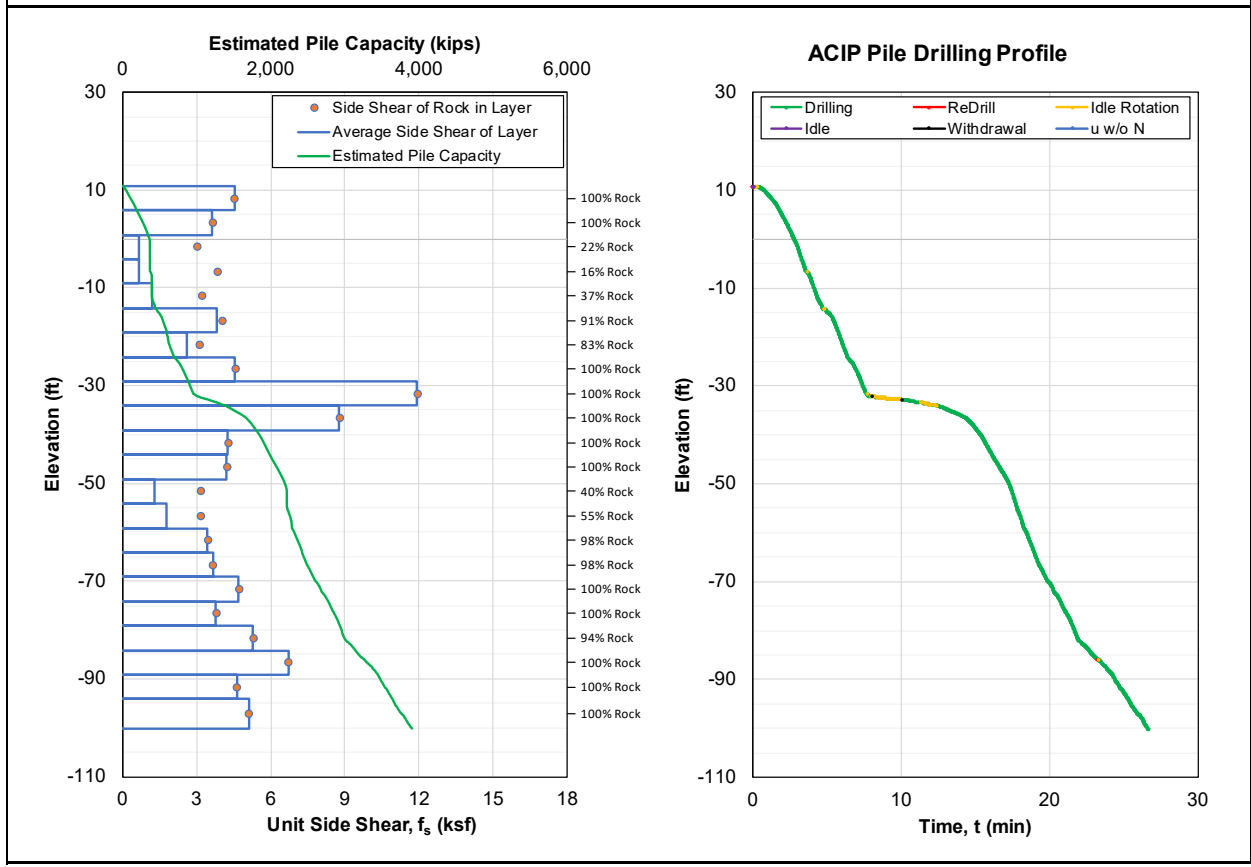


Figure A-33. ACIP pile capacity QA/QC report for Group C-2 Pile 7.

Project	Location	Engineer	Pile ID
I-395	Miami, Florida	Rodgers, McVay, Kelch	C2-8
Station	Offset (ft)	Drill Rig	Drill Bit Diameter (in)
100+00.01	10.00	Drill Rig A	30
Top of Pile Elevation (ft)	Bottom of Pile Elevation (ft)	Depth Increment Analyzed (cm)	ISO-MWD Assessment
10.64	-100.81	1	Class 1

Specific Energy Above Threshold, e (psi)	
Specific Energy Threshold (psi)	1,250
Mean	3,400
Median	2,204
Standard Deviation	5,817
Coefficient of Variation (CV)	1.71
Maximum	165,743
Minimum	1,250
Number of Data Points	2,145

ACIP Pile Capacity QA/QC	
Pile Length (ft)	111.45
Total Rock Socket Length (ft)	70.4
Average Pile Side Shear, $f_s$ (ksf)	3.81
Unfactored Pile Capacity (kips)	3,338
Factored Pile Capacity (kips)	2,003
Factored Design Load (kips)	980
C/D Ratio for LRFD $\Phi = 0.6$	2.04
Design Requirement Inspection	<b>Passed</b>

Unconfined Compressive Strength Above Threshold, $q_u$ (psi)	
$q_u$ Threshold (psi)	88
Mean	207
Median	150
Standard Deviation	209
Coefficient of Variation (CV)	1.01
Maximum	4,081
Minimum	88
Number of Data Points	2,145

Pile Installation Summary	
Drilling Time (min)	25.9
ReDrill Time (min)	0.1
Idle Rotation Time (min)	5.6
Idle Time (min)	2.3
Withdrawal Time (min)	0.1
Penetration w/o Rotation Time (min)	0.2
Total Time (min)	34.2
Drilling Efficiency (%)	76%

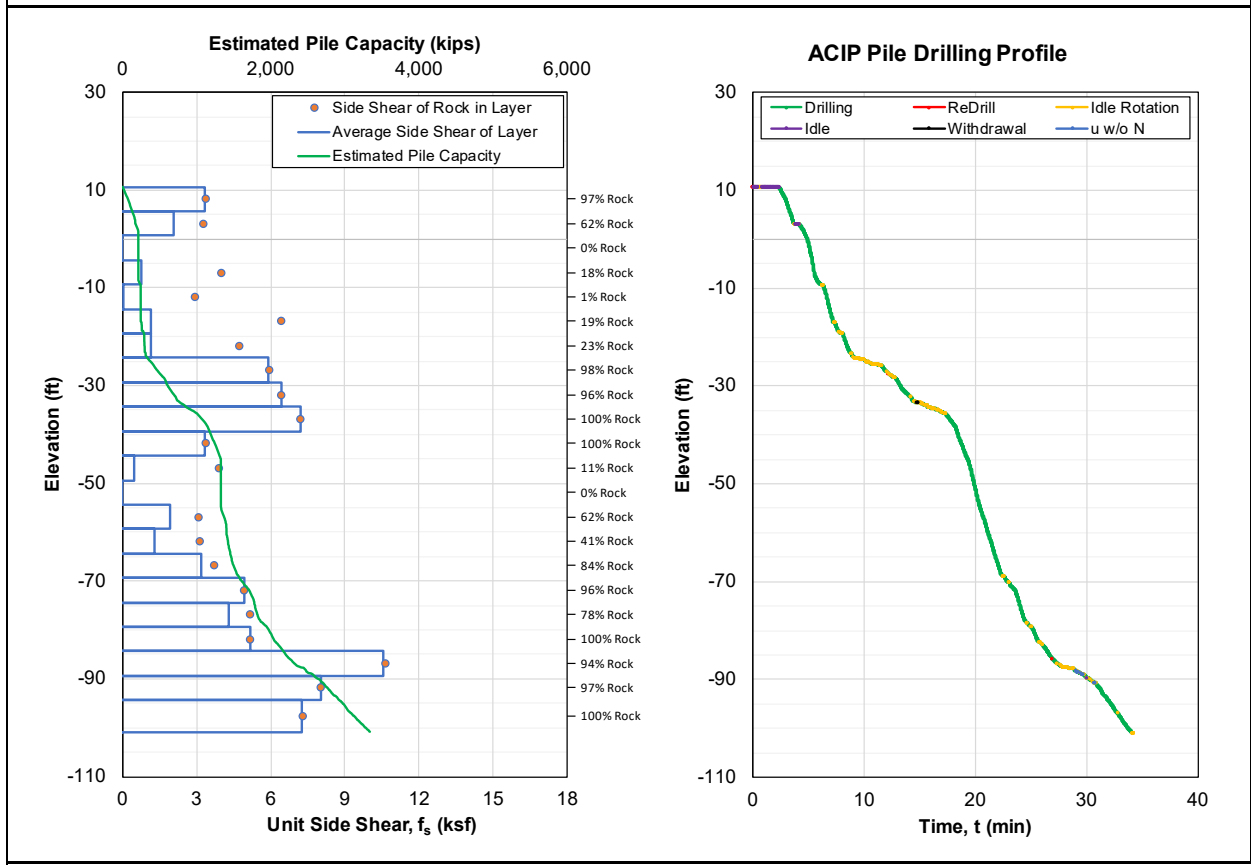


Figure A-34. ACIP pile capacity QA/QC report for Group C-2 Pile 8.

Project	Location	Engineer	Pile ID
I-395	Miami, Florida	Rodgers, McVay, Kelch	D4
Station	Offset (ft)	Drill Rig	Drill Bit Diameter (in)
100+00.01	10.00	Drill Rig A	30
Top of Pile Elevation (ft)	Bottom of Pile Elevation (ft)	Depth Increment Analyzed (cm)	ISO-MWD Assessment
4.09	-130.92	1	Class 1

Specific Energy Above Threshold, e (psi)	
Specific Energy Threshold (psi)	1,250
Mean	3,971
Median	1,893
Standard Deviation	12,937
Coefficient of Variation (CV)	3.26
Maximum	354,406
Minimum	1,250
Number of Data Points	3,233

ACIP Pile Capacity QA/QC	
Pile Length (ft)	135.01
Total Rock Socket Length (ft)	106.1
Average Pile Side Shear, $f_s$ (ksf)	4.98
Unfactored Pile Capacity (kips)	5,276
Factored Pile Capacity (kips)	3,166
Factored Design Load (kips)	1,050
C/D Ratio for LRFD $\Phi = 0.6$	3.02
Design Requirement Inspection	<b>Passed</b>

Unconfined Compressive Strength Above Threshold, $q_u$ (psi)	
$q_u$ Threshold (psi)	88
Mean	220
Median	130
Standard Deviation	311
Coefficient of Variation (CV)	1.41
Maximum	6,364
Minimum	88
Number of Data Points	3,233

Pile Installation Summary	
Drilling Time (min)	31.6
ReDrill Time (min)	0.2
Idle Rotation Time (min)	42.3
Idle Time (min)	3.1
Withdrawal Time (min)	0.2
Penetration w/o Rotation Time (min)	1.4
Total Time (min)	78.9
Drilling Efficiency (%)	40%

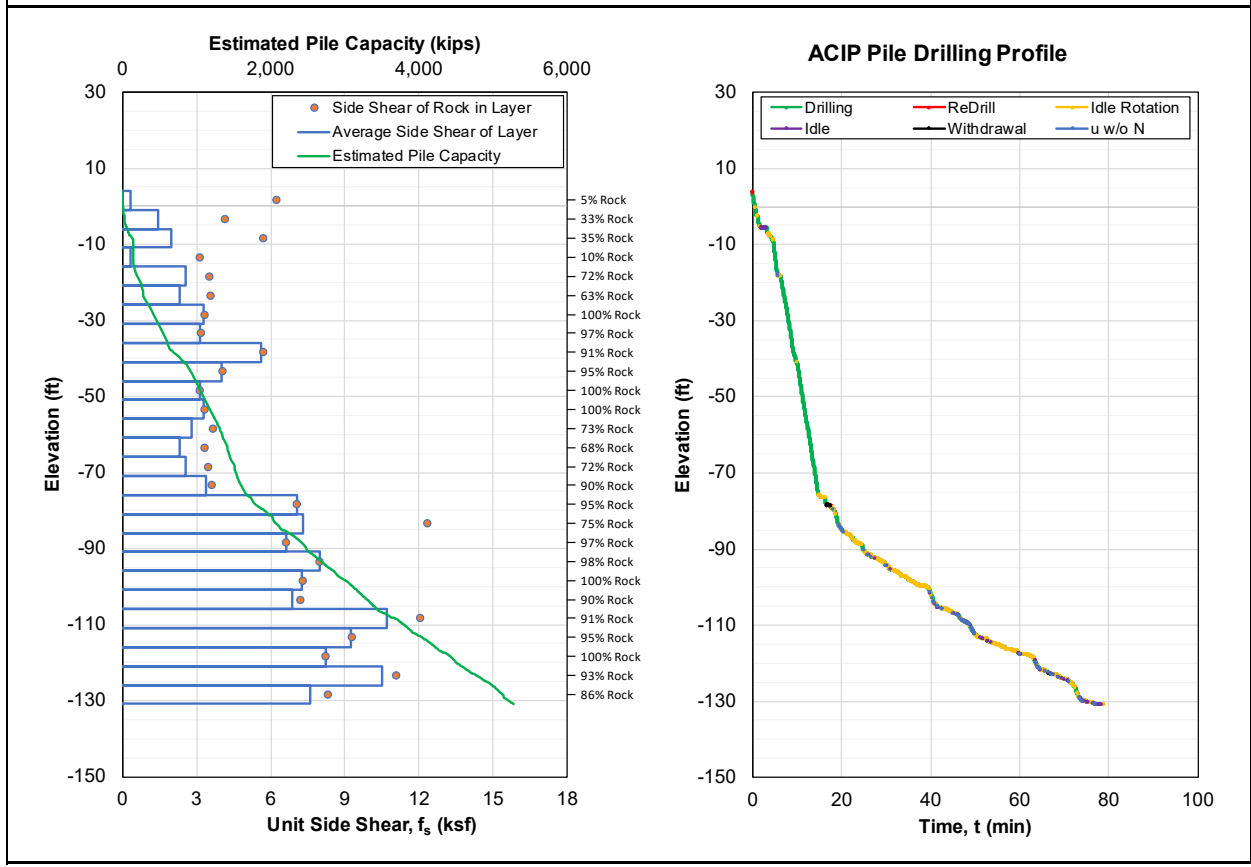


Figure A-35. ACIP pile capacity QA/QC report for Group D Pile 4.

Project	Location	Engineer	Pile ID
I-395	Miami, Florida	Rodgers, McVay, Kelch	D5
Station	Offset (ft)	Drill Rig	Drill Bit Diameter (in)
100+00.01	10.00	Drill Rig A	30
Top of Pile Elevation (ft)	Bottom of Pile Elevation (ft)	Depth Increment Analyzed (cm)	ISO-MWD Assessment
3.74	-131.27	1	Class 1

Specific Energy Above Threshold, e (psi)	
Specific Energy Threshold (psi)	1,250
Mean	5,363
Median	2,737
Standard Deviation	15,196
Coefficient of Variation (CV)	2.83
Maximum	379,268
Minimum	1,251
Number of Data Points	2,718

ACIP Pile Capacity QA/QC	
Pile Length (ft)	135.01
Total Rock Socket Length (ft)	89.2
Average Pile Side Shear, $f_s$ (ksf)	5.25
Unfactored Pile Capacity (kips)	5,569
Factored Pile Capacity (kips)	3,341
Factored Design Load (kips)	1,050
C/D Ratio for LRFD $\Phi = 0.6$	3.18
Design Requirement Inspection	<b>Passed</b>

Unconfined Compressive Strength Above Threshold, $q_u$ (psi)	
$q_u$ Threshold (psi)	88
Mean	283
Median	184
Standard Deviation	382
Coefficient of Variation (CV)	1.35
Maximum	6,615
Minimum	88
Number of Data Points	2,718

Pile Installation Summary	
Drilling Time (min)	34.9
ReDrill Time (min)	0.6
Idle Rotation Time (min)	43.5
Idle Time (min)	2.9
Withdrawal Time (min)	0.4
Penetration w/o Rotation Time (min)	1.5
Total Time (min)	83.7
Drilling Efficiency (%)	42%

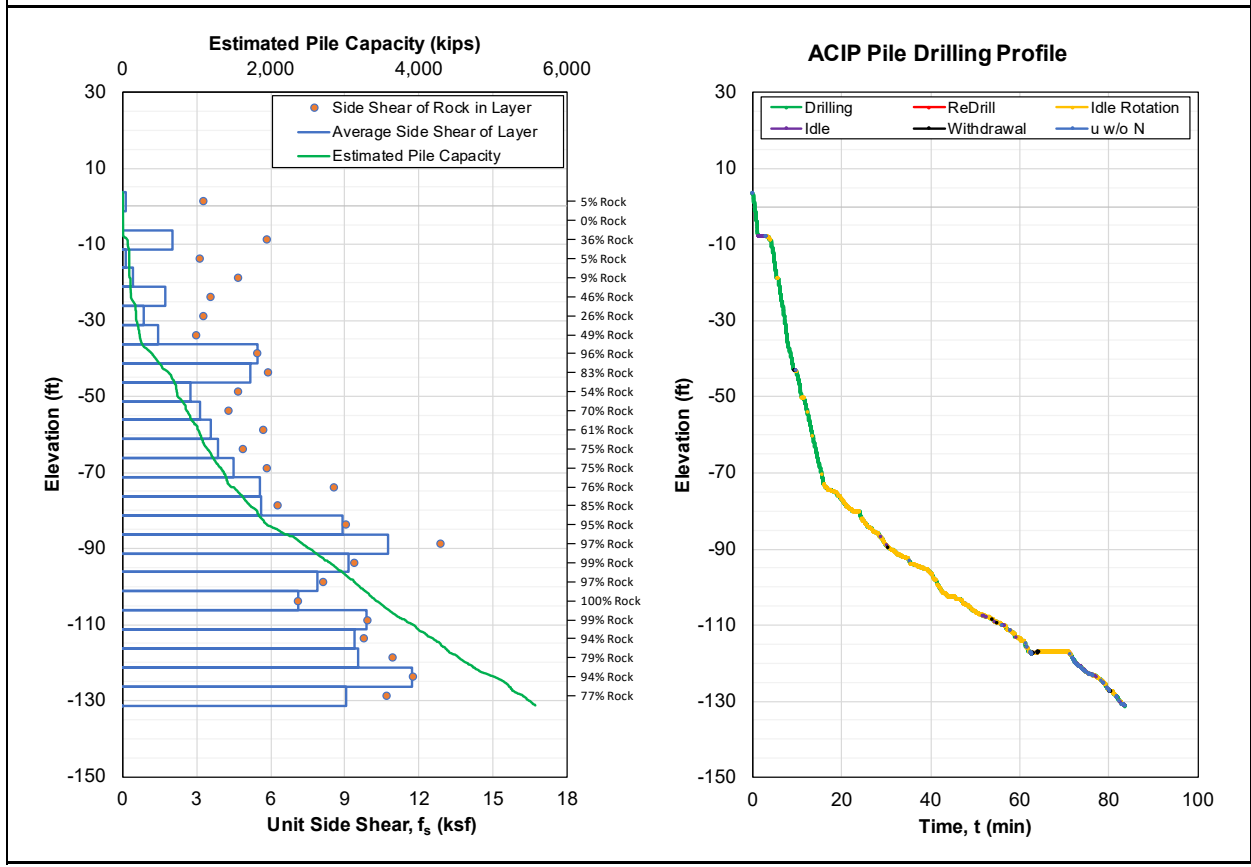


Figure A-36. ACIP pile capacity QA/QC report for Group D Pile 5.

Project	Location	Engineer	Pile ID
I-395	Miami, Florida	Rodgers, McVay, Kelch	D6
Station	Offset (ft)	Drill Rig	Drill Bit Diameter (in)
100+00.01	10.00	Drill Rig A	30
Top of Pile Elevation (ft)	Bottom of Pile Elevation (ft)	Depth Increment Analyzed (cm)	ISO-MWD Assessment
3.42	-131.55	1	Class 1

Specific Energy Above Threshold, e (psi)	
Specific Energy Threshold (psi)	1,250
Mean	4,697
Median	2,488
Standard Deviation	11,804
Coefficient of Variation (CV)	2.51
Maximum	283,593
Minimum	1,250
Number of Data Points	3,377

ACIP Pile Capacity QA/QC	
Pile Length (ft)	134.97
Total Rock Socket Length (ft)	110.8
Average Pile Side Shear, $f_s$ (ksf)	5.97
Unfactored Pile Capacity (kips)	6,331
Factored Pile Capacity (kips)	3,799
Factored Design Load (kips)	1,050
C/D Ratio for LRFD $\Phi = 0.6$	3.62
Design Requirement Inspection	<b>Passed</b>

Unconfined Compressive Strength Above Threshold, $q_u$ (psi)	
$q_u$ Threshold (psi)	88
Mean	256
Median	168
Standard Deviation	338
Coefficient of Variation (CV)	1.32
Maximum	5,600
Minimum	88
Number of Data Points	3,377

Pile Installation Summary	
Drilling Time (min)	37.9
ReDrill Time (min)	0.2
Idle Rotation Time (min)	52.1
Idle Time (min)	0.2
Withdrawal Time (min)	0.2
Penetration w/o Rotation Time (min)	0.0
Total Time (min)	90.6
Drilling Efficiency (%)	42%

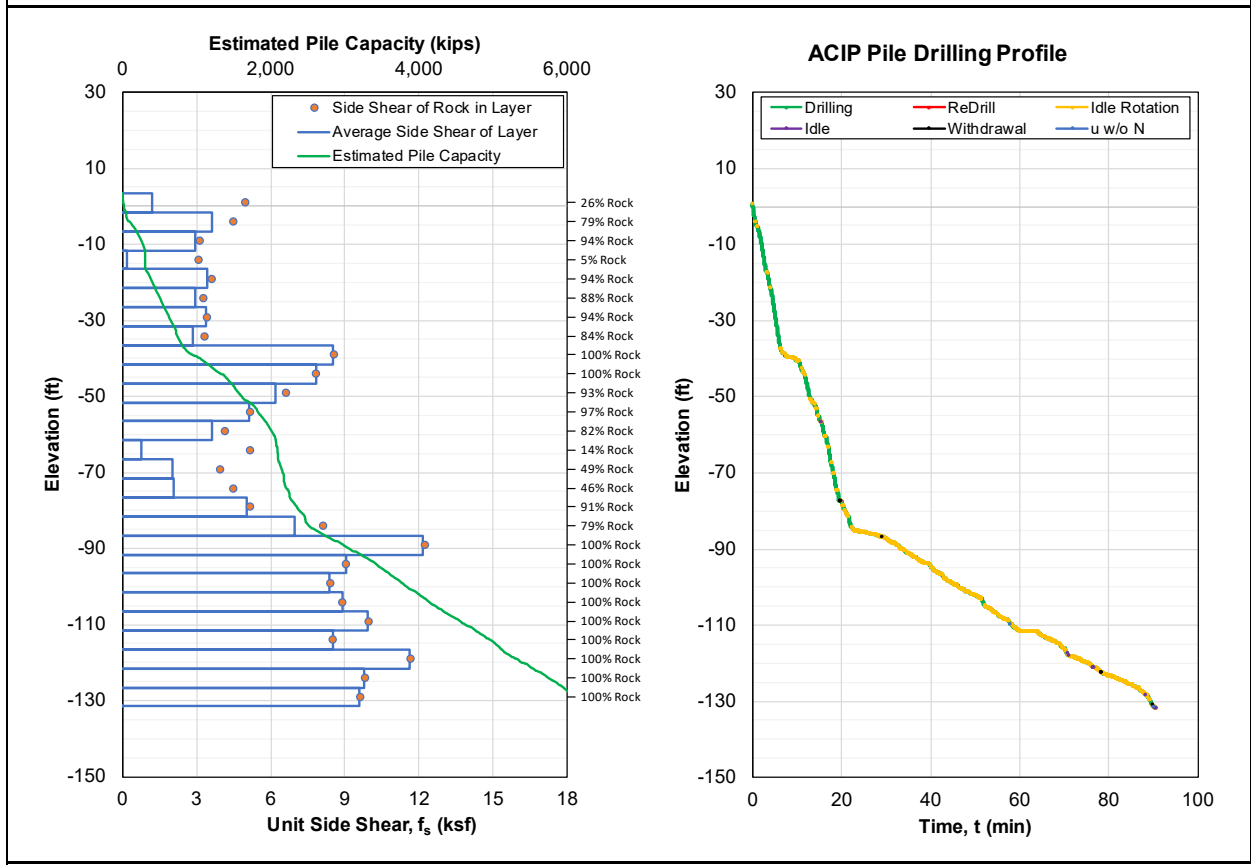


Figure A-37. ACIP pile capacity QA/QC report for Group D Pile 6.



Project	Location	Engineer	Pile ID
I-395	Miami, Florida	Rodgers, McVay, Kelch	D7
Station	Offset (ft)	Drill Rig	Drill Bit Diameter (in)
100+00.01	10.00	Drill Rig A	30
Top of Pile Elevation (ft)	Bottom of Pile Elevation (ft)	Depth Increment Analyzed (cm)	ISO-MWD Assessment
3.39	-131.58	1	Class 1

Specific Energy Above Threshold, e (psi)	
Specific Energy Threshold (psi)	1,250
Mean	5,317
Median	2,930
Standard Deviation	12,871
Coefficient of Variation (CV)	2.42
Maximum	357,846
Minimum	1,252
Number of Data Points	2,842

Unconfined Compressive Strength Above Threshold, q <sub>u</sub> (psi)	
q <sub>u</sub> Threshold (psi)	88
Mean	287
Median	196
Standard Deviation	357
Coefficient of Variation (CV)	1.24
Maximum	6,400
Minimum	88
Number of Data Points	2,842

ACIP Pile Capacity QA/QC	
Pile Length (ft)	134.97
Total Rock Socket Length (ft)	93.2
Average Pile Side Shear, f <sub>s</sub> (ksf)	5.59
Unfactored Pile Capacity (kips)	5,924
Factored Pile Capacity (kips)	3,554
Factored Design Load (kips)	1,050
C/D Ratio for LRFD $\Phi = 0.6$	3.39
Design Requirement Inspection	<b>Passed</b>

Pile Installation Summary	
Drilling Time (min)	34.2
ReDrill Time (min)	0.3
Idle Rotation Time (min)	40.9
Idle Time (min)	4.3
Withdrawal Time (min)	0.3
Penetration w/o Rotation Time (min)	0.8
Total Time (min)	80.8
Drilling Efficiency (%)	42%

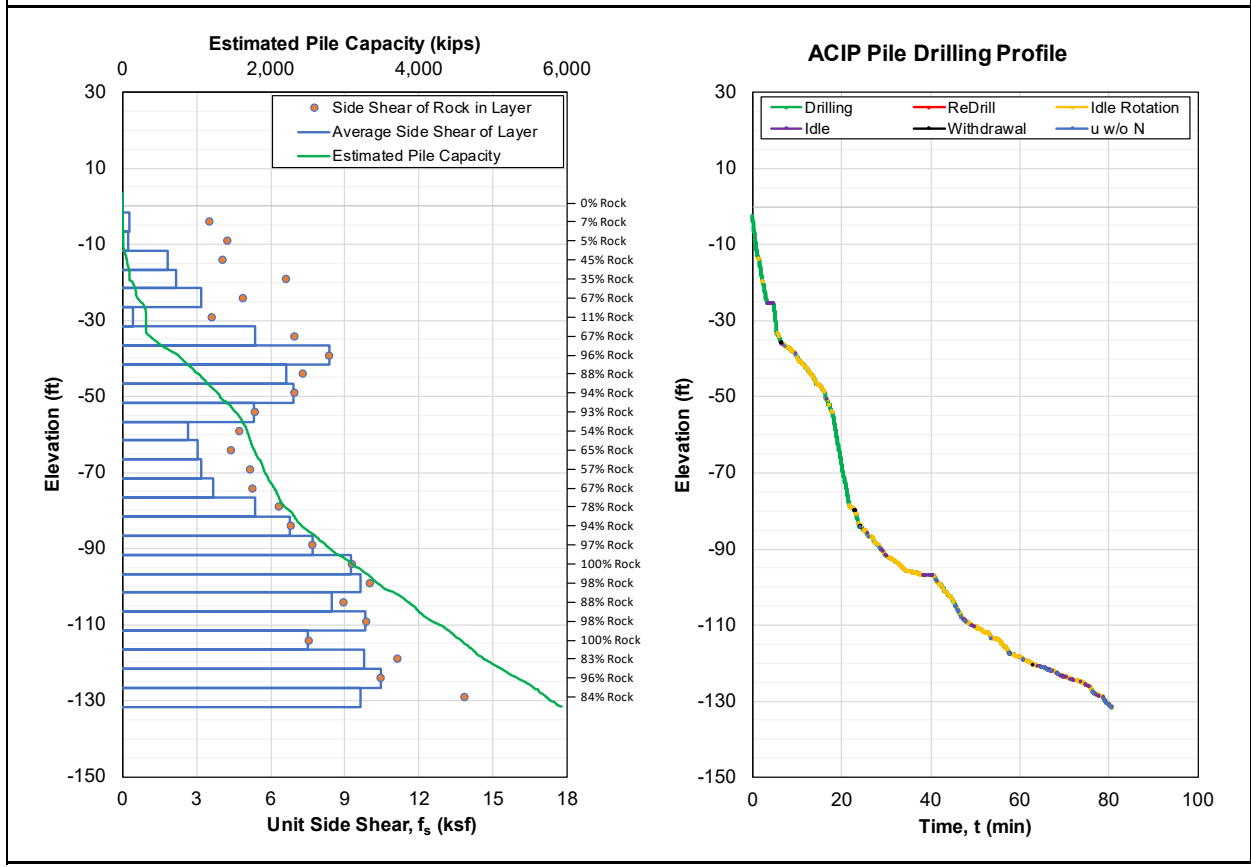


Figure A-38. ACIP pile capacity QA/QC report for Group D Pile 7.

Project	Location	Engineer	Pile ID
I-395	Miami, Florida	Rodgers, McVay, Kelch	D12
Station	Offset (ft)	Drill Rig	Drill Bit Diameter (in)
100+00.01	10.00	Drill Rig A	30
Top of Pile Elevation (ft)	Bottom of Pile Elevation (ft)	Depth Increment Analyzed (cm)	ISO-MWD Assessment
3.24	-131.73	1	Class 1

Specific Energy Above Threshold, e (psi)	
Specific Energy Threshold (psi)	1,250
Mean	5,309
Median	2,596
Standard Deviation	18,030
Coefficient of Variation (CV)	3.40
Maximum	377,008
Minimum	1,253
Number of Data Points	3,284

ACIP Pile Capacity QA/QC	
Pile Length (ft)	134.97
Total Rock Socket Length (ft)	107.7
Average Pile Side Shear, $f_s$ (ksf)	6.07
Unfactored Pile Capacity (kips)	6,438
Factored Pile Capacity (kips)	3,863
Factored Design Load (kips)	1,050
C/D Ratio for LRFD $\Phi = 0.6$	3.68
Design Requirement Inspection	<b>Passed</b>

Unconfined Compressive Strength Above Threshold, $q_u$ (psi)	
$q_u$ Threshold (psi)	88
Mean	270
Median	175
Standard Deviation	413
Coefficient of Variation (CV)	1.53
Maximum	6,592
Minimum	88
Number of Data Points	3,284

Pile Installation Summary	
Drilling Time (min)	36.0
ReDrill Time (min)	0.1
Idle Rotation Time (min)	37.6
Idle Time (min)	3.0
Withdrawal Time (min)	0.0
Penetration w/o Rotation Time (min)	0.4
Total Time (min)	77.1
Drilling Efficiency (%)	47%

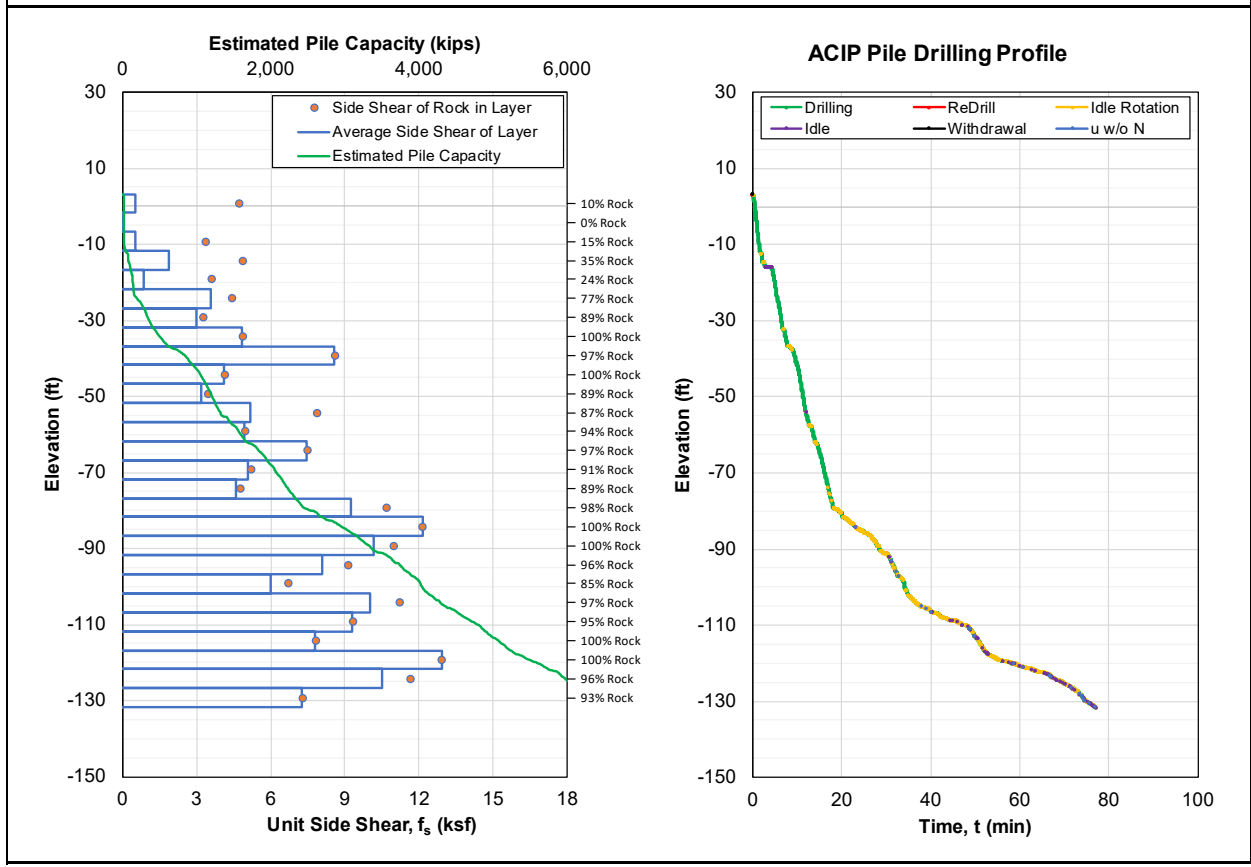


Figure A-39. ACIP pile capacity QA/QC report for Group D Pile 12.

Project	Location	Engineer	Pile ID
I-395	Miami, Florida	Rodgers, McVay, Kelch	D13
Station	Offset (ft)	Drill Rig	Drill Bit Diameter (in)
100+00.01	10.00	Drill Rig A	30
Top of Pile Elevation (ft)	Bottom of Pile Elevation (ft)	Depth Increment Analyzed (cm)	ISO-MWD Assessment
3.32	-131.65	1	Class 1

Specific Energy Above Threshold, e (psi)	
Specific Energy Threshold (psi)	1,250
Mean	5,764
Median	2,691
Standard Deviation	16,979
Coefficient of Variation (CV)	2.95
Maximum	384,918
Minimum	1,251
Number of Data Points	2,993

ACIP Pile Capacity QA/QC	
Pile Length (ft)	134.97
Total Rock Socket Length (ft)	98.2
Average Pile Side Shear, $f_s$ (ksf)	5.90
Unfactored Pile Capacity (kips)	6,252
Factored Pile Capacity (kips)	3,751
Factored Design Load (kips)	1,050
C/D Ratio for LRFD $\Phi = 0.6$	3.57
Design Requirement Inspection	<b>Passed</b>

Unconfined Compressive Strength Above Threshold, $q_u$ (psi)	
$q_u$ Threshold (psi)	88
Mean	291
Median	181
Standard Deviation	431
Coefficient of Variation (CV)	1.48
Maximum	6,670
Minimum	88
Number of Data Points	2,993

Pile Installation Summary	
Drilling Time (min)	35.9
ReDrill Time (min)	0.3
Idle Rotation Time (min)	21.5
Idle Time (min)	2.7
Withdrawal Time (min)	0.2
Penetration w/o Rotation Time (min)	2.2
Total Time (min)	62.7
Drilling Efficiency (%)	57%

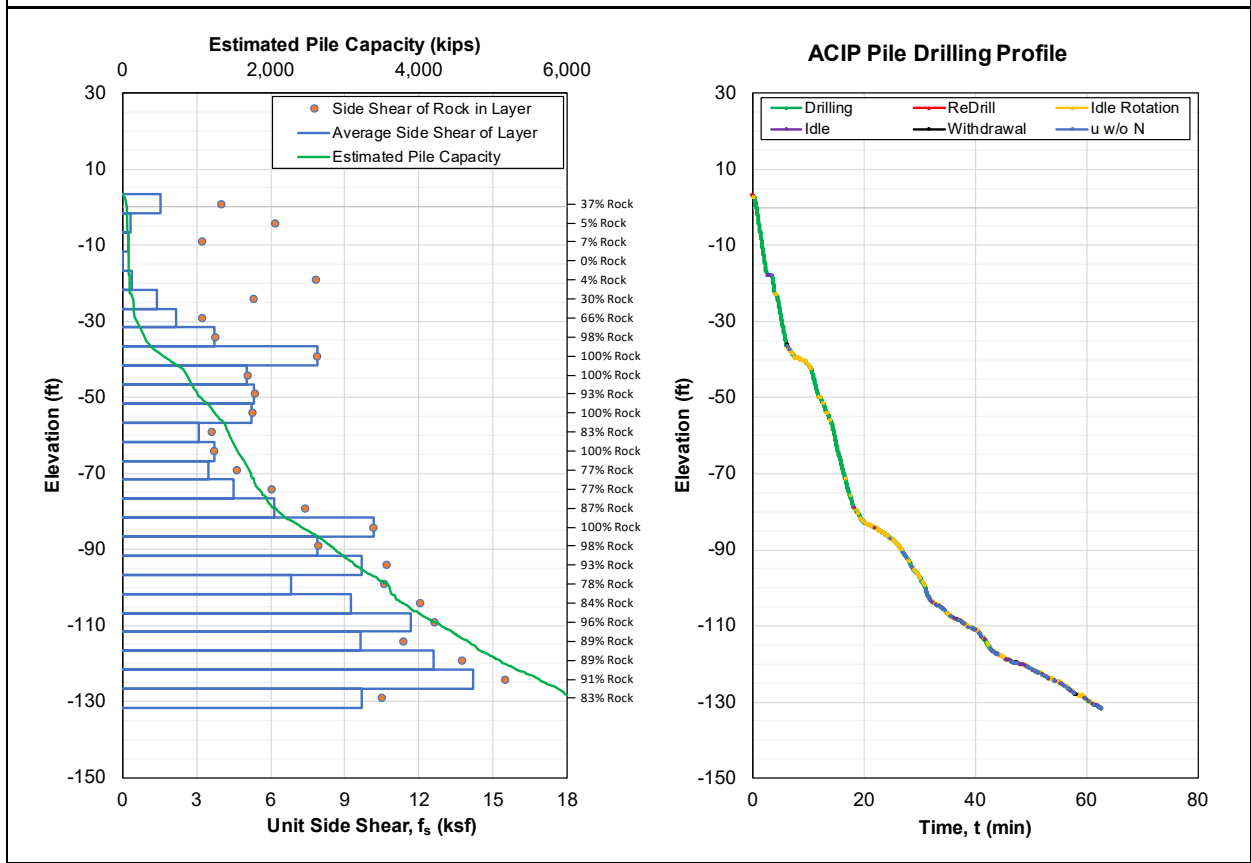


Figure A-40. ACIP pile capacity QA/QC report for Group D Pile 13.

Project	Location	Engineer	Pile ID
I-395	Miami, Florida	Rodgers, McVay, Kelch	D14
Station	Offset (ft)	Drill Rig	Drill Bit Diameter (in)
100+00.01	10.00	Drill Rig A	30
Top of Pile Elevation (ft)	Bottom of Pile Elevation (ft)	Depth Increment Analyzed (cm)	ISO-MWD Assessment
3.27	-131.70	1	Class 1

Specific Energy Above Threshold, e (psi)	
Specific Energy Threshold (psi)	1,250
Mean	5,304
Median	2,754
Standard Deviation	13,832
Coefficient of Variation (CV)	2.61
Maximum	290,056
Minimum	1,255
Number of Data Points	2,920

ACIP Pile Capacity QA/QC	
Pile Length (ft)	134.97
Total Rock Socket Length (ft)	95.8
Average Pile Side Shear, $f_s$ (ksf)	5.59
Unfactored Pile Capacity (kips)	5,931
Factored Pile Capacity (kips)	3,558
Factored Design Load (kips)	1,050
C/D Ratio for LRFD $\Phi = 0.6$	3.39
Design Requirement Inspection	<b>Passed</b>

Unconfined Compressive Strength Above Threshold, $q_u$ (psi)	
$q_u$ Threshold (psi)	88
Mean	280
Median	185
Standard Deviation	379
Coefficient of Variation (CV)	1.35
Maximum	5,673
Minimum	88
Number of Data Points	2,920

Pile Installation Summary	
Drilling Time (min)	35.4
ReDrill Time (min)	0.5
Idle Rotation Time (min)	24.9
Idle Time (min)	3.0
Withdrawal Time (min)	0.5
Penetration w/o Rotation Time (min)	2.0
Total Time (min)	66.2
Drilling Efficiency (%)	53%

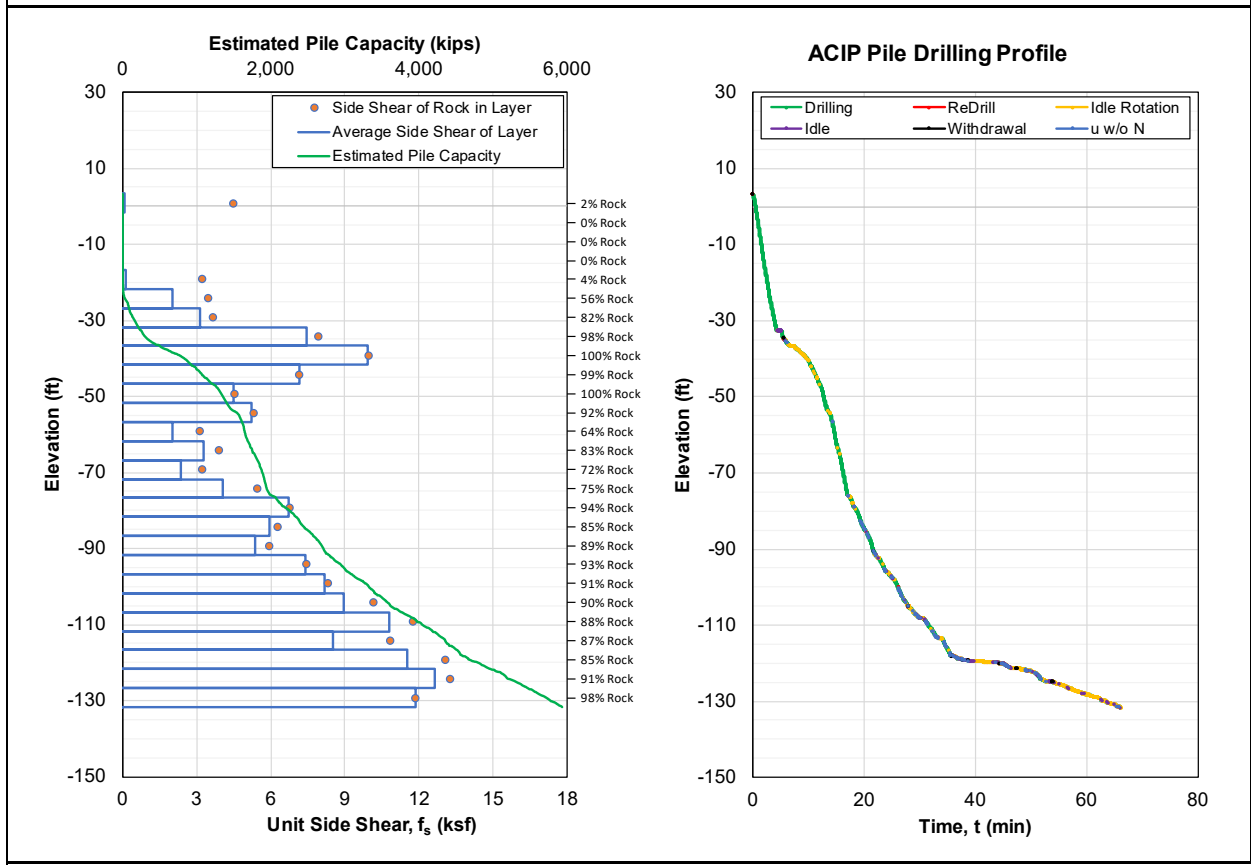


Figure A-41. ACIP pile capacity QA/QC report for Group D Pile 14.

Project	Location	Engineer	Pile ID
I-395	Miami, Florida	Rodgers, McVay, Kelch	D20
Station	Offset (ft)	Drill Rig	Drill Bit Diameter (in)
100+00.01	10.00	Drill Rig A	30
Top of Pile Elevation (ft)	Bottom of Pile Elevation (ft)	Depth Increment Analyzed (cm)	ISO-MWD Assessment
3.15	-131.82	1	Class 1

Specific Energy Above Threshold, e (psi)	
Specific Energy Threshold (psi)	1,250
Mean	5,123
Median	2,875
Standard Deviation	10,099
Coefficient of Variation (CV)	1.97
Maximum	210,587
Minimum	1,251
Number of Data Points	3,171

Unconfined Compressive Strength Above Threshold, q <sub>u</sub> (psi)	
q <sub>u</sub> Threshold (psi)	88
Mean	285
Median	192
Standard Deviation	322
Coefficient of Variation (CV)	1.13
Maximum	4,706
Minimum	88
Number of Data Points	3,171

ACIP Pile Capacity QA/QC	
Pile Length (ft)	134.97
Total Rock Socket Length (ft)	104.0
Average Pile Side Shear, f <sub>s</sub> (ksf)	6.21
Unfactored Pile Capacity (kips)	6,578
Factored Pile Capacity (kips)	3,947
Factored Design Load (kips)	1,050
C/D Ratio for LRFD $\Phi = 0.6$	3.76
Design Requirement Inspection	<b>Passed</b>

Pile Installation Summary	
Drilling Time (min)	40.3
ReDrill Time (min)	0.3
Idle Rotation Time (min)	31.1
Idle Time (min)	2.5
Withdrawal Time (min)	0.2
Penetration w/o Rotation Time (min)	0.3
Total Time (min)	74.8
Drilling Efficiency (%)	54%

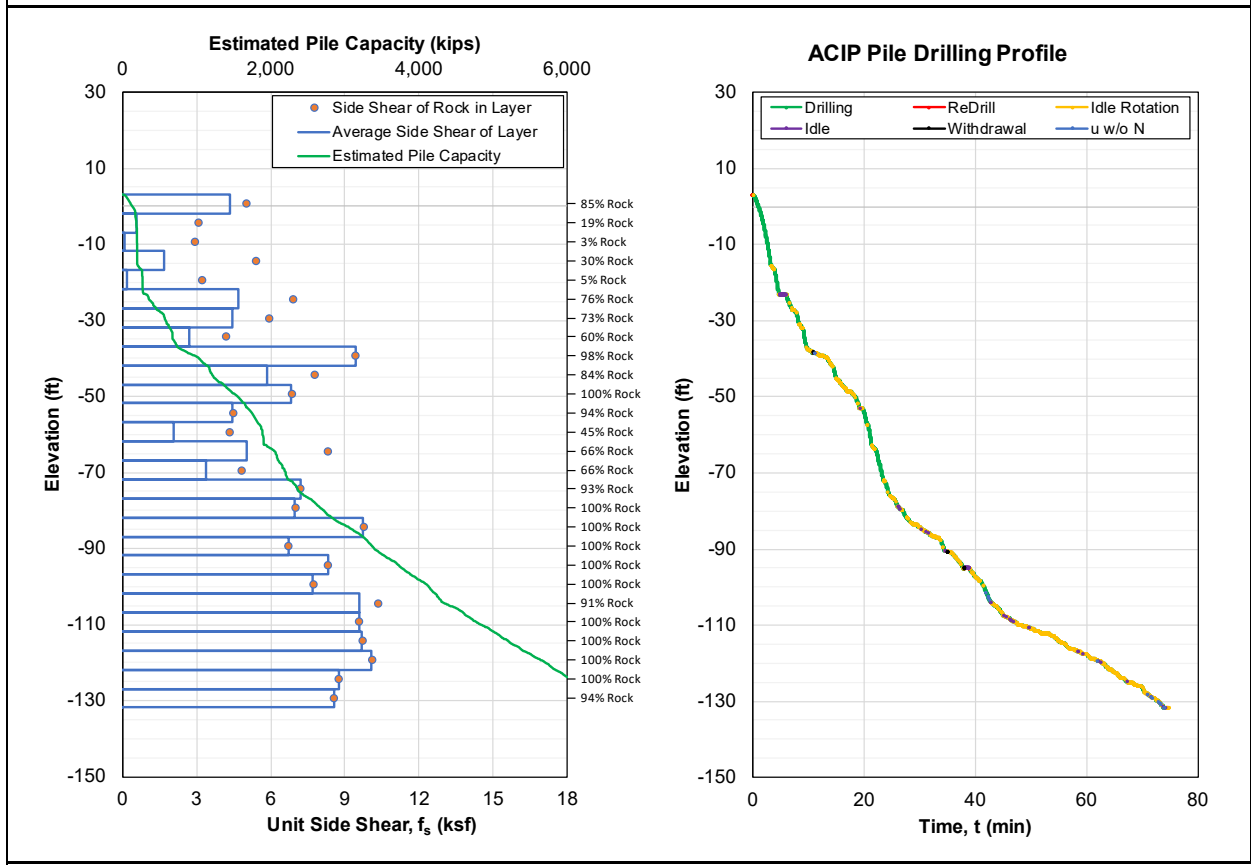


Figure A-42. ACIP pile capacity QA/QC report for Group D Pile 20.

Project	Location	Engineer	Pile ID
I-395	Miami, Florida	Rodgers, McVay, Kelch	D21
Station	Offset (ft)	Drill Rig	Drill Bit Diameter (in)
100+00.01	10.00	Drill Rig A	30
Top of Pile Elevation (ft)	Bottom of Pile Elevation (ft)	Depth Increment Analyzed (cm)	ISO-MWD Assessment
3.29	-131.68	1	Class 1

Specific Energy Above Threshold, e (psi)	
Specific Energy Threshold (psi)	1,250
Mean	4,502
Median	2,424
Standard Deviation	11,321
Coefficient of Variation (CV)	2.51
Maximum	348,448
Minimum	1,251
Number of Data Points	2,767

Unconfined Compressive Strength Above Threshold, q <sub>u</sub> (psi)	
q <sub>u</sub> Threshold (psi)	88
Mean	250
Median	164
Standard Deviation	320
Coefficient of Variation (CV)	1.28
Maximum	6,303
Minimum	88
Number of Data Points	2,767

ACIP Pile Capacity QA/QC	
Pile Length (ft)	134.97
Total Rock Socket Length (ft)	90.8
Average Pile Side Shear, f <sub>s</sub> (ksf)	4.78
Unfactored Pile Capacity (kips)	5,071
Factored Pile Capacity (kips)	3,042
Factored Design Load (kips)	1,050
C/D Ratio for LRFD $\Phi = 0.6$	2.90
Design Requirement Inspection	<b>Passed</b>

Pile Installation Summary	
Drilling Time (min)	30.3
ReDrill Time (min)	2.2
Idle Rotation Time (min)	13.8
Idle Time (min)	29.0
Withdrawal Time (min)	1.4
Penetration w/o Rotation Time (min)	1.7
Total Time (min)	78.4
Drilling Efficiency (%)	39%

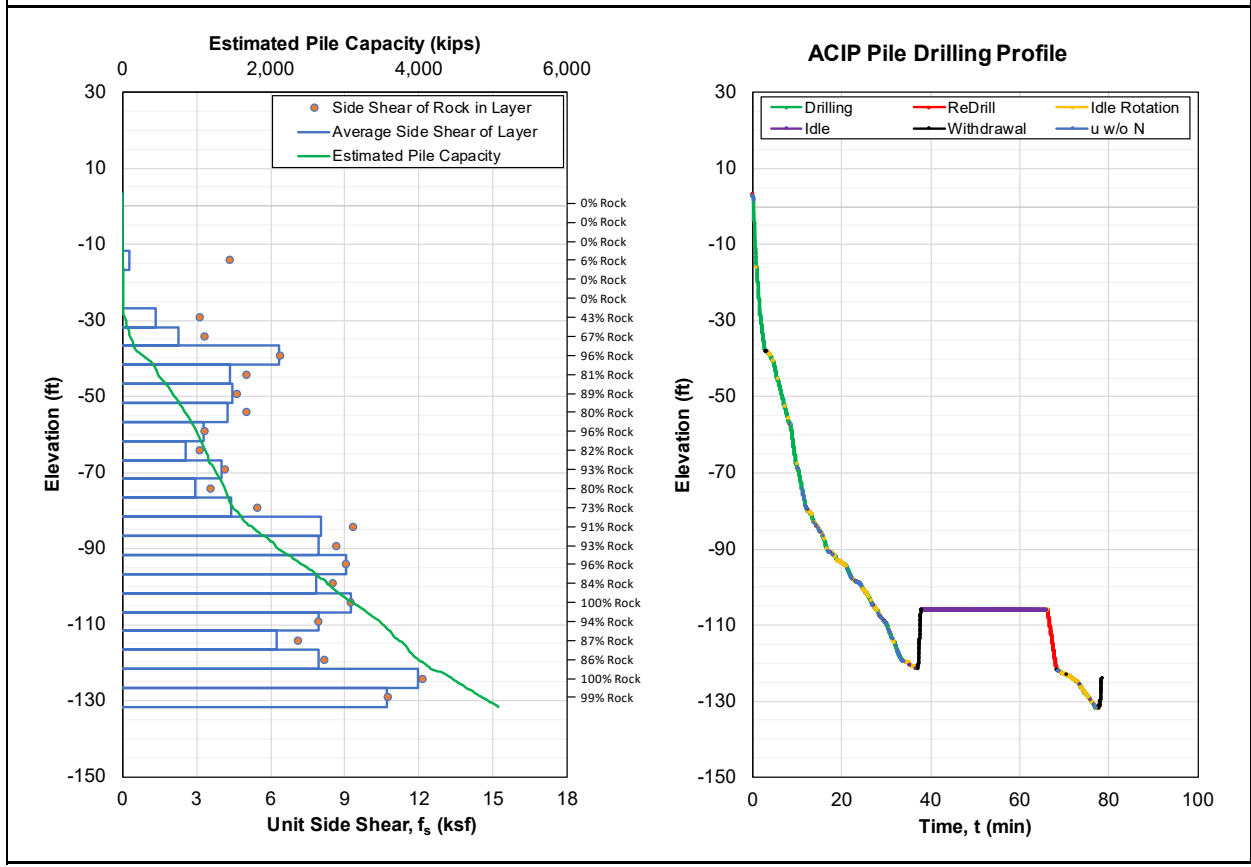


Figure A-43. ACIP pile capacity QA/QC report for Group D Pile 21.

Project	Location	Engineer	Pile ID
I-395	Miami, Florida	Rodgers, McVay, Kelch	D28
Station	Offset (ft)	Drill Rig	Drill Bit Diameter (in)
100+00.01	10.00	Drill Rig A	30
Top of Pile Elevation (ft)	Bottom of Pile Elevation (ft)	Depth Increment Analyzed (cm)	ISO-MWD Assessment
3.27	-131.90	1	Class 1

Specific Energy Above Threshold, e (psi)	
Specific Energy Threshold (psi)	1,250
Mean	4,620
Median	2,247
Standard Deviation	14,433
Coefficient of Variation (CV)	3.12
Maximum	378,855
Minimum	1,251
Number of Data Points	3,000

Unconfined Compressive Strength Above Threshold, q <sub>u</sub> (psi)	
q <sub>u</sub> Threshold (psi)	88
Mean	245
Median	153
Standard Deviation	363
Coefficient of Variation (CV)	1.48
Maximum	6,611
Minimum	88
Number of Data Points	3,000

ACIP Pile Capacity QA/QC	
Pile Length (ft)	135.17
Total Rock Socket Length (ft)	98.4
Average Pile Side Shear, f <sub>s</sub> (ksf)	5.07
Unfactored Pile Capacity (kips)	5,382
Factored Pile Capacity (kips)	3,229
Factored Design Load (kips)	1,050
C/D Ratio for LRFD $\Phi = 0.6$	3.08
Design Requirement Inspection	<b>Passed</b>

Pile Installation Summary	
Drilling Time (min)	31.2
ReDrill Time (min)	0.5
Idle Rotation Time (min)	27.1
Idle Time (min)	3.5
Withdrawal Time (min)	0.6
Penetration w/o Rotation Time (min)	1.9
Total Time (min)	64.8
Drilling Efficiency (%)	48%

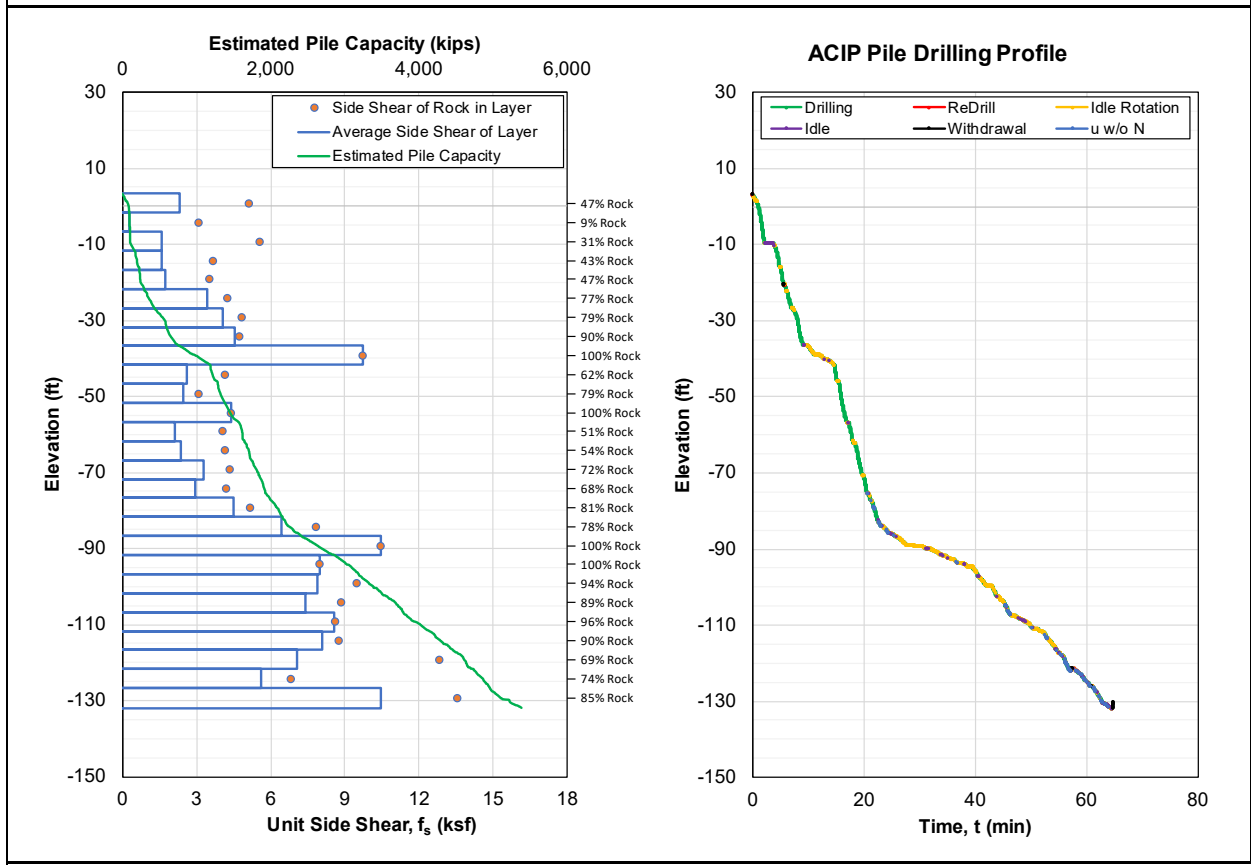


Figure A-44. ACIP pile capacity QA/QC report for Group D Pile 28.

Project	Location	Engineer	Pile ID
I-395	Miami, Florida	Rodgers, McVay, Kelch	D10
Station	Offset (ft)	Drill Rig	Drill Bit Diameter (in)
100+00.01	10.00	Drill Rig A	30
Top of Pile Elevation (ft)	Bottom of Pile Elevation (ft)	Depth Increment Analyzed (cm)	ISO-MWD Assessment
2.94	-132.00	1	Class 1

Specific Energy Above Threshold, e (psi)	
Specific Energy Threshold (psi)	1,250
Mean	6,249
Median	2,982
Standard Deviation	20,634
Coefficient of Variation (CV)	3.30
Maximum	392,942
Minimum	1,250
Number of Data Points	2,421

Unconfined Compressive Strength Above Threshold, q <sub>u</sub> (psi)	
q <sub>u</sub> Threshold (psi)	88
Mean	307
Median	199
Standard Deviation	464
Coefficient of Variation (CV)	1.51
Maximum	6,749
Minimum	88
Number of Data Points	2,421

ACIP Pile Capacity QA/QC	
Pile Length (ft)	134.94
Total Rock Socket Length (ft)	79.4
Average Pile Side Shear, f <sub>s</sub> (ksf)	5.03
Unfactored Pile Capacity (kips)	5,328
Factored Pile Capacity (kips)	3,197
Factored Design Load (kips)	1,050
C/D Ratio for LRFD $\Phi = 0.6$	3.04
Design Requirement Inspection	<b>Passed</b>

Pile Installation Summary	
Drilling Time (min)	31.4
ReDrill Time (min)	0.3
Idle Rotation Time (min)	21.5
Idle Time (min)	2.2
Withdrawal Time (min)	0.3
Penetration w/o Rotation Time (min)	2.2
Total Time (min)	57.8
Drilling Efficiency (%)	54%

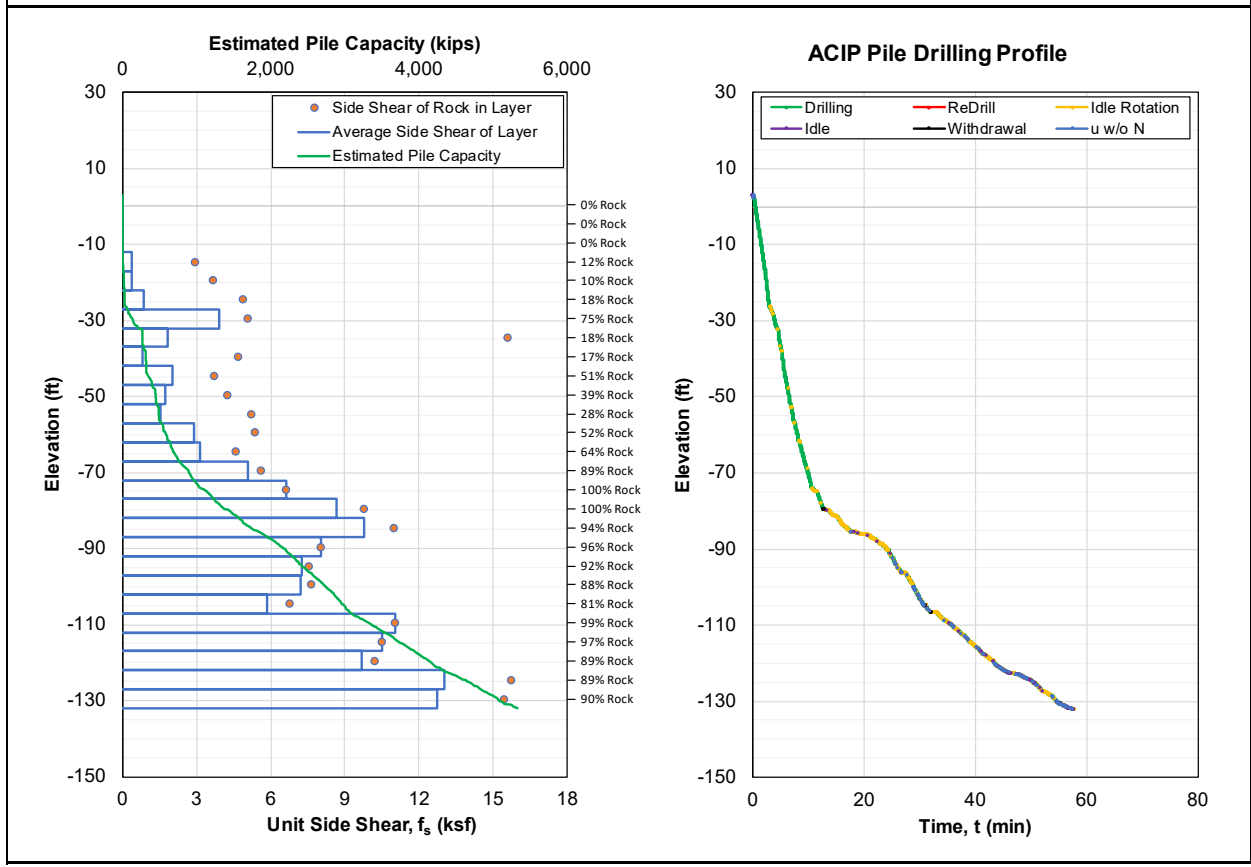


Figure A-45. ACIP pile capacity QA/QC report for Group D Pile 10.



Project	Location	Engineer	Pile ID
I-395	Miami, Florida	Rodgers, McVay, Kelch	D18
Station	Offset (ft)	Drill Rig	Drill Bit Diameter (in)
100+00.01	10.00	Drill Rig A	30
Top of Pile Elevation (ft)	Bottom of Pile Elevation (ft)	Depth Increment Analyzed (cm)	ISO-MWD Assessment
3.09	-132.38	1	Class 1

Specific Energy Above Threshold, e (psi)	
Specific Energy Threshold (psi)	1,250
Mean	4,624
Median	2,321
Standard Deviation	15,508
Coefficient of Variation (CV)	3.35
Maximum	373,766
Minimum	1,252
Number of Data Points	2,962

Unconfined Compressive Strength Above Threshold, q <sub>u</sub> (psi)	
q <sub>u</sub> Threshold (psi)	88
Mean	244
Median	158
Standard Deviation	368
Coefficient of Variation (CV)	1.51
Maximum	6,560
Minimum	88
Number of Data Points	2,962

ACIP Pile Capacity QA/QC	
Pile Length (ft)	135.47
Total Rock Socket Length (ft)	97.2
Average Pile Side Shear, f <sub>s</sub> (ksf)	4.97
Unfactored Pile Capacity (kips)	5,293
Factored Pile Capacity (kips)	3,176
Factored Design Load (kips)	1,050
C/D Ratio for LRFD $\Phi = 0.6$	3.02
Design Requirement Inspection	<b>Passed</b>

Pile Installation Summary	
Drilling Time (min)	31.2
ReDrill Time (min)	0.4
Idle Rotation Time (min)	25.2
Idle Time (min)	1.5
Withdrawal Time (min)	0.8
Penetration w/o Rotation Time (min)	1.0
Total Time (min)	60.0
Drilling Efficiency (%)	52%

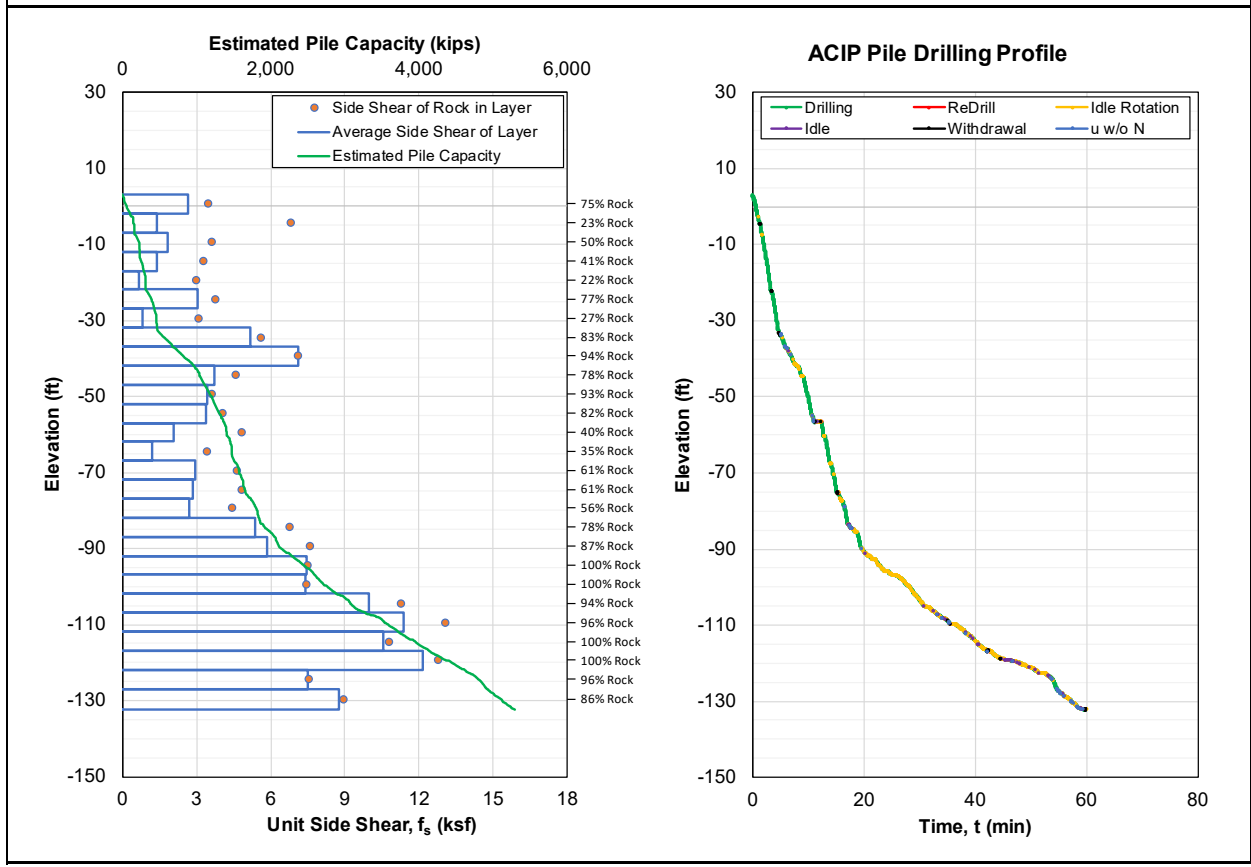


Figure A-46. ACIP pile capacity QA/QC report for Group D Pile 18.

Project	Location	Engineer	Pile ID
I-395	Miami, Florida	Rodgers, McVay, Kelch	D19
Station	Offset (ft)	Drill Rig	Drill Bit Diameter (in)
100+00.01	10.00	Drill Rig A	30
Top of Pile Elevation (ft)	Bottom of Pile Elevation (ft)	Depth Increment Analyzed (cm)	ISO-MWD Assessment
3.05	-131.92	1	Class 1

Specific Energy Above Threshold, e (psi)	
Specific Energy Threshold (psi)	1,250
Mean	5,330
Median	2,621
Standard Deviation	15,142
Coefficient of Variation (CV)	2.84
Maximum	391,905
Minimum	1,250
Number of Data Points	3,060

Unconfined Compressive Strength Above Threshold, q <sub>u</sub> (psi)	
q <sub>u</sub> Threshold (psi)	88
Mean	278
Median	177
Standard Deviation	391
Coefficient of Variation (CV)	1.41
Maximum	6,739
Minimum	88
Number of Data Points	3,060

ACIP Pile Capacity QA/QC	
Pile Length (ft)	134.97
Total Rock Socket Length (ft)	100.4
Average Pile Side Shear, f <sub>s</sub> (ksf)	5.82
Unfactored Pile Capacity (kips)	6,165
Factored Pile Capacity (kips)	3,699
Factored Design Load (kips)	1,050
C/D Ratio for LRFD $\Phi = 0.6$	3.52
Design Requirement Inspection	<b>Passed</b>

Pile Installation Summary	
Drilling Time (min)	34.6
ReDrill Time (min)	0.2
Idle Rotation Time (min)	29.3
Idle Time (min)	9.0
Withdrawal Time (min)	0.2
Penetration w/o Rotation Time (min)	1.7
Total Time (min)	75.0
Drilling Efficiency (%)	46%

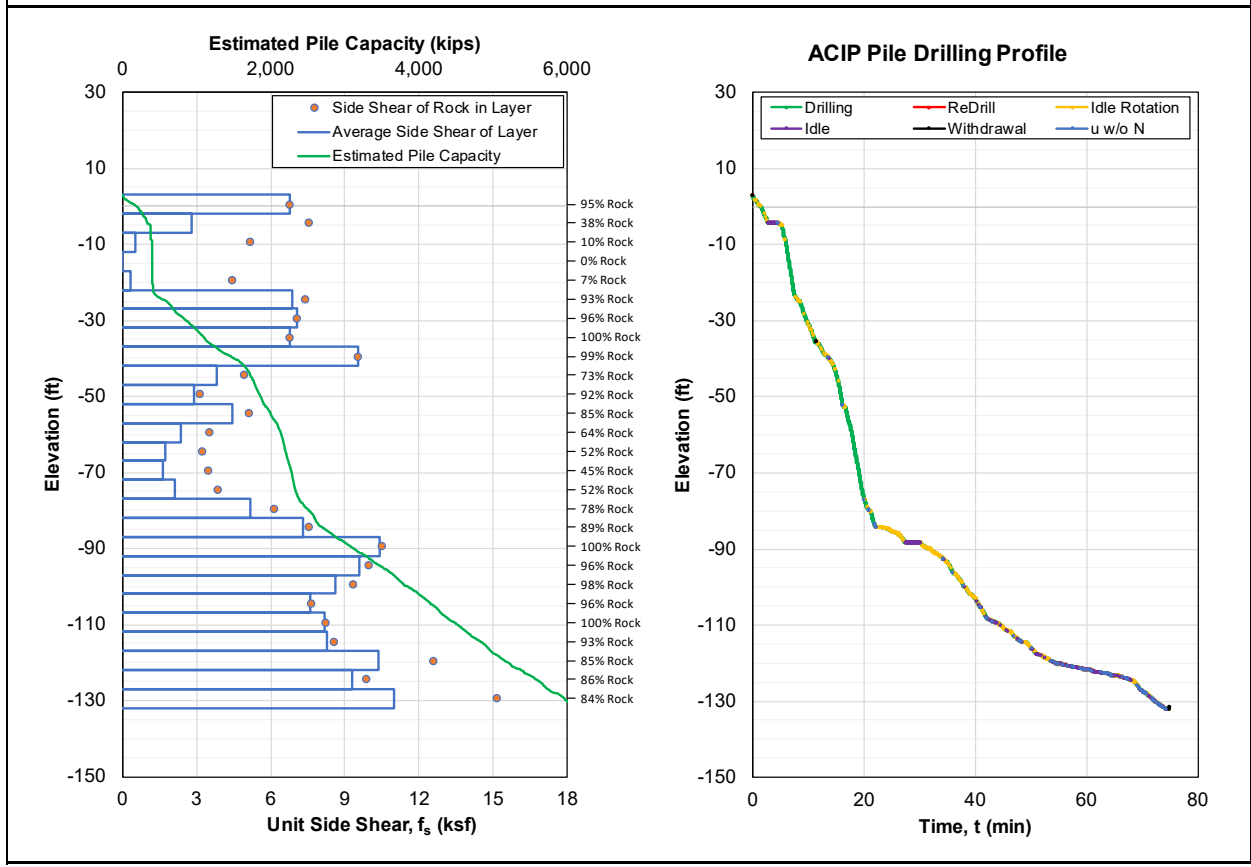


Figure A-47. ACIP pile capacity QA/QC report for Group D Pile 19.

Project	Location	Engineer	Pile ID
I-395	Miami, Florida	Rodgers, McVay, Kelch	D26
Station	Offset (ft)	Drill Rig	Drill Bit Diameter (in)
100+00.01	10.00	Drill Rig A	30
Top of Pile Elevation (ft)	Bottom of Pile Elevation (ft)	Depth Increment Analyzed (cm)	ISO-MWD Assessment
3.12	-131.85	1	Class 1

Specific Energy Above Threshold, e (psi)	
Specific Energy Threshold (psi)	1,250
Mean	5,111
Median	2,812
Standard Deviation	13,081
Coefficient of Variation (CV)	2.56
Maximum	356,445
Minimum	1,254
Number of Data Points	3,267

ACIP Pile Capacity QA/QC	
Pile Length (ft)	134.97
Total Rock Socket Length (ft)	107.2
Average Pile Side Shear, $f_s$ (ksf)	6.25
Unfactored Pile Capacity (kips)	6,624
Factored Pile Capacity (kips)	3,974
Factored Design Load (kips)	1,050
C/D Ratio for LRFD $\Phi = 0.6$	3.78
Design Requirement Inspection	<b>Passed</b>

Unconfined Compressive Strength Above Threshold, $q_u$ (psi)	
$q_u$ Threshold (psi)	88
Mean	278
Median	188
Standard Deviation	346
Coefficient of Variation (CV)	1.24
Maximum	6,385
Minimum	88
Number of Data Points	3,267

Pile Installation Summary	
Drilling Time (min)	40.6
ReDrill Time (min)	0.2
Idle Rotation Time (min)	34.3
Idle Time (min)	3.3
Withdrawal Time (min)	0.1
Penetration w/o Rotation Time (min)	1.2
Total Time (min)	79.5
Drilling Efficiency (%)	51%

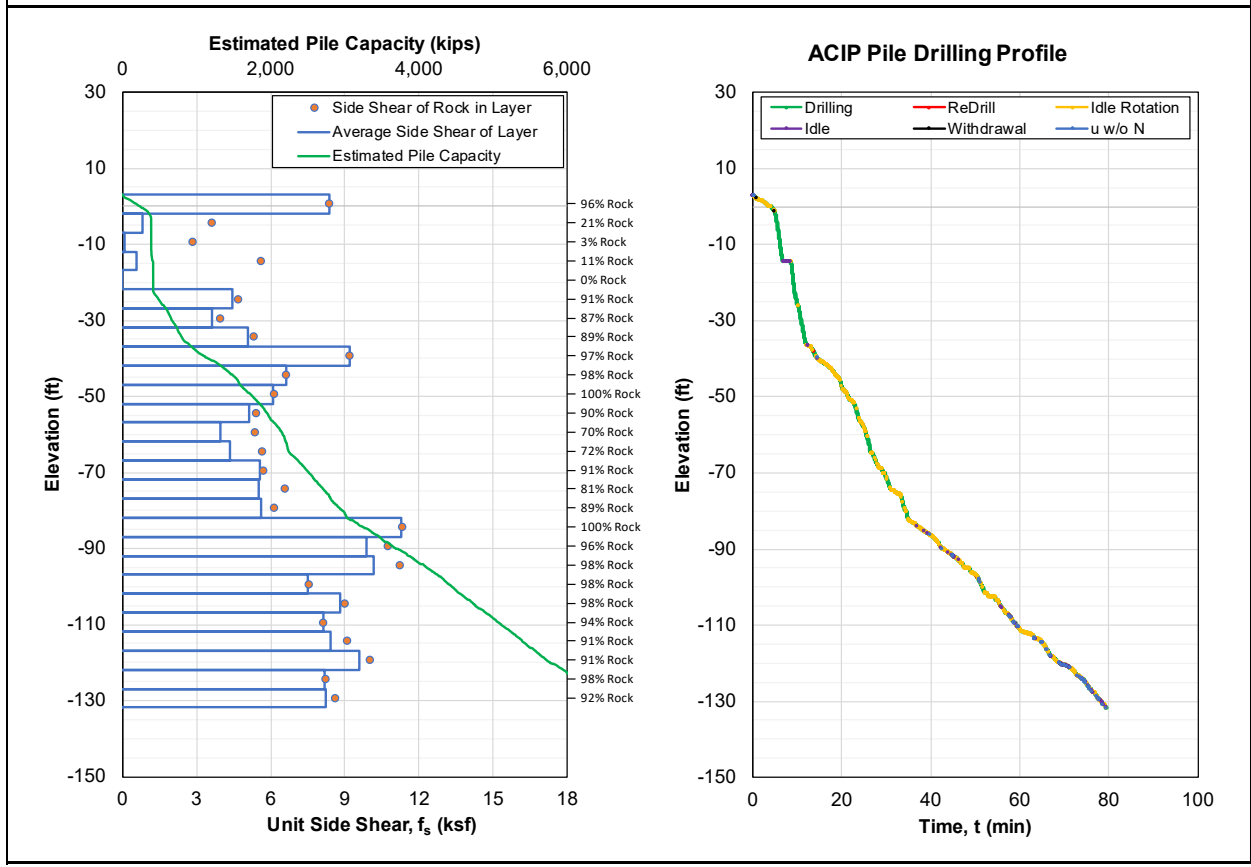


Figure A-48. ACIP pile capacity QA/QC report for Group D Pile 26.

Project	Location	Engineer	Pile ID
I-395	Miami, Florida	Rodgers, McVay, Kelch	D27
Station	Offset (ft)	Drill Rig	Drill Bit Diameter (in)
100+00.01	10.00	Drill Rig A	30
Top of Pile Elevation (ft)	Bottom of Pile Elevation (ft)	Depth Increment Analyzed (cm)	ISO-MWD Assessment
3.15	-131.86	1	Class 1

Specific Energy Above Threshold, e (psi)	
Specific Energy Threshold (psi)	1,250
Mean	6,242
Median	3,326
Standard Deviation	17,631
Coefficient of Variation (CV)	2.82
Maximum	375,366
Minimum	1,256
Number of Data Points	3,210

Unconfined Compressive Strength Above Threshold, q <sub>u</sub> (psi)	
q <sub>u</sub> Threshold (psi)	88
Mean	319
Median	220
Standard Deviation	428
Coefficient of Variation (CV)	1.34
Maximum	6,576
Minimum	88
Number of Data Points	3,210

ACIP Pile Capacity QA/QC	
Pile Length (ft)	135.01
Total Rock Socket Length (ft)	105.3
Average Pile Side Shear, f <sub>s</sub> (ksf)	6.92
Unfactored Pile Capacity (kips)	7,338
Factored Pile Capacity (kips)	4,403
Factored Design Load (kips)	1,050
C/D Ratio for LRFD $\Phi = 0.6$	4.19
Design Requirement Inspection	<b>Passed</b>

Pile Installation Summary	
Drilling Time (min)	45.8
ReDrill Time (min)	0.2
Idle Rotation Time (min)	33.3
Idle Time (min)	2.2
Withdrawal Time (min)	0.2
Penetration w/o Rotation Time (min)	1.1
Total Time (min)	82.7
Drilling Efficiency (%)	55%

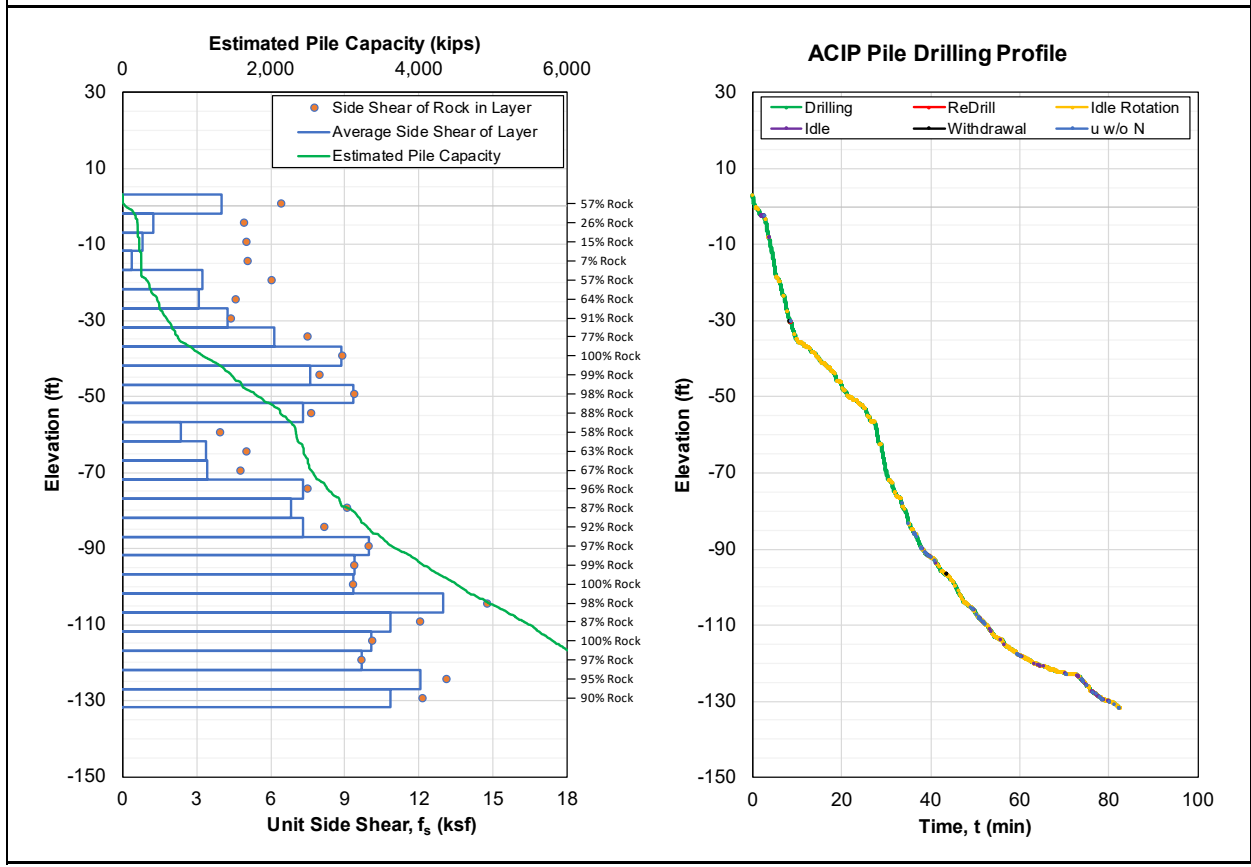


Figure A-49. ACIP pile capacity QA/QC report for Group D Pile 27.

Project	Location	Engineer	Pile ID
I-395	Miami, Florida	Rodgers, McVay, Kelch	D35
Station	Offset (ft)	Drill Rig	Drill Bit Diameter (in)
100+00.01	10.00	Drill Rig A	30
Top of Pile Elevation (ft)	Bottom of Pile Elevation (ft)	Depth Increment Analyzed (cm)	ISO-MWD Assessment
3.4	-131.64	1	Class 1

Specific Energy Above Threshold, e (psi)	
Specific Energy Threshold (psi)	1,250
Mean	5,596
Median	2,858
Standard Deviation	17,403
Coefficient of Variation (CV)	3.11
Maximum	370,892
Minimum	1,250
Number of Data Points	3,148

Unconfined Compressive Strength Above Threshold, q <sub>u</sub> (psi)	
q <sub>u</sub> Threshold (psi)	88
Mean	289
Median	191
Standard Deviation	406
Coefficient of Variation (CV)	1.40
Maximum	6,531
Minimum	88
Number of Data Points	3,148

ACIP Pile Capacity QA/QC	
Pile Length (ft)	135.04
Total Rock Socket Length (ft)	103.3
Average Pile Side Shear, f <sub>s</sub> (ksf)	6.20
Unfactored Pile Capacity (kips)	6,579
Factored Pile Capacity (kips)	3,947
Factored Design Load (kips)	1,050
C/D Ratio for LRFD $\Phi = 0.6$	3.76
Design Requirement Inspection	<b>Passed</b>

Pile Installation Summary	
Drilling Time (min)	37.1
ReDrill Time (min)	2.5
Idle Rotation Time (min)	32.4
Idle Time (min)	12.4
Withdrawal Time (min)	2.4
Penetration w/o Rotation Time (min)	1.6
Total Time (min)	88.4
Drilling Efficiency (%)	42%

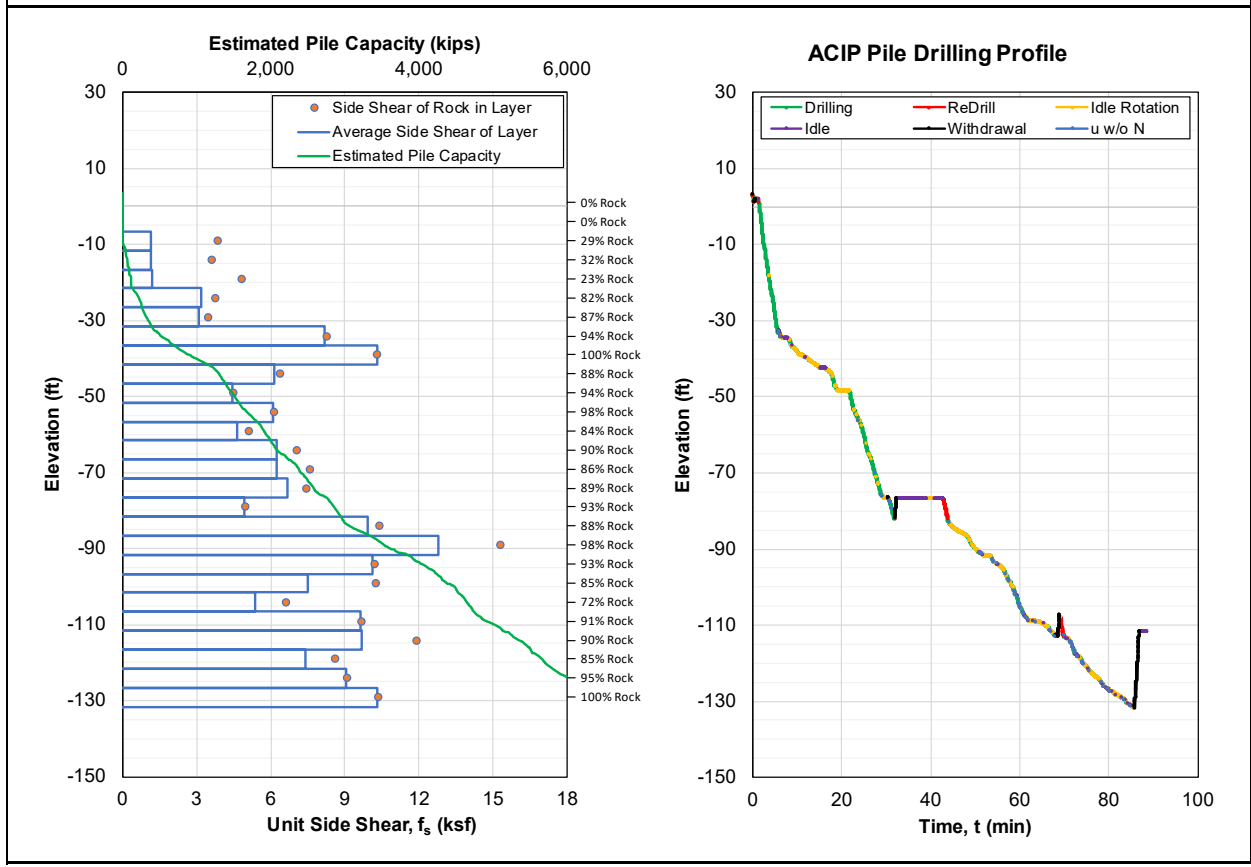


Figure A-50. ACIP pile capacity QA/QC report for Group D Pile 35.

## Appendix B – Sample Calculations

The following provides simulated sample calculations to first convert hydraulic torque and crowd into physical measures compatible with Teale’s (1965) specific energy equation. Next, the simulated time-referenced-data is converted to depth-referenced-data for compatibility. Then, the depth-referenced-data is converted into specific energy for QA/QC monitoring. For the calculation simulations, the following drill rig specifications were generated by the UF research team and do not reflect the actual specifications provided by the drilling contractor (Note: the actual specifications are not provided to protect the proprietary nature of the contractor’s drill rigs):

- Maximum Torque ( $T_{max}$ ) = 1,629,747 in-lbs
- Torque Baseline Pressure ( $T_{BP}$ ) = 0 psi
- Maximum Operating Pressure ( $P_{max}$ ) = 4,000 psi
- Hydraulic Flow Rate ( $Q$ ) = 40,000 in<sup>3</sup>/min
- Maximum displacement ( $\delta_{max}$ ) = 8.0 in<sup>3</sup>/rev
- Minimum displacement ( $\delta_{min}$ ) = 4.0 in<sup>3</sup>/rev
- Number of motors ( $X$ ) = 2
- Gearcase reduction for first gear ( $R_1$ ) = 160
- Gearcase reduction for second gear ( $R_2$ ) = 80
- Maximum Crowd ( $F_{max}$ ) = 90,000 lbf
- Maximum Operating Pressure ( $P_{max}$ ) = 4,000 psi
- Crowd Baseline Pressure ( $F_{BP}$ ) = 0 psi

### Converting Torque

From the specifications gathered, the minimum rotational speed ( $N_{min}$ ) that coincides with the maximum torque ( $T_{max}$ ) was determined for first gear:

$$N_{min} = \frac{Q}{\delta_{max} * R_1 * X} = \frac{40,000 \text{ in}^3/\text{min}}{8 \text{ in}^3/\text{rev} * 160 * 2} = 15.625 \text{ RPM}$$

The value of  $N_{min}$  indicates the maximum torque available on the drill rig can be achieved within a rotational speed range of 0 to 15.625 RPM. This is often referred to as, “rock drilling mode”. The maximum torque is then determined:

$$T_{max} = \frac{P_{max} * Q}{2 * \pi * N_{min}} = \frac{4,000 \text{ psi} * 40,000 \text{ in}^3/\text{min}}{2 * \pi * 15.625 \text{ RPM}} = 1,629,747 \text{ in} - \text{lbs}$$

At rotational speeds above  $N_{min}$ , the maximum torque available begins to decrease and can be determined by the following equation (Note:  $N = 20$  RPM for the example):

$$T = \frac{P_{max} * Q}{2 * \pi * N} = \frac{4,000 \text{ psi} * 40,000 \text{ in}^3/\text{min}}{2 * \pi * 20 \text{ RPM}} = 1,273,240 \text{ in} - \text{lbs}$$

The transition from first gear to second gear can be determined by finding the maximum rotational speed that can be achieved while in first gear:

$$N_{max1} = \frac{Q}{\delta_{min} * R_1 * X} = \frac{40,000 \text{ in}^3/\text{min}}{4 \text{ in}^3/\text{rev} \times 160 \times 2} = 31.25 \text{ RPM}$$

This indicates that at rotational speeds above  $N_{max1}$  the drill rig has transitioned into second gear. The maximum rotational speed that can be achieved for second gear is found using the same equation with the gearcase reduction for second gear:

$$N_{max2} = \frac{Q}{\delta_{min} * R_2 * X} = \frac{40,000 \text{ in}^3/\text{min}}{4 \text{ in}^3/\text{rev} \times 80 \times 2} = 62.5 \text{ RPM}$$

The maximum torque at the highest rotational speed is then determined:

$$T = \frac{P_{max} * Q}{2 * \pi * N_{max2}} = \frac{4,000 \text{ psi} \times 40,000 \text{ in}^3/\text{min}}{2 * \pi * 62.5 \text{ RPM}} = 407,437 \text{ in} - \text{lbs}$$

From the data generated, the following torque-rotational (T-N) chart can be developed:

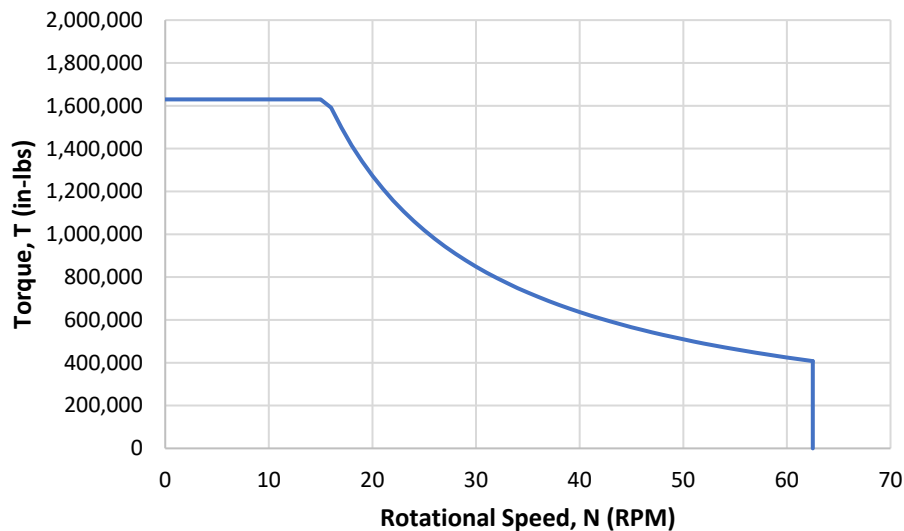


Figure B-1. Simulated torque vs. rotational speed chart.

### Converting Crowd

To convert crowd, a conversion coefficient ( $K_F$  - lbf/psi) must be developed. Using the specifications gathered for crowd, and the baseline hydraulic crowd pressure ( $F_{BP}$ ) solve for  $K_F$  using the identified and measured input parameters:

$$K_F = \frac{F_{max}}{P_{max} - F_{BP}} = \frac{90,000 \text{ lbf}}{4,000 \text{ psi} - 0 \text{ psi}} = 22.5 \frac{\text{lbf}}{\text{psi}}$$

The developed conversion coefficient was then used to transform the “real time” measured crowd hydraulic pressures to physical measures (lbf) as presented in the following equation, where the crowd operating pressure,  $F_p = 800$  psi for this demonstration.

$$F \text{ (lbf)} = 22.5 \left( \frac{\text{lbf}}{\text{psi}} \right) \times (800 \text{ psi} - 0 \text{ psi}) = 18,000 \text{ lbf}$$

### Transforming Time-Referenced Data to Depth-Referenced Data

Table B-1 presents simulated time-referenced-data recorded using a 1 Hz sampling rate that will be transformed into depth-referenced-data with an average value provided for every 1 cm of penetration. As observed in Table B-1, four time-based measurements were collected for the 1 cm increment at a depth of 2.00 feet.

Table B-1. Simulated time-referenced data.

Depth (ft)	Penetration Rate (ft/min)	Rotational Speed (RPM)	Torque Pressure (psi)	Crowd Pressure (psi)
2.00	0.54	18	2,000	800
2.00	0.51	17	2,200	800
2.00	0.48	15	2,400	800
2.00	0.44	14	2,600	800

The first step is to convert each drilling parameter to compatible units of measure for the calculation of specific energy, Table B-2.

Table B-2. Converted depth-referenced data.

Depth (ft)	Penetration Rate (in/min)	Rotational Speed (RPM)	Torque (in-lbs)	Crowd (lbf)
2.00	6.48	18	707,355	18,000
2.00	6.12	17	823,861	18,000
2.00	5.76	15	977,848	18,000
2.00	5.28	14	1,059,335	18,000
Average	5.91	16	892,100	18,000

From Table B-2, rotational speed does not require conversion, penetration rate is simply converted from ft/min to in/min, and the crowd conversion was previously calculated for a crowd pressure of 800 psi. For torque conversion, two sample calculations are provided for this demonstration. The first sample calculation is for the first set of drilling parameters where  $N = 18$  RPM and  $T_p = 2,000$  psi.

$$T = \frac{P \cdot Q}{2 \times \pi \times N} = \frac{2,000 \text{ psi} \times 40,000 \text{ in}^3/\text{min}}{2 \times \pi \times 18 \text{ RPM}} = 707,355 \text{ in} - \text{lbf}$$

The second sample calculation is for the last set of drilling parameters where  $N = 14$  RPM and  $T_p = 2,600$  psi. In this scenario,  $N = 14$  RPM which is less than  $N_{\min}$  defined as  $N = 15.625$  RPM



in the prior calculations. Consequently, a value of  $N = 15.625$  RPM is used for the rotational speed range of 0 RPM to 15.625 RPM.

$$T = \frac{P \cdot Q}{2 \cdot \pi \cdot N_{min}} = \frac{2,600 \text{ psi} \times 40,000 \text{ in}^3/\text{min}}{2 \cdot \pi \cdot 15.625 \text{ RPM}} = 1,059,335 \text{ in} - \text{lbs}$$

### Calculating Specific Energy

Once the conversions are complete, an average value recorded over the 1-cm depth increment is calculated for each drilling parameter as indicated in Table B-2. Once the average for each drilling parameter is calculated, the drilling parameters are now transformed into depth-referenced-data that are compatible with the specific energy equation. Specific energy is calculated as follows with a drill bit diameter ( $d$ ) of 30 inches ( $\text{Area} = 706.86 \text{ in}^2$ ) used for this demonstration.

$$e = \frac{F}{A} + \frac{2\pi NT}{Au} = \frac{18,000 \text{ lbf}}{706.86 \text{ in}^2} + \frac{2 \times \pi \times 16 \text{ RPM} \times 892,100 \text{ in-lbs}}{706.86 \text{ in}^2 \times 5.91 \text{ in/min}} = 21,494 \text{ psi}$$

Where:

- $e$  = Specific Energy (psi);
- $T$  = Torque (in-lbs);
- $F$  = Crowd or downward axial force (lbf);
- $u$  = Penetration rate (in/min);
- $N$  = Rotational speed (RPMs); and
- $A$  = Cross-sectional area of the excavation ( $\text{in}^2$ ) defined by the bit diameter,  $d$  (in).

### Calculating Adjusted Specific Energy

In the QA/QC section of the ACIP Pile MWD Analysis spreadsheet, the adjusted specific energy is calculated for specified pile segments/layers. The following example will display how the adjusted specific energy ( $e_{\text{adjusted}}$ ) is calculated. First, a simulated 10 centimeter thick layer is considered (Table B-3) where the recorded depth increment is set to 1 centimeter (i.e., measurements recorded every centimeter of penetration) and the specific energy threshold is set to 1,250 psi. From Table B-3, it is observed that the average specific energy for the segment is 1,586 psi when all 10 data points are considered. Once the  $e_{\text{threshold}}$  is applied, the four data points that fell below the threshold are removed from the analysis and the average specific energy above the threshold is calculated as  $e_{\text{above}} = 2,274$  psi.

Table B-3. Simulated data used as an example to calculate the segment adjusted specific energy.

<b>e Threshold = 1,250 psi</b>		
<b>Depth (cm)</b>	<b>e (psi)</b>	<b>e<sub>above</sub> (psi)</b>
1	3,129	3,129
2	2,868	2,868
3	2,481	2,481
4	1,335	1,335
5	625	
6	358	
7	549	
8	679	
9	1,529	1,529
10	2,302	2,302
<b>Average</b>	1,586	2,274
<b>Count</b>	10	6

Once the data points are removed, the spreadsheet calculates the length of the rock socket within the segment in the following way:

$$L_{rock} = Count \times recorded\ depth\ increment = 6\ data\ points \times 1\ cm/data\ point = 6\ cm$$

Next, the percentage of rock is calculated:

$$\% of\ Rock = \frac{L_{rock}}{L_{Layer}} = \frac{6\ cm}{10\ cm} \times 100\% = 60\%$$

Finally, the average specific energy above the threshold ( $e_{above}$ ) is adjusted by the percentage of rock present within the specified segment/layer:

$$e_{adjusted} = \frac{\% of\ Rock}{100} \times e_{above} = \frac{60}{100} \times 2,274\ psi = 1,364.4\ psi$$

The  $e_{adjusted}$  value is then reported in the QA/QC portion of the strength analysis and displayed in the QA/QC plots in the “Strength Analysis” and “Pile Summary Report” tabs.